E-733-65-1

FINAL REPORT
VOLUME I
FOR
MILLIMETER COMMUNICATION PROPAGATION PROGRAM
(1 NOV., 1964 – 1 NOV., 1965)

Contract No. NAS 5-9523

Prepared by
RAYTHEON COMPANY
SPACE & INFORMATION SYSTEMS DIVISION
Sudbury, Massachusetts
Raytheon Report No. FR-65-334-1

for

GODDARD SPACE FLIGHT CENTER
SYSTEMS DIVISION
COMMUNICATIONS RESEARCH BRANCH
CODE 733
Greenbelt, Maryland

RAYTHEON COMPANY
SPACE AND INFORMATION SYSTEMS DIVISION

E-733-65-1

FINAL REPORT
VOLUME I
FOR
MILLIMETER COMMUNICATION PROPAGATION PROGRAM
(1 NOV., 1964 - 1 NOV., 1965)

Contract No. NAS 5-9523

Prepared by
RAYTHEON COMPANY
SPACE & INFORMATION SYSTEMS DIVISION
Sudbury, Massachusetts
Raytheon Report No. FR-65-334-1

for

GODDARD SPACE FLIGHT CENTER
SYSTEMS DIVISION
COMMUNICATIONS RESEARCH BRANCH
CODE 733
Greenbelt, Maryland

RAYTHEON COMPANY
SPACE AND INFORMATION SYSTEMS DIVISION
RAYTHEON

SUMMARY

This document is Volume I of the final report for the Millimeter Communication Propagation Program being performed under NASA Contract No. NAS5-9523 by Raytheon's Space and Information Systems Division for Goddard Space Flight Center. This program is a study to design experiments which will determine the effects of the propagating medium on millimeter-wave (10 to 100 gigacycles) space-earth communications.

The First Quarterly Report discussed the effects of the propagating medium as they are known today and described a one-year space-earth experiment to be performed in 1968 with a 6000 nautical mile medium altitude satellite. The Second Quarterly Report described a one-year space-earth experiment using a synchronous stationary satellite. It also described in detail the ground and satellite equipment to be used in an experiment, most of which is compatible with either the medium altitude or synchronous altitude Applications Technology Satellites.

This final report consists of three volumes with Volume I being a report on the complete experiment design study. Volume II is actually the third quarterly report which, along with the other quarterly reports, provides detailed backup to Volume I. Volume II describes how the raw data, which is collected during the propagation experiments, should be processed and evaluated and includes an introduction to the design of communication and propagation experiments for low altitude and synchronous altitude manned spacecraft. Volume III contains a descriptive bibliography of related reports and a recommended outline for a propagation data handbook.

This summary of Volume I gives a list of specific recommendations which NASA should consider in order to carry out an effective millimeter-wave propagation program. Problem areas, which require immediate attention, are also identified.

For the most part, this experiment design study was conducted with NASA's Applications Technology Satellites (ATS) in mind. The specific ATS satellites are described as follows:

a.	ATS-A	MAGGE	Medium altitude, gravity gradient stabilized satellite at 28.5° inclination.
b.	ATS-B and C	SASSE	Synchronous altitude, spin stabilized, stationary satellites.
c.	ATS-D and E	SAGGE	Synchronous altitude, gravity gradient, stationary satellites.

At present, Flight ATS-E, which is due to be launched late in 1968, is being strongly considered as the space platform for the initial millimeter-wave propagation experiment.

With the establishment of the NASA APOLLO Applications Program (AAP) and the Air Force Manned Orbiting Laboratory (MOL) Program, it was considered appropriate to include, as much as possible, experiment design information involving low altitude and synchronous altitude manned spacecraft.

This final report recommends a specific payload configuration for the initial space-earth experiment which consists of two separate modules: one having a 35 Gc transmitter and 94 Gc receiver/signal processor and the other having a 16 Gc transmitter. However, mainly because of prime power limitations aboard the spacecraft and a deep concern for reliability, a compromise payload, namely, a 16 Gc transmitter and a 35 Gc receiver/signal processor, is being considered for Flight ATS-E. The body of this report does not specifically discuss this compromise because the study was

essentially completed before this course of action was taken. However, practically all of the experiment design information is still valid and all recommendations presented in this summary still apply.

Since the design of space-earth communication links represents the ultimate objective of the propagation program, consideration for the water vapor and oxygen absorption regions around 22 Gc and 60 Gc were excluded. The original design of the experiments was therefore centered around the frequencies of 16 Gc, 35 Gc and 94 Gc because they are representative of the 10 Gc to 100 Gc band. From these three frequencies, the primary frequency for the initial experiment was chosen to be 35 Gc because most of the existing millimeter ground facilities being considered are easiest to instrument with receivers at this frequency. Reasons for choosing a down-link instead of an up-link will be discussed in the recommendations.

For the initial experiments a secondary frequency was chosen to be 16 Gc. Although the atmospheric effects are not as dramatic at this frequency, it nevertheless represents the frequency band in which the next generation of space-earth communication channels will fall. Down-links were recommended for the 16 Gc experiments for the same reasons given for the 35 Gc experiments. However, because of prime power limitations, it was considered not possible for 35 Gc and 16 Gc to be transmitted simultaneously, thus the reason for two separate payload modules.

The third frequency was chosen to be 94 Gc because it represents the next useful atmospheric window above the 60 Gc band. Unfortunately, a down link was not recommended for the initial experiments because of the risk in attempting to develop a spaceworthy transmitter of adequate power within a two year time period.

In an experiment utilizing the compromise configuration, the primary frequency simply becomes 16 Gc because it is transmitted from the space-craft and the secondary frequency becomes 35 Gc.

The existing ground facilities which were evaluated are those located at: the Aerospace Corporation, El Segundo, California; the University of Texas, Austin, Texas; Air Force Cambridge Research Laboratories (AFCRL), Lexington, Massachusetts; and Lincoln Laboratory, Lexington, Massachusetts. A facility at Goddard Space Flight Center (GSFC) which is presently being established, would be the chief participant. Since more emphasis is being placed on 16 Gc, additional existing facilities should be considered such as those located at Defense Research Telecommunications Establishment (DRTE), Ottawa, Canada; Ohio State University, Columbus, Ohio; Naval Ordnance Laboratory (NOL), Corona, California; and Applied Physics Laboratory (APL), Howard County, Maryland.

RECOMMENDATIONS

1. General

NASA should consider the millimeter-wave propagation program as a long-range effort with the initial phase involving simple channel probes (test waveforms) and the payload configurations mentioned above. The program plans should outline subsequent phases which: investigate higher frequencies, investigate frequencies within the water vapor and oxygen absorption bands, demonstrate communications feasibility with actual modulation systems, and utilize manned spacecraft.

2. Channel Characterization

The basic goal of the millimeter-wave propagation program should be to characterize various channels, which represent the 10 Gc to 100 Gc band in terms of space and frequency and time. This information should be presented in the form which is not only useful in increasing our scientific understanding of the effects of the propagating medium but also provides the communication systems engineer with the necessary data to design space-earth

communications links.

2.1 The two-dimensional, frequency-time correlation function is an important portion of this channel characterization which is measured by those experimenters who need fading statistics and which has direct application to the design of communication systems using frequency diversity. Coherence time, coherence bandwidth and fading rates can be determined directly from the two-dimensional correlation function. A two-dimensional Fourier Transform of this correlation function can be taken in order to describe the scattering function and obtain information regarding doppler and multipath spreading by the channel.

2.2 The space-time (lateral coherence) correlation function, for two parallel spatial channels receiving the same signal, is another important characterization of the millimeter channel. From this function the coherence aperture can be determined, which is an important measure of the maximum size antenna to be efficiently employed. In situations where space diversity schemes are being considered, the spatial correlation function specifies the antenna separation required in order to receive uncorrelated signals. A spatial spectral density function can be derived from the two-dimensional Fourier Transform of the spatial correlation function. This function describes the spatial spectrum of the wavefront and the lateral motion of wavefront with respect to the antenna baseline.

2.3 In the initial propagation experiments it is not practical to develop the complete functions just described. Modified two-dimensional correlation functions and their Fourier Transforms should be generated which give reasonable estimates of the boundaries of the space-earth channel in all three dimensions. From this boundary data subsequent experiments can be intelligently designed.

3. Correlative Measurements

Basic correlative measurements are required to classify the weather model existing in each test in order to give statistical merit to the channel characterization functions. Proper emphasis must be placed upon correlative data processing in order to classify the atmospheric conditions existing during each measurement period and determine the probability of each class of conditions during the annual cycle. Good correlative measurements will also help explain why certain things are happening to the test signals which are being propagated through the complex atmosphere.

3.1 In addition to the usual surface meteorological data which must be collected at each ground terminal, radiometric measurements in coincidence with the basic signal measurements are a necessity. The apparent sky temperature, which is the result of these radiometric measurements, directly relates to the total atmospheric attenuation due to the water and oxygen content of the atmosphere. Since the test signals could undergo fading due to multipathing as well as variations in water content within the receiving beam, the radiometric measurements will therefore help distinguish between various mechanisms producing fading. Modified autocorrelations of radiometer signals, cross correlations of radiometer signals with the amplitude envelopes of the test signals and modified two-dimensional space-time correlation functions of radiometer signals should be processed and used in the evaluation of the signal data.

3.2 If a NASA facility is established for the expressed purpose of making propagation measurements throughout a long range program then it is considered worthwhile to employ a 3 Gc weather radar specifically instrumented to record estimates of the rainfall rate

along the propagation path. In experiments involving stationary satellites where the propagation path is fixed, surface rate data from rain gauges underneath the path would be a practical supplement to the radar data. Millimeter-wave radar should not be considered for measuring rainfall rate profiles because the radar backscatter is attenuated on its return and knowledge of the water, temperature, and pressure profiles along the propagation path with sufficient accuracy will not be available. A clear definition of the useful four-dimensional, space-time radar resolution cell must be firmly established before a radar is procured.

4. The Measurement Waveform

The basic test waveform to be transmitted in the first experiment should be a carrier and one pair of AM sidebands. A choice between an unmodulated carrier and a modulated carrier must be provided with the modulating frequency being variable in several discrete steps up to at least 50 megacycles. This simple arrangement which uses a passive modulator in the satellite will provide some useful estimates of the space-frequency-time boundaries of the propagation channel. Although other more sophisticated waveforms are discussed, these are left for use in future experiments which are based on the results of this initial experiment.

5. Formulation of Experiments

5.1 Three types of satellites, classified according to orbital altitude, were evaluated in terms of their suitability as space platforms with which to conduct space-earth millimeter-wave propagation experiments. In addition, high altitude aircraft were compared with the satellites because they could play a definite role in the propagation program.

A series of propagation experiments using aircraft would constitute a useful phase in the overall millimeter-wave propagation program. This phase of the program should precede, if possible, the final spacecraft equipment design phase for the initial space-earth experiments. Air-ground experiments, however, should not be considered as a satisfactory substitute for the complete space-earth experiments because of the costs involved in achieving an accurate statistical model. Slow moving aircraft which can fly above most of the sensible atmosphere can provide qualitative data, on the frequency-time characteristics of the channel within a shorter equipment design and fabrication period than that required for spacecraft. This qualitative data would be helpful in designing more intelligent space-earth experiments which are more complete and which yield quantitative results. The aircraft can also be used to evaluate experiment equipment which is to be used aboard a spacecraft.

The synchronous stationary satellite is the best space platform with which to conduct the initial space-earth experiment because considerable operational expense is saved by; not having to generate precise and timely ephemeris data which is required for acquiring and tracking non-synchronous satellites with narrow millimeter-wave beams and; not performing costly modifications for automatic track capability in the existing millimeter-wave facilities. This is the only vehicle, including aircraft, with which accurate spatial characterization can be achieved. The big disadvantage with synchronous spacecraft is that it could be placed beyond line-of-site of many of the important ground facilities including the one planned for GSFC. Early identification of the satellite longitudinal position is required to insure that proper planning can be made regarding useful ground

facilities. The optimum position for the propagation experiment would be either 27° W Lg. over the Atlantic or 145° W Lg. over the Pacific.

In the long range program, the medium altitude (6000 n miles) satellite would be a useful space platform with which to conduct propagation experiments. The angular elevation rate of the medium altitude satellite is slow enough to permit ample viewing time per pass with sufficient data samples per degree of elevation and, yet the elevation angular rate is still fast enough to complete a continuous elevation profile before significant weather changes can occur.

The design of experiments using low altitude (100 to 300 n miles) manned spacecraft should be based on the assumption that propagation experiments using aircraft and synchronous altitude satellites have already been performed during preceding phases of the program. Low orbiting spacecraft are not ideal vehicles for basic propagation experiments because they are too close to earth to permit reasonable time for gathering quantitative data by any one aircraft or ground station. Multiple aircraft and ground stations are expensive especially since the spacecraft is traveling at high angular rates relative to the other terminal. Low orbiting spacecraft do, however, offer payload capacities which often surpass that which is available at higher altitudes. Furthermore, the availability of man in a low orbiting spacecraft is of inestimable value in determining the operational potential of millimeter-wave communications, to support future manned spacecraft missions such as the later generations of the AAP and MOL programs.

5.2 For the initial propagation experiments it is recommended that down-links be used instead of up-links whenever possible. The key to a successful experimental program which involves the assistance of several existing ground installations, each controlled by a different agency, depends on the ease with which these facilities can participate.

All of the existing sites which were evaluated are equipped with millimeter-wave receivers which are used in radio astronomy. Since these facilities use interchangeable rf heads to change frequency of operation, it is very reasonable to assume that modifications for receiving test signals from satellites are much easier than those required for transmitting test signals to the satellites.

Another very important reason for wanting to use satellite transmitters is that less coordination is required during the data collection operation and several stations can make measurements simultaneously without interfering with one another. When ground transmitters are used, a closed loop is required to confirm that the transmitted signal is being properly received.

One objection to the down-link has been the high prime power requirements of the space transmitter. However, a satellite receiver would have to be on longer than a space transmitter in order to accommodate each ground station individually.

One of the prime objectives of the propagation experiments is to define the two-dimensional lateral coherence function with at least some points along the spatial axis. These measurements can only be made with a down-link.

When up-links are used, the participating agencies do not have immediate access to the raw data which is being collected. There is a certain delay in obtaining this information which prevents the station operators from evaluating their performance in real time. and taking corrective action. It is certain that in addition to satisfying NASA's requirements, these agencies will want to make specific measurements or data recordings which fulfill special requirements of their own.

An early space-earth experiment has to depend completely on present technology and a satellite receiver is considerably closer to meeting longevity and environmental requirements than a satellite transmitter. For this reason plus the fact that receivers require less power, a 35 Gc up-link for the ATS-E spacecraft is a logical choice.

5.3 A typical work cycle with a stationary satellite which would be satisfactory for the propagation experiments would be to operate during a dozen five day work weeks seasonally spaced throughout the year. A full work week every four or five weeks may be the most attractive arrangement from a manpower scheduling view point and the down time between tests will provide ample opportunity for examining data and making changes in test procedure and ground equipment before the next test.

Each work week should consist of four data collection sessions with a minimum of four to six hours duration for each; and appropriately spaced so that each station collects data during dawn and dusk and near noon and midnight. These sessions must include pre-test and post-test data collection check-out and calibration with the spacecraft simulator which is located at a remote boresight facility. Little planning would be made with

regard to weather since it is unpredictable and since work schedules must be established well in advance. Enough samples would be taken during the year which should result in a reasonable cross-section of the normal meteorological variables.

The importance of early mission profile planning cannot be over-emphasized because of the competition with other experiments aboard the spacecraft for prime power and telemetry and competition with other experiments being conducted by the participating ground facilities.

6. Ground Facilities

A primary experimental ground facility should be established under the control of NASA which, when supplemented by the facilities of other agencies, can be expanded to meet the needs of the long-range program. Decisions on facility siting and major equipment designs and procurements should be based on a series of flights rather than a single flight, such as the ATS-E.

6.1 The basic element in the primary experimental facility, the antenna pedestal system, must be equipped to automatically track low altitude spacecraft and high altitude aircraft as well as slow moving satellites. The pedestal yoke must be large enough to accommodate a receiver-transmitter compartment which provides easy access to interchangeable r-f packages.

6.2 The equipment layout for the primary facility should include a system of auxiliary antennas and mirrors which can be employed to investigate the two-dimensional lateral coherence function using stationary satellites. This system of reflectors must be designed such that variable baseline configurations are possible. The additional antennas may also be used to solve difficult diplexing problems created by multiple frequency operations.

6.3 The equipment layout for all of the participating facilities should include a well equipped boresite facility which, in addition to the signal sources required for antenna system alignment and receiver calibration, it contains receivers, waveform generators and signal processors which function like those aboard the spacecraft.

6.4 The longitudinal position of the stationary satellite is critical in that the right combination of elevation angles from two or more existing ground stations may not be possible. Under these circumstances, it is reasonable to consider addition of transportable non-tracking antenna-receiver installations at locations, other than those of the existing facilities, to serve as gap fillers in the elevation angle profile. These auxiliary installations under some circumstances may not have sufficient antenna gain to investigate the coherence bandwidth of the medium but they could supply important signal fading statistics on a single carrier.

7. Spacecraft Equipment

There are many problems associated with the millimeter-wave 16 Gc transmitter/35 Gc receiver module for the ATS-E spacecraft in the areas of: critical design in the r-f section and; interfaces with supporting sub-systems, other experiment modules and the space-frame.

The small amount of prime power (in the neighborhood of 25 watts) which is available from the electrical power subsystem is the chief cause for concern. Since the efficiencies of transmitters at 16 Gc are poor, the amount of radiated power is limited to approximately 200 milliwatts. This small amount of r-f power in the experimental 16 Gc space-earth down-link demands that careful attention be given to:

a. the stability of the transmitter and ground receiver local oscillator;
b. the sensitivity of the ground receiver;
c. performance of the ground receiver carrier phase-lock loop;
d. the gain of the satellite antenna and;
e. the losses in the path from the transmitter to the antenna (that is, those of the passive AM modulator, decoupler for the 35 Gc receiver frequency doubler and the waveguide).

Stability and reliability requirements make a strong case for a solid state transmitter whose frequency output is derived from some multiple of a good crystal. However, sufficient power output from solid state devices at 16 Gc poses a problem. Attention to "d" and "e" above involves the placement of the module with respect to the antenna to minimize waveguide runs and involves the performance of the spacecraft stabilization subsystem. An antenna beam whose width is smaller than the angle subtended by the Earth is required in order that sufficient effective radiated power (ERP) (20 dbw) is produced.

If the output power is 200 milliwatts, the antenna gain must be 27 db (7.5 degree beam, 7.2" diameter aperture). Unfortunately, this antenna has to be pointed away from the satellite vertical toward the United States and therefore its design has a greater dependency on the stabilization accuracy and the longitudinal position of the spacecraft. The 20 dbw ERP was based on a 15-foot diameter receiving aperture on earth. If 30 to 60 foot apertures are available, the ERP could be reduced.

The 35 Gc up-link is less of a problem because of the 100 watt ground transmitter which is planned. This amount of power provides a 27 db advantage over the 16 Gc down-link which

should more than compensate for the propagation losses, high noise figure and receiver sensitivity degradation over the life of the satellite. The main problem with the 35 Gc up-link is the transmission of propagation data back to earth. The PCM telemetry subsystem restricts the sampling rate to three cycles per second (10 cycles per second is desired). Analog data transmission with the 4 Gc/6 Gc communication transmitter may be a better arrangement.

The spacecraft payload for ATS-E poses many questions which require early answers if a useful flight qualified package is to be integrated into the spacecraft in time for a late 1968 launch. The first series of questions to be answered is:

a. What is the longitudinal position of the satellite?
b. What changes in position are anticipated during the first year of operation?
c. What ground facilities can be used?
d. What is the maximum size antenna which can be employed on the spacecraft?

Early laboratory breadboard work must be performed to determine estimates of:

a. Power output level which can be reliably generated at 16 Gc with solid state devices.
b. Efficiency of a solid state 16 Gc transmitter.
c. Values of minimum signal-to-noise density for phase lock receiver acquisition and track using r-f frequency stabilities which are expected to prevail.
d. Noise figure for the 35 Gc receiver.
e. Highest acceptable modulation frequency for the passive AM modulator.

8. Data Processing and Evaluation

The propagation data collected at the various cooperative ground facilities should be processed and evaluated by NASA at a central facility. For the most part, existing computer facilities are equipped to handle the data processing required for the propagation data collection program. Special computer programs can be derived to transform the raw data into estimates of the millimeter-wave channel characteristics. An extensive quantity of data will result from the experimental program, and of course, it is not necessary to statistically process all of the data collected. However, it is necessary to look at the analog presentations for the occurrence of unusual propagation effects to insure that the data which is processed adequately represents the statistical model.

Each ground facility receiver participating in the program should be equipped with identical signal processors and analog magnetic tape recorders to minimize data processing expense. Each ground receiver should share its RF head with a radiometer so that sky temperature measurements can be recorded on the same tape in synchronism with the signal phase and amplitude measurements. When available, short term and long term variations of tracking antenna azimuth and elevation should also be recorded on the same tape. Real-time analog strip line recorder presentations of the same data which was recorded on magnetic tape should be made at each site for calibration check-out and operational monitoring; and to provide the cooperating agencies with immediate access to the raw data. The taped analog data from satellites and ground facilities should be converted to digital form at a central data processing facility.

Once the space-frequency-time characterization of the channel is developed to a reasonable degree, then established computational methods can be used to infer the effects of the atmosphere on conventional modulation systems. Much of this information is already available in existing literature.

PRINCIPAL CONTRIBUTORS

The technical officers at Goddard Space Flight Center who were responsible for this study were Mr. Abe Kampinsky and Mr. Walter Elder of the Communications Research Branch in the Systems Division. The key Raytheon participants are given in Table I.

Valuable advice regarding existing theoretical and experimental propagation data and existing experimental ground facilities was received from the following agencies:

Aerospace Corporation, El Segundo, California

Air Force Cambridge Research Laboratories,
Bedford, Massachusetts

MIT, Lincoln Laboratory, Lexington, Massachusetts

Electrical Eng. Research Lab., University of Texas,
Austin, Texas

TABLE 1

KEY RAYTHEON PARTICIPANTS IN MILLIMETER-WAVE COMMUNICATION PROPAGATION STUDY

Name	Raytheon Organization	Technical Area
Mr. Ira Smith	SISD[1], Sudbury, Mass.	Study Director
Dr. Eli Brookner		Atmospheric Propagation Effects, Waveform Analysis, Data Processing
Mr. Joseph Clougherty		Atmospheric Propagation Effects, Plasma Effects
Mr. Edward Gifford		Equipment Design
Mr. Ronald Porter		Correlative Measurements, Meteorology
Mr. Louis Romano		Atmospheric Propagation Effects, Signal Analysis, Equipment Design
Mr. Thomas Servey		Atmospheric Propagation Effects, Meteorology
Mr. Arthur Robichaud	(now with National Radio Astronomical Observatory)	Facilities Survey, Equipment Design
Mr. Robert Savage	SBO[2], SISD, Santa Barbara, California	Equipment Design
Mr. David Barton	SURANO[3], Equipment Division, Wayland, Mass.	Atmospheric Propagation Effects
Dr. Joseph deBettencourt	CADPO[4], Equipment Division, Norwood, Mass.	Atmospheric Propagation Effects
Dr. John Myers	Research Division, Waltham, Mass.	Atmospheric Propagation Effects
Dr. Barret Hazeltine	Consultant, Brown University, Providence, R.I.	Correlative Radiometric & Radar Measurements
Mr. Donald Snyder	Consultant, MIT, Cambridge, Mass.	Data Processing

(1) SISD - Space and Information Systems Division
(2) SBO - Santa Barbara Operation
(3) SURANO - Surface Radar and Navigation Operation
(4) CADPO - Communications and Data Processing Operation

CONTENTS

CONTENTS (Continued)

CONTENTS (Continued)

CONTENTS (Continued)

CONTENTS (Continued)

ILLUSTRATIONS

ILLUSTRATIONS (Continued)

ILLUSTRATIONS (Continued)

ILLUSTRATIONS (Continued)

ILLUSTRATIONS (Continued)

TABLES

TABLES (Continued)

Section I
INTRODUCTION

This document is Volume I of the final report for the Millimeter Communication Propagation Program being performed under NASA Contract No. NAS5-9523 by Raytheon's Space and Information Systems Division for Goddard Space Flight Center. This program is a study to design experiments which will determine the effects of the propagating medium on millimeter-wave (EHF) space-earth communications.

The scope of work for this study program was defined in Exhibit "A" of Contract NAS5-9523 and supplemented by the Raytheon Proposal, "A Millimeter Communication Propagation Program," BR-3011, 3 June 1964. Another report which supplements Exhibit "A" is, "Program Definition Plan for Millimeter Communication Propagation Program," FR-4-498-B, 29 January 1965. The Program Definition Plan defines the objective of the program, lists the tasks to be performed, and describes the various work activities under each task, including their time relationships with one another.

The objective of this experiment design study was to design a series of experiments which show how the objectives of a millimeter propagation program can be met. Wherever design problems could not be solved, courses of action in the form of component tests and breadboard design were recommended. This objective includes development of experiment cost estimates and time schedules, including that for data processing and evaluation. Results of the study include equipment design, source of key components, definition of basic measurements and description of how these basic measurements can be used to meet the objectives of the experiment.

The First Quarterly Report, which was a report of work accomplished during the period 1 November 1964 to 1 February 1965, described the effects of the propagating medium as they are known today and discussed a one-year space-earth experiment to be performed in 1968 with a 6000 nautical mile medium altitude satellite. The Second Quarterly Report, which was a report of work accomplished during the period 1 February 1965 to 1 May 1965, described a one-year space-earth experiment using a synchronous stationary satellite. The Second Quarterly Report also described in detail the ground and satellite equipment to be used in the experiment, most of which is compatible with either the medium altitude or synchronous altitude Applications Technology Satellites.

The final report consists of three volumes. Volume I is a summary of all the work performed during the program. Volume II is a detailed report of work accomplished during the third quarter, 1 May 1965 to 1 August 1965. The most significant technical areas covered in Volume II are: The usefulness of correlative radiometric and weather radar data; introduction to design of communication and propagation experiments for low altitude and synchronous altitude manned spacecraft; and millimeter-wave propagation data processing and evaluation. Volume III has a descriptive bibliography of reports which were used during the study and contains an outline of a propagation data handbook which is recommended as the final product of the experimental program.

This report, Volume I, does not contain all of the important technical information published in Volumes II and III and the First and Second Quarterly Reports. Instead, it summarizes the basic issues down to a certain level and references sections of the other reports which contain the detailed back-up.

Section 2 of this report, "The Potential of Millimeter-waves in Space-Earth Communication Systems," is a general discourse on the incentives for

determining the effects of the propagating medium on millimeter-wave signals.

Section 3, "Millimeter-wave Channel Characterization," has two parts. The first part describes the general model for a communication channel in an attempt to provide an understanding of the basic physics involved. The second part gives the standard definitions of the mathematical correlation and spectral density functions for communication channels separated in frequency and separated spatially.

Section 4, "Propagation of Millimeter-waves," describes the effects of the atmosphere on millimeter-wave propagation within the limits of our present understanding. Atmospheric absorption and refraction, antenna temperature, flat fading, selective frequency fading, coherence bandwidth, spatial decorrelation and plasma effects are among the items discussed.

The next section which follows defines the basic measurements which should be made to increase our knowledge of atmospheric effects. Section 5, "Definition of Basic Measurements," describes the basic test waveforms or channel probes which could be used to obtain the basic signal measurements from which the channel can be characterized. In addition, basic correlative measurements using meteorological radiometric and radar instrumentation are defined. These correlative measurements will help to explain why certain things are happening to the channel probes. They also classify the weather conditions at the time of the tests in order to establish some statistics from the propagation data.

Section 6, "System Performance Analysis," explains how the channel correlation and spectral density functions can be used to estimate performance of various common modulation systems.

Section 7, "Formulation of Experiments," provides the basic information required to evaluate various candidate concepts. Orbital constraints placed upon the experiment by synchronous, medium and low altitude satellites are

given. Up-link experiments are compared with down-link experiments. The candidate waveforms, which were discussed in Section 5 in terms of the basic signal data they could provide, are now discussed in terms of hardware implementation. Ground antenna configurations are suggested for measuring various spatial correlation and spectral density functions. The proper use of aircraft in the propagation measurements program is defined.

Section 8, "Equipment Design," provides the schematic block diagrams for the ground and spacecraft hardware which could be used in a measurements program. In addition to the block diagrams and the weight, volume, and prime power estimates for the spacecraft equipment; critical design problems are outlined.

Section 9, "Ground Facilities Evaluation," summarizes the capabilities of existing and planned experimental millimeter-wave ground facilities which could play an important role in the propagation measurements program. The meteorological conditions which prevail at each of these facilities is also given.

Section 10, "Signal Processing," describes the signal processor configuration which makes the basic measurements on the test waveform to be used. A signal flow analysis is summarized which describes the spectrum of the test waveform as it moves through the transmitter, the atmosphere, the receiver, and finally the signal processor. A signal level analysis is summarized which includes carrier aquisition and track conditions, effective receiver bandwidth, amplitude measurement and phase detection. Finally the design of the signal processor is given.

Section 11, "Data Processing," describes the general concept of data processing for the propagation data collection program and summarizes the mathematical formulation required to generate the correlation and spectral density functions to be computed from the basic signal measurements.

Section 12 is a bibliography of reports referenced in this volume.

Section 2
THE POTENTIAL OF MILLIMETER WAVES IN SPACE-EARTH COMMUNICATIONS SYSTEMS

The first and foremost incentive for determining the effects of the propagation medium on millimeter wave signals (EHF) is to develop new communication bands to relieve the overcrowding of the lower frequency bands. Establishment of 10 percent frequency bands for space-earth communications at 35 Gc and 94 Gc would represent an order of magnitude with more capacity than all the lower frequency bands presently assigned. This increase in available bandwidth is necessary if future aerospace communication links are to handle the steadily increasing quantities of information which must be transmitted from space vehicles. Use of millimeter waves is inevitable, the principle question being when. Propagation data is required to guide the development of millimeter wave component technology and to indicate to space communication planners when millimeter systems will be technically and economically competitive.

Another very important reason for learning more about millimeter wave propagation is the wide bandwidth offered by millimeter wave components. If the propagation medium does not severely limit the coherent bandwidth of signals transmitted through it, then real-time transmission of information from sophisticated space-borne sensors is possible, particularly if they are manned and they are performing low altitude missions.

Spacecraft weight and power is at a precious premium as is room on space vehicles for antennas. If the transmitter portion of an aerospace communication link is contained in a spacecraft, then the distribution of the product of radiated power and antenna gain is an important factor in the design of the communication link. As an example, assume that an aerospace communication link were performing satisfactorily at a frequency of 9400 Mc

with 10 watts of radiated rf power and a two-foot diameter paraboloid antenna. Neglecting atmospheric attenuation for a moment, the same link performance, assuming identical receiving terminal characteristics, could be obtained at a frequency of 94 Gc with the same two-foot dish by using only 100 milliwatts of radiated rf power. Considering that tube conversion efficiencies might typically be 10 percent, the X-band system would require 100 watts of satellite power while the EHF system would require one watt of satellite power. The savings of almost 100 watts of primary power in only one instance is an important consideration when the scarcity of spacecraft power is considered.

Another advantage that is obtained by operating aerospace communication links at EHF is the aspect of transmission privacy. This advantage is due primarily to EHF atmospheric attenuation characteristics and the narrow antenna beamwidths obtainable at EHF. These two factors also help to reduce any possible interference or RFI from other EHF signals. For a given size antenna, the half power beamwidth is inversely proportional to the operating frequency. Thus, an antenna operating at 94 Gc would have 1/10th the beamwidth of the same size antenna operating in X-band. The privacy of transmission which is obtainable due to atmospheric attenuation characteristics is particularly noticeable in the 60 Gc frequency band. In this frequency band, transmissions from a satellite to an aircraft at 45,000 feet would not be received by a ground station because of the large additional attenuation due to the intervening atmosphere below the aircraft.

A vehicle which re-enters the earth's atmosphere at hypersonic velocities becomes enveloped in an ionized plasma of compressed and heated air. This plasma severely attenuates communication to and from the vehicle, increases the effective noise temperature of the vehicle antenna thus degrading receiver sensitivity, and limits the amount of power that can be radiated from the vehicle. Because of the uncertanties in the plasma parameters for a typical re-entry condition, it is evident that the use of millimeter-wave signals holds

considerable promise. This study is not directly related to the problem of propagating through a plasma; however, it must be pointed out that one must determine the effects of propagating through the atmosphere before an optimum re-entry communications frequency can be chosen which represents the best trade-off between plasma effects and propagation effects.

Present operational equipments which are radiating power at fundamental frequencies in the millimeter band are comparatively few. Most of these EHF emitters are limited to low radiated power levels and transmission paths along the earth. As a result of these characteristics and well confined antenna sidelobes, radiated EHF power at angles other than along the earth's surface is very small. In addition, any radiated EHF power along the earth's surface is subject to comparatively high attenuation due to atmospheric losses. Consequently, there is currently little possibility of interference to EHF aerospace links from fundamental EHF emitters, either accidental or intentional. Another possible source of interfering EHF signals lies in the harmonics of high power C-band and X-band radars. These harmonic signal levels can be of sizeable magnitudes and the antennas from which they are radiated are quite often pointed skyward. In general, however, the signal density in the EHF band is several orders of magnitude less than the signal density in the present SHF communication links.

In communication systems, where meduim or synchronous altitude satellites are used to relay information from one point on the earth's surface to another, several hardware areas also require concentrated attention. Directional millimeter wave satellite antennas are needed to provide increased receiving aperture and increased transmitting gain to overcome the penalties of atmospheric attenuation and fading. Likewise, more investigation into larger receiving apertures for the ground terminals are required. Unlike radio telescope antenna systems which operate only in good weather, the communications systems must have an all weather capability.

Turbulent atmospheric conditions, as well as antenna surface errors, seriously limit the maximum receiving aperture size, especially in the power-starved space-to-earth communication links. If suitable propagation data is available, it may be possible to design millimeter wave multiple reflector antenna systems which avoid the large reflector mechanical problems and automatically restore loss in antenna gain due to wavefront distortion from atmospheric inhomogeneities. These antenna arrays would employ self-adaptive techniques which would compensate for random phase fluctuations.

For all applications, of course, more stable, efficient and space-worthy millimeter wave sources are required. For satellite communication systems, millimeter wave ground transmitters must be developed which are comparable in output power level to that of present lower frequency systems. Since radio telescopes have requirements for low noise receivers, it appears that this area of hardware technology has received attention for some time and therefore is not as critical as the other areas.

Thus, there are many possible operational advantages to be obtained from aerospace communication links at EHF. However, the EHF band has not received anywhere near the attention that the SHF band has received and, consequently, the EHF band got a late start and has been developing at a much slower pace than the SHF band. However, various Government agencies are now encouraging the development of the EHF state-of-the-art and considerable information and capability is being developed.

Section 3
MILLIMETER-WAVE CHANNEL CHARACTERISTICS

A systematic procedure for evaluating performance capabilities and limitations of communication links is best initiated by formulating a mathematical model of the channel itself. A general model for a communications channel which represents the physical processes associated with propagation effects is presented. The ideal waveforms for determining the characteristics of such a channel model is included in the discussion.

Following the general model, mathematical definitions of the channel characteristics is given which apply to any communication channel. The effects of the atmosphere on these channel characteristics at millimeter-wave frequencies is given in Section 4. The basic measurements which must be obtained in order to describe these effects are given in Section 5 and finally in Section 11, the mechanics of processing the basic measurements are presented.

3.1 The General Model

It must be emphasized that the presentation of this general model is only an attempt to provide an understanding of the basic physics involved and, that an experimental measurements approach based on this model would clearly not be the most effective nor expedient method for two reasons. First, it is not clear that it is feasible to carry out measurements of the properties of the channel to the degree of fineness necessary in such a model. Second the complexity of the descriptive relationship of the processes may not permit exact solution, and mathematical approximation that may have to be made might compromise the validity of results to such an extent where it becomes necessary to carry out an experimental program for their substantiation anyway. It is better therefore to employ a semi-empirical phenomenological

model whose parameters can be adjusted on the basis of experimental measurements which describes the propagation effects directly.

3.1.1 Mathematical Model

To obtain the form of the general model, consider the most general type of communications channel. It will be comprised of many paths through which the signal can propagate from the transmitter to the receiver as shown in Figure 3-1. These paths will have different delay times. One can group together the paths which have nearly the same delay to within some $\Delta\tau$. Thus, the ith path is made up of a set of subpaths whose delays are all within $\Delta\tau$ of each other. The signal propagating through this ith path will thus be composed of the sum of delayed versions of the transmitted signal. In a communications channel, the values of the subdelays vary in a random manner. As a result, the signal received from the ith delayed channel will be composed of the sum of vectors having arbitrary phases which vary

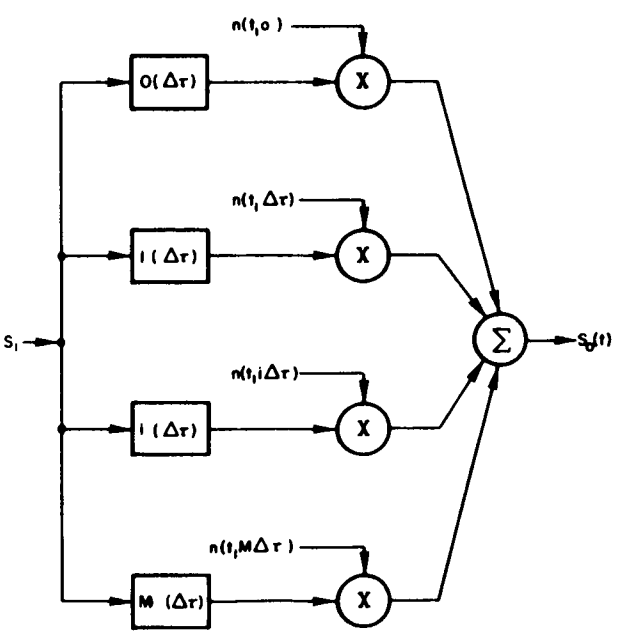

Figure 3-1 Communication Channel Model

randomly and will consequently introduce fading onto the signal from the ith channel. This fading or scintillation is generally Rayleigh distributed. Figure 3-1 characterizes such a communication channel in terms of a delay line network. The noise voltage $n_i(t)$ multiplying the signals of the ith channel introduces the fading or, equivalently, the scintillation of the signal. These noise voltages could be independent or dependent. In this model, it is assumed that there are delay paths having delays from 0 to T in steps of $\Delta\tau$. If one of the delay paths did not actually exist, the modulation voltage would be zero.

The model given in Figure 3-1 represents the general form of any time-variable stochastic network.[1] This model characterizes a communications channel having flat fading (which occurs for any narrow band communications channel) and one having frequency selective fading.[2, 3]

The above model, however, does not take into account the variations of the path with frequency, that is, a system having frequency dispersion. Nor does it take into account the possibility that the scintillation may depend on the signal frequency and also on the delay path. To extend the above model to include frequency dispersion and the possibility of a dependence of the scintillation on frequency, each path of the model shown in Figure 3-1 should include a bank of narrow band filters followed by noise modulators and a summer as shown in Figure 3-2.

Other characteristics of the communications channel of interest which are not included in the above model are the dependence of the received signal on the antenna's:

1) Spatial location
2) Pointing angle
3) Polarization

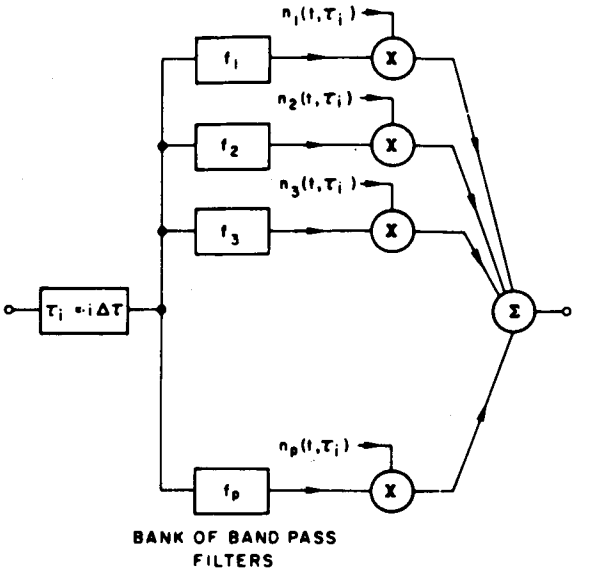

Figure 3-2 Model for ith Delay Path

As shall be shown later, these factors are the bases of diversity techniques for compensating the degradation due to the presence of multiple channels in the communications path.

On the basis of the above model, it can be established that certain specific data must be derived, based on measurements, to fully characterize the channel with regard to its influence on signal propagation. This will be discussed in the following section.

3.1.2 Ideal Waveform Requirements

From the general discussion above, the optimum signal for determining the characteristics of the communications channel is seen to be one which indicates the number of paths, the delay τ_i of each path and the auto-correlation function or equivalently the power spectral density function of the scintillation introduced into the signal by each path. This problem is

similar to the radar problem in which one desires to measure range and doppler velocity simultaneously. Accordingly, as in the radar case, the optimum signal for obtaining the channel characteristics is generally a signal having a noise-like structure.[4] That this is indeed the case was shown by a mathematical proof given in Appendix III of the First Quarterly Report.

Signals having a simple rectangular structure are suggested. Such signals have certain capabilities and limitations in measuring channel characteristics.

First, consider the transmission of a single narrow pulse which has a width less than $\Delta\tau$. This signal will enable one to determine the number of multipaths and delays of each multipath. However, it will not permit the determination of the spectrum of the scintillation introduced by each path. To obtain the power spectral density of the scintillation introduced by each path, a train of such pulses having equal spacings between them could be used if certain conditions are met. In particular, these conditions are: the spacing between pulses must be greater than the difference in the delay between the shortest delay path and the longest delay path and, at the same time, the bandwidth of the scintillation must be less than one over the spacing between samples. The first requirement permits unambiguous resolution of the different delay paths. The second requirement allows the unambiguous measurement of the scintillation spectrum since the sampling rate is higher than the bandwidth of the scintillation. If these conditions cannot be met, that is, if the reciprocal of the bandwidth of the scintillation is greater than the maximum difference in delay, then the ambiguities will not be resolved in the determination of the scintillation spectrum of unambiguous path resolution is to be obtained. Assuming conditions are met and the above signals are used, the pulses would be processed coherently in the receiver.

3.2 Definition of Channel Parameters

A pictorial display, provided by Green[5], which shows the functions of a single channel to be defined as well as their interrelationships, is given in Figure 3-3. A second pictorial display showing the functional relationships between two spatial channels is given in Figure 3-4. An explanation of each of the single and dual channel functions now follows.

3.2.1 The Two-Dimensional Correlation Function

The Two-Dimensional Correlation Function for a single spatial channel is an important quantity characterizing the millimeter channel. This function is measured by those experimentors who measure fading and fading statistics and it has direct application to the design of communication systems using frequency diversity. The importance of this function is discussed by Green[5], Gallagher[6], and Price and Green[7].

The following quantities may be determined directly from the two-dimensional correlation function, $R(\Delta f, \Delta t)$: the coherence time and the coherence bandwidth of the channel; the duration of fades; the Echo-Correlation Function, $R(\Delta t)$; and the Spaced-Frequency Correlation Function, $R(\Delta f)$. Moreover, the Scattering Function, $\sigma(\tau, f)$, which is the two-dimensional Fourier Transform of $R(\Delta f, \Delta \tau)$, provides direct information regarding doppler and multipath spreading by the channel.

That $R(\Delta f, \Delta \tau)$ and $\sigma(\tau, f)$ are important is demonstrated by the fact that $\sigma(\tau, f)$ can be used to determine the probability of error in deciding which of m waveforms has been transmitted through the channel[8, 9, 10]. The function, $\sigma(\tau, f)$ also arises in the consideration of optimum analog communication systems and bounds on their performance[11].

For the purposes of investigating the physical significance of the various quantities associated with $R(\Delta f, \Delta \tau)$ and $\sigma(\tau, f)$, the observations of Green[5] and Gallagher[6] are summarized.

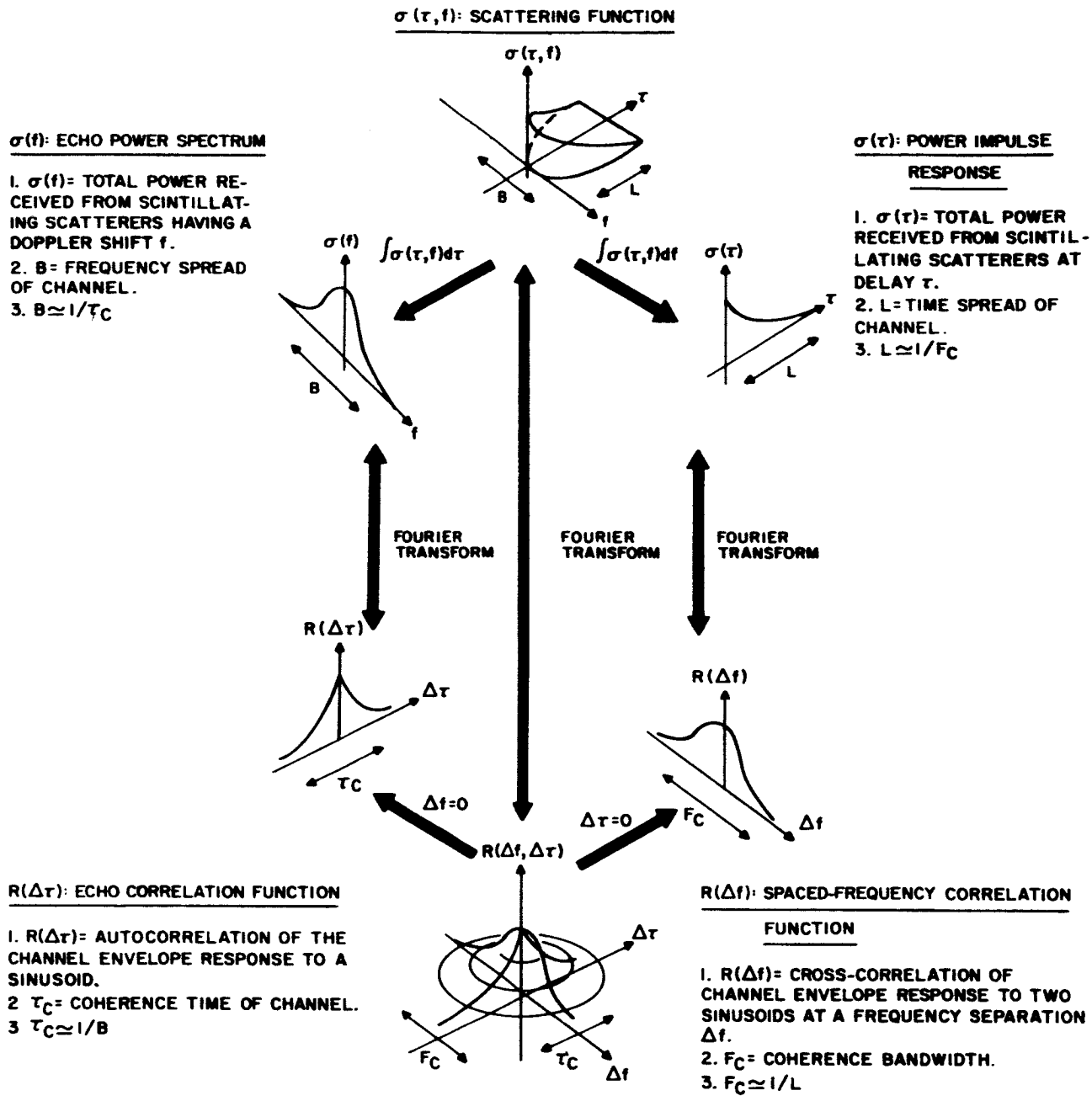

Figure 3-3. Functional Interrelationship of a Single Spatial Channel

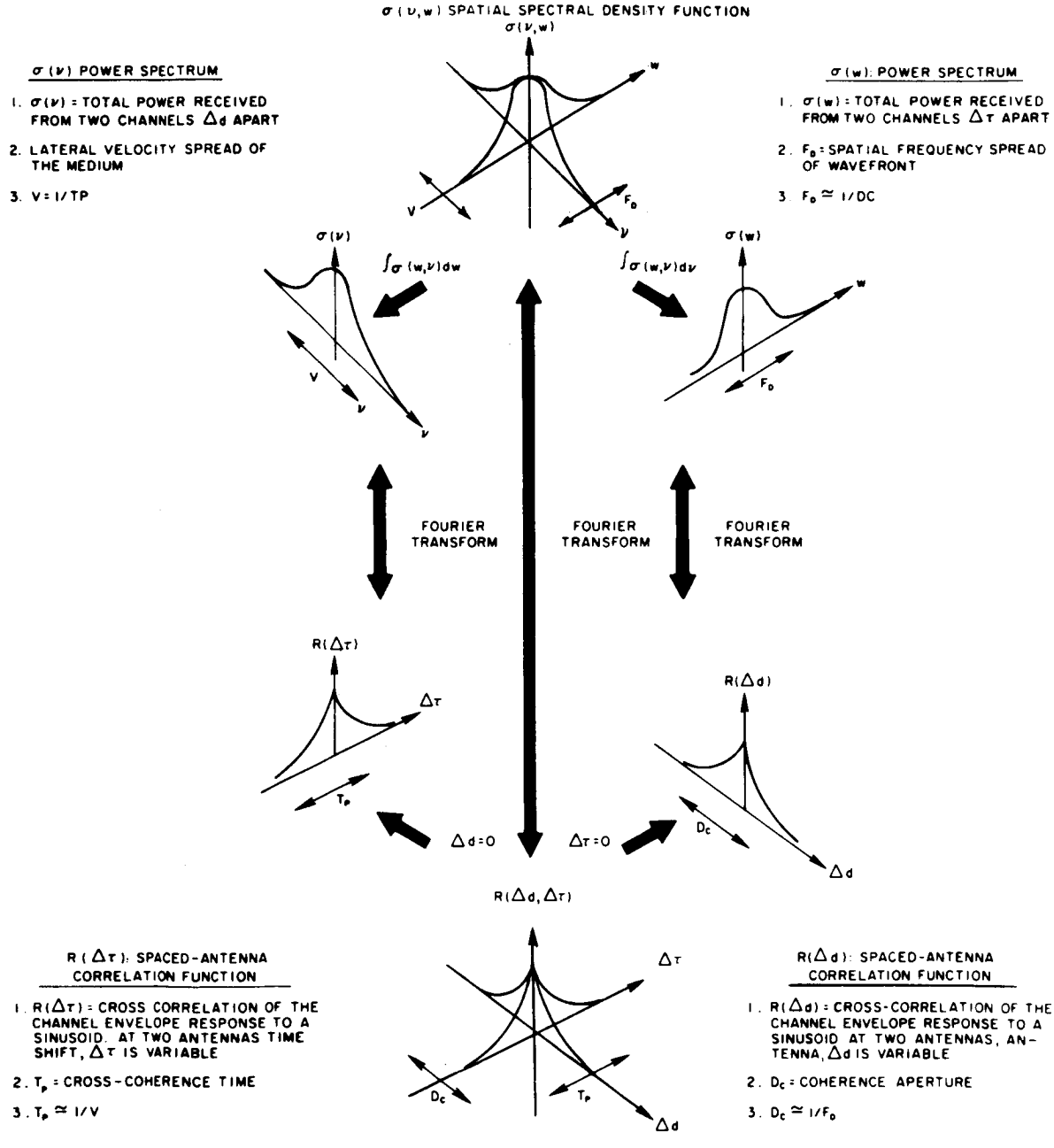

R(Δd), Δr): Two-Dimensional Spatial Correlation Function

Figure 3-4. Functional Relationships Between Two Spatial Channels

The time-frequency-spread channels under considerations have the property that a transmitted sinusoid is received as a narrow-band random process. That is, a transmitted signal of the form:

$$s_t(\tau) = \mathrm{Re}\left\{ e^{j2\pi f \tau} \right\} \tag{3-1}$$

is received as

$$s_r(\tau) = \mathrm{Re}\left\{ \tilde{s}_r(f,\tau)\ e^{j2\pi f \tau} \right\}, \tag{3-2}$$

where $\tilde{s}_r(f,\tau)$ is the complex envelope of the received signal; since $s_r(\tau)$ is narrow-band, the envelope of the received signal is $\left| \tilde{s}_r(f,\tau) \right|$ where $\tilde{s}_r(f,\tau)$ may be interpreted as a randomly-varying transfer function.

The Two-Dimensional Correlation Function is defined in terms of complex envelopes by:

$$R(\Delta f, \Delta\tau) = E\left\{ \tilde{s}_r^{\,*}\left(f - \frac{\Delta f}{2}, \tau\right) \tilde{s}_r\left(f + \frac{\Delta f}{2}, \tau + \Delta\tau\right) \right\}, \tag{3-3}$$

where "E" signifies taking the expected value of the bracketed quantity and "*" indicates complex conjugate.

In order to interpret $R(\Delta f, \Delta\tau)$, we closely follow Gallagher[6] and consider $R(o, \Delta\tau)$ and $R(\Delta f, o)$ separately.

Referring to Equation (3-3), $R(o, \Delta\tau)$ is seen to be the auto-correlation function of the complex envelope of the channel response to an input sinusoid of frequency f cps. This autocorrelation function, $R(\Delta\tau) = R(o, \Delta\tau)$, is called the "Echo-Correlation Function," it provides coherence time and fading duration information.

The coherence time of the channel, τ_c, is loosely defined as the range in $\Delta\tau$ over which $R(\Delta\tau)$ is non-zero. Very often τ_c is taken to be the solution to:

$$R(T_c) = 1/2\ R(o). \qquad (3\text{-}4)$$

The fact that $R(\Delta t)$ approaches zero largely results from fading in the channel. τ_c is related, therefore, to the duration of fades.

Again referring to Equation (3-3), $R(\Delta f, o)$ is seen to be the cross-correlation function of the complex envelope of the channel response to a sinusoid at $f - \frac{\Delta f}{2}$, cps. with the complex envelope of the response to a sinusoid at $f + \frac{\Delta f}{2}$. The cross correlation function, $R(\Delta f) = R(\Delta f, o)$, is called the "Spaced-Frequency Correlation Function;" it provides coherence bandwidth information.

The coherence bandwidth, F_c, of the channel is loosely defined to be the range in Δf over which $R(\Delta f)$ is non-zero. If frequency diversity modulation schemes are used to transmit information, the F_c is a measure of how far apart the separate channels must be in order to receive uncorrelated signals on each.

If a signal of bandwidth W, centered around f, is transmitted and W is such that $R(W, o) \simeq R(o,o)$, then the received signal will be the same as the transmitted signal except for an overall amplitude and phase that change over a period of time which is on the order of τ_c. Conversely, if $R(W,o) \simeq o$, the amplitude and phase of different frequency components of the input signal will be changed relative to each other, and the received waveform will no longer bear a simple resemblance to the transmitted waveform.

If $R(\Delta f, \Delta \tau)$ is unimodal, the τ_c is approximately the reciprocal of the doppler spreading and F_c is approximately the reciprocal of the time spreading of the channel.

3.2.2 The Scattering Function

The channel scattering function, which is the two-dimensional Fourier transform of the correlation function, is directly applicable to communication system design. The scattering function, $\sigma(\tau, f)$ has a convenient physical interpretation; it represents the power received from a scintillating scatterer at delay τ and doppler shift f.

Consider the two functions, $\sigma(f) = \int \sigma(\tau, f)\, dt$ and $\sigma(\tau) = \int \sigma(\tau, f)\, df$, separately. $\sigma(f)$ is called the "Echo Power Spectrum" and $\sigma(t)$ is called the "Power Impulse Response."

The scattering function represents the total power received from all scatters producing a doppler shift of f cps. The doppler spread of the channel, B, is loosely defined to be the range in f over which $\sigma(f)$ is non-zero. As previously mentioned, if $\sigma(\tau, f)$ and $R(\Delta f, \Delta \tau)$ are well behaved, then $B \simeq 1/\tau_c$.

The functions, $\sigma(\tau)$ represent the total power received from all scatterers at a delay τ. The time spread of the channel, L, is loosely defined to be the range in τ over which $\sigma(\tau)$ is non-zero. If $\sigma(\tau, f)$ and $R(\Delta f, \Delta \tau)$ are well behaved, then $L \simeq 1/F_c$.

The Echo-Correlation Function, $R(\Delta \tau)$, is the Fourier Transform of the Echo Power Spectrum, $\sigma(f)$, and the Spaced-Frequency Correlation Function $R(\Delta f)$, is the Fourier Transform of the Power Impulse Response, $\sigma(t)$.

3.2.3 The Modified Two-Dimensional Correlation Function

A frequently measured quantity, which has no simple relation to $R(\Delta f, \Delta\tau)$, is a modified two dimensional correlation function. The modified function, which is denoted by $\hat{R}(\Delta f, \Delta\tau)$, is defined in terms of the channel envelope response by:

$$\hat{R}(\Delta f, \Delta\tau) = 2E\left\{\left|\tilde{s}_r\left(f - \frac{\Delta f}{2}, \tau\right)\right|\left|s_r\left(f + \frac{\Delta f}{2}, \tau + \Delta\tau\right)\right|\right\} \tag{3-5}$$

Since $\hat{R}(\Delta f, \Delta\tau)$ depends on the envelope of the channel response, rather than the complex envelope, it is insensitive to phase fluctuations, and therefore provides less information than $R(\Delta f, \Delta\tau)$. $\hat{R}(\Delta f, \Delta\tau)$ is used in practice because of the relative ease in measuring it compared to measuring $R(\Delta f, \Delta\tau)$, (by 14). Associated with $\hat{R}(\Delta f, \Delta\tau)$ is a complete set of quantities; $\hat{R}(\Delta f)$, $\hat{R}(\Delta\tau)$, $\hat{\tau}_c$, $\hat{F}_c$, $\hat{\sigma}(\tau, f)$, etc., each of which is defined, in a parallel fashion, to its counterpart associated with $R(\Delta f, \Delta\tau)$.

3.2.4 The Two-Dimensional Spatial Correlation Function

The two-dimensional correlation function for two parallel spatial channels receiving the same signal will provide the communication system designer with information on spatial diversity, limitations of atmosphere on antenna size, and the physical structure of the propagating medium. The correlation function is obtained by receiving a single sinusoid at two receivers separated by a distance (Δd) and correlating them with time shift ($\Delta\tau$).

The two-dimensional spatial correlation function, $R(\Delta d, \Delta\tau)$ which is shown in Figure 3-4 is defined by:

$$\hat{R}(\Delta d, \Delta\tau) = 2E\left\{\tilde{s}_r^*\left(d - \frac{\Delta d}{2}, \tau\right)\tilde{s}_r\left(d + \frac{\Delta d}{2}, \tau + \Delta\tau\right)\right\} \tag{3-6}$$

which is analogous to the two-dimensional correlation function given in Equation 3-3).

The coherence aperture, D_c, of a channel is loosely defined as the range in Δd over which $R(\Delta d)$ is non-zero. If very large antennas are to be used in a communication system D_c is an important measure of the maximum diameter aperture which can be efficiently employed. In situations where space diversity schemes are being considered as a means of enhancing channel reliability, D_c is a measure of antenna separation required in order to receive uncorrelated signals. When Δd is zero and $\Delta\tau$ is variable, the two-dimensional spatial correlation function becomes the echo correlation function for a single channel. In Figure 3-4, D_c is thought of in seconds, that is, the coherence distance (in units of length) divided by the speed of propagation.

The cross coherence time, T_p, is loosely defined as the range in $\Delta\tau$ over which $R(\Delta\tau)$ is non-zero. $R(T_p)$ is often referred to as $1/2\ R(o)$. If $R(\Delta\tau)$ is maximum at some point other than $\Delta\tau = 0$, it indicates that the relative structure of the atmosphere has remained essentially unchanged as it moves a certain distance (Δd).

3.2.5 The Spatial Spectral Density Function

The dual channel spectral density function, $\sigma(v,w)$, which is the two-dimensional Fourier Transform of the spatial correlation function, is useful in understanding the physical structure of the atmosphere.

The spatial frequency spread, F_D, is loosely defined to be the range in wavefront frequency W over which $\sigma(w)$ is non-zero. If $\sigma(w,v)$ and $R(\Delta d, \Delta\tau)$ are well behaved, then $F_D \simeq {}^{1}/_{D_c}$. In other words, the larger the coherence aperture, the narrower the spatial spectrum of the wavefront. When D_C is expressed in seconds, F_D becomes cycles per second.

The lateral velocity, V_s is loosely defined as the velocity of the propagating medium across a distance (Δd); and it is the range of the lateral velocity v over which $\sigma(v)$ is non-zero. If $\sigma(w, v)$ and $R(\Delta d, \Delta \tau)$ are well behaved, then $V \simeq 1/T_p$ (in cycles per second). When multiplied by Δd in units of length, V is expressed in linear velocity dimensions.

3.2.6 The Modified Two-Dimensional Spatial Correlation Function

In simpler experiments, a modified spatial correlation function, $\hat{R}(\Delta d, \Delta \tau)$, is usually measured. It is defined in terms of the envelopes of the received signals by:

$$\hat{R}(\Delta d, \Delta \tau) = 2 E \left\{ \left| \tilde{s}_r \left(d - \frac{\Delta d}{2}, \tau\right) \right| \left| \tilde{s}_r \left(d + \frac{\Delta d}{2}, \tau + \Delta \tau\right) \right| \right\} \tag{3-7}$$

The function $\hat{R}(\Delta d, \Delta \tau)$ provides no information about decorrelation effects due to phase fluctuations because of the use of only amplitude envelopes rather than complex envelopes.

Section 4
PROPAGATION OF MILLIMETER WAVES

The potential of millimeter-waves in space-earth communications cannot be fully assessed until the effects of the atmosphere on millimeter-wave propagation are well understood. This section describes these effects as they are known today. It discusses the effects of atmospheric water vapor, rain and oxygen on attenuation of millimeter waves, atmospheric noise generation and atmospheric refraction. Considerable effort has been made to estimate the effects of atmospheric turbulence on fading, coherence bandwidth, integration time limitations and antenna aperture limitations. A brief review is given on effects of rain on antennas and radomes and the propagation of millimeter waves through plasma.

4.1 Atmospheric Attenuation

In the millimeter wave region of the spectrum, the atmosphere produces attenuation through resonance absorption of its constituent gases. This attenuation is determined principally by oxygen and water vapor. Prominent water vapor peaks occur at 22 Gc, 184 Gc, and 324 Gc, and there are approximately 150 water lines in the submillimeter region. A cluster of oxygen lines occurs at both 60 Gc and 118 Gc. Since this study was primarily concerned with space-earth communications channels, the atmospheric "windows" at 16 Gc, 35 Gc and 94 Gc received most of the attention and therefore dominates the discussion in this section on atmospheric attenuation. Only a brief review of attenuation in the oxygen absorption region is given.

4.1.1 Attenuation Due to Water

Millimeter wave signals are subject to attenuation from fog, rainfall, snowfall, and the melting layer or "bright band." Figure 4-1 shows the water vapor attenuation at sea level and four altitudes above sea level.[12]

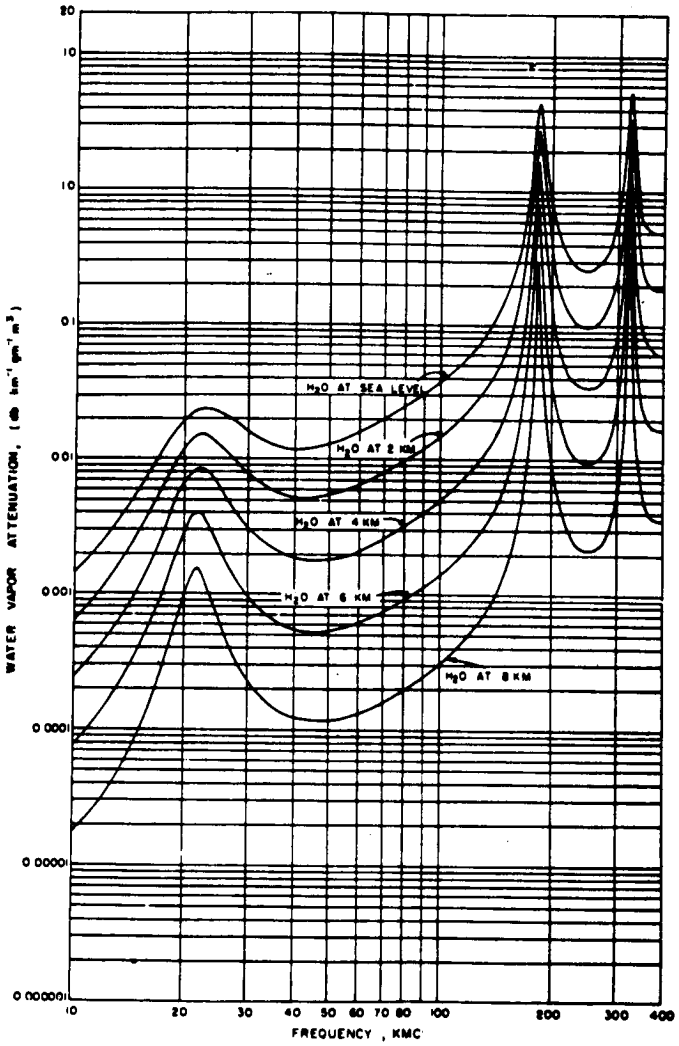

Figure 4-1 Attenuation Due to Water Vapor at Five Elevations

Theoretical models of rainfall attenuation based on experimental data indicate that attenuation per unit length is directly proportional to rainfall rate. Attenuations for various rates of rainfall in the microwave and millimeter-wave region are shown in Figure 4-2. Attenuation for clouds and fogs are shown in Figure 4-3.[13, 14]

The primary purpose of this portion of the study was to determine how the specific weather conditions, which prevail at the locations of existing and planned millimeter-wave facilities, affect the design and conduct of the communication propogation experiments. The existing experimental facilities which might participate in this program were assumed to be those located at Aerospace Corporation, El Segundo, California; University of Texas, Austin, Texas; Air Force Cambridge Research Laboratories and MIT, Lincoln Laboratory near Lexington, Massachusetts. A planned facility for GSFC at Greenbelt, Maryland, was also included. The nearby cities whose available weather statistics are considered to be representative of conditions at these sites were: Los Angeles, Austin, Boston, Washington and Baltimore.

Computed values of apparent sky temperature and atmospheric transmission factors for the range of weather conditions expected at these four sites showed no significant variation between sites or for weather changes at a particular site. Based on the obvious factors of rainfall rate, temperature, and relative humidity, certain generalizations can be made about the design and conduct of the communication experiment. For example, measurements made during a one month period in the Boston area seem to give all the necessary data about atmospheric and weather effects. In addition, it will be shown that the percentage of time during a year in which the rainfall rate, R, is equal to or greater than 0.2 inches per hour is approximately the same for the four cities that were analyzed even though the total annual rainfall varies by a factor 3:1.

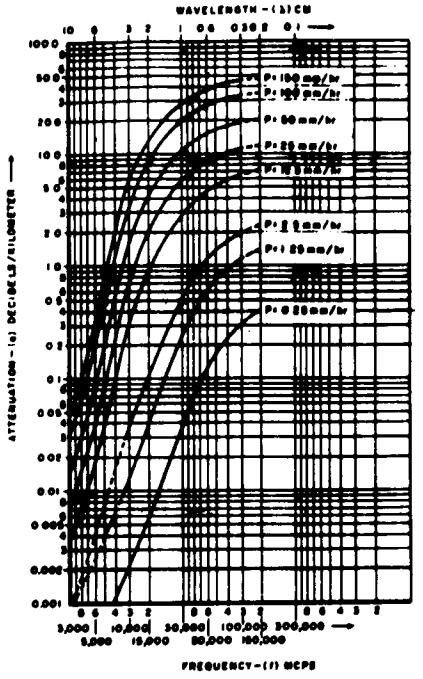

Figure 4-2 Rainfall Attenuation vs Frequency for Various Precipitation Rates

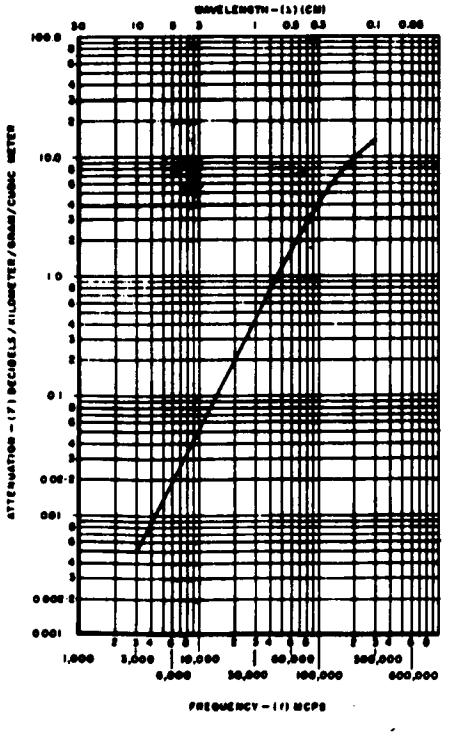

Figure 4-3 Attenuation Due to Clouds of Fog

Basic data was obtained from the U.S. Weather Bureau,[15, 16] from which profiles of surface temperature, relative humidity, rainfall rates, and rainfall intensity/duration were generated. Some of this data is tabulated in Table 4-1. Climatological summaries are given for each city in Section 9 under Geographical and Meterological Profiles. The water vapor content (ρ) data was obtained from equation (4-1).

$$\rho = \frac{2.17\ e \times 10^2}{T}\ f,\ \text{grams meter}^{-3} \qquad (4\text{-}1)$$

where

e is the saturated water vapor pressure in millibars from a standard characteristics diagram[17]

T is air temperature in ^{o}Kelvin, and

f is relative humidity in percent

Using the above weather data and a program for the Raytheon IBM-7044 digital computer, values of atmospheric transmission factor versus antenna elevation angle were computed for the four frequencies 16, 35, 70, and 94 Gc for several weather models. Standard meteorological lapse rates for temperature and pressure versus altitude were used. The detailed results of the computations was given in Section 3.1 of the First Quarterly Report and the computer program which was used was described in Appendix II of the First Quarterly Report.

This investigation was intended to cover a representative range of seasonal and diurnal conditions with more detailed calculations to be done after the first set was analyzed. It was discovered, upon analyzing the resulting data, that there is no apparent effect on the design or conduct of the experiment due to weather variances among the ground stations.

TABLE 4-1

LOCAL WEATHER DATA FOR FOUR SITES

Weather Factor (3)	Boston	Washington, D.C.	Baltimore (1)	Los Angeles	Austin
Temperature (°F)					
High	82	87	87	83	96
Low	23	30	30	46	40
Relative Humidity (%)					
High (2)	54	52	52	53	43
Low (2)	69	67	72	45	73
Annual Rain (inches)	42.8	40.8	44.2	14.7	32.6
Mean Days					
Clear	99	105	121	185	119
Partly Cloudy	106	105	123	107	113
Cloudy	160	155	121	73	133
Heavy Fog	24	14	15	17	23
Rain (4)	130	114	123	35	81
Sleet, Snow (5)	11	5	6	0	0
Thunderstorms	20	30	32	6	40
Water Vapor Content (g/m^3)					
High	11.5	19.1	18.8	14.7	18.8
Low	1.65	3.3	3.2	5.2	4.8

(1) Baltimore is included to help describe GSFC.
(2) Relative Humidity figures are associated with high and low temperature data. That is, high relative humidity number occurred at high temperature reading.
(3) All data based on 30 year records.
(4) Days on which .01 inch or more was recorded.
(5) Days on which 1.0 inch or more was recorded.

After completing the above analysis, a representative weather model was developed which was based upon consultation with and published material[18] by Dr. Atlas of AFCRL's Weather Branch.

Dr. Atlas and his associates have worked for years on the radar analysis of weather systems. As a result of this work they have developed curves which show how water vapor and rainfall rate vary with altitude. Their results are based on a dependence between updraft velocity and raindrop fall velocity and the moisture holding ability of the atmosphere at a given temperature and pressure. Based on their results and the surface conditions estimated for our work, the curves in Figure 4-4 were developed to serve as a representative weather model. The cloud condition represents a heavy cloud cover for a temperate zone area, and the rainfall rate corresponds to a surface rate of 0.2 inches per hour (5.2 mm per hour). The major difference between candidate ground stations is expected to be the number of days of heavy cloud cover and days of rain, as indicated in Table 4-1.

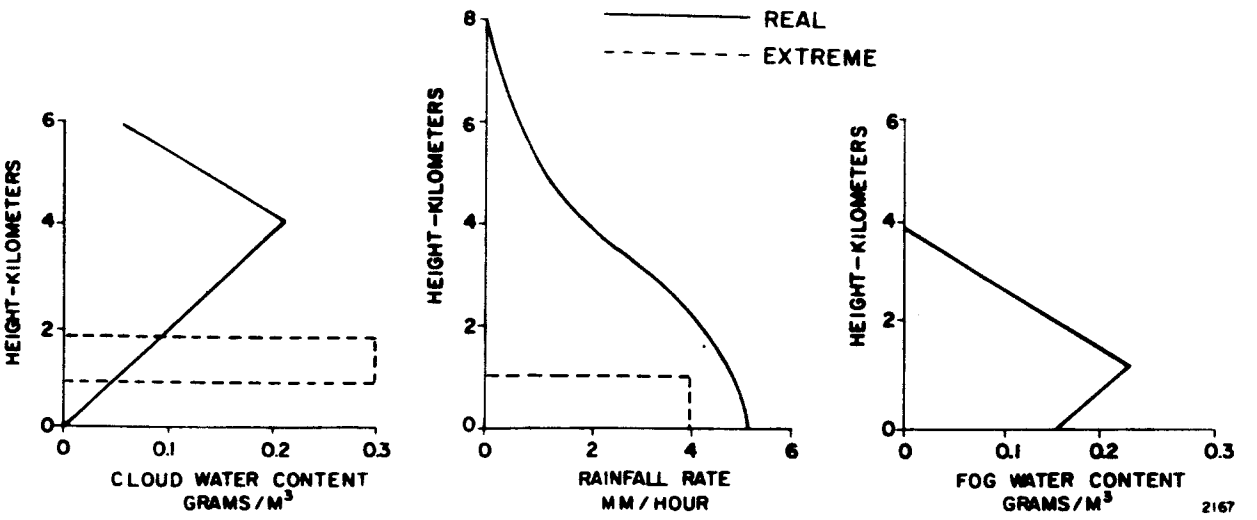

Surface Temperature = 300 Degrees Kelvin
Surface Pressure = 760 Millimeters

Figure 4-4 The Weather Model

This weather model was incorporated into the computer program and atmospheric attenuation as a function of elevation angle for 16 Gc, 35 Gc, 70 Gc and 94 Gc was derived for clear, cloudy (plus fog), and rainy (plus clouds and fog) weather conditions. The results of these calculations is given in Figures 4-5 through 4-8. Associated curves for apparent sky temperature are discussed in Section 4.2. This data show the expected results that atmospheric attenuation increases with increasing frequency and that there is a superimposed oxygen attenuation peak at frequencies near the oxygen absorption peak at 60 Gc.

U.S. Weather Bureau Technical Paper 40 [16] contains maps of the continental United States with iso-pluvial lines for rainfall duration from 30 minutes to 24 hours from data gathered over 1, 2, 5, 10, 25, 50, and 100 year periods. Data from these maps was extracted for the candidate ground station sites and is tabulated in Table 3-IV of the First Quarterly Report.

This data was used in conjunction with data from Table 4-1 and the method given in Reference 19 to develop the curves of Figure 4-9. A surface rainfall rate of 0.2 inches per hour was chosen from these curves as a design point. This is a rate which will be exceeded only about 45 hours per year (0.5 percent) at any one of the four candidate sites.

Figure 4-10, taken from Reference 19, shows the percentage time for exceeding a precipitation rate for rates of 0.06 in/hour, 0.12 in/hour, and 0.18 in/hour. The average daily rain is derived from Table 4-1 where values of annual precipitation and number of days with precipitation exceeding 0.1 inch are given for each site. The curves of Figure 4-10 are then used to find the percentage of time that the given rates will be exceeded. This given three points on each curve of Figure 4-9. A fourth point was established for the one hour position on each curve from the data in Reference (16) in the 1 hour-2 year set of data. This means

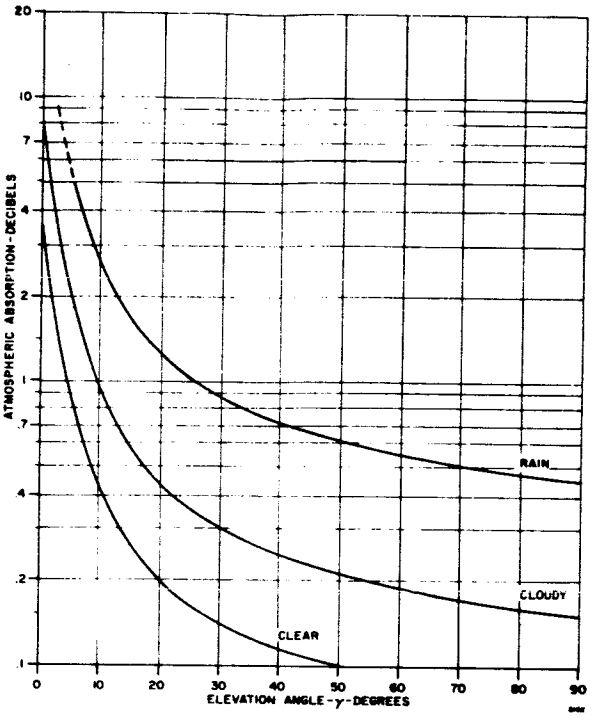

Figure 4-5. Atmospheric Absorption at 16 Gc

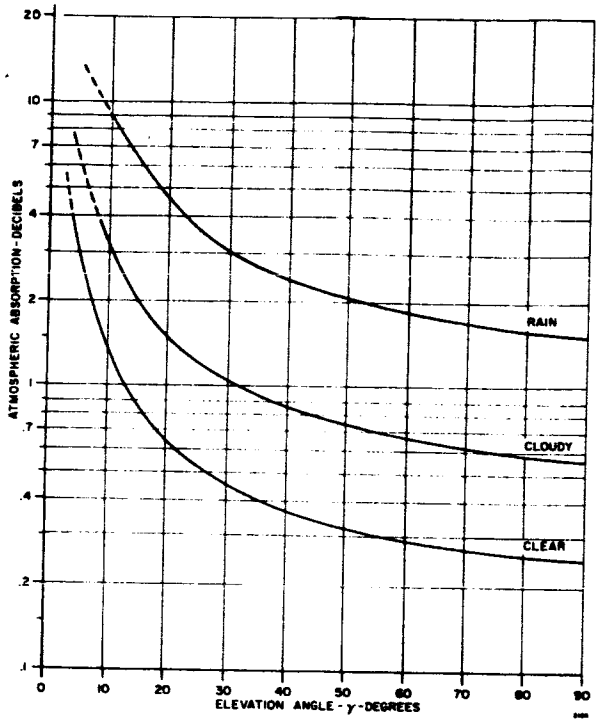

Figure 4-6. Atmospheric Absorption at 35 Gc

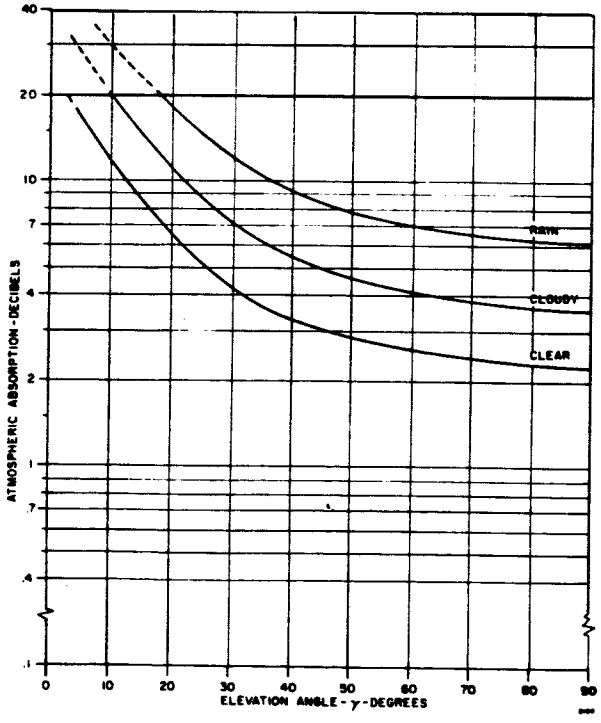

Figure 4-7. Atmospheric Absorption at 70 Gc

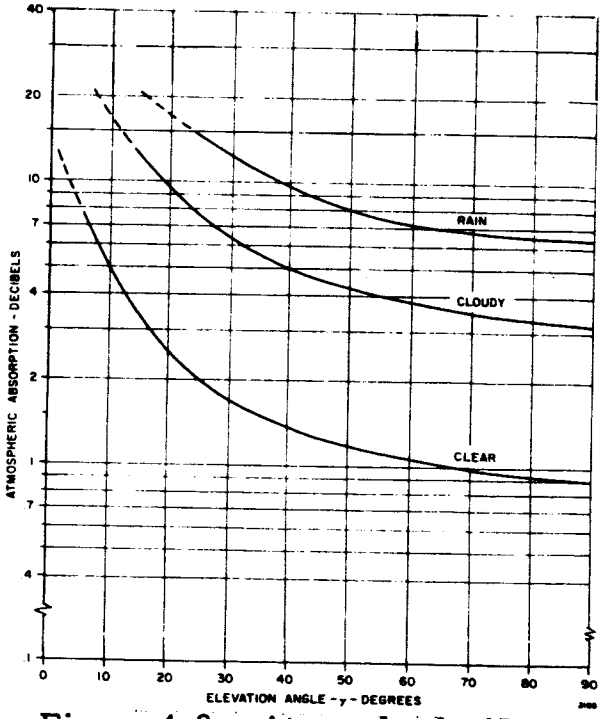

Figure 4-8. Atmospheric Absorption at 94 Gc

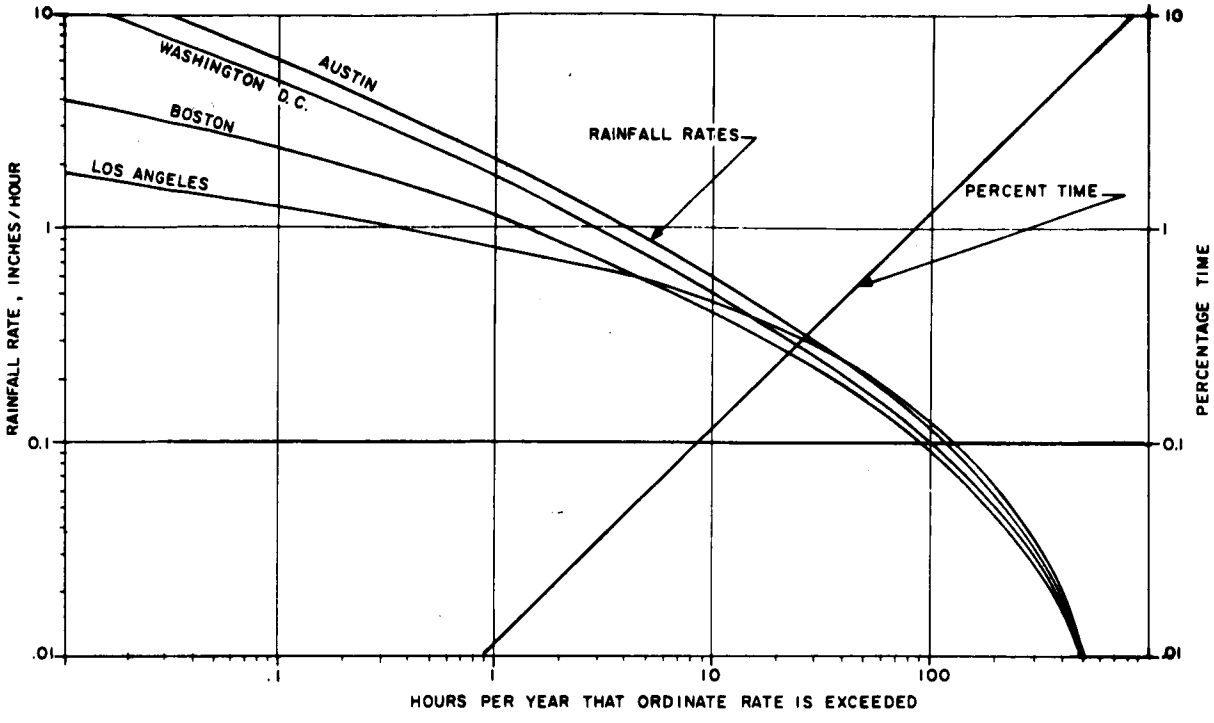

Figure 4-9 Frequency of Occurrence of Rainfall at a Given Intensity

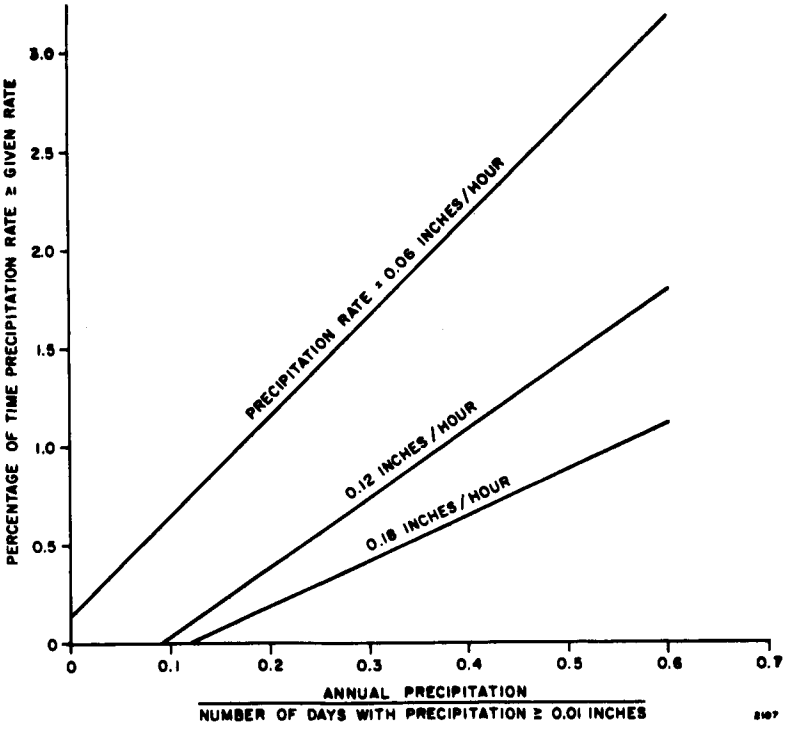

Figure 4-10 Precipitation Rate Occurrence Based on Annual Precipitation

that the curves in Figure 4-9 are subject to some error to the left of the 10 hour line, but in the area of the 40 hour line the error is negligible.

4.1.2 Attenuation Due to Oxygen

Satellite-to-aircraft experimental communication links are essential when investigating the effects of the atmosphere on the propagation of frequencies near the 60 Gc oxygen absorption region. The opacity of the atmosphere to frequencies near 60 Gc has been pretty well predicted. Meeks and Lilley[20] give detailed estimates of the limitations that oxygen places on millimeter-wave propagation. Straiton and Tolbert[12] have also investigated this band using a 500-foot absorption cell at the University of Texas. What is not completely predictable is the bandwidth that the propagation medium will support and the minimum useful horizon as a function of altitude. Experimental verification with satellite-aircraft communication links using special signal waveforms are required. Opacity per unit bandwidth can vary from 2 db per megacycle near a resonant frequency such as 60.44 Gc, to 0 db per megacycle near the adjacent window at 60.8 Gc. This can have drastic effects on the phase and amplitude characteristics of broadband communication channels.

In designing space-air experimental links operating in the 60 Gc oxygen absorption band, the required system analysis will be a bit different. From Meeks and Lilley horizontal and vertical attenuation due to oxygen is shown in Figure 4-11 and 4-12. Zenith opacity versus altitude, and opacity versus zenith angle, have been derived for 60.8 Gc and is shown in Figure 4-13 and 4-14.

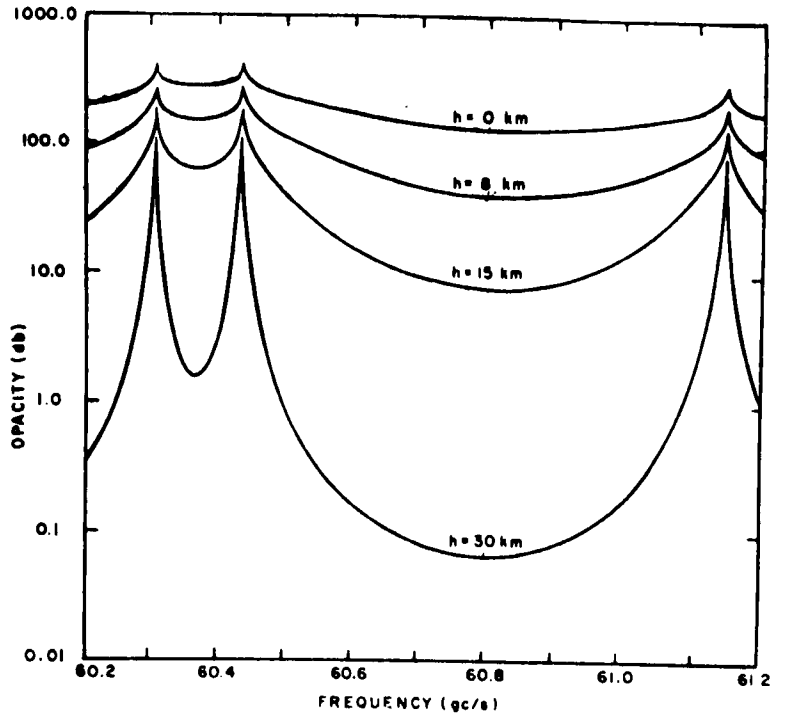

Figure 4-11. Horizontal Attenuation Due to Oxygen

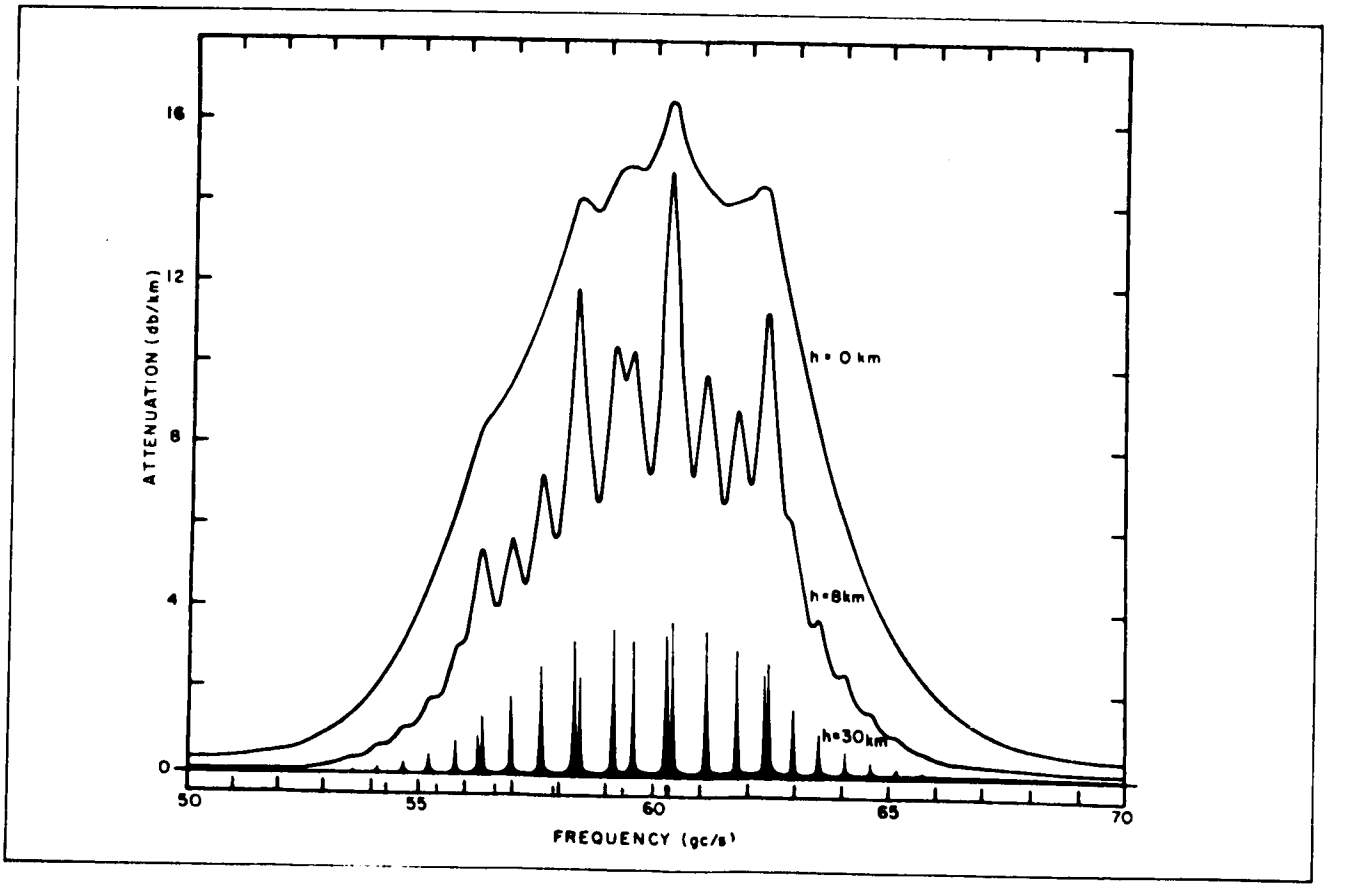

Figure 4-12. Vertical Opacity Due to Oxygen

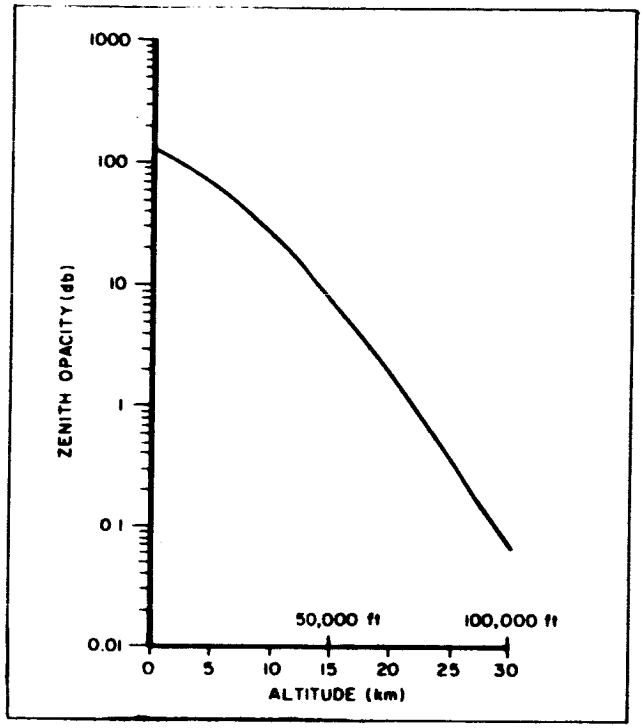

Figure 4-13. Zenith Opacity of the Atmosphere Due to Oxygen Absorption at 60.8 Gc.

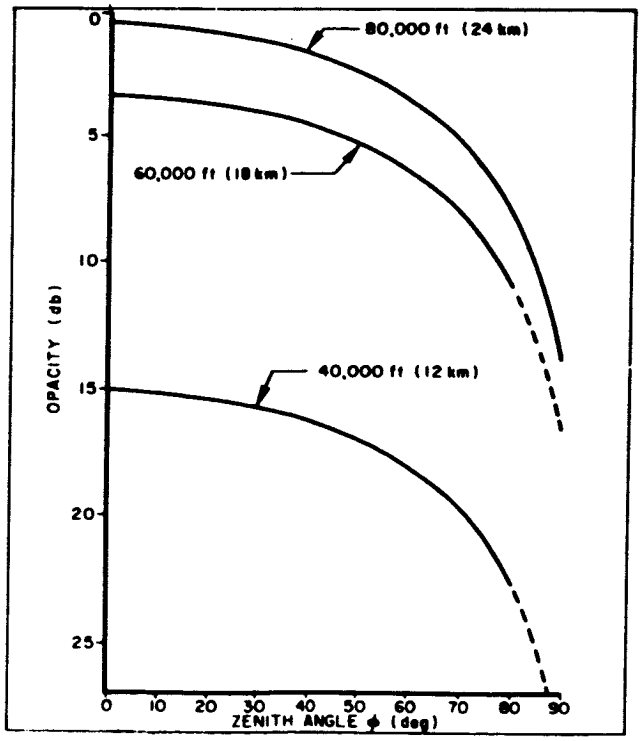

Figure 4-14. Opacity vs Zenith Angle Due to Oxygen Absorption at 60.8 Gc.

4.2 Atmospheric Temperature

In addition to atmospheric attenuation, another well known effect on propagation of millimeter waves is the additive noise received with the communication signals. The computer program mentioned in Section 4.1, was used to calculate the effect of this noise in the form of apparent antenna temperature based on the weather model in Figure 4-4. Temperature as a function of elevation angle for ground receivers in clear, cloudy and rainy weather is given in Figures 4-15 through 4-18 for frequencies of 16 Gc, 35 Gc, 70 Gc and 94 Gc. For spacecraft receivers the situation is different, for as long as the receiver antenna beam is subtended by the earth, the apparent temperature will be 290°K for all frequencies between 10 Gc and 100 Gc (see Figure 4-19). [12] The use of apparent antenna temperature data as a correlative measurements tool is explained in Section 5.2 "Basic Correlative Measurements".

4.3 Effects of Rain on Radomes and Antennas

Considerable attention has been given to the effects of water vapor and rain in the propagation medium between the earth terminal and the satellite. In millimeter wave communication systems, all weather operational capability is required and consideration of the effects of rain on the ground antenna installation itself is necessary. Until now these effects of rain have been largely overlooked.

Under normal operating conditions the effect on systems with radomes is much worse than that on antennas without radomes, providing, of course, that the antenna feeds are adequately protected. The transmission losses and reflection losses of the water film on a radome has been presented by Blevis[21]. His analysis was based on values for complex relative dielectic constant of water obtained by Grant, Buchanan and Cook[22], and certain mathematical treatments by Leaderman and Turner[23]. According to

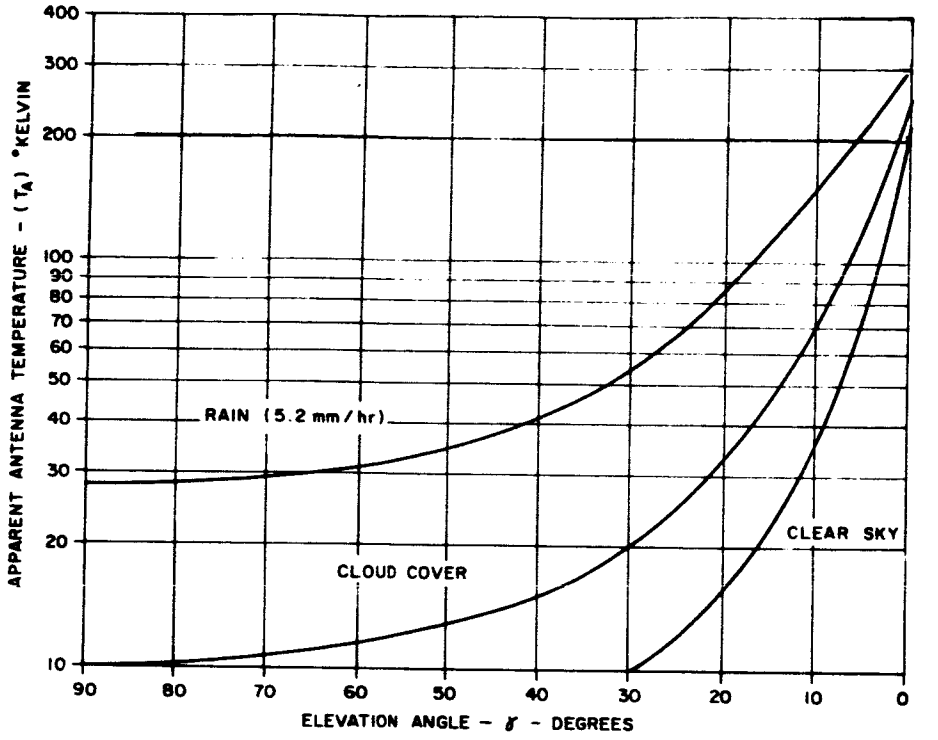

Figure 4-15 Apparent Temperature of the Atmosphere at 16 Gc

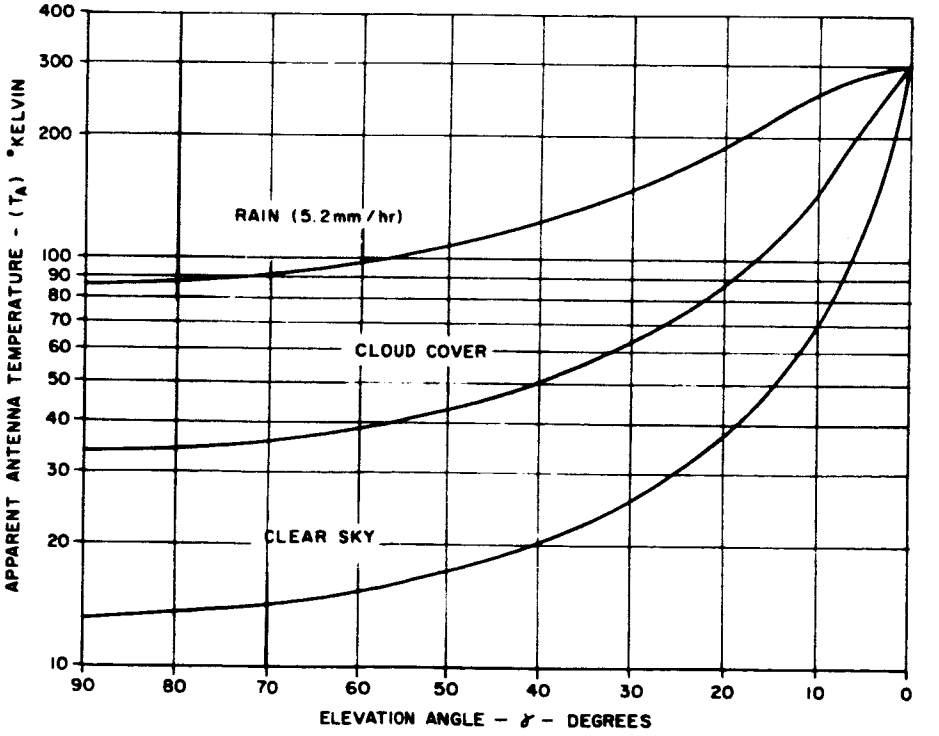

Figure 4-16 Apparent Temperature of the Atmosphere at 35 Gc

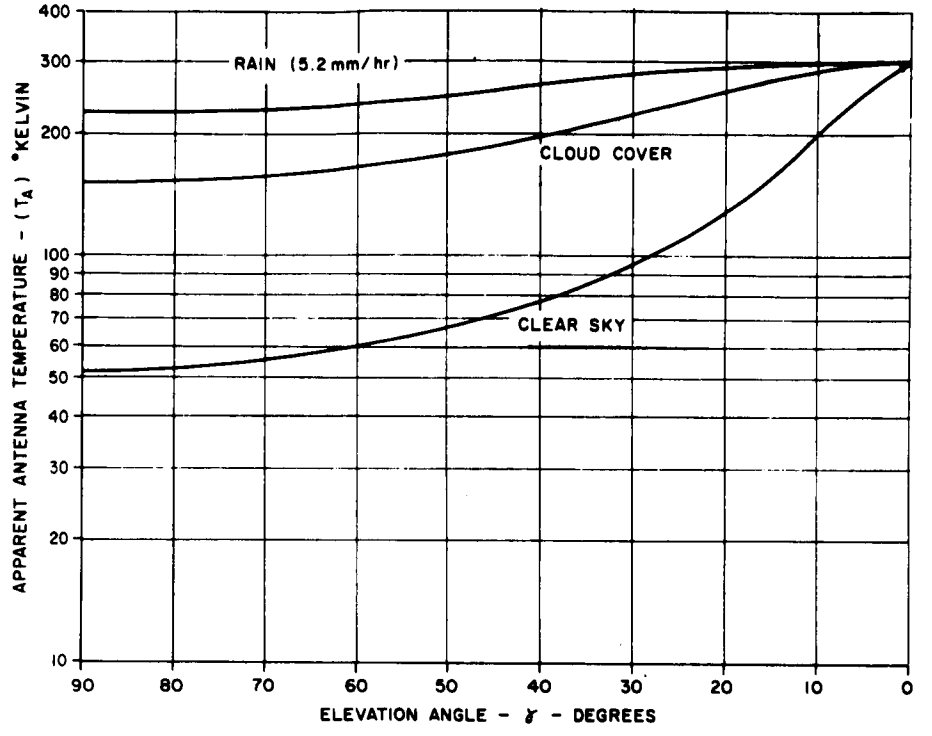

Figure 4-17 - Apparent Temperature of the Atmosphere at 94 Gc

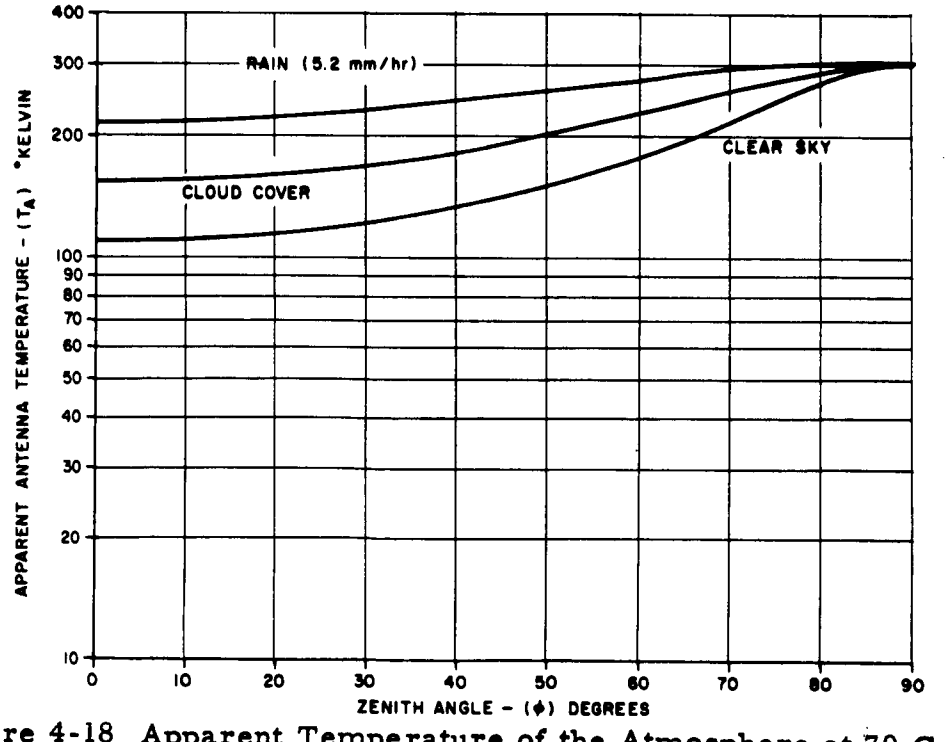

Figure 4-18 Apparent Temperature of the Atmosphere at 70 Gc

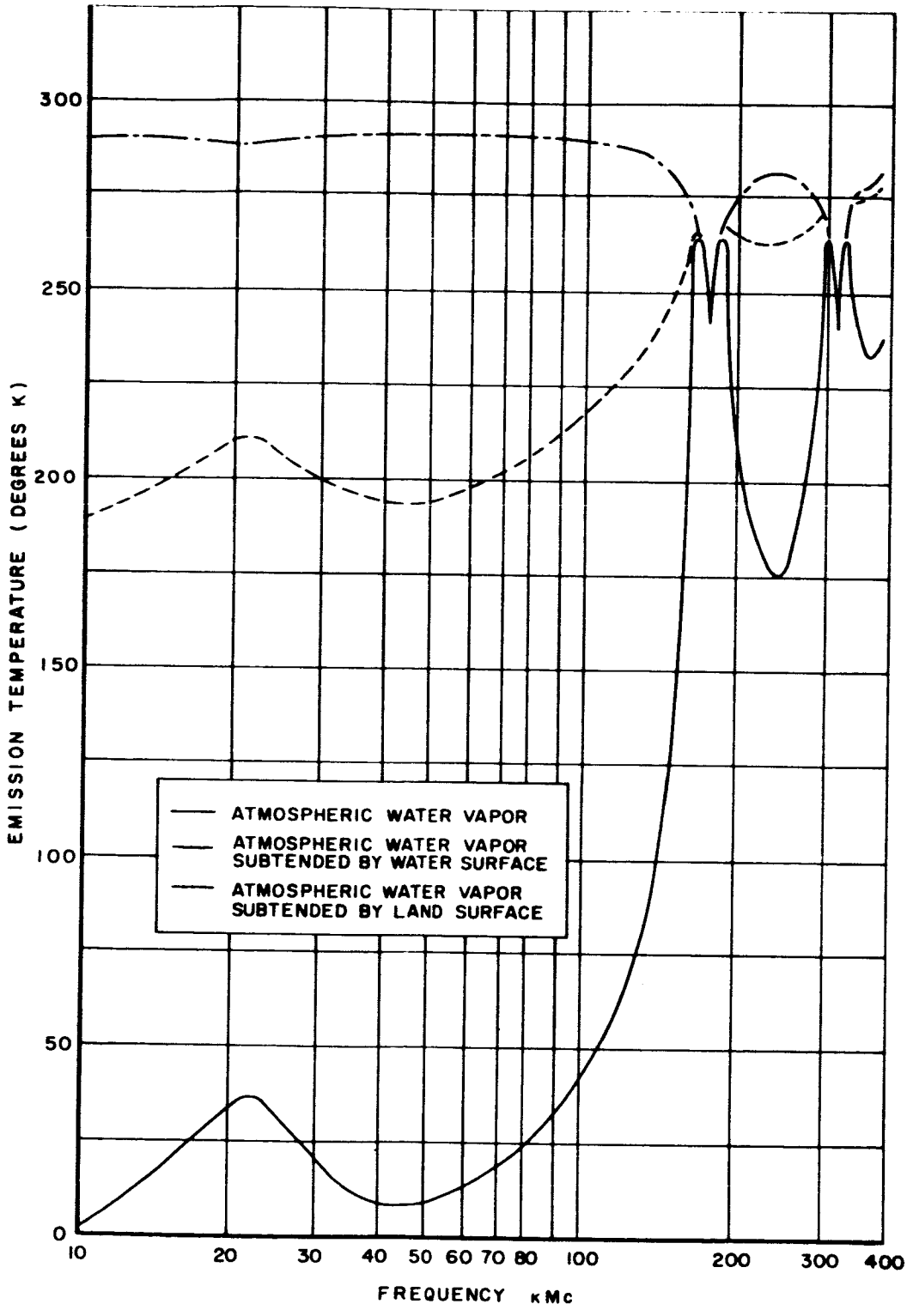

Figure 4-19 Calculated Emission Temperatures into Space from the Earth and its Atmospheric Water Vapor

Gibble,[24] there is an interesting approximation for water film thickness as a function of rainfall rate over a spherical radome:

$$d^3 = \frac{3}{2} \quad \frac{\mu r R}{W}$$

where

μ - viscosity of water
W - weight density of water
r - radius of the radome
R - rainfall rate

(4-2)

To illustrate the magnitude of the problem the water film thickness for a 25 foot radome and a 0.2 inch per hour rainfall was calculated using Equation (4-2). The thickness was 5×10^{-3} inches over the upper hemisphere of the radome, thus, according to curves in Reference (21) the transmission and reflection losses total 5.3 db for a frequency of 16.0 Gc and it appears that they might be 2 or 3 db more for a frequency of 35.0 Gc. The effects of increase in antenna noise temperature and degradation of antenna gain are other factors which must also be considered.

Since a rainfall rate of 0.2 inch per hour occurs 45 hours per year, about 0.5 percent of the time in most regions of the United States, then the effects of rain on antennas and radomes is of definite concern in the design of the propagation experiments and the use of the experimental results in designing communication systems.

4.4 Atmospheric Refraction

The use of millimeter wavelengths for earth-satellite communications is suggested by the large operating bandwidth, increased antenna gain, and smaller antenna beamwidths. Antenna systems operating with these smaller beamwidths demand positioning to a greater accuracy, thus the effects of refraction on pointing millimeter-wave antennas must be evaluated. Section 3.4 of the First Quarterly Report is a summary of refraction effects on satellite angle tracking for any frequency band. The information presented in this report is a summary of Section 2.1, Volume II of the Final Report which deals with the effects of refraction on pointing millimeter-wave ground terminal and spacecraft communication antennas.

A ground based automatic tracking and acquisition facility utilized for millimeter-wave space-earth communication would not require that the refraction of the propagating wave be known to a high degree of accuracy. However, if this same system were to supply data required for predicting the orbit of the satellite, in addition to being a communication terminal, then the pointing error due to atmospheric refraction would be of prime importance.

Refraction or bending of electromagnetic propagation through the atmosphere is due to both the troposphere and the ionosphere. However, the ionosphere has very little effect on propagating frequencies above 10 Gc and, as seen in Figure 4-20 [25] energy propagating at zero degrees elevation angle would exhibit an error in elevation angle of approximately 1 microradian when viewing a 270 nautical mile satelite from the Earth. Thus, the refraction due to the ionosphere is insignificant and need not be considered for millimeter-wave propagation. However, this is not the case for the troposphere as shown with the pointing error curves in Figure 4-21.[25] Incidentally, the pointing error in elevation due to tropospheric refraction when observing a satellite from the surface of the earth is one to two orders of magnitude greater than that which exists when viewing a point on the earth from a satellite.

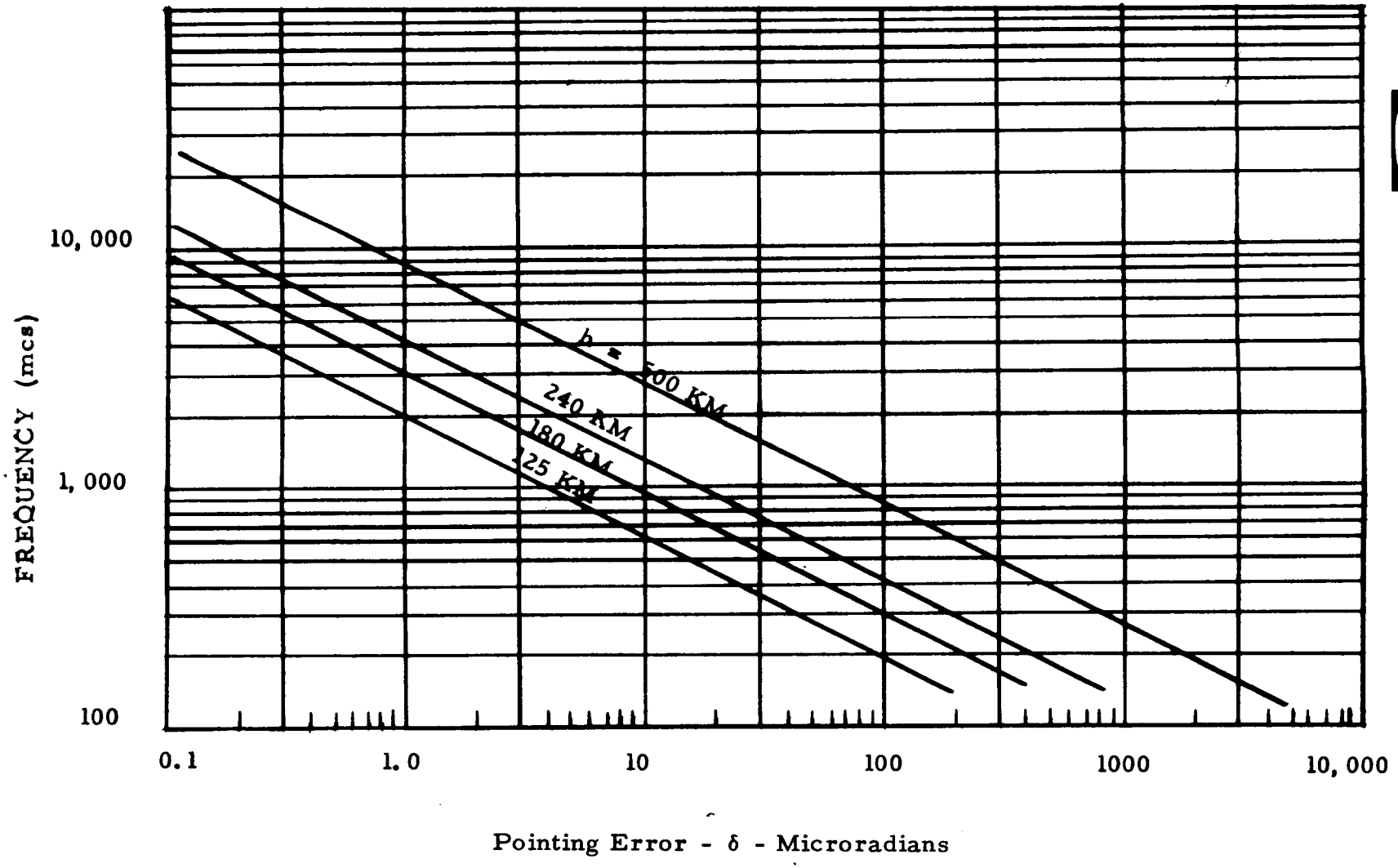

Figure 4-20 Pointing Error at Ground Station Due to Ionospheric Refraction

(Elevation Angle of 0°)

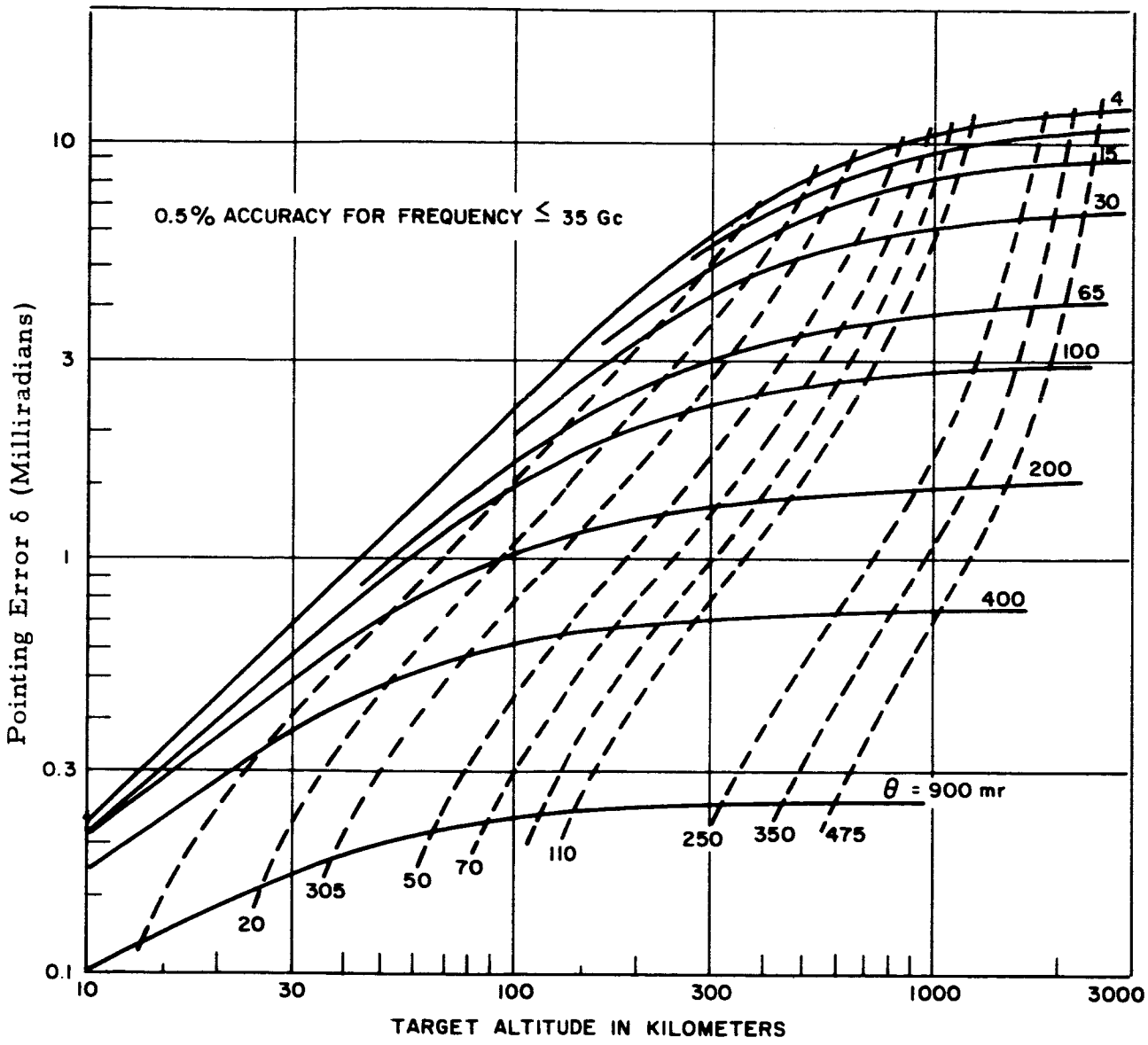

Figure 4-21 Ground Station Pointing Error Due to Tropospheric Refraction for Satellites Below 500 n. Miles

Figure 4-22 gives pointing errors at a satellite as a function of altitude and elevation angle.

This angular error in elevation is the difference in angle between the angle of incidence of the received energy and the true line-of-site of the radiating source. As depicted in Figure 4-23 an angular error due to tropospheric refraction is experienced at both the ground terminal and at the orbiting spacecraft. However, the error as viewed from the ground station, is greater than the error at the spacecraft by orders of magnitude. The error as observed from the ground station is a function of both elevation angle and altitude of the vehicle as readily observed in Figure 4-21 [25]. For vehicles at altitudes greater than 925Km (500 n mi) and elevation angles greater than 5 degrees, the tropospheric refraction error is approximated by:

$$\delta = N_o \times 10^{-6} \cot \theta \qquad (4\text{-}3)$$

where:

δ = Error in radians

N_o = Refractivity at observing station

θ = Elevation angle of target

Curves for δ vs elevation angle for atmospheres of 100% and 0% relative humidity are shown as Figure 4-24.

The angular error as viewed from the vehicle is much less than the errors plotted in Figure 4-24. This error has been computed for satellites orbiting at altitudes ranging from 100 to 6000 nautical miles, by dividing the atmospheric refractivity profile of Figure 4-25[26, 27] into six stratified layers, as shown in Figure 4-26. The angles specified in Figure 4-26 were determined through application of Snell's law for the spherically symmetrical surface.[28] The refractive angle errors were then computed for satellites in 100 - 6000 nautical mile orbits and plotted in Figure 4-22.

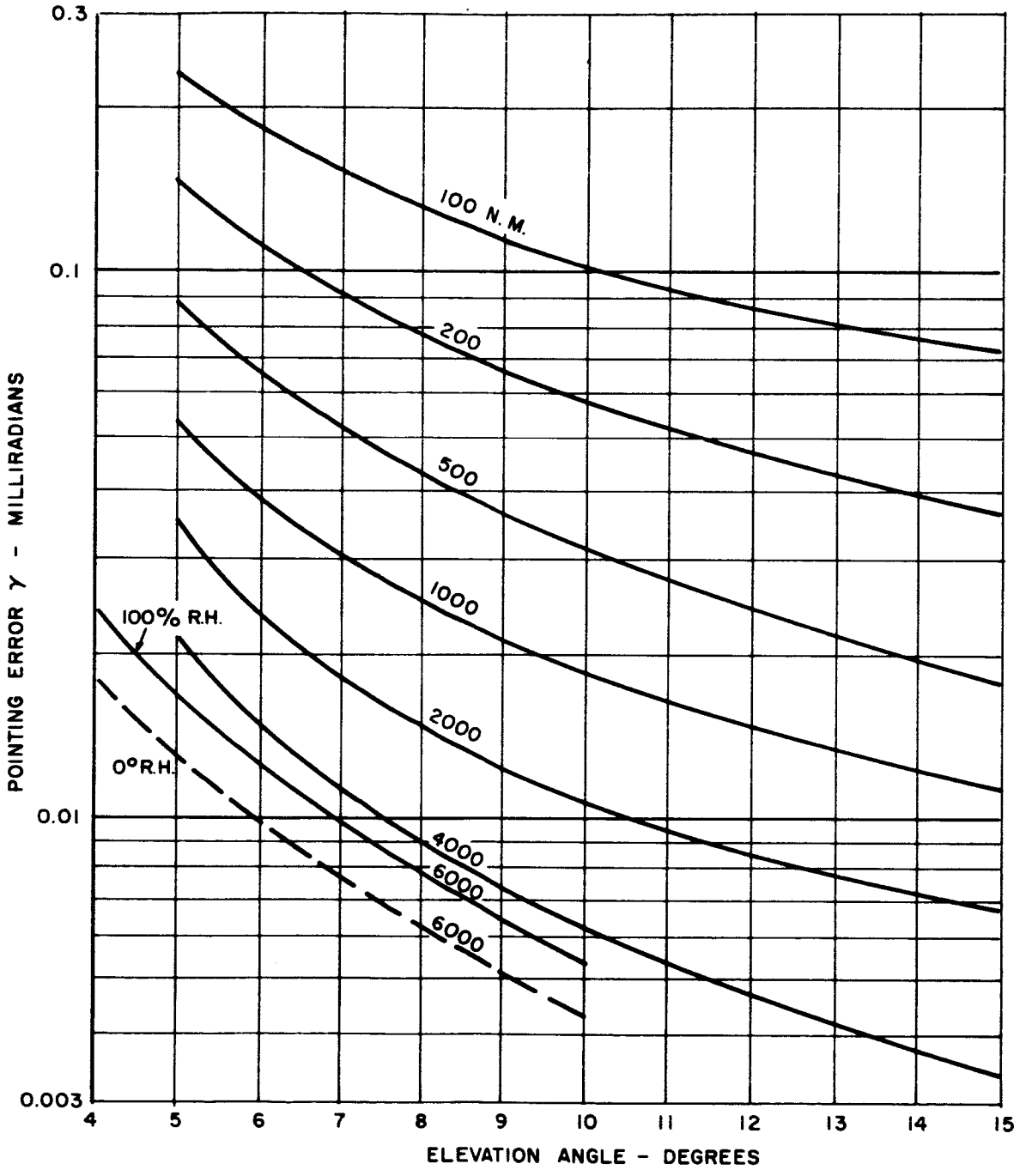

Figure 4-22 Satellite Pointing Error Due To Tropospheric Refraction

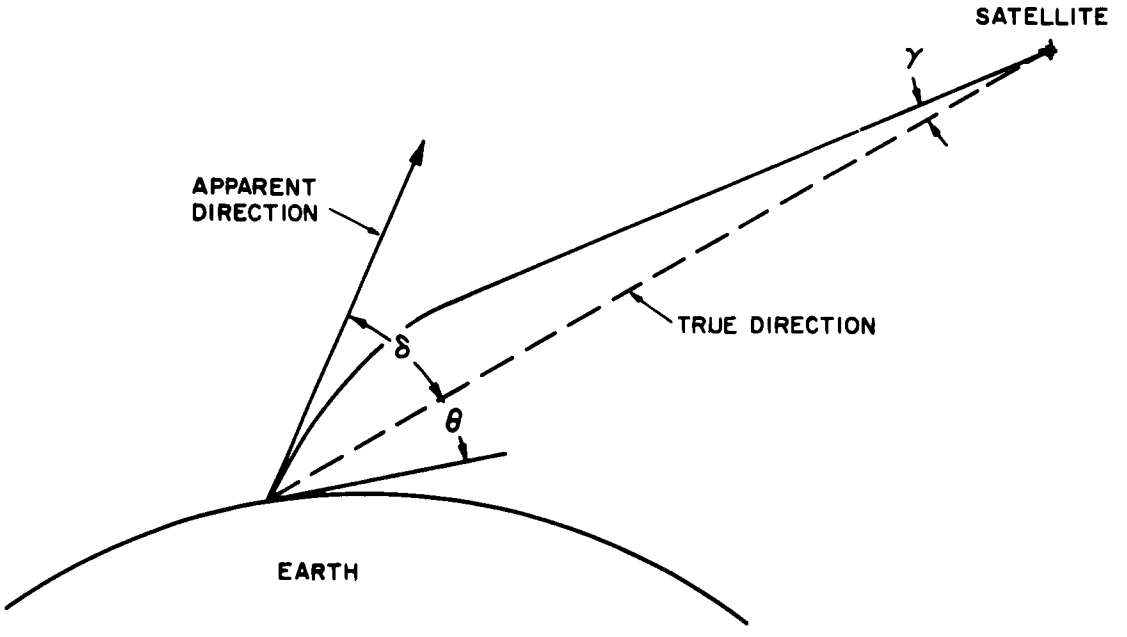

γ = Error in direction as viewed from satellite.

δ = Error in direction as viewed from earth.

Figure 4-23 Path of a Propagating Wave

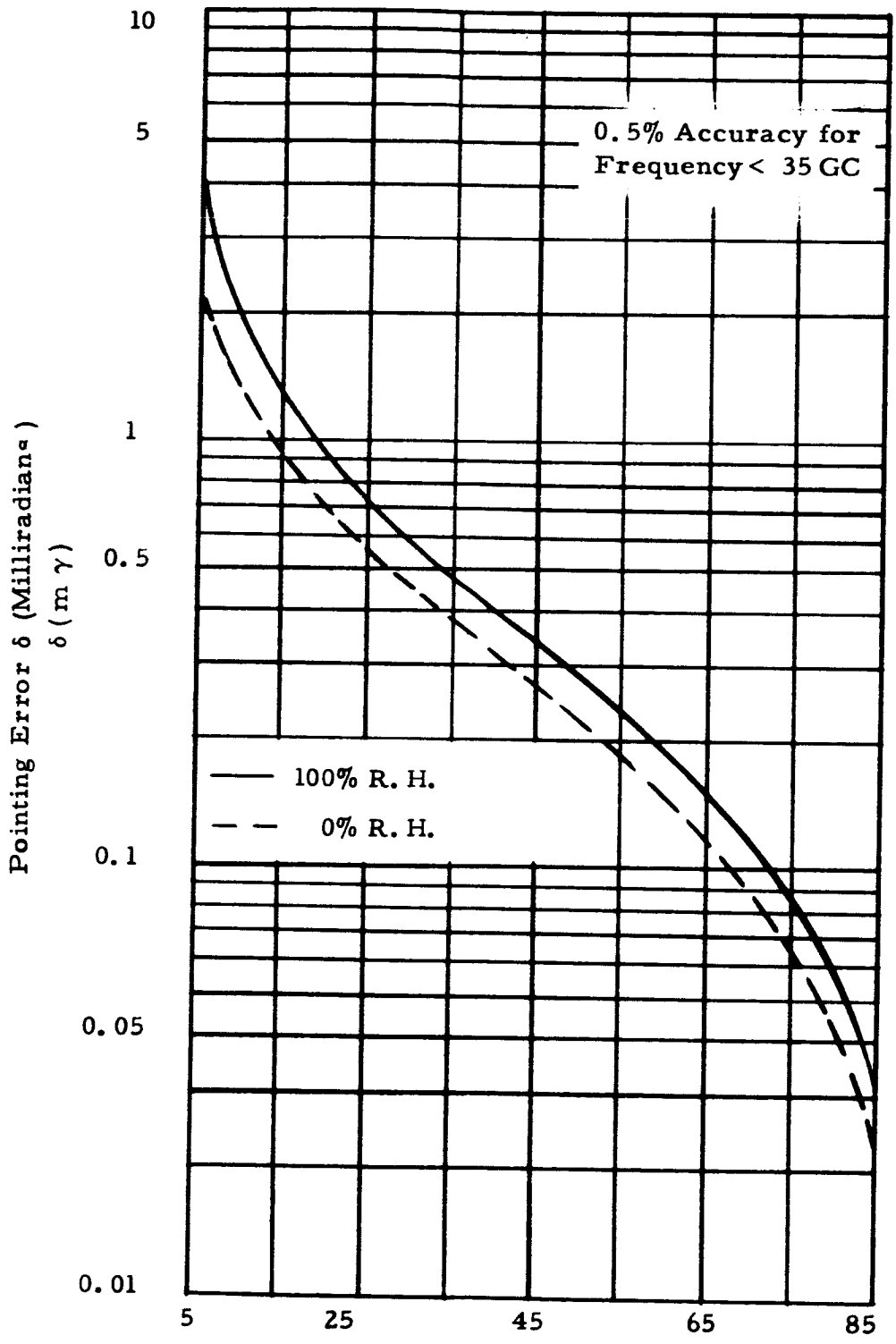

Figure 4-24 Ground Station Pointing Error Due to Tropospheric Refraction for Satellites Above 500 n. Miles

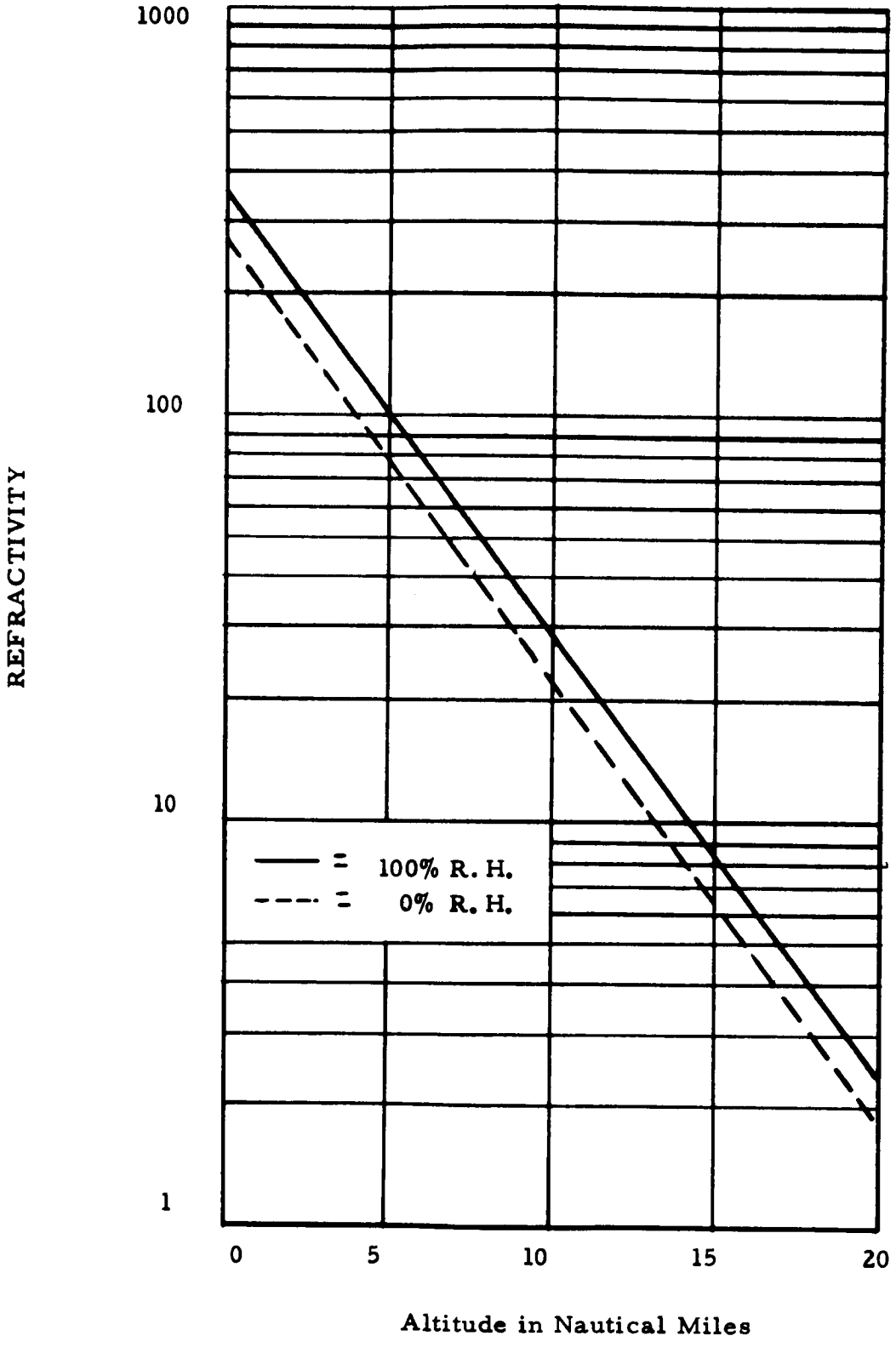

Figure 4-25 Refractivity of the Troposphere

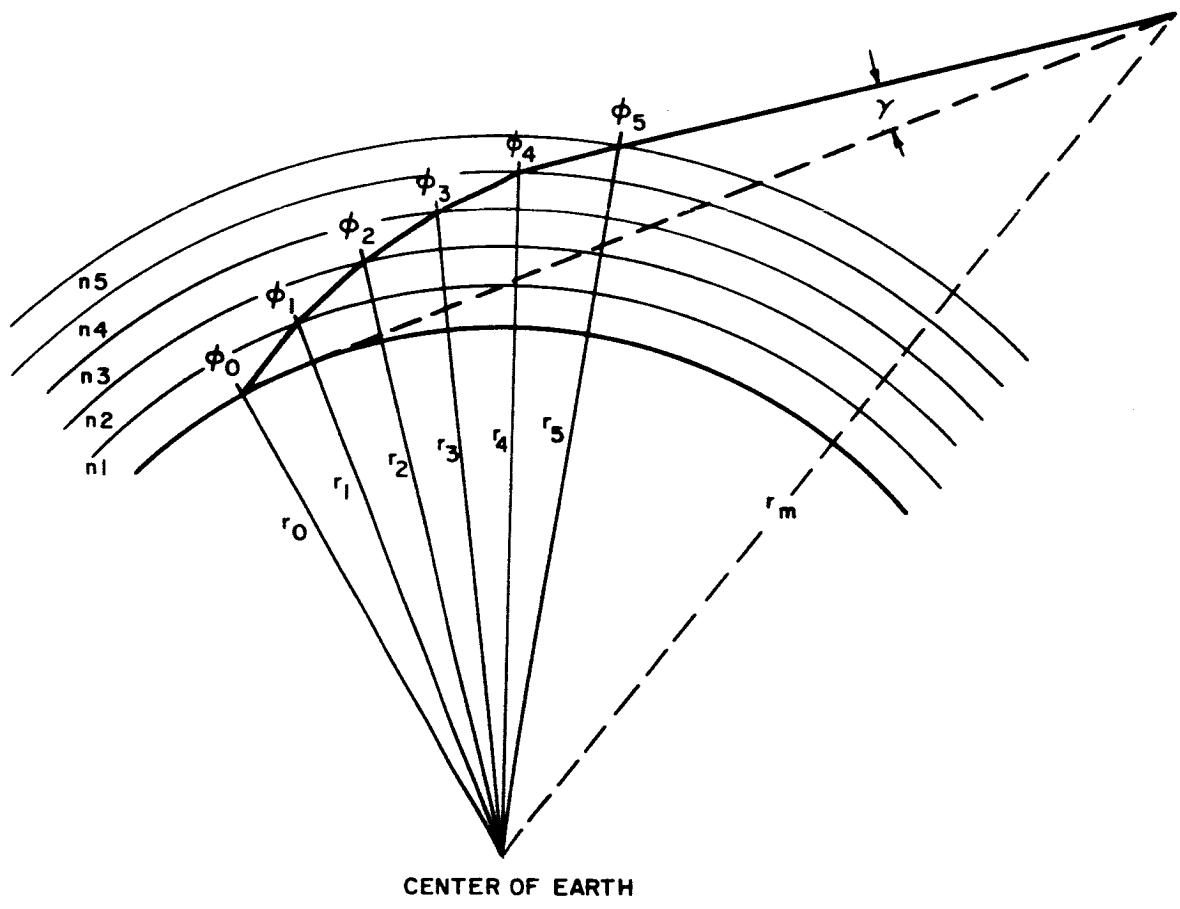

Figure 4-26 Atmospheric Layer Stratification

4.5 Refraction Effects on Maximum Integration Time, Signal Phase Variations, Signal Frequency Spectrum and Antenna Gain

Propagation of millimeter waves through a turbulent atmosphere at low elevation angles has an effect upon the maximum useful receiver signal integration time and the maximum useful receiving antenna size. Variations in index of refraction along a propagation path are caused by changes in the inhomogeneous atmosphere by wind and the angular movement of a satellite with respect to the ground terminal. These variations in index of refraction, which are a function of wind velocity and satellite angular velocity, degrade the spectral purity of the transmitted signal, thus affecting the maximum useful integration time. This useful integration time increases with aperture size. These effects upon integration time are of particular significance in the design of phase-lock receivers for ground communication terminals which receive millimeter signals from low altitude spacecraft.

The gain of large millimeter antennas might also be affected by the turbulent atmosphere. As the antenna becomes larger, the wavefront of the receiver signal incident upon the aperture becomes less and less planner. The resulting effects upon antenna performance are very similar to those effects caused by reflector mechanical errors. The relative motion between the atmosphere and the propagation path does not have an effect upon the gain of the antenna.

Data taken from National Bureau of Standards experiments are analyzed to estimate the magnitude and spectra of fluctuations in earth-satellite radio paths. Range fluctuations over a period of a day can be expected to reach a level of about 25 cm (rms) at a 6^{o} elevation angle under poor weather conditions. The corresponding fluctuation over a period of one minute would be about 0.4 cm. For the case of the 100 nmi satellite, the rms velocity fluctuation could be as great as 72.5 cm/sec for an antenna of 6 inch diameter at 94 Gc, corresponding to a frequency fluctuation of 228 cps. The rms velocity fluctuation for a 15 foot diameter paraboloid at a frequency

of 94 Gc (considered to be the maximum useful antenna size at this frequency) would be 7.1 cm/sec, corresponding to a frequency fluctuation of 22 cps. For the 6000 nmi satellite, and the 15 foot diameter paraboloid at 94 Gc, the rms velocity fluctuation would be .06 cm/sec, corresponding to a frequency fluctuation of less than one cps. Range fluctuations over a 15 foot aperture will be of the order of .01 cm, indicating little beam broadening or loss of gain at a frequency of 94 Gc.

4.5.1 Spectrum of Path Length Fluctuation or Equivalently Signal Phase Spectrum

The influence of the troposphere on the apparent lengths of fixed radio paths has been investigated for several years by the National Bureau of Standards at Boulder, Colorado. The best statistical summary of voluminous results takes the form of a composite power spectrum, extending from 10^{-8} to 10 cps. Such curves have been published for paths in Colorado, Hawaii, and Florida[29, 30, 31]. In each case, the path considered is about 15 miles long and leaves a flat surface at an angle of about 6 degrees. Considerable variation in amplitude can be expected from site to site and from time to time, but a typical spectrum for an atmosphere containing cumulus clouds can be expressed as:

$$W(f) = W_o \qquad f < f_a$$

$$W(f) = W_o\left(\frac{f_a}{f}\right)^{8/3} \qquad f < f_a$$

$$W_o = 10^7 \text{ (ppm)}^2/\text{ cps}$$

$$f_a = 10^{-5} \text{ cps}$$

The spectral density is expressed here in units of (parts per million)^2 per cps. For a path length of 36 km (120,000 feet), the low-frequency spectral density W_o would correspond to 1.3×10^8 cm^2/cps. The spectrum given

above may be applied to path lengths from about 20 to 40 km at altitudes below 5 km without modification. A plot of this spectrum is given in Figure 4-27. For convenience in interpretation, the spectrum may be replotted as in Figure 4-28, where the ordinate represents the weighted spectral density f W(f). The effect of the weighting is to show the relative contribution to the total area of each octave or decade in the spectrum. Thus it is seen that the predominant frequency components in the fluctuation spectrum will lie between 10^{-6} and 10^{-4} cps.

The results given above indicate that the phase variation will be very slow and hence of no consequence. In particular, the phase variation is expected to be 98 degrees in one minute for a stationary beam due to a 10-foot per second wind velocity and not be much greater for beam tracking a satellite at an altitude of 6,000 miles. Such a slow variation in phase could easily be tracked by a phase lock receiver if need be.

4.5.2 Magnitude of Path Length Fluctuation

The magnitude of range fluctuation observed over a given time interval t_1 may be estimated by integrating the product of the spectral density times a filter function G_1 (f) which expresses the effect of the finite observation interval[30].

$$\sigma_r^2 = \int_o^\infty G_1 (f)\, W (f)\, dg$$

$$G_1 (f) = (f\, t_1/2)^2 \qquad f < 2/t_1$$

$$G_1 (f) = 1 \qquad f > 2/t_1$$

The filter functions for observation periods of one day and one minute are applied to the basic spectrum in Figure 4-29. The predominant frequencies

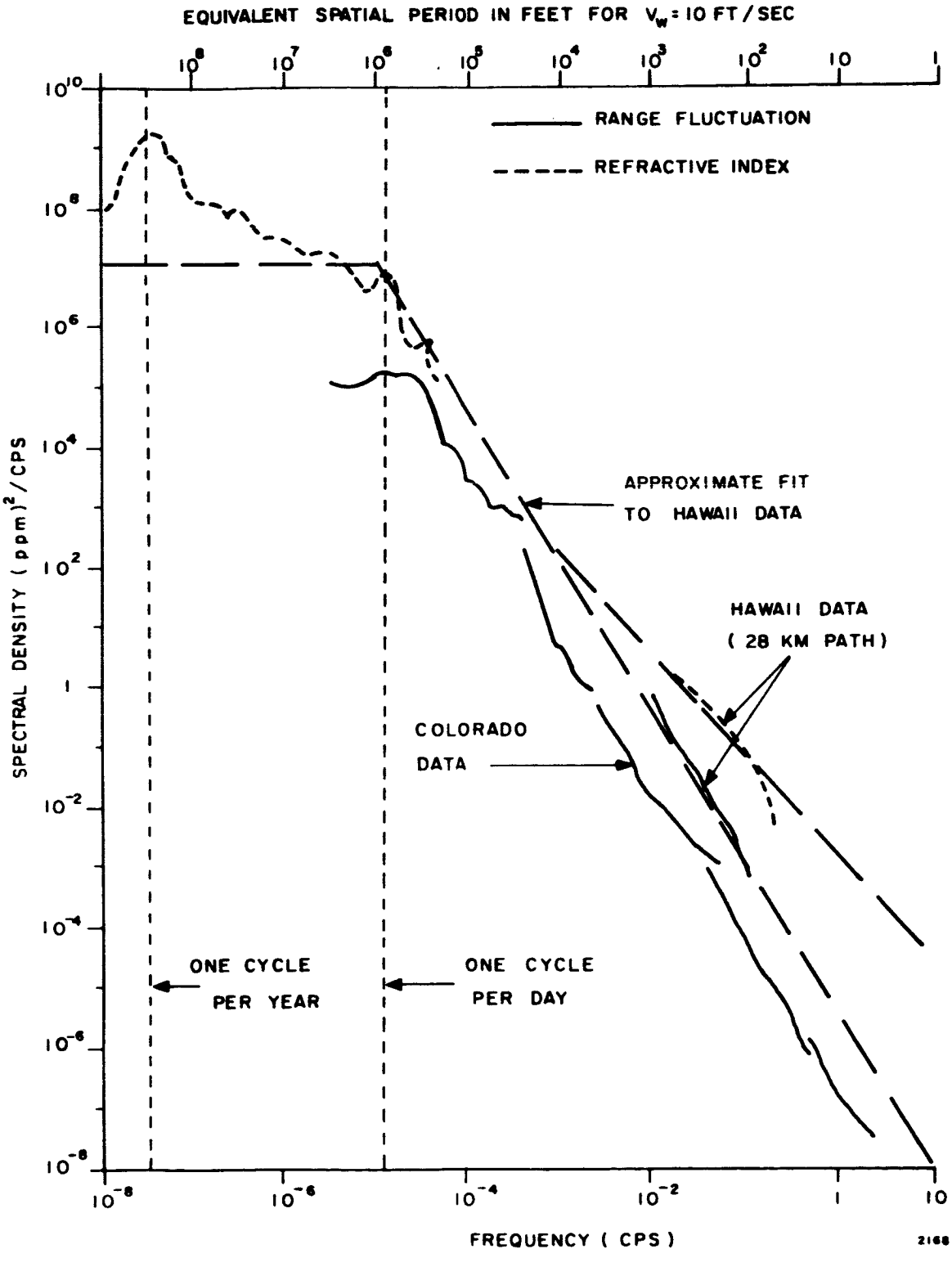

Figure 4-27 - Spectra of Refractivity and Range Fluctuation (NBS Data)

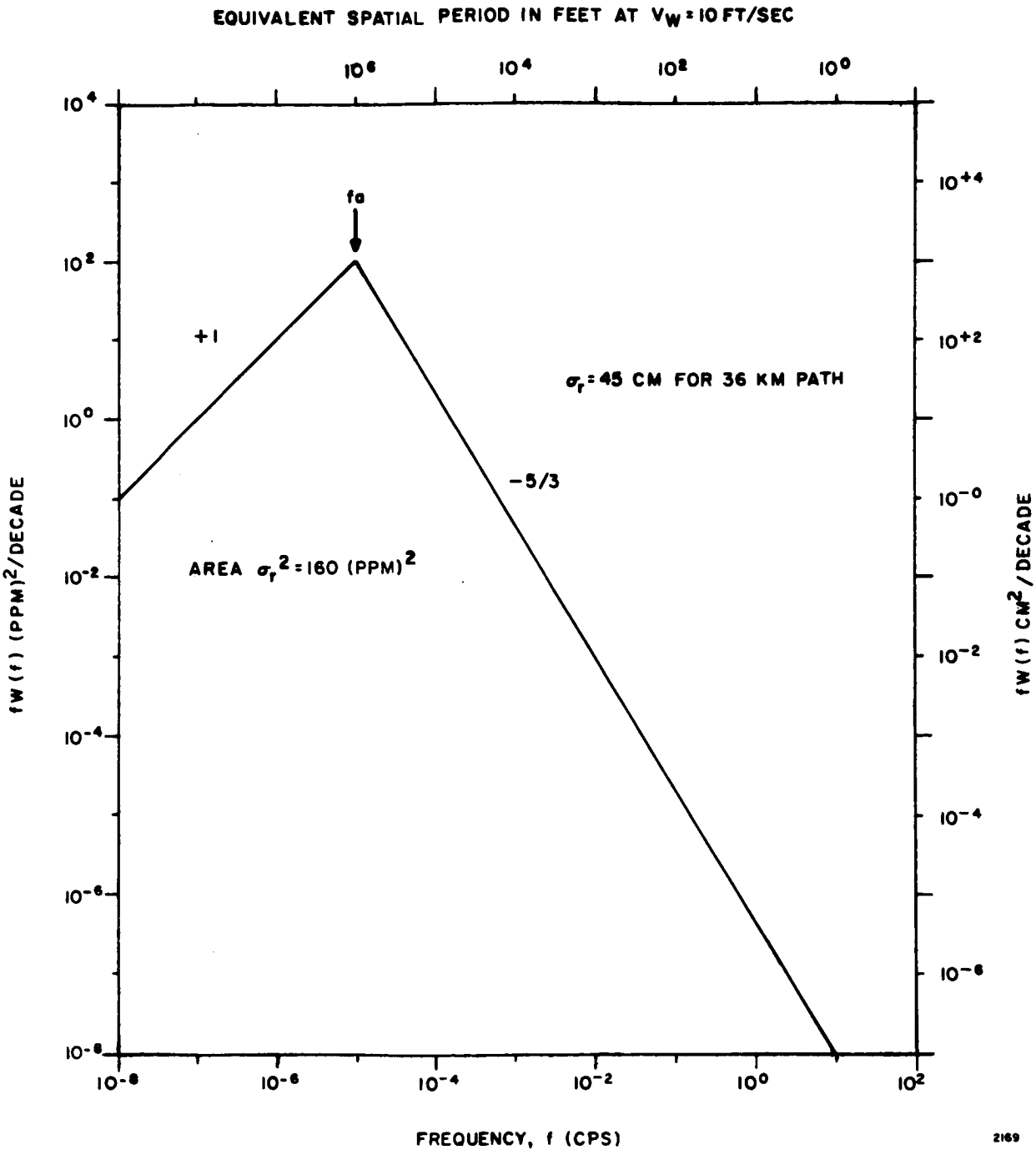

Figure 4-28 - Modified Plot of Range Fluctuation Spectrum

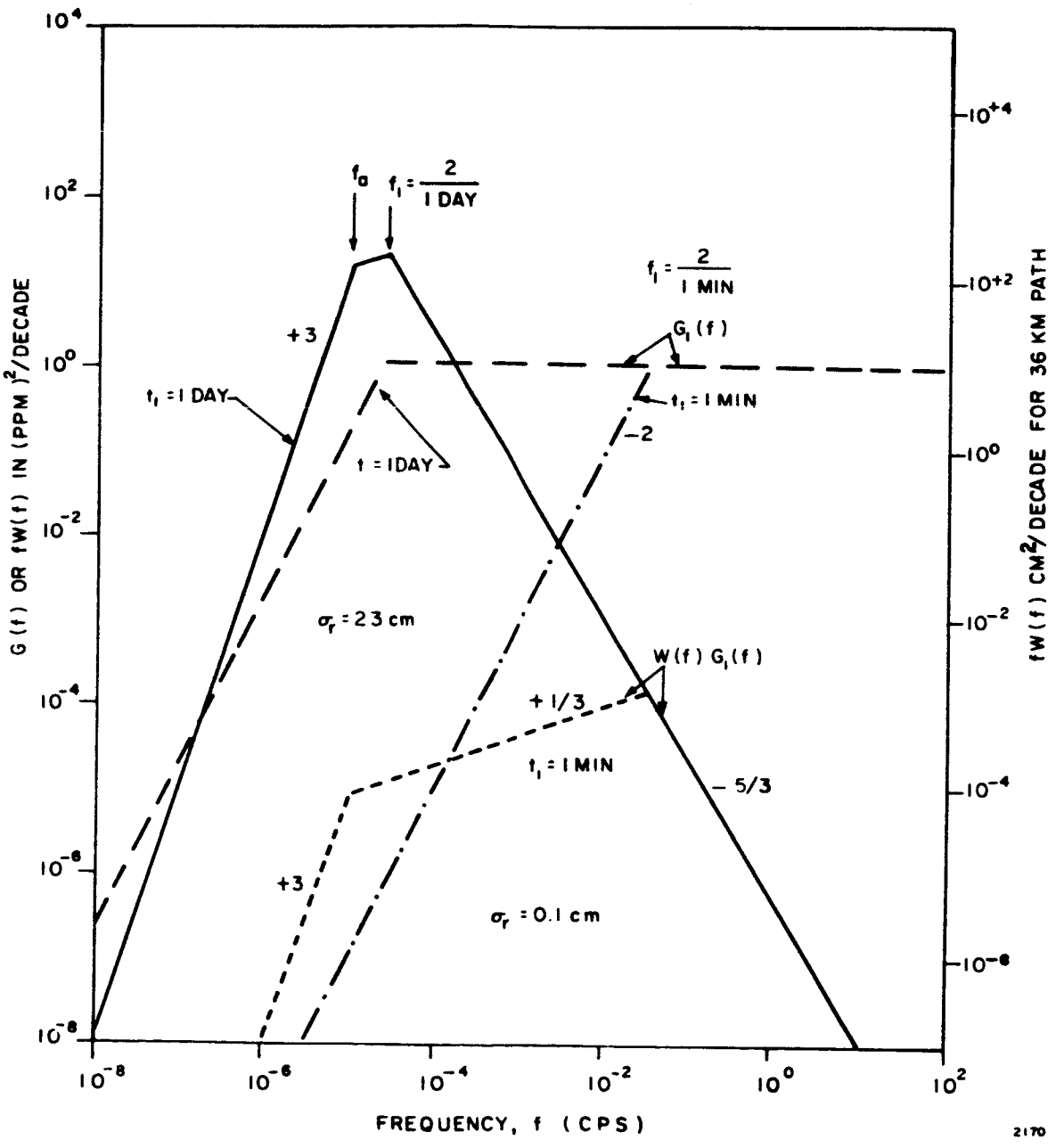

Figure 4-29 - Range Fluctuation Spectra for Finite Observation Periods

of fluctuation are in the region near $f_1 = 2/t_1$, and lower frequency components are lost, appearing as "trends" of greatly reduced amplitude in the short samples of data. The rms fluctuations will be about 23 cm over a day, and 0.1 cm over a minute (for periods shorter than a day, the rms fluctuation will vary as the 5/6 power of the observation period).

4.5.3 Velocity (On Signal Frequency) Fluctuation

The rate of change of fluctuation in range gives the velocity fluctuation, and this quantity, divided by the wavelength, gives the frequency fluctuation in cps. The spectral density of velocity fluctuation is just $(2\pi f)^2$ times that of range fluctuation (Figure 4-30). The rms velocity fluctuation is the integral of this spectrum. Since the predominant frequencies are near the high end of the spectrum, the observation time is no longer of great importance. However, the upper limit of the -8/3 portion of the spectrum will be important in establishing velocity fluctuation. This limit, set either by aperture size or by physical properties of the atmosphere, will lie between 0.1 and 10 cps for the case of the fixed path. An aperture of diameter d will tend to filter out fluctuations lying above a frequency $f_d = V_w/2d$, where V_w is the wind velocity component normal to the antenna axis. The equivalent aperture filter function is

$$G_d(f) = \left(\frac{f_d}{f}\right)^2 \qquad f > f_d$$

$$G_d(f) = 1 \qquad f < d_d$$

This function is shown in Figure 4-30, superimposed on the velocity spectrum, for d = 50, 15, 5 and 0.5 feet.

The velocity fluctuation may now be computed from:

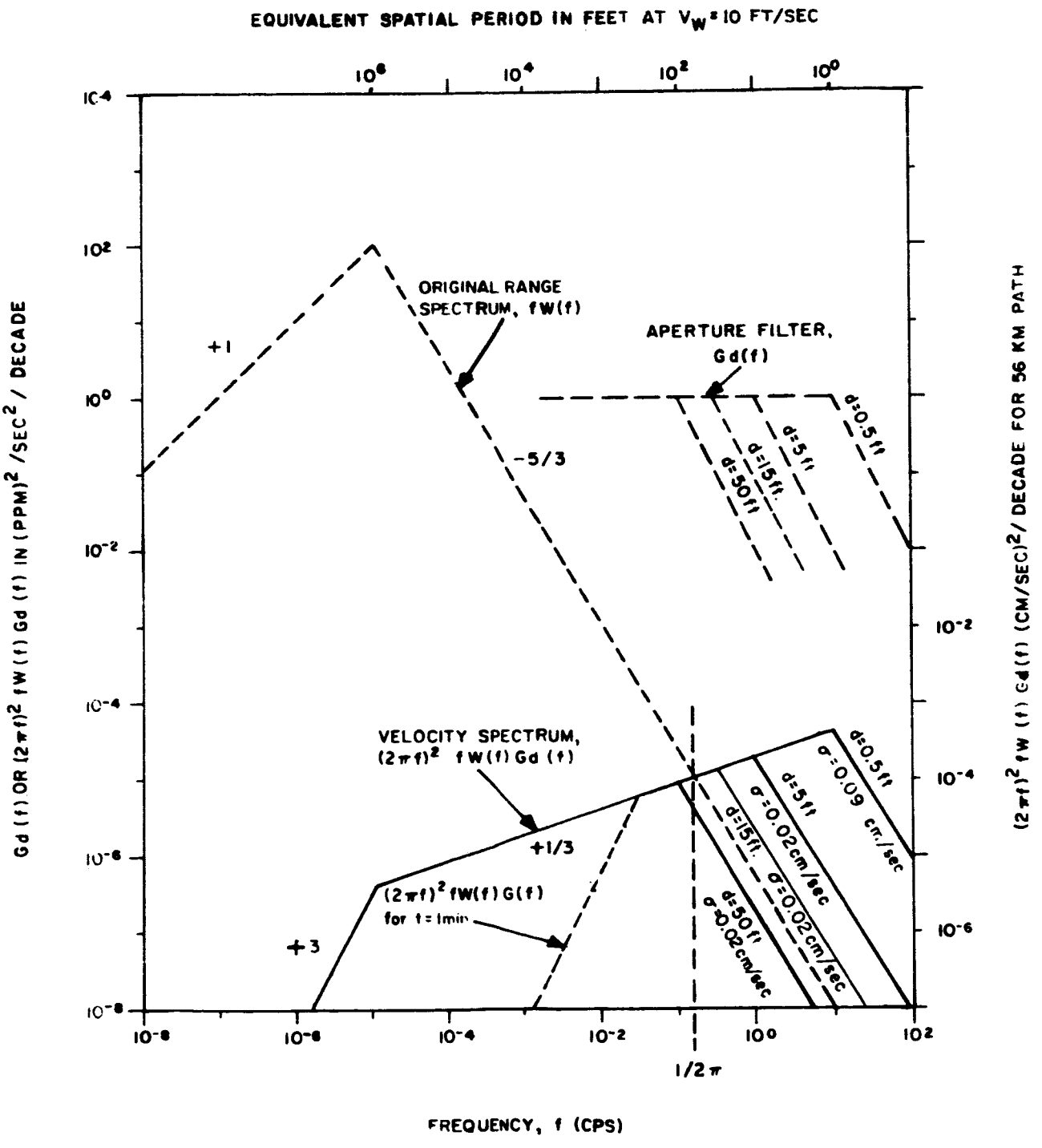

Figure 4-30 Velocity Fluctuation Spectrum for Different Aperture Diameters

$$\sigma_f^2 = (2\pi)^2 \int_o^\infty f^2 W(f)\, G_1(f)\, G_d(f)\, df$$

$$(2\pi)^2 \int_o^\infty f^2 W(f)\, G_d(f)\, df$$

Expected values for the fixed path will run from 0.02 to 0.09 cm/sec, depending on aperture. This corresponds to an rms frequency deviation of 0.02 to 0.09 cps at f_o = 30 Gc (λ = 1 cm).

4.5.4 Path Length Fluctuation for Moving Spacecraft

The preceding results may be applied directly to communication paths to a synchronous satellite, where the fluctuations result entirely from atmospheric drift across the path and temporal variations in the refractivity along the path. If the satellite moves, relative to the ground terminal, a further effect is introduced by angular motion of the radio path through the atmosphere. Although this angular motion cannot be simulated exactly in fixed-path experiments, its effect can be estimated with reasonable accuracy by considering an average velocity of the antenna beam relative to the tropospheric features which cause fluctuation. This velocity is used to modify the spectrum of Figures 4-27 and 4-28, by assuming that the tropospheric features are "frozen" in the air mass and pass through the beam at a frequency proportional to the total velocity of the air relative to the beam. The following analysis will assume that this relative velocity at an altitude of 12,000 feet is an appropriate weighted average for tropospheric effects. At an elevation angle of 6 degrees, the path from a terminal at sea level to this point will be about 120,000 feet in length. The "apparent" wind velocities as determined from Figure 4-31 for 100 nmi and 6000 nmi satellites are 813 and 25 ft/sec., respectively. Addition of the typical wind velocity to the "apparent" wind velocity (actually the velocity of the satellite) yields values of 823 and 35 ft/sec for v_b used in the computations.

The range and velocity fluctuation spectra for the moving beam case will be as shown in Figures 4-32 and 4-33. The frequency scale has been multiplied by the factor v_b/v_w, and the density scale in W(f) divided by the same quantity preserving the area under the curve. However, the variances observed in short time periods will be increased approximately by the factor $(v_b/v_w)^{5/3}$. The fluctuations for fixed and moving beams are compared in Table 4-2. Table 4-3 gives the resulting frequency fluctuations at 94 Gc for a 100 nmi satellite.

4.5.5 Phase-Difference Fluctuations or Spatial Coherence

Information on the magnitude of phase-difference fluctuations across a large aperture can also be obtained from the NBS data. If we assume that the "frozen" model of the atmosphere is valid, at least for tropospheric features whose dimensions are smaller than several aperture widths, the rms range-difference fluctuations between two points separated by a distance b are found by applying the following transfer function[30] to the

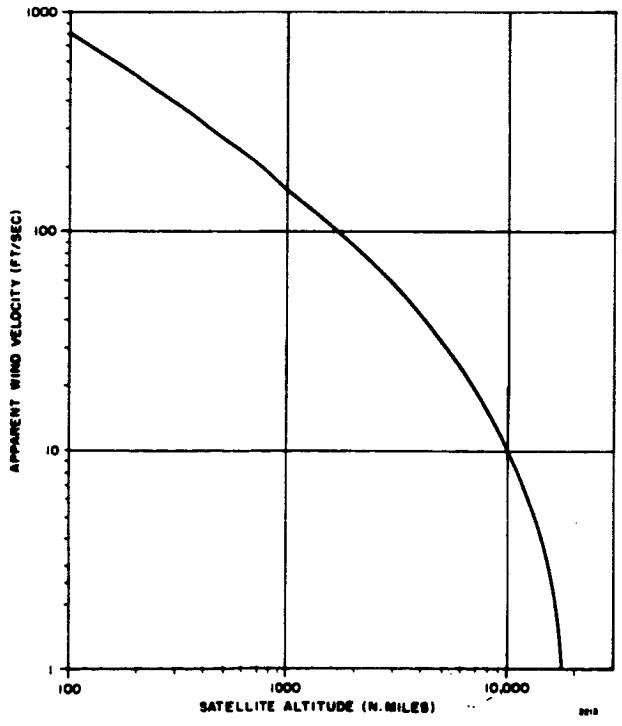

Figure 4-31 Apparent Wind Velocity vs Satellite Altitude

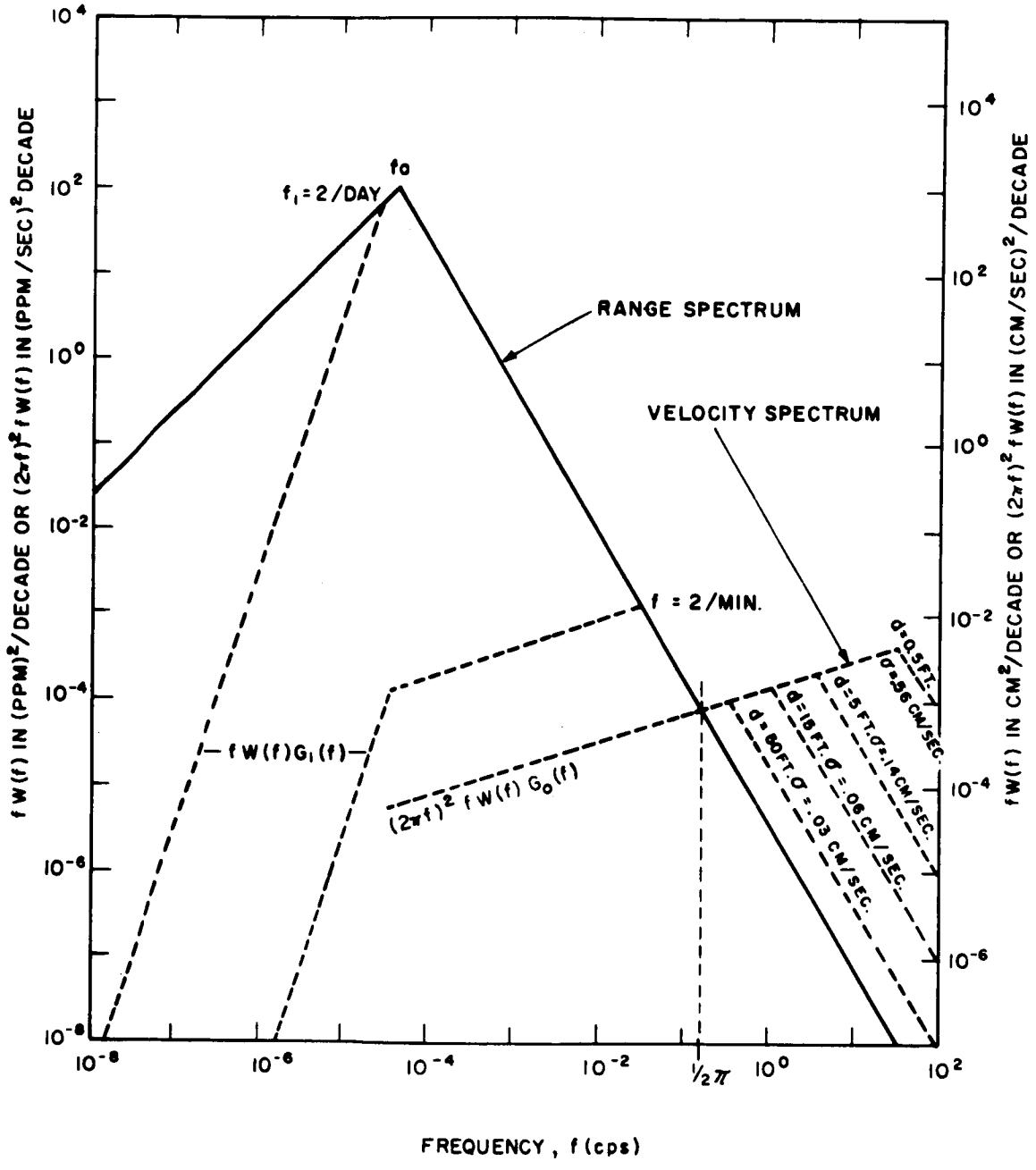

Figure 4-32 Range and Velocity Spectra for Moving Path, 6000 nmi Satellite

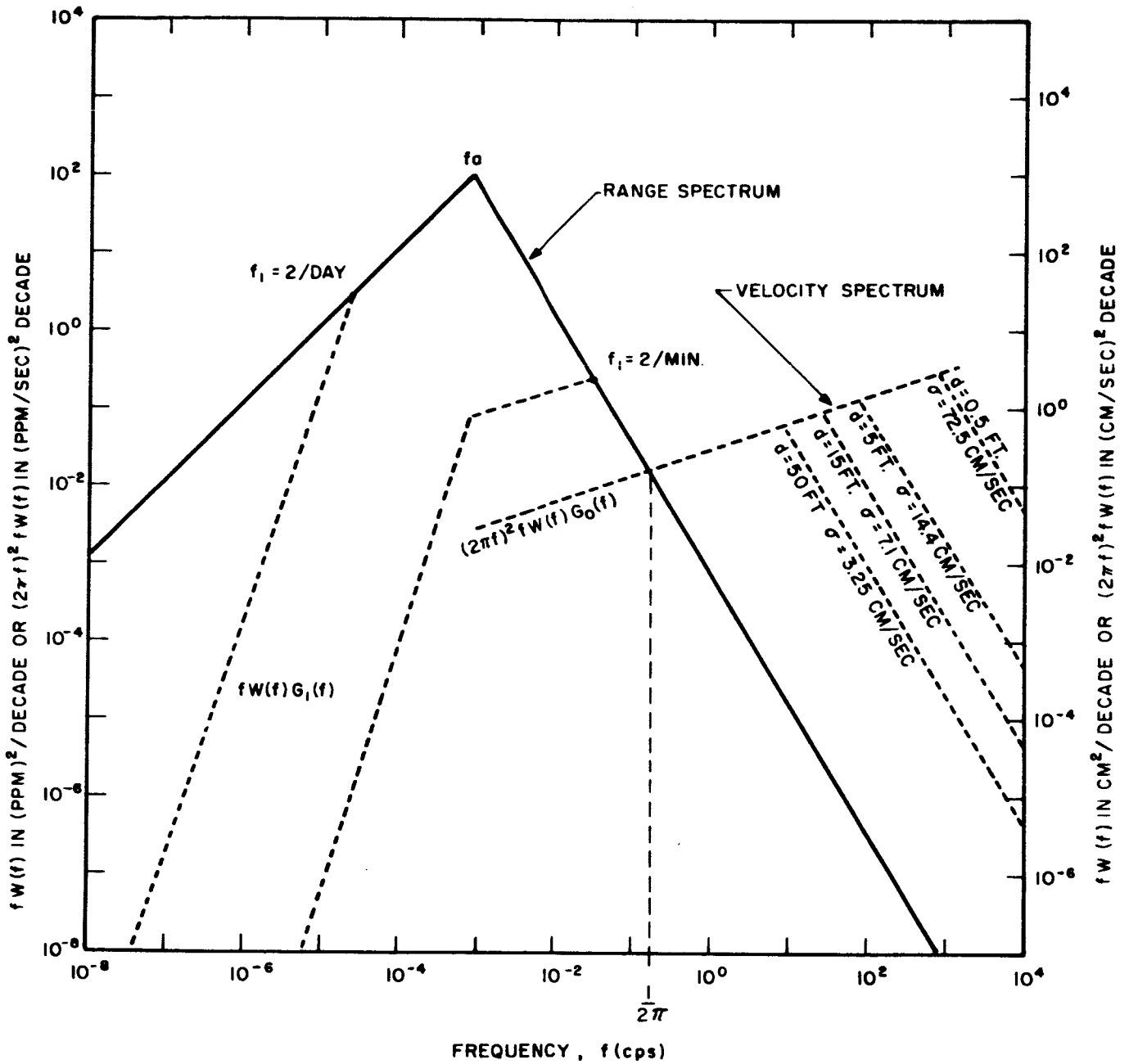

Figure 4-33 Range and Velocity Spectra for Moving Path, 100 nmi Satellite

TABLE 4-2

FLUCTUATIONS FOR FIXED AND MOVING BEAMS

	Fixed Path (v_n=10 ft/sec)	Moving Path 6000 nmi satellite (v_b=35 ft/sec)	Moving Path 100 nmi satellite (v_b=823 ft/sec)
Total range fluctuation	45 cm	45 cm	45 cm
Fluctuation in one day	23 cm	23 cm	23 cm
Fluctuation in one minute	0.1 cm	.36 cm	
Velocity fluctuation(d=50 ft)cm/sec	.02 cm/sec	.03 cm/sec	3.3 cm/sec
Velocity fluctuation(d=15 ft) cm/sec	.02 cm/sec	.06 cm/sec	7.1 cm/sec
Velocity fluctuation(d=5 ft)cm/sec	.02 cm/sec	.14 cm/sec	14.4 cm/sec
Velocity fluctuation (d=0.5 ft)cm/sec	.09 cm/sec	.56 cm/sec	72.5 cm/sec

TABLE 4-3

FREQUENCY FLUCTUATIONS AT 94 Gc FOR A 100 nmi SATELLITE

Antenna Diameter (ft)	Frequency Fluctuation (cps)
15.0	22
5.0	45
0.5	228

basic spectrum:

$$G_b(f) = 2\,(f/f_b)^2 \qquad f < f_b$$

$$G_b(f) = 2 \qquad f > f_b$$

$$f_b = 0.22\, v_w / b$$

This is a "high-pass" filter function, as shown in Figure 4-34. Fluctuations at frequencies below f_b will introduce linear variations in phase across an aperture of width b, changing the apparent angle of arrival. Frequencies near f_b will cause broadening of the antenna beam, while those above f_b will increase sidelobes. The number of sidelobes affected will be proportional to the increase in frequency beyond f_b. The amount of broadening or sidelobe increase will depend on the rms phase-difference contributed by the corresponding portion of the error spectrum $w(f)\, G_b(f)$. Significant reduction in gain will occur when the rms phase error across the aperture exceeds about 0.3 radian (or when the rms range difference fluctuation exceeds $\lambda/20$).

Figures for range-difference fluctuations shown on Figure 4-34 indicate fluctuations of less than 0.08 cm for a 50 foot aperture and of the order of 0.01 cm for a 15 foot aperture. At a frequency of 94 Gc, .01 cm is equivalent to 0.3, indicating no appreciable deteoration in gain.

4.6 Amplitude Fading

Amplitude fading arises from a number of factors. These are:

a. Variations in the water vapor content in the atmosphere.

b. Atmospheric turbulence.

c. Direct and reflected wave interference.

Variations in the water vapor give rise to slow variations in signal amplitude. The variations are diurnal in nature, although more rapid

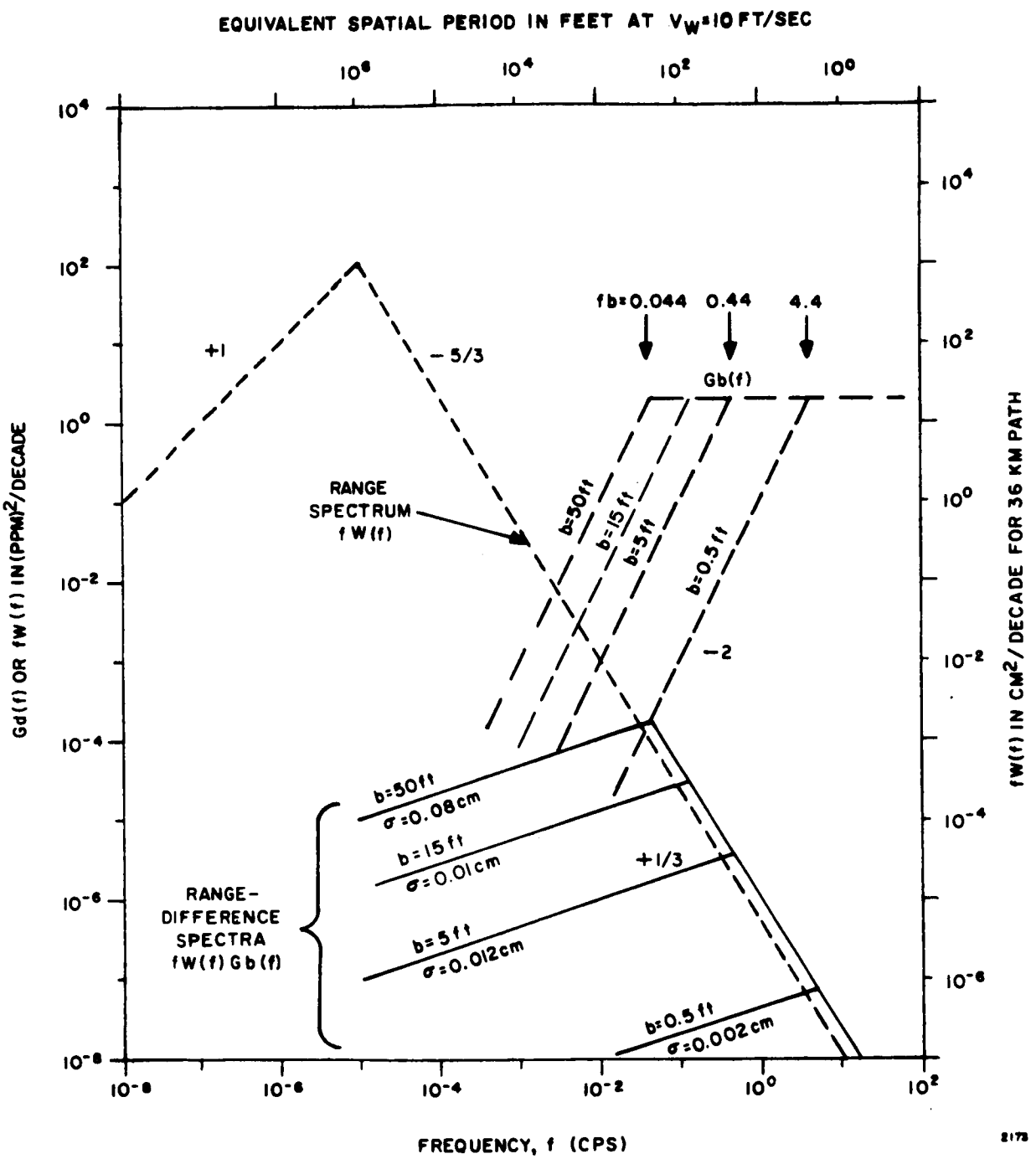

Figure 4-34 Range-Difference Spectra for Separations From 0.5 to 50 Feet

fluctuation can occur due to the passing of clouds across the communications path and the occurrence of rain, snow or hail.

Atmospheric turbulence gives rise to multipathing in the communications channel. This results from the stochastic-temporal variations of the index of refraction in the atmosphere in the presence of turbulence. Experimental data indicate that the decorrelation distance for the index of refraction is of the order of 100 to 200 feet.[32] Furthermore, the frequency components of the spectrum of these fluctuations are usually 10 cps or less[33]. Hence, the frequency of the fading should be 10 cps or less. Moreover, the Telstar data[34] which used a 6 mc carrier, indicated a frequency rate for the fading of 1/2 cps for an elevation angle of 4 degrees or less.

The fluctuation due to the interference of the direct and reflected wave will occur at low elevation angles and is identical to the interference experienced in ground wave propagation[35]. Moreover, the fluctuation due to turbulence also occurs at low elevation. The experiment to be performed will determine how deep the fluctuations are and the fluctuation rate as a function of elevation angle, geographical location and weather conditions.

An analysis of the degree of fading due to inhomogeneities in the troposphere has been carried out by Bergmann[36]. He considered the problem solely as one in geometrical optics, neglecting the diffraction effects and assuming that the variation of the index of refraction is isotropic in space. His analysis indicates that the rms intensity fluctuation in db on a one-way path is given by:

$$E_{rms} = 0.0785\, R^{3/2} \sqrt{r_o\, (\nabla^2 n)^2} \qquad (4\text{-}4)$$

where R is the range, r_o is the patch size of the inhomogeneities, ∇^2 is the Laplacian of the refracted index, and the averaging is to be taken over all space.

For propagation vertically through the troposphere, the width of the region in which the inhomogeneities lie is about 10,000 yards. The size of the inhomogeneities is about 40 yards and the peak deviation in the index of refraction is about 10^{-5} (36). Using these values, one finds that the rms intensity fluctuation (that is, the fading) is only about 0.05 db. For low elevation angles, however, the length of the path over which the inhomogeneities may lie might be of the order of 60,000 yards for the earth-satellite channel. For this value of R, one finds from Equation 4-4 that the intensity of the scintillation is about 0.8 db. Hence, as one might expect, there will be greater scintillation at low elevation angles which will diminish rapidly toward the zenith. (Measurements recently made at Aerospace at 94 Gc indicate rms fluctuation having considerably larger values than that indicated here. Values of 10 db depth of fading were obtained for a 20,000 yard path.)

Tatarsky(37) has also studied this problem and he shows that the mean-squared value, σ^2, of the logarithmetic variation of the amplitude of signal transmitted through a turbulent medium is:

$$\sigma^2 = 1.23\, C_n^{\,2}\, k^{7/6}\, L^{11/6} \qquad (4\text{-}5)$$

where,

$C_n^{\,2} = 10^{-9}/\text{cm.}$

$k = 2\pi/\lambda$

λ = wavelength of signal

L = pathlength in cm.

The value of C_n was calculated using optical data but Tatarsky indicates the value is useful at frequencies as low at UHF. Using representative values for λ and L, one finds there is essentially no fluctuation in the output signal due to scattering from turbulence in the atmosphere. (This agrees with some

experimental results [38] which show little scientillation at elevation angles above 4 degrees.)

4.7 Multipathing Phenomena and Coherence Bandwidth

There are several phenomena which give rise to multipathing in the atmosphere. One phenomenon arises from scattering, in particular, scattering from blobs distributed randomly in the atmosphere. These scattered rays interfere with the direct rays. For large size antennas, a second phenomenon, giving rise to multipathing, results from the fact that there can exist two direct paths far enough separated from each other so that they see completely different inhomogeneities.

Multipathing can also arise from non-random inhomogeneities in the atmosphere such as distinct clouds, vortex columns, etc. The contribution from this third type of perturbation must be evaluated for the situation at hand and from direct experiments. While it might be possible to calculate the effect of a cloud of specified shape and droplet density, the character of real weather is not known in enough detail to be able to predict the frequency of clouds of various sizes, shapes and densities. The associated vortex columns and other completely transparent structured (that is, non-random) irregularities which abound in the atmosphere are even less predictable.

In the remainder of this section, consideration is given to multipathing arising from the first two homogeneous phenomena mentioned above.

Figure 4-35 which illustrates the multipathing arising from scattering, indicates the direct ray and the scattered ray. The received signal will consist in this case of the major return from the direct ray path plus the returns from the scatter paths. In the illustration only single scattering is pictured. Some consideration to multiple scattering was given in Section 3.5 of the First Quarterly Report.

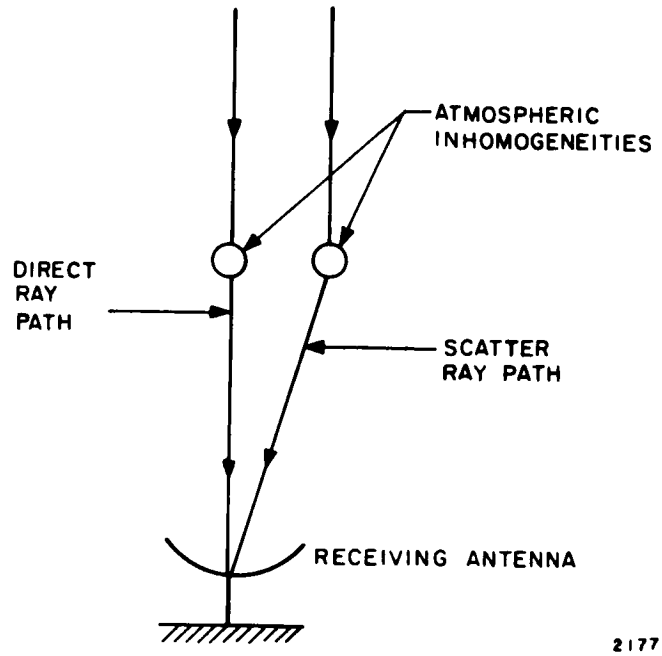

Figure 4-35 Scatter Paths

Generally, the scatter returns will arrive after the direct path return. Furthermore, the return via the direct path will be very much larger than that from the scatter paths in general and will not be scintillating. The difference in delay between the direct and scatter paths is very small. In particular, based on a first order Born approximation, Muchmore and Wheelon[39] estimated it to be much less than a nanosecond (the contribution resulting from higher order terms is not known).

It is convenient to total the contributions from the scatter paths. Due to the fact that there are many scatter paths and the returns from each scatter path will add up in random phase, the contribution from the scatter paths will consist of a randomly fluctuating term in the receiver. This randomly fluctuating term can be expected to have a Gaussian distribution as far as its instantaneous voltage is concerned and a Rayleigh distribution

as far as its envelope is concerned. It follows from the above discussion that if only the multipathing due to scattering from inhomogeneities in the atmosphere is considered the return signal can be written as

$$e_r(t) = s(t - \tau)\left[\alpha e^{-j\delta} + \beta_e e^{-je}\right] \qquad (4\text{-}6)$$

where

$s(t)$ = the transmitted signal

τ = the propagation time

α = the amplitude of the return received over the direct path

δ = the phase of the return received over the direct path

β = the instantaneous amplitude of the sum of the scattered signals

e = the phase of the sum of the contributions from the scattered terms

The quantity α is non-random; δ will have a slow random variation which will be discussed later; β has a Rayleigh distribution; ϵ has a uniform distribution. The variance of β is designated here for convenience as 2σ.

The ratio of the intensity of the direct term and the sum total of the scatter terms is dependent on the elevation angle of the satellite. Estimates of the ratios of these two terms can be obtained from the results of Bergmann[36].

These results were given in Section 4.6 where it was shown that for vertical propagation, in which case the path length is about 10,000 yards, the rms intensity of the fluctuations of the received signal is only 0.05 db. This implies that the combinations from the scatter components is only about one-half percent of the contribution from the direct path. For low

elevation angles the same theory predicts that the depth of the amplitude fading would be about 0.8 db. Hence for low elevation angles (elevation angles resulting in path lengths of about 60,000 yards), the contributions from the scattering in the atmosphere can be appreciable.

The multipathing from the second phenomenon is illustrated in Figure 4-36. Since the scale size for the inhomogeneities is of the order of 100feet, such multipathing would be observed for antennas having a size greater than 100 feet. Such an antenna is the Haystack antenna. If the antenna size is slightly over 100 feet, there will be more than one direct path, hence the return signal will have the form

$$e_r(t) = s(t-\tau)\left[\alpha_1 e^{-j\delta_1} + \alpha_2 e^{-j\delta 2} + \beta_e^{-j\epsilon}\right] \qquad (4\text{-}7)$$

where the direct signal by two direct paths of intensities α_1 and α_2 and phase δ_1 and δ_2 have been approximated. Assuming that the satellite is at a low elevation angle such that the path through the atmosphere is

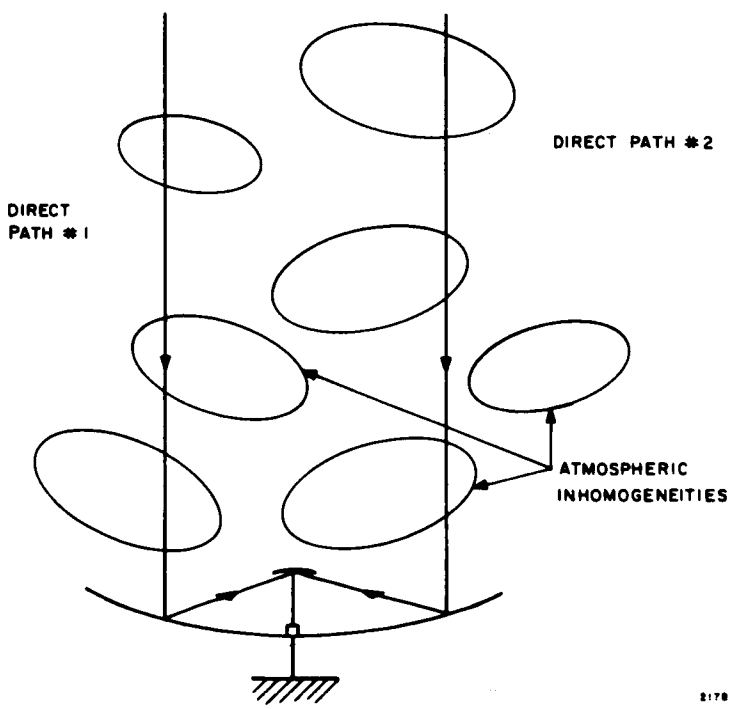

Figure 4-36 Direct Path Multipaths

100,000 feet and the scale size is 100 feet and that the intensity of the index fluctuations is of the order of 0.2 N units (this is a reasonable value based on results given by Crain, et al,[33], it follows that the difference in delays between the two paths would be of the order of only 0.6 millinanoseconds and hence is inconsequential. The curve given in Figure 4-34 indicates that the rms value of the path length differences over a 50 foot dish is 0.08 cm. or, equivalently, 2.7 millinanoseconds indicating that the above estimate is perhaps somewhat optimistic, but still the effect can be neglected.

The coherence bandwidth for the channel is determined by the multipath spread, that is, the maximum difference in delay between the earliest arriving signal and the latest arriving multipath signal. The analysis given by Muchmore and Wheelon[39] predicts that the multipath spread due to scattering should be less than a nanosecond. Although there is some question as to the validity of Muchmore and Wheelon's analysis, assume for the moment that their prediction is correct. As was pointed out above, the direct path multipath spread for low elevation angles, where the path is about 100,000 feet, is negligible even when very large antennas are used. Hence the expected coherence bandwidth can be expected to be larger than one gigacycle at the millimeter-wave frequencies of interest.

4.8 Propagation Through a Plasma

A vehicle which re-enters the earth's atmosphere while traveling at hypersonic velocities becomes enveloped in a shock layer of compressed and heated air. As the vehicle descends into the atmosphere, the air temperature in the shock layer rises to several thousand degrees Kelvin. While in the region of elevated temperatures, the air in the shock layer becomes thermally ionized, and consequently, electrically conducting. This phenomenon can effect communications in several ways: telemetry signals can be severally attenuated; the plasma can have an effect on the

effective noise temperatute of an antenna and consequently degrade receiver sensitivity; and the plasma can lower the breakdown level of the antenna.

Millimeter-wave communication systems can be used when the communicating vehicle is enveloped in plasma because:

a. The attenuation of the plasma decreases with increasing frequency;
b. The degradation in receiver sensitivity is negligible when the signal frequency is greater than the plasma frequency; and
c. The breakdown power level increases with increasing frequency.

Experimental evidence indicates that antenna breakdown is not a problem for the satellite transmitter power levels contemplated in the millimeter wave communications program.

Although this study was not directly related to the problem of propagating through a plasma, it must be pointed out that one must determine the effects of propagating through the atmosphere before an optimum re-entry communications frequency can be chosen which represents the best tradeoff between plasma effects and propagation effects. As a convenience for those readers interested in evaluating millimeter-waves for communication with vehicles re-entering the earth's atmosphere, a detailed review of available literature was given in Section 3.6 of the First Quarterly Report.

Section 5
DEFINITION OF BASIC MEASUREMENTS

Three channel probes or test waveforms, based on AM, PAM and PAM/FM type modulation schemes, are discussed analytically to show how they represent most modulation systems and to explain how basic signal measurements using these waveforms can be used to describe the communication channel functions which were defined in Section 3.2. Hardware implementation of these three test waveforms is discussed in Section 7.5.

Since it is essential that the weather model involved, at the time the channel is being probed, be accurately described in order to explain certain atmospheric effects on the transmitted waveforms, the basic meteorological radiometric and radar correlative measurements are also discussed in this section.

5.1 Basic Signal Measurements

In order to determine the performance of the space-earth link at millimeter wave frequencies when various types of analog and digital modulations are used, it is necessary to characterize the channel. In order to know the characteristics of the channel, it is desirable to obtain a reasonable channel model and, in turn, a measure of the parameters specifying the channel model. A somewhat detailed description of a general channel model that can represent any communications link was given in Section 3.1 and a description of the anticipated channel model for the millimeter communication link is given in Section 4. In summary, the pertinent characteristics which describe the channel are:

1) The multipath structure of the channel.
2) The dispersion introduced by each of the multipaths.

3) The time variations of gain and delay for each of the multipaths.

4) The amplitude and phase characteristics as a function of frequency for the overall channel.

5) The noise characteristics of the channel.

Knowledge of the above characteristics would give a fairly complete description of the channel. In particular, it would give the total coherence bandwidth, the selective fading, and the flat fading of the channel. Other factors, not included in the above model, which are also of interest are the spatial decorrelation distance, the polarization diversity exhibited by the channel, and any angle diversity introduced by the channel. Knowledge of all of the above characteristics, as a function of meteorological conditions, location of the ground system and the elevation and velocity of the satellite, would provide a basis for determining the performance of the communications system using various types of modulations.

Ideal waveforms can be specified which give a measurement of the first four characteristics listed above. Such a waveform would have an impulse-like characteristic which enables it to measure the scattering function of the channel. A detailed discussion of optimum test waveforms and their properties was given in Section 3.1.2. In the discussion which follows, waveforms are presented which, although not optimum, provide information on the channel characteristics that apply for determining the system performance for most modulations of interest. Three types of test waveforms are considered. These are an AM waveform with two side bands, a PAM test waveform which is a time quantized pulse amplitude modulated waveform, and a PAM/FM test waveform, which involves modulating the FM carrier with a PAM waveform. The AM probe yields basic phase and amplitude data while the PAM probe yields indication of communication system performance for the PAM, PWM, PPM, PAM/AM and PPM/AM family of modulation systems; and the PAM/FM probe yields indication of communication system performance for the PAM/FM,

PWM/FM, PCM/FM, PPM/FM, and FM/FM family of modulation systems. Where possible, it would be desirable to design the system so that it could transmit all of these waveforms in a programmed manner.

5.1.1 AM Test Waveform

The simplest waveform under consideration consists of an amplitude modulated carrier. The carrier is modulated by a single sinusoidal signal so as to produce two sidebands, one below and one above the carrier, each a distance away from the carrier equal to the modulation frequency. The modulation index is made as close to 100 percent as is deemed safe without risking the possibility of distortion due to having a modulation greater than 100 percent.

The receiver for this type of waveform would filter out the carrier and phase lock a local oscillation signal to the incoming carrier waveform. The phase lock signal is used in order to enable measurements of the phase shift of each of the sidebands relative to the carrier signal. The phase shifts are measured in both magnitude and sign. In addition to measuring the phase shifts of the sidebands, the amplitudes of the sidebands as a function of time would be measured. The amplitude of the carrier as a function of time would also be measured. The time between samples would be determined by the coherence and the strength of the transmitted signal. It is expected that the integration time required in order to obtain a good signal-to-noise ratio for the receiver signal is from 0.01 to 0.1 seconds. Hence the time between the samples of the phase and amplitudes of the carrier and side bands would be in the same range.

The amplitude modulated test waveform just described has the advantage of providing a measure of the phase and amplitude transfer characteristics of the channel at three frequencies in one measurement. By using a different modulation frequency for different measurements, the transfer characteristics can be obtained over different points in the channel bandwidth.

Considerations are being given to modulating with various signals between 5 mc and 50 mc to measure the coherence bandwidth for high data rate systems and perhaps with a 5 kc signal to measure the characteristics for the channel for a telemetry signal.

It is important to point out that a measurement of the channel characteristics can be obtained almost as readily with the use of AM waveforms as with the optimum test waveform mentioned in Section 3.1.2. That is, theoretically the same information can be obtained about the channel with measurements involving the use of AM test signals as with the ideal test waveforms. This was shown to be true in the mathematical discussion, which is based on References 40 and 41 in Section 4.1.1 in the First Quarterly Report.

The circuitry by which the test waveform can be used to obtain the sum of the phase shifts introduced on each sideband is presented in Section 10.1. An alternate method involving the use of a frequency discriminator was described in Appendix IV of the First Quarterly.

A discussion of the data processing requirements centering around the use of the AM waveform was given in Section 7 of Volume II.

5.1.2 PAM Test Waveform

The AM test waveform described above has the advantage of providing the transfer characteristics of the channel as a function of frequency. The test waveform also provides information on selective frequency fading if such fading exists and information on the coherence bandwidth and multipath structure of the channel. From this information the performance of various modulations can be determined for the channel under consideration. However, rather than indirectly obtaining information on the performance of various modulations from transfer characteristic measurements, it would be more desirable to measure the effects on the types of modulations to be used directly and from these obtain an indication of the performance of channel for these modulations. To do this, it is desired to use a test waveform which

comes as close as possible to the actual types of modulations to be used. In particular, if a PAM/AM waveform is to be transmitted, then a test waveform which is similar to a PAM/AM waveform should be transmitted. In this way, it can be determined directly if the channel has sufficient bandwidth to carry the PAM/AM waveform under consideration, by measuring the rise time, pulse width and increase in sidelobe level. Such a test waveform is suggested in this subsection. The PAM test waveform under consideration applies to other types of modulation as well as PAM/AM modulation. In particular, it would provide an indication of how well the system performs for PAM, PWM, PPM, PWM/AM, and PPM/AM. This test waveform involves the transmission of narrow pulses and at the same time permits transmission at the same power level and reception with the same integration time as that for the AM waveform.

The waveform involves the transmission periodically of a narrow pulse. The pulsewidth is made as narrow as possible and the duty cycle for the pulse train is chosen to be about 0.1. At present the receiver appears to be limited to a bandwidth of about 100 mc. Hence, a reasonable pulsewidth appears to be about 10 nanoseconds and the time between pulses would be about 100 nanoseconds. Figure 5-1a shows the amplitude modulation on the carrier signal applied by the test waveform. The spectrum for the test waveform is shown in Figure 5-1b.

The question arises as to how to process the signal in order to remove the noise. In order to suppress the noise from the waveform, a processor is used in the receiver which is essentially a matched filter. It is noted from Figure 5-1b that the spectrum of the test waveform consists of a line spectrum. About 90 percent of the total signal energy is contained in the spectral lines within the band from -100 mc to +100 mc. Nearly all the energy would be contained within a bandwidth from -200 mc to +200 mc. Assume that a 10-cycle integration filter was required to process the received signal if no

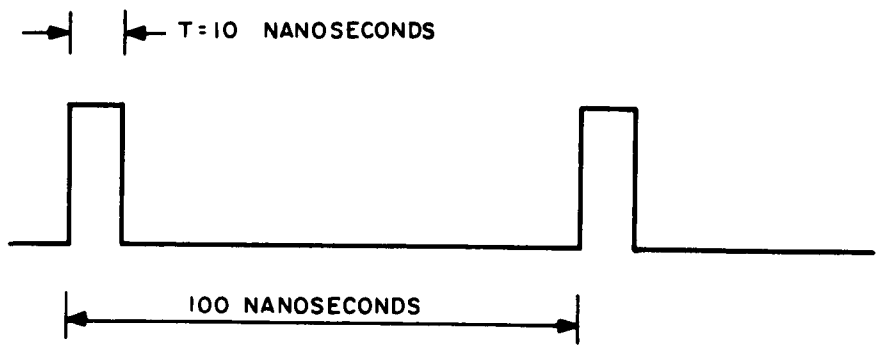

a. Amplitude Modulation

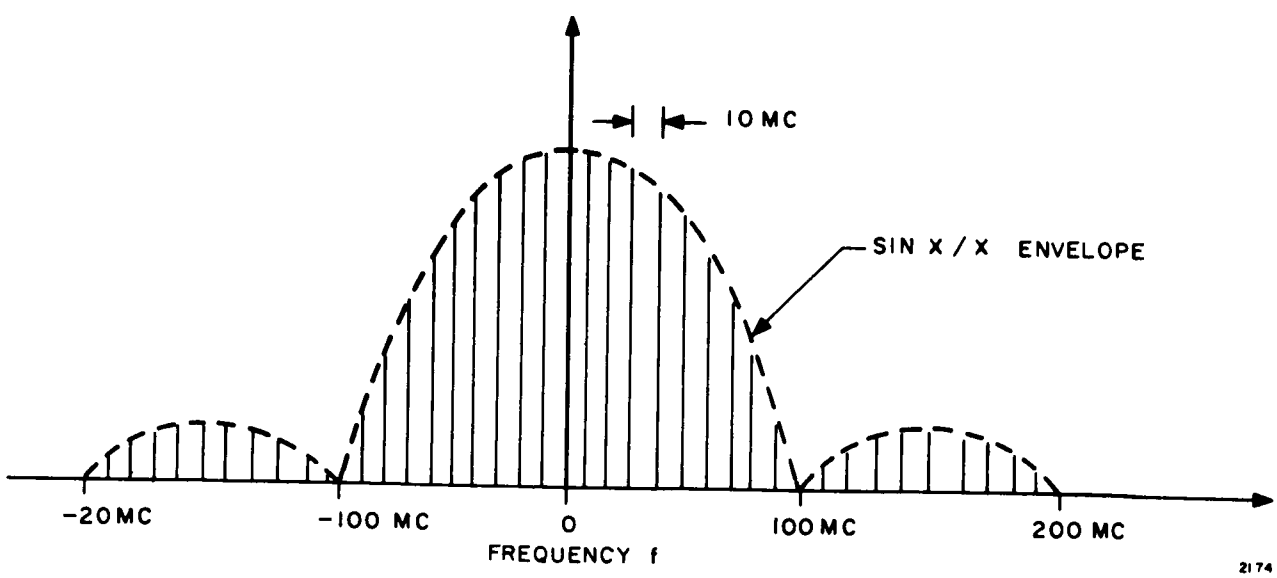

b. Line Spectrum

Figure 5-1 AM Test Waveform

modulation were placed on the carrier, that is, if only the carrier were transmitted and all the energy were in the carrier. To process the modulated waveform, 10-cycle filters are placed at each line in the spectrum shown in Figure 5-1b. For the modulation specified about a total of 40 filters would be required in the receiver. By adding the outputs of these filters the received pulse train could be obtained without the noise, or at least with a low noise level. The outputs of the filters are weighted before adding. In particular, greater weight is given to the filters in which the signal-to-noise ratio is larger. In other words, the weights are in proportion to the signal-to-noise ratios anticipated for each of the filters. In an actual train of 10 nanosecond pulses, the line spectrum would not, of course, extend out as far as indicated. Instead, because of rounding of the pulses, the line spectrum would drop off faster so that fewer than 40 receiver filters would be required.

To determine how effective the receiver comb filter processor is, in suppressing the noise, a comparison needs to be made of the signal-to-noise ratio obtained with the pulse amplitude modulation test waveform described above (and its receiver processing) with the signal-to-noise ratio achieved if only the carrier were transmitted and all the energy of the transmitted waveform were in the carrier and a 10-cycle integration filter were used for the carrier signal. To do this the $\frac{\sin x}{x}$ envelope for the line spectrum of the test waveform given in Figure 5-1b shall be approximated by a rectangular envelope extending from -50 mc to +50 mc. Hence, to process the signal in the receiver, 11 filters would be required with signal-to-noise ratio in each filter being the same at the receiver. Since there are 11 filters, the noise at the output of the summer will be 11 times greater than the noise at the output of one filter or, in particular, 11 times greater than the noise for the CW system. The signal power at the output of the summer will be the same, however. Hence, the average signal power-to-noise ratio at the output of the summer will be 1/11 that for the case where just the carrier is transmitted and all the energy is in the carrier. However, since the duty cycle is 0.1 during the time when

the signal peaks, the signal power-to-noise ratio will be 10 times greater than the average; hence, the signal power-to-noise ratio for the pulse amplitude modulated test waveform is about the same as for the case when just the carrier is transmitted.

Of course the above conclusion applies only if for a given prime power the same average output power can be achieved for the CW and pulse system. This would be the case if a hard tube or power line type modulation system is used for the generation of the pulse train. However, in the event that an RF line modulator is used to generate the train, the output power is reduced by the duty cycle of the pulse system.

Due to the complexity of the receiver processor for the pulse amplitude modulated test waveform, this waveform could be used only for down transmission from the satellite, where the processing would be done on the ground receiver. The parameters given above for the test waveform correspond to testing out the performance of the channel for a high data rate system, or for a time multiplex telemetry system. In order to check out the performance anticipated for one channel of a frequency multiplexed telemetry system, a modulation is transmitted in which the pulse width is 200 microseconds and the time between pulses is 2 milliseconds.

The data observed on the received signal would be the rise time, the pulsewidth, the sidelobe level, and the fading rate of the signal. Computations would be made of the probability distribution of the fading and the time autocorrelation function of the fading.

5.1.3 PAM/FM Test Waveform

In many systems, frequency modulation is used. For example, in the Applications Technology Satellite (ATS) program the communications system uses wide band 4 Gc and 6 Gc FM/FM TV links. Other types of FM considered for satellite applications are PAM/FM, PWM/FM, PCM/FM, and PPM/FM. A test waveform is described in this subsection which comes close in form to

the type of FM to be considered in many of the satellite applications. As in the case of the PAM/AM test waveform, it is possible with this test waveform to operate at the same transmitter power level and integrate between 0.01 and 0.1 seconds in order to suppress the background noise.

One of the frequency modulations for the carrier being considered is shown in Figure 5-2. The period T, shown in the figure is made as narrow as possible. Due to the receiver limitations already mentioned, it appears that the minimum period, T, is about 100 nanoseconds to take advantage of the noise suppression characteristics of FM by using a modulation index of three and at the same time remains in a 100 mc bandwidth. For this modulation index and for the above mentioned pulsewidth of 100 nanoseconds, the signal bandwidth would be about 30 percent larger than the total deviation of 60 mc. To arrive at this anticipated bandwidth, use is made of the results obtained by Corrington [42] as to the bandwidth for various modulations.

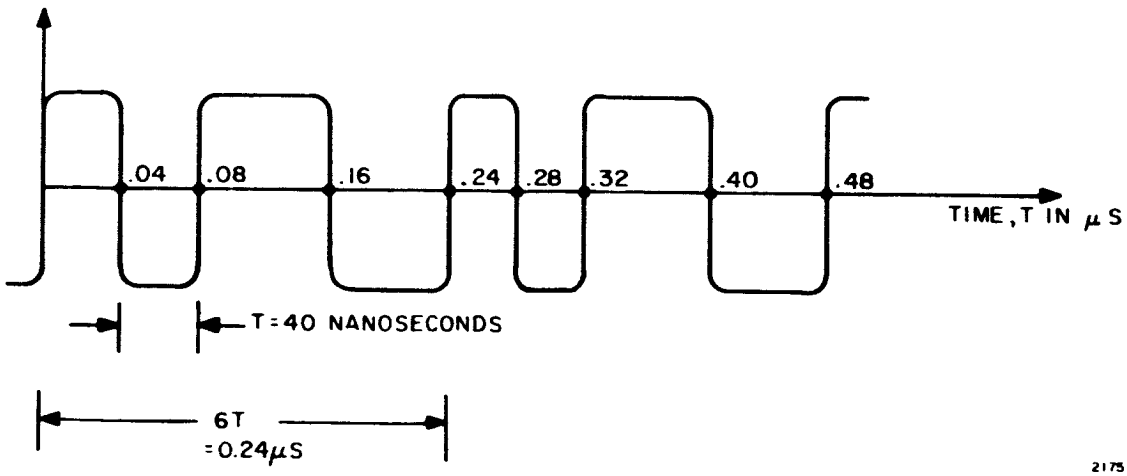

Figure 5-2 Frequency Modulation

In particular, the bandwidth is approximated to be equal to the bandwidth obtained for a triangular modulation; the results obtained for a triangular modulation being somewhat worse than for a sinusoidal modulation. Figure 5-3 shows the curve for the increase in bandwidth above the total deviation for the case where the carrier is modulated by a triangular waveform. The figure gives the signal bandwidth as a function of the modulation index. Three different types of signal bandwidths are given. These are indicated by curves A, B, and C. Curve A gives the signal bandwidth occupied by the triangular wave modulated carrier which is defined as the distance between the two frequencies beyond which none of the side frequencies is greater than 1 percent of the carrier amplitude obtained when the modulation is removed. Curves B and C give the bandwidth defined as the distance between two frequencies beyond which none of the side frequencies is greater than 0.1 and 0.01 percent, respectively. For 100 mc bandwidth receivers it is apparent from the figure that a bandwidth between curve A and B is being used in the system.

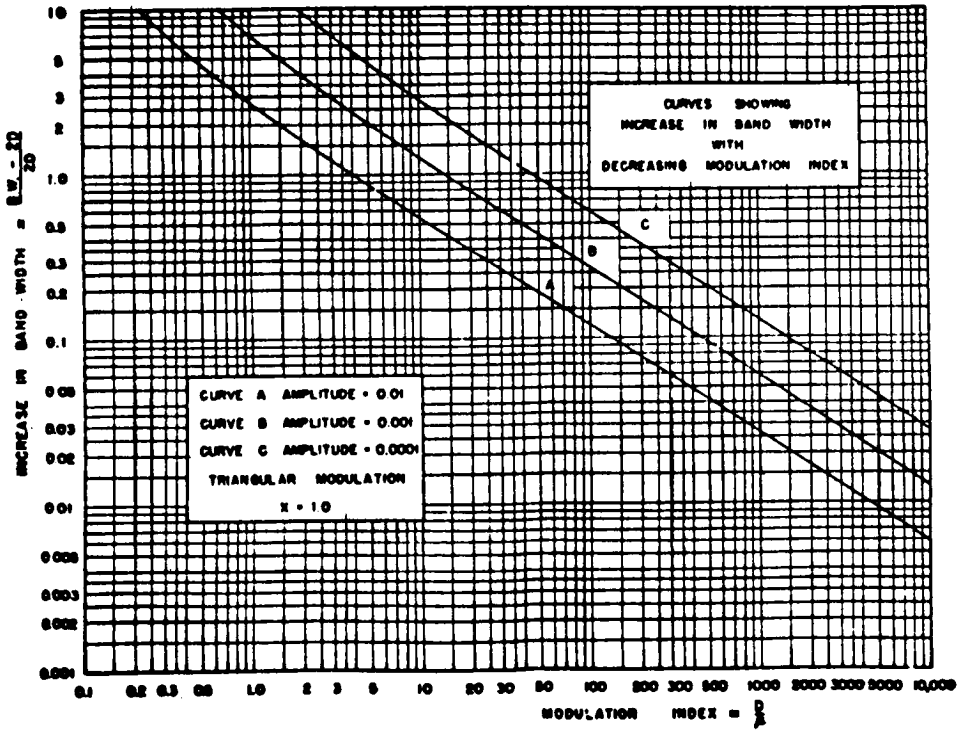

Figure 5-3 Variation of Bandwidth with Modulation Index

The receiver processor for the FM waveform would be similar to that used for the PAM test waveform. Figure 5-4 gives a rough sketch of the line spectrum for the FM test waveform. Most of the energy in the test waveform is anticipated to be centered about the frequencies ±30 mc away from the carrier frequency. The major portion of the energy should be in about 11 tones about the frequencies -30 mc and +30 mc away from the carrier. A total of about 80 filters would be required in the receiver in order to process essentially all the signal energy. Weightings would be used at the output of each filter before the summation takes place. The weightings would be proportional to the signal-to-noise ratios anticipated for each of the filter tones. The FM test waveform can be expected to yield a signal-to-noise ratio at the output of the processor not far below that obtained if a CW waveform were transmitted with the same energy contained in the FM test waveform. This arises from the noise suppression due to the comb filtering and the inherent noise suppression of an FM system.

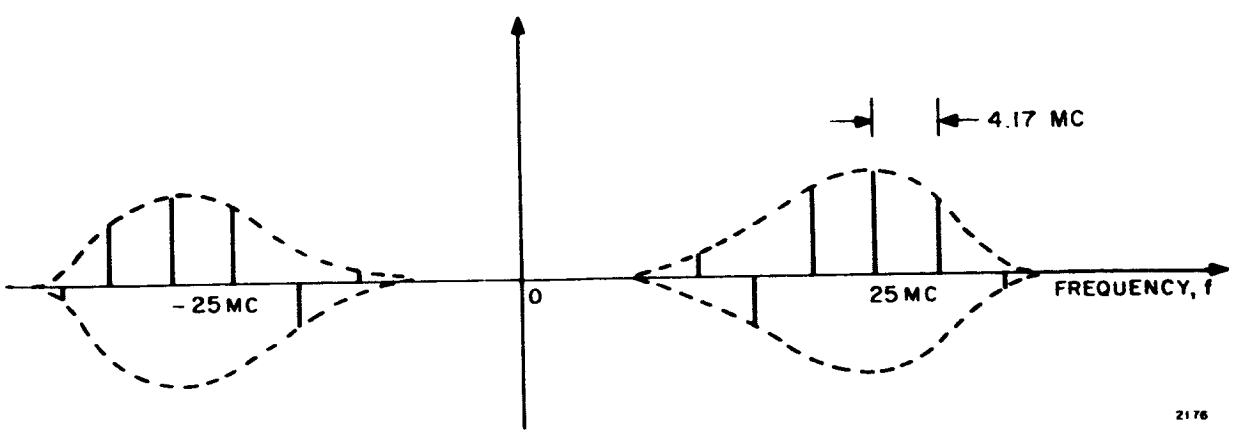

Figure 5-4 Line Spectrum of Frequency Modulation

The waveform parameters given above correspond to those that would be used to test out the channel for high data rate systems. For checking the performance of the channel for telemetry data transmitted on a PCM/FM or simular modulation, the period T would be made equal to 200 microseconds.

Other basic types of modulation waveforms for the FM carrier are possible. However, the one given in Figure 5-2 seems to be the most suitable. One reason for this is that as much of the energy as possible is placed at the frequencies with maximum deviation from the carrier, with as little energy as possible being placed at the carrier frequency. This is desirable since when the signal is at the carrier frequency, the output of the FM discriminator is zero, being at the carrier corresponding to having a zero modulation signal or a zero output so that all the energy at the carrier would be wasted as far as the modulation waveform is concerned. Since no phase locking is employed in the receiver when an FM test waveform is used, this does not offer any disadvantage because the receiver uses frequency locking.

As in the case of the PAM test waveform, measurements are made on the demodulated waveform of its rise time, pulse width, and sidelobe levels. Also, measurements are made of the fading of the signal. These measurements would enable the determination of the distribution of the fading and its time autocorrelation function.

5.2 Basic Correlative Measurements

Basic correlative measurements are required to classify the weather model existing in each test in order that the statistical propagation data can be translated to other geographical locations which experience similar meteorological conditions. Good correlative measurements will also help explain why certain things are happening to the test signals which are being propagated through the complex atmosphere. In addition to the usual surface meteorological data which must be collected at each ground terminal, radiometric measurements in coincidence with the basic signal measurements are a

necessity. The apparent sky temperature, which is the result of these radiometric measurements, directly relates to the atmospheric attenuation due to the water and oxygen content of the atmosphere.

The test signals undergo fading due to multipathing as well as fading due to variations in water content within the receiving beam. The radiometric measurements should, therefore, help us to isolate these two fading effects. A weather radar, preferably located right at the ground terminal, could provide another correlative input - a rainfall rate profile along the communication path. The total effect of rain absorption and scattering can then be deduced by integration of this profile.

5.2.1 Meteorological Measurements

Since weather effects will markedly influence the performance of communications channels in the 10 to 100 Gc frequency range, it is clear that correlative meteorological data should be taken to facilitate communications data analysis. Fortunately, the instrumentation required for this purpose is relatively inexpensive. A description of a low-cost system capable of recording wind speed, wind direction and temperature at the surface is given in Reference 43. Other sensors can be substituted for, or added to, those listed in Reference 43 to cover pressure, relative humidity, and precipitation rate.

Basically, the minimum requirement for meteorological data, to be used in communication channel performance evaluation, is as follows:

- -- Atmospheric temperature
- -- Atmospheric pressure
- -- Atmospheric relative humidity
- -- Precipitation rate
- -- Wind velocity and direction

These measurements should be made at least at ground level at the transmitter site and, if possible, at other points along the transmission path. If accurate

data is available on pressure, temperature and relative humidity, it will be possible to compute the index of refraction. Knowledge of this parameter will assist in determining the reasons for signal fluctuations at a particular time.

Radiosonde correlative measurements would be highly useful since atmospheric temperature, pressure and relative humidity vary with height above the surface. Accurate measurements can be made of these parameters up to an altitude of approximately 50,000 feet; however, radiosondes are capable of rising to altitudes of 125,000 feet. The maximum errors involved in radiosonde measurements are as follows:

Temperature:	$\pm 1^{\circ}$ C referred to surface temperature
Pressure:	±1.5 millibars, over a range of 100 - 1000 millibars ±4 millibars, over a range of 0 - 1000 millibars
Relative Humidity:	±5 percent up to 40°C, dry bulb reading 5 - 10 percent up to 30,000 feet altitude 20 - 50 percent above 30,000 feet

The above performance figures apply to the AMT-4, MT-12 and AMG-9 radiosonde transmitters, except that the last-mentioned equipment does not measure pressure.

The surface and radiosonde measurements should be supplemented with Weather Bureau data during analysis of communications channel performance. This information includes surface, radiosonde, weather radar,and weather satellite data. The Weather Bureau can furnish the necessary information from central data collection and storage facilities.

5.2.2 Radiometric Measurements

Ground based radiometers will measure apparent sky temperature which varies with weather and evaluation angle as shown in Section 4.2. The amount of attenuation due to absorption is well correlated with the apparent sky temperature T_a measured by a radiometer, especially if the apparent sky temperature is less than about 180°K. This relationship is discussed in great detail in Section 3.1, Volume II, Final Report. The relationship between the apparent sky temperature T_a and the attenuation, σ, in decibels for a signal transmitted through the entire atmosphere is shown in Figure 5-5. The curve divides about 180°K to show the area of uncertainty in our present knowledge of the relationship.

Figure 5-5 is based on results of calculations using the method given by Barrett and Chung [44]. The computer program for performing the calculations was described in Appendix II, First Quarterly Report. Points calculated for several clear, cloudy and rainy weather models at frequencies of 10 Gc, 35 Gc and 94 Gc for all elevation angles were plotted to give the average curve shown in Figure 5-1. These models, which are homogenous in the horizontal plane, were described in Section 3.1 of the First Quarterly Report. When using this curve for those models in which the surface atmospheric pressure, P, and surface atmospheric temperature, T, is other than 760 millimeters and 293°K, the abscissa must be multiplied by $\frac{PT}{760 \times 290}$ in order to accomplish the proper temperature attenuation conversion.

The interesting result in this exercise was the lack of spread of the calculated points about the curve of Figure 5-5 for different weather models and different frequencies at temperatures below 180° K. One weather model representing an extreme, and unrealistic, water vapor distribution, was even considered in order to investigate the boundaries of the temperature-attenuation relationships. The extreme weather model is compared with the "standard" weather model in Figure 5-6. The extreme weather model for cloudy weather

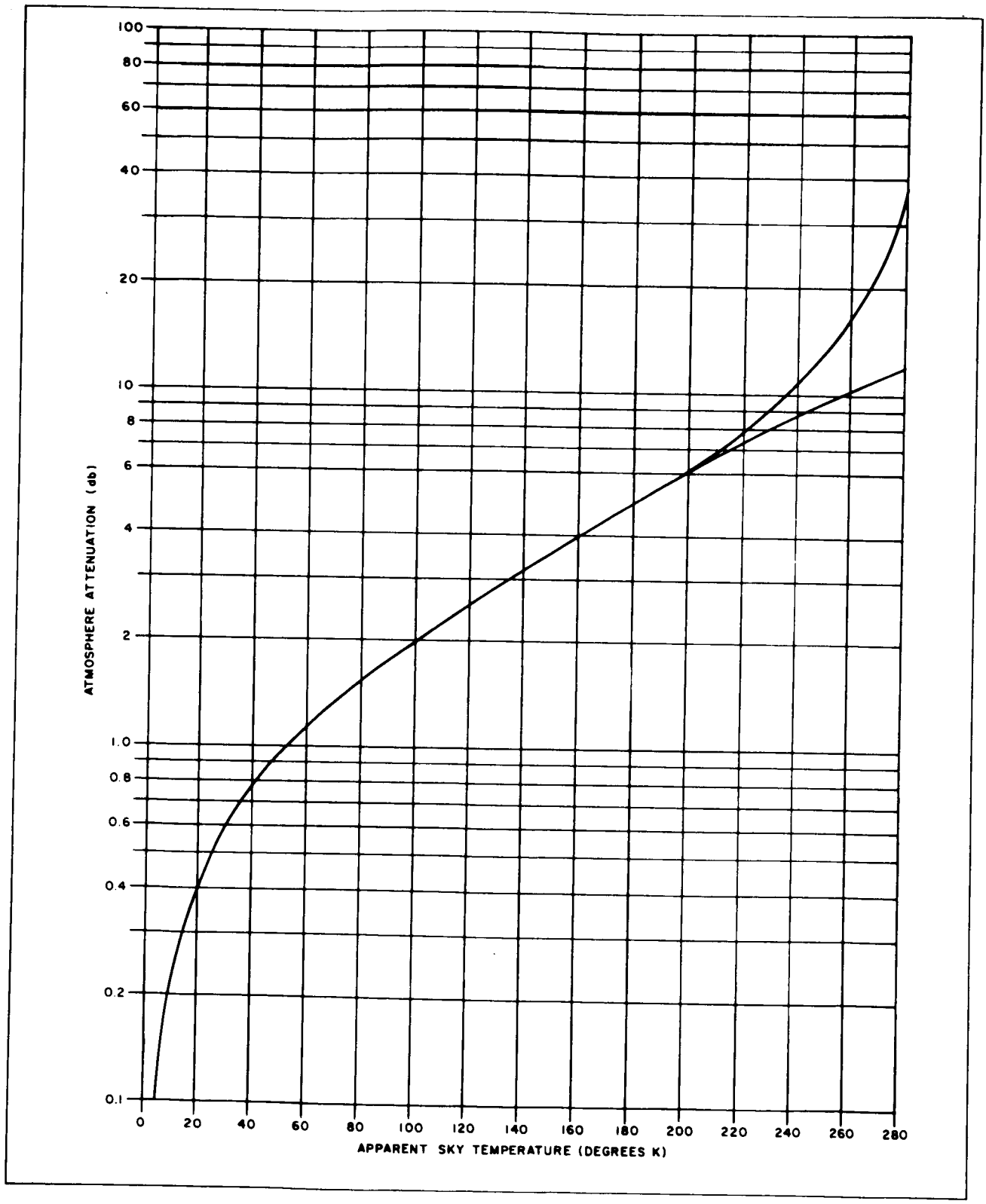

Figure 5-5. Atmospheric Attenuation as a Function of Apparent Sky Temperature

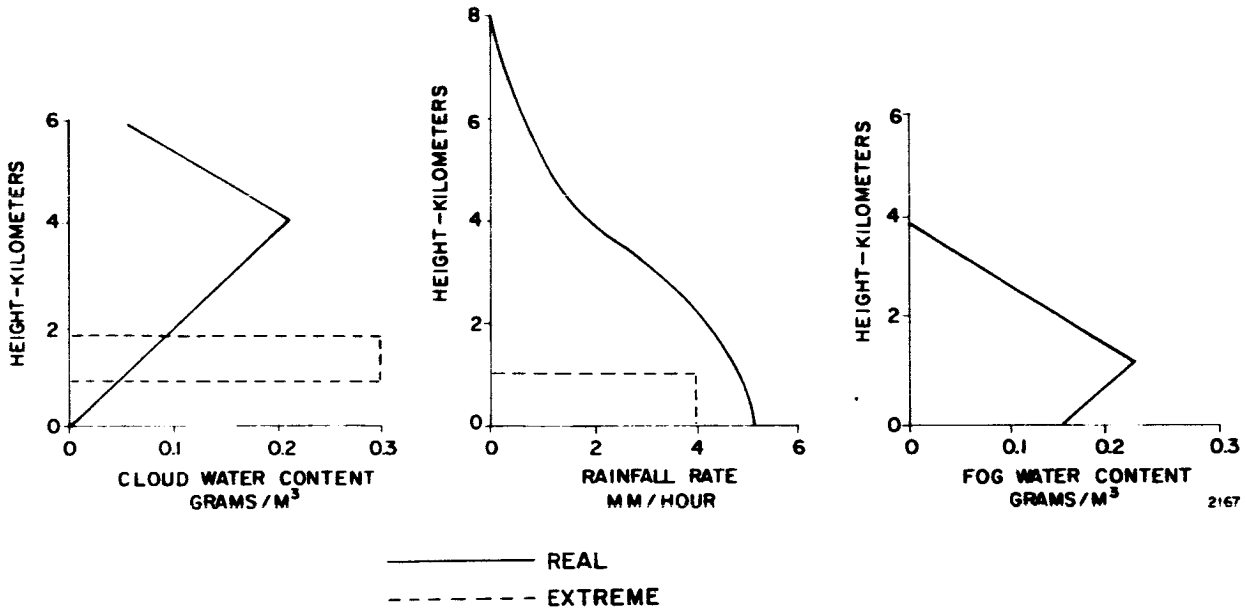

Figure 5-6 Realistic and Extreme Weather Models

consists of a cloud with a uniform water content of 0.3 grams/cubic meter extending from 0.9 kilometers to 1.8 kilometers. The rainy weather models consist of the same cloud and a uniform rainfall between 0.9 kilometers and k sea level. The rainfall rate is 4 millimeters per hour. The comparison between the attenuation-temperature characteristics of the extreme and realistic models, as shown in Figure 5-7, lends validity to the universal characteristic curve of Figure 5-5.

Several important conclusions which can be drawn from Figure 5-5 are:

1) For $T_a \leq 200^{\circ}K$ ($\sigma \leq 6$ db) the uncertainty of σ is $<< 0.1$ db. With a radiometer error of 5% ($\Delta T_a = 10^{\circ}K$ at $T_a = 200^{\circ}K$), the error in σ is ≤ 0.5 db.

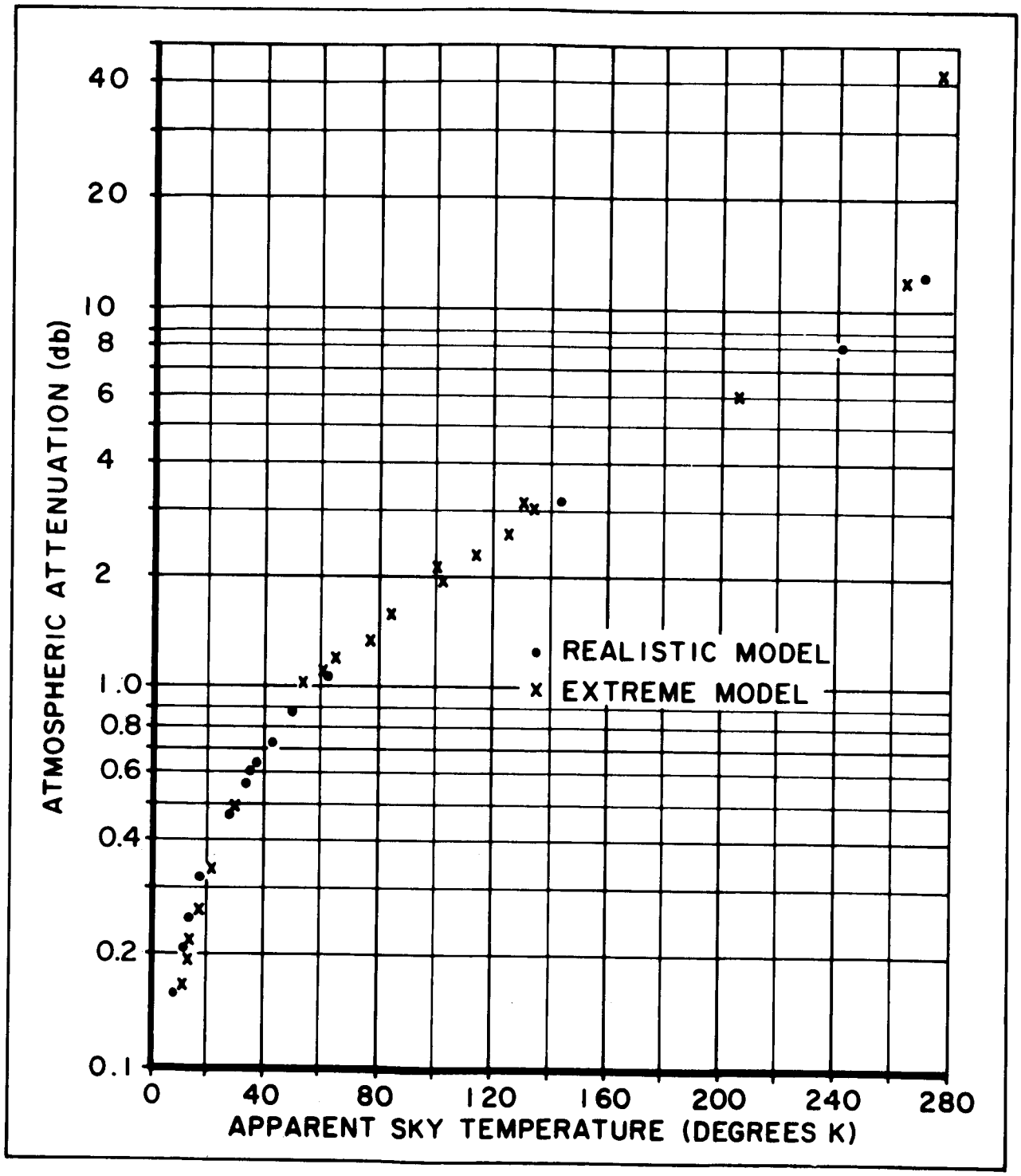

Figure 5-7 Attenuation As A Function of Apparent Sky Temperature For Realistic and Extreme Weather Models at 35 Gc

2) For $T_a \leq 240^oK$ ($\sigma \leq 10$ db) the uncertainty of σ is ≤ 1.0 db. With a radiometer error of 5% ($\Delta T_a = 12^oK$ at $T_a = 240^oK$), the uncertainty in σ is 8.0 to 14.0 db.

3) In the data processing operation T_a can be automatically converted to σ (within the accuracies mentioned above) using curves similar to Figure 5-5 which take into account the surface temperature and pressure underneath the propagation path, the receiver altitude and the carrier frequency.

4) In the data processing operation, the σ obtained from radiometric temperature can be compared with total signal losses obtained from the signal receiver data to determine if fading other than that due to atmospheric absorption exists. As Figure 5-5 shows this can only be done effectively at $T_a \leq 240^oK$ ($\sigma \leq 10$ db) because of present uncertainties in the T_a to σ conversion. If we are interested in fading when $\sigma >$ 10 db (most space-earth system applications are probably not interested in that much of a penalty) then further effort is required. Table 5-1 which was derived from σ versus elevation angle data, given in Figures 4-2 through 4-5 of of Section 4-1, gives the elevation angles at which $\sigma = 10$ db.

TABLE 5-1

ELEVATION ANGLES BELOW WHICH ATTENUATION DUE TO ATMOSPHERIC ABSORPTION IS 10 DB OR GREATER
(degrees)

Weather Conditions	16 Gc	35 Gc	94 Gc
Clear	0	< 5	5
Cloudy	0	5	20
Rain	< 5	10	40

The conversion from radiometric sky temperature to signal attenuation in a space-earth communications link is most accurate when the atmosphere is homogeneous in the horizontal plane. The apparent sky temperature, as measured by a radiometer, represents an average temperature of the medium within the antenna beam while the attenuation of the actual signal depends only on the conically shaped medium between the satellite and the ground atenna. The point is that, if the medium is horizontally inhomogeneous, the received radiation may have gone through a portion of the atmosphere which absorbs significantly more or less than the average absorption indicated by the radiometer. Incidentally, the larger the antenna used by the radiometer and the signal receiver, the more accurate will be the conversion.

To get an indication of the degree of inhomogeneity in the atmosphere, a second signal receiver/radiometer located some distance from the first, could be used. The signals from the two receiver/radiometers would be cross-correlated for various relative delay times. The amount of cross-correlation function could be used to give information on the atmospheric mechanism producing the fading. For example, if the altitude of the inhomogeneities is known, the velocity of motion can be determined from the relative delay time at which the cross-correlation function is a maximum.

5.2.3 Radar Measurements

At ground terminals where considerable millimeter-wave propagation measurements are to be made, it appears worthwhile to employ a weather radar as a correlative tool to determine precipitation rates along the propagation path. A radar such as the WSR-57 rating at 10 cm should detect precipitation at rates greater than 1 mm/hr at most altitudes of interest. In experiments involving synchronous satellites, that is, when the propagation path is fixed, surface rate data from rain gauges underneath the path could be a practical supplement or alternative to the radar data.

A good general introduction to the capabilities of weather radar is given in "Radar Meteorology".[45, 46] There are two types of weather phenomena which will produce a radar return. One is moisture droplets in the atmosphere where there is a marked change in the index of refraction, but no water or ice particles. (Returns from this latter type of phenomena are called "angels.") Both of these phenomena will affect the propagation of millimeter waves, the moisture particles producing absorption and scattering, and the angels producing scattering and multipath effects.

One might expect, therefore, that the number of angels detected by a weather radar would give significant information about the amount of scatter of millimeter waves or the amount of signal degradation due to multipath. Unfortunately, this does not seem to be true. For one thing, there is some disagreement as to the exact cause of angels.[47, 48] Even knowing the mechanisms, it is difficult to predict theoretically the relation between the power scattered in different directions from turbulent variations in the refractive index.[49, 50] The signal observed by a radar is, of course, a result of radiation scattered directly back to the radar, while the signal received from a satellite is the result of radiation scattered in the forward direction. Furthermore, no applicable experimental results are available. It is expected, therefore, that while a weather radar will be quite useful in indicating if there is something invisible in the atmosphere which is producing fading, a weather radar probably cannot be used to determine whether the cause of fading is due to scattering or due to multipath.

Moisture particles in the atmosphere produce a radar return. The amplitude of the return depends upon the wavelength of the radiation. Short wavelengths (about 1 cm) can be used to detect some clouds but on one experiment only about 50% of the clouds produced a return.[51] Furthermore, because the detected clouds absorb as well as reflect, it is difficult to make quantitative estimates of the water content of the clouds from radar returns.

Therefore, it does not appear to be useful to attempt to use short wavelength radars to estimate the absorption due to the water content of clouds.[58]

Radiation at 10 cm wavelengths is not appreciably scattered by the small moisture particles making up clouds, but is scattered by the larger particles making up rain, snow or hail. Therefore, a 10 cm radar would be useful in looking through a cloud cover to determine if there is precipitation along the propogation path.

A great deal of work both theoretical and experimental, relating to the amplitude of the power return from a rainstorm to the rainfall rate has been done.[45, 46] The major result is Equation (5-1).

$$\bar{P}_r = \frac{C}{r^2} R^{1.6} \qquad (5\text{-}1)$$

where,

$\bar{P}_r$ = the power, in watts, received from a rainstorm

r = the slant range, in meters, from the radar to the storm

R = the rainfall rate in mm/hr.

C = constant depending on the radar

The formula for C is given in Equation (5-2)

$$C = 128\pi^7 \frac{P_t A_p \gamma \beta \tau}{\tau} K^2 N \qquad (5\text{-}2)$$

where,

P_t = transmitted power in watts

A_p = area of antenna in square meters

γ = antenna azimuth beamwidth in degrees

β = antenna elevation beamwidth in degrees

τ = pulse width in seconds

λ = wavelength in meters

$K^2 = \frac{m^2 - 1}{m^2 + 2}$ where m is the complex index of refraction. A value of 0.93 for K^2 is assumed which corresponds to liquid water at about 10^{o}C.

N = empirical constant which relates power backscatter to rainfall rate at those frequencies where the Rayleigh approximation applies. A value of 0.4×10^{-16} is used as representative for most rains which includes a 0.2 correction factor to make the theoretical results agree with experimental data.

Based on the characteristics for the WSR-57 radar, which are given in Table 5-2, the constant C comes out to be 7×10^{-4} and, using Equation (5-1) the minimum detectable rainfall rate at any given slant range is:

$$R_{min} \simeq \left[100 \quad P_r \quad r^2\right]^{.625} \qquad (5\text{-}3)$$

Figure 5-8 is a curve of minimum detectable rainfall rate as a function of range for the radar constant $C = 7 \times 10^{-4}$. Using this curve and the altitude versus slant range curves of Figure 5-9 (corrected for atmospheric refracting using refractive index, $n(h) = 1 + 0.000313\, e^{-0.04385h}$ with h in thousands of feet), the performance of the WSR-57 radar can be estimated. This radar should detect most rainfall rates of interest and accurately determine rates greater than 1 mm/hr at all slant ranges of interest above 2^{o} elevation.

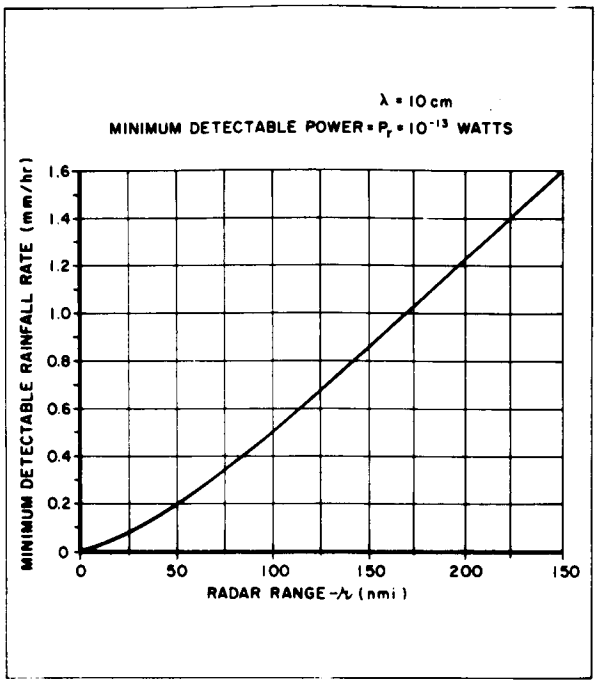

Figure 5-8 Minimum Detectable Rainfall

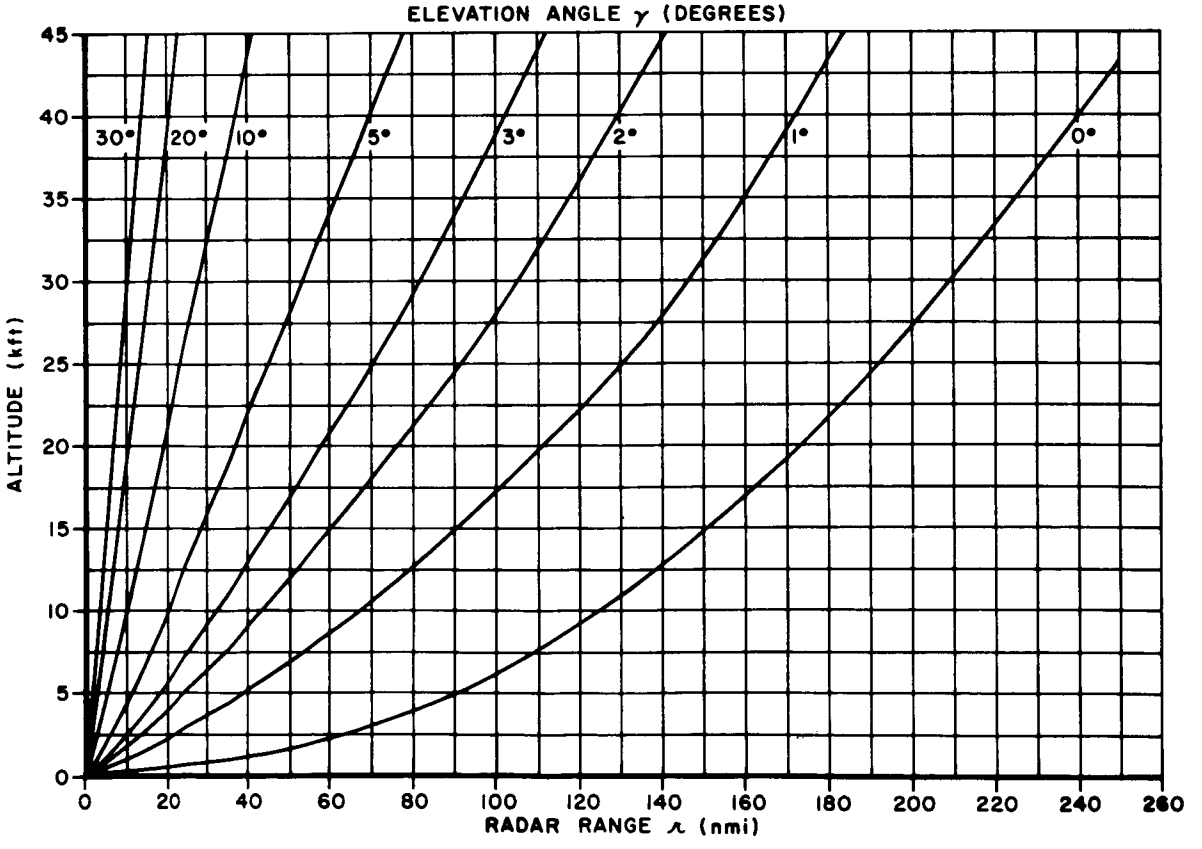

Figure 5-8 Altitude Versus Slant Range

TABLE 5-2

S-BAND CHARACTERISTICS OF THE WSR-57 WEATHER RADAR

Antenna Gain	38.5 db
Antenna Beamwidth	1.8 degrees
Antenna Diameter	12.0 feet (3.7 meters)
Peak Power	500 kilowatts
Pulse Width	0.25 & 4.0 microseconds
Pulse Repetition Frequency	658, 154 pps
Resolution	1.6 mm/hr. at 250 n mi.
Elevation Scan	-10 degrees to 45 degrees
Azimuth Scan	360 degrees

Battan[45] shows that the value of the rainfall rate calculated from radar data with Equation (5-3) can actually vary by plus or minus 50% from the rate measured by a network of rain gauges. This conclusion is also implied by the results of Hathaway and Evans.[53] Some of this spread results from the wide variation in rainfall rates within a storm. It seems clear that the network of rain gauges was not nearly dense enough to give close estimates of rainfall rates in the experiment of Hathaway and Evans and also in other experiments.[54,55]

It should be pointed out that the antenna beamwidth for a weather radar will be much wider than that of the receiver for the millimeter waves. This will mean that the weather radar return will indicate the average amount of rainfall in a volume which may be different from the actual rainfall through which the signal from the satellite passes. There are two ways to improve the resolution of the radar:

1) Instead of letting the radar beam track the millimeter-wave beam, the radar antenna drive system is programmed to scan the beam first in the elevation plane containing the

propagation path and then in the azimuth plane containing the propagation path. By knowing the shape of the beam and applying the proper coordinate conversion, the accuracy of the rate profile can be improved.

2) The WSR-57 radar also has C-band and X-band heads. With the same antenna size, each angular dimension of the resolution volume can be reduced by factors of 0.55 and 0.3 respectively. However, when operating at wavelengths below 10 cm, attenuation corrections must be made or else the conversion from power received to rainfall rate will be in error. Radiometers provide the total attenuation for the millimeter-wave signals but it does not provide an attenuation profile along the propagation path from which to make the necessary corrections. Therefore, if we increase the frequency of the radar to improve resolution we probably do not gain much in rainfall rate accuracy.

Once the rainfall rate has been estimated, the amount of attenuation due to rain can be calulated. This attenuation is caused both by absorption and scattering. This problem has been studies theoretically and experimentally. [45,56,57] The theoretical result is that the attenuation is given by Equation (5-4):

$$\text{Attenuation (db)} = K_2 \int R^{\gamma} \, dr \qquad (5\text{-}4)$$

where,

R is the rainfall rate as a function of slant range r and,

K_2 = a constant dependent on the wavelength (at 1 cm, the value of K_2 is about 0.2 db/km per mm/hr)

γ = another constant also dependent on the wavelength (at 1 cm, the value of γ is about 1.0). (45)

Experimental results (56) are summarized in Table 5-3 and Table 5-4. Table 5-3 indicates the spread in the value of the attenuation (per unit length, per unit rainfall) at different wavelengths and Table 5-4 indicates how well the experimental data fits the theoretical results, at least at one frequency.

It would appear then that the weather radar would be useful in giving an estimate of the rainfall rate along the propagation path and subsequently the total signal attenuation. Such an estimate could also be obtained from a line of rain gauges along the propagation path (assuming a synchronous satellite is used) and such a line might be valuable as a check on the radar estimates if one can assume accurate altitude profiles of rainfall rate. Incidentally, there is evidence of precipitation in the atmosphere which does not reach the ground. The weather radar is especially useful for night time measurements or for measurements in the presence of fog, when the millimeter wavelength receiver operator cannot observe weather conditions along the propagation path.

TABLE 5-3

SUMMARY OF ATTENUATION MEASUREMENTS

Organization	Wavelength λ(cm)	Attenuation, db/km per mm/hr.		
		Upper Bound	Lower Bound	Average
BTL	3.2	0.090	0.012	0.019
RL	1.25	0.40	0.09	0.17
NRSL	1.25	0.34	0.23	0.25
BTL	1.09	0.27	0.15	0.18
Clarendon	0.96	0.25	0.10	0.15
BTI	0.62	0.37	0.27	0.31

TABLE 5-4

COMPARISON OF EXPERIMENTAL AND THEORETICAL ATTENUATION

(λ = 0.6 cm)

Rainfall Rate	Attenuation (db)	
R(mm/hr)	Experimental	Theoretical
10	3.7	3.8
20	7.4	7.0
30	10.6	10.0
40	13.6	12.7
50	16.0	15.4
70	20.4	20.0
100	26.5	27.0

Section 6
SYSTEMS PERFORMANCE ANALYSIS

Based on the measurements made with the test waveforms specified in Section 5.1, data on the characteristics of the communications channel will be determined and, from these characteristics, the performance of the channel for various modulations can be inferred.

First, consideration is given to the effect of fading on an FSK system. Next, the effects of large dispersions over the signal band on binary AM, PM and FM signals are given. Finally, the effects of multipathing on a wideband FM system are discussed.

6.1 Effects of Fading on FSK Systems

The results given by Turin (58) can be used to determine the performance of an FSK system in a fading channel, in particular, in a Rician channel which is characterized by the signal given by equation (6-1).

$$e_r(t) = s(t - \tau) \left[a\, e^{-j\delta} + \beta\, e^{-j\epsilon} \right] \qquad (6\text{-}1)$$

where

$s(t)$	=	the transmitted signal
τ	=	the propagation time
a	=	the amplitude of the return received over the direct path
δ	=	the phase of the return received over the direct path
β	=	the instantaneous amplitude of the sum of the scattered signals
ϵ	=	the phase of the sum of the contributions from the scattered terms

coherent receiver it is assumed that α and δ are not known and that the receiver processes the returned signal optimally on the basis of an unknown α and δ. Assume that it is desired to design for a bit error rate of 10^{-3} when there is no random term, that is, when there is no scattering term so that $\gamma = \infty$. From Figure 6-1 it follows that the signal-to-noise ratio required in the receiver per bit is 5. For low elevation angles where γ might be assumed to be equal to 2, it is apparent from the curve that to maintain the same bit error rate, nearly a 100-fold increase in the transmitted power would be required.

The above discussion of course assumed that no diversity is used. If spatial diversity is implemented in the ground receiver system by the use of two antennas, then the increase in power required to maintain the same error rate would be considerable less. In particular, if two antennas are used having the same gain, instead of one, and maximum diversity ratio is used in the receiver, the results given by Lindsey(59, 60) indicate that only a 2-fold increase in power is required to maintain the 10^{-3} error rate.

6.2 Effects of Large Delay Dispersion and Fading on Binary AM and FM Systems

For a digital AM, PM, or FM system, the presence of multipathing or, equivalently, delay distortion will give rise to pulse distortion and resultant intersymbol interference. The same is true of time multiplexed systems such as PAM/AM and PAM/FM. In this section the distortion resulting from delay dispersion, as well as fading, on the error rate of binary AM, PM and FM systems is given.

Sunde (61) gives results on the increase in error rate for the above mentioned binary systems due to delay dispersion and fading. Sunde's results for assumptions on the channel do not apply completely to the mm channel under consideration. However, his results are close enough to serve as an estimate and in certain cases as a boundary to the error rates anticipated

for the millimeter channel. He points out that the error rate in the presence of fading, noise and delay dispersion is equal to the sum of the error rates when only delay dispersion is present, which he refers to as $P_3^{(1)}$, (no fading or noise is assumed present), plus the error rate due to the presence of fading and noise alone, which he refers to as $P_3^{(3)}$. The results are given by Sunde for the case where, in the received signal there is only the fading term of Equation (6-1), that is, the signal is completely fading with $\gamma = 0$. Actually γ is expected to be slightly greater than zero, hence, with respect to this assumption, the results given by Sunde provide a lower bound on the error rates. For the results given, it is also assumed that all the multipath paths have equal gain and that there are an infinite number of multipaths having delays between the minimum and maximum delays.

Consider first the error due to delay dispersion. As a result of the linear delay dispersion shown in Figure 6-2, a pulse having a raised cosine spectrum will be distorted as indicated in the figure. In the figure, B equals the bandwidth of the pulse and $T = 1/B$. The quantity d equals the delay dispersion, Δ, is equal to 2d. The resultant maximum reduction in tolerable noise (the noise margin reduction) is given in Figure 6-3 for a binary AM with envelope detection, binary FM with frequency discrimination detection, binary PM with synchronous detection. Using the results of Figures 6-2 and 6-3 and the distribution for Δ anticipated by Sunde (61), the following expressions were obtained for the error probability due to delay dispersion for binary AM FM, PM (with differential phase detection) systems.

$$P_e^{(1)} = \frac{\Delta^2 \hat{B}^2}{6} \left[1 + \ell n \left(1 + m \frac{3}{2\pi \Delta^2 \hat{B}^2} \right) \right]^m \qquad (6\text{-}2)$$

For $\Delta = 1.0$ nanosecond and B = 100 mc, Equation (6-2) yields that $P_e^{(1)} = 8 \times 10^{-3}$.

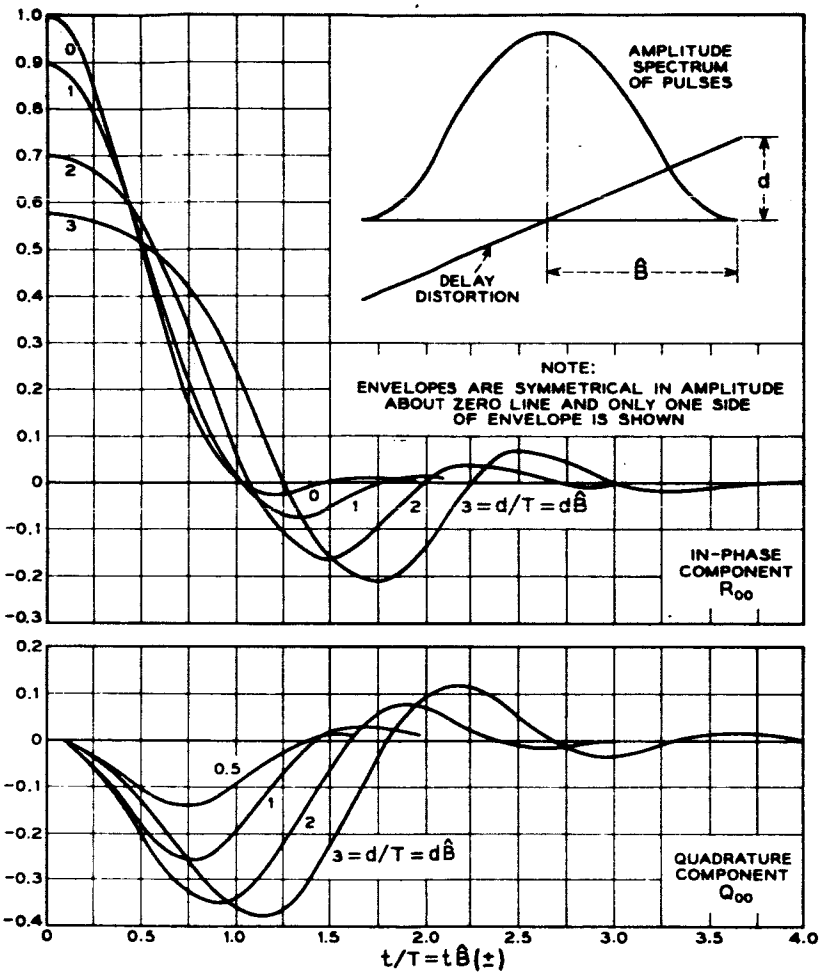

Figure 6-2. Pulse Distortion

The error due to Rayleigh fading and noise for the above AM, FM, and PM systems are, respectively

$$P_e^{(3)} = \frac{1}{2}\left[\frac{\ell n\, \bar{p}}{p-1} + e^{-\ell n p}\right] \qquad (6\text{-}3)$$

$P_e^{(1)} = 1/2 \ \bar{p}$

and $P_e^{(3)} = 1/2 \ (\bar{p} + 1)$

where $\bar{p}$ = average power signal-to-noise ratio at the receiver.

For the AM system it was assumed in obtaining Figure 6-3 that an optimum threshold which gives minimum error is used. Values for $P_e^{(3)}$ for FM and PM systems are tabulated below.

$P_e^{(3)}$	$\bar{p}$ (db)
$1/2 \times 10^{-2}$	20
$1/2 \times 10^{-3}$	30
$1/2 \times 10^{-4}$	40
$1/2 \times 10^{-5}$	50

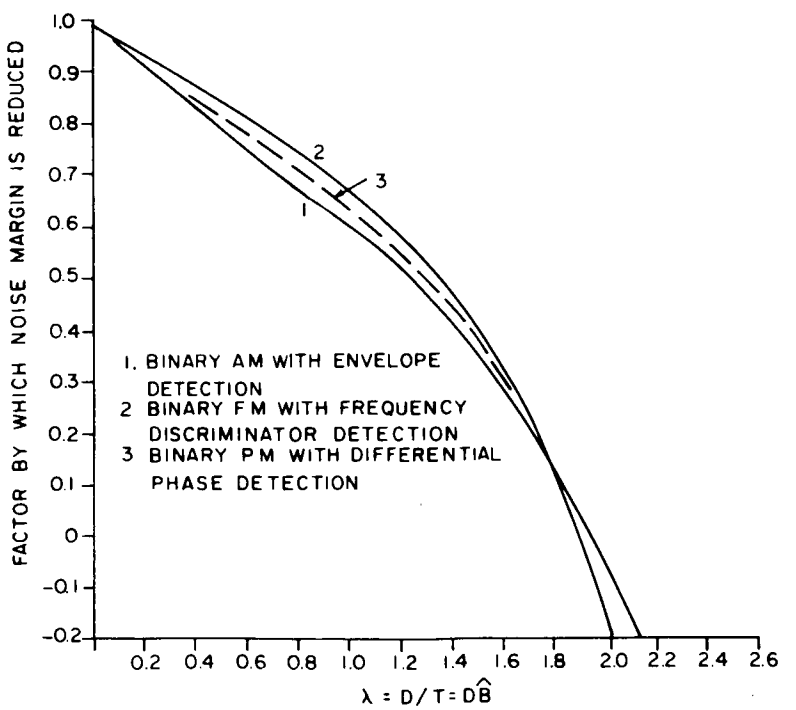

Figure 6-3. Maximum Reduction in Noise Margin Owing to Linear Delay Distortion

In many cases one uses frequency devision multiplexing to avoid intersymbol interference of a time-multiplexed system. For a frequency multiplexed systemone must be concerned with intermodulation distortion. Sunde (62) points out that intermodulation interference will cause less transmission impairment than intersymbol interference in direct digital transmission, if a cost of a two-fold increase in bandwidth and carrier power can be tolerated.

6.3 Effects of Multipathing on a Wide Band FM System (62)

First, consider the case where the bandwidth of the signal is not large enough (that is, in wideband TV) so as to have the frequency dispersion and multipath spread affect the system performance. In this case only the fading introduced onto the signal would affect the fidelity of the transmission. The effect of fading in FM system is to raise the threshold level required before system performance degrades.

Now consider the effects of multipath spread, Δ , when the signal bandwidth is large enough so that $B \geq 1/\Delta$. The discussion of the effects of multipathing on wideband FM systems, in this case, can be broken down into two cases. First, the case where there is only one main path component as indicated by Equation (6-1). Second, the case where there are one or more main path components as represented by Equation (6-4).

$$e_r^{(t)} = s\ (t - \tau\ ) \left[\alpha_1 e^{-j\delta_1} + \alpha_2 e^{-j\delta_2} + \beta\, e^{-j\epsilon} \right] \qquad (6\text{-}4)$$

For the first case, if the main path component is larger than the scatter components, then, due to the capture phenomena of FM systems, only the main path component would be observed and no distortion will result. The beat frequency interference is suppressed relative to the full signal by a ratio equal to the ratio of the deviation to the emphasis frequency.

In the case where there are two or more main path components (as would occur for a very large receiving antenna), and the one which domi-

nates varies from one time to the next, then no one main component will be captured. Instead, alternately, one main component and then another would be captured. This switching from one main component to another can introduce excessive noise and distortion into the system. Hence wideband FM modulation would not be suitable in this situation.

Section 7
FORMULATION OF EXPERIMENTS

This section evaluates various approaches to each segment of the experiment design philosophy, and selects the best combination of approaches as the recommended experiment configuration. The candidate platforms to be used were evaluated principally in terms of their orbital constraints. High altitude aircraft were compared with satellites to determine their ability to simulate space-earch channels and their cost effectiveness in the communication program. A discussion on up-links versus down-links recommends that down-links be used whenever possible. The waveforms discussed in Section 5 are considered in terms of hardware implementation and it is recommended that the simple AM waveform be used during the initial propagation experiments. Finally, the experiment configuration is selected which best meets the basic measurements requirements stated in Sections 3 and 5. The equipment design details will be given in Section 8.

7.1 Candidate Satellite Evaluation

Three candidate satellites, classified according to orbital altitude, were evaluated in terms of their suitability as space platforms with which to conduct space-earth millimeter-wave propagation experiments. High altitute aircraft are compared with the satellites because they could play a definite role in the communications program. Table 7-1 summarizes the results of the evaluation. Appendix III of the Second Quarterly Report gives the general orbital characteristics as a function of altitude which can be used in the consideration of other satellites should they become identified.

7.1.1. Synchronous Satellites

This is a summary of the detailed analysis on synchronous stationary satellites which was given in Section 2.2 of the Second Quarterly Report. Orbital data is also given in Appendix III of Volume II, Final Report. Non-stationary synchronous satellites were also discussed in the above quarterly report but they are not considered as serious candidates at this time.

TABLE 7-1

EVALUATION OF SATELLITES AND AIRCRAFT FOR USE IN SPACE-EARTH MILLIMETER-WAVE PROPAGATION EXPERIMENTS

Vehicle	Altitude	Specific Comments	Chief Roles
Aircraft	30K' to 50K'	(1) High performance ground antenna tracking system required. (2) Less reliable flight equipment necessary. (3) Reasonable data collection periods. (4) Complete elevation profiles. (5) Short lead times. (6) Short path lengths. (7) Ample vehicle prime power.	(1) Initial qualitative experiments on a single spatial channel by simulating space-earth links under representative meteorological conditions at all elevation angles. (2) Evaluation of spacecraft flight hardware. (3) Exploration of oxygen absorption region using space-aircraft links.
Synchronous Satellites	19,500 n miles (stationary)	(1) No ground antenna tracking system necessary. (2) Flight equipment designed to operate for period of one year. (3) Continuous access for data collection. (4) Significant limitations on elevation profile and ground station siting. (5) Long lead times. (6) Long path lengths. (7) Limited vehicle prime power.	(1) Qualitative experiments on parallel spatial channels. (2) Quantitative data on single channels and multiple spatial channels under representative meteorological conditions at specific elevation angles.
Medium Altitude Satellites	5,000 n mi to 6,000 n mi at inclinations $\geq 28.5°$	(1) Medium performance ground antenna tracking system required. (2) Flight equipment designed to operate for period of one year. (3) Reasonable data collection periods three to four times per day. (4) Complete elevation profiles. (5) Long lead times. (6) Long path lengths. (7) Limited vehicle prime power.	(1) Quantitative and qualitative data on single spatial channels under representative meteorological conditions at all elevation angles.
Low altitude satellites	100 n mi to 300 n mi at inclinations $\geq 28.5°$	(1) High performance ground antenna tracking system required. (2) Flight equipment designed to operate for period of 30 to 60 days. (3) Extremely limited data collection periods. (4) Complete elevation profiles. (5) Long lead times. (6) Medium path lengths. (7) Reasonable vehicle prime power.	(1) Operational evaluation for the development of low altitude manned spacecraft space-earth data links.

Figure 7-1 gives elevation angle versus difference in longitude between the satellite and the ground station for ground station latitudes between 30^{o} and 50^{o}. From this chart, elevation angles versus satellite longitude for a specific ground station location can be quickly sketched. For example, Figure 7-2 gives the elevation angle profiles for the ATS (Applications Technology Satellites) ground stations at: Rosmon, North Carolina; Mojave, California; and Canberra, Australia. As a point of interest, London and Berlin are also shown. It is important to note that the most likely satellite positions were assumed to be near those given in Table 7-2. These positions were chosen because they optimize the elevation angles for the links or combinations of links mentioned in Table 7-2.

TABLE 7-2

ASSUMED POSITIONS OF ATS SYNCHRONOUS SATELLITES

Position	Longitude	Symbol	Links
Primary Atlantic	45^{o} W	PA-45	Rosman-Europe and Rosman-Mojave
Secondary Atlantic	30^{o} W	SA-30	Rosman-Europe
Primary Pacific	145^{o} W	PP-145	Mojave-Canberra and Mojave-Rosman
Secondary Pacific	165^{o} W	SP-165	Mojave-Canberra

Figures 7-3 and 7-4 give elevation data for the millimeter ground facilities located at Aerospace Corporation, University of Texas, Goddard Space Flight Center (GSFC), Defense Research Telecommunications Establishment (DRTE), Lincoln Laboratory and Air Force Cambridge Research Labs (AFCRL). In addition, a transportable millimater auxiliary antenna-receiver terminal located at either White Sands Missile Range (WSMR) or Rosman is considered as a gap filler to improve the elevation angle profile for the propagation experiments. Table 7-3 gives the possible points along the elevation profile for the satellite positions given in Table 7-2.

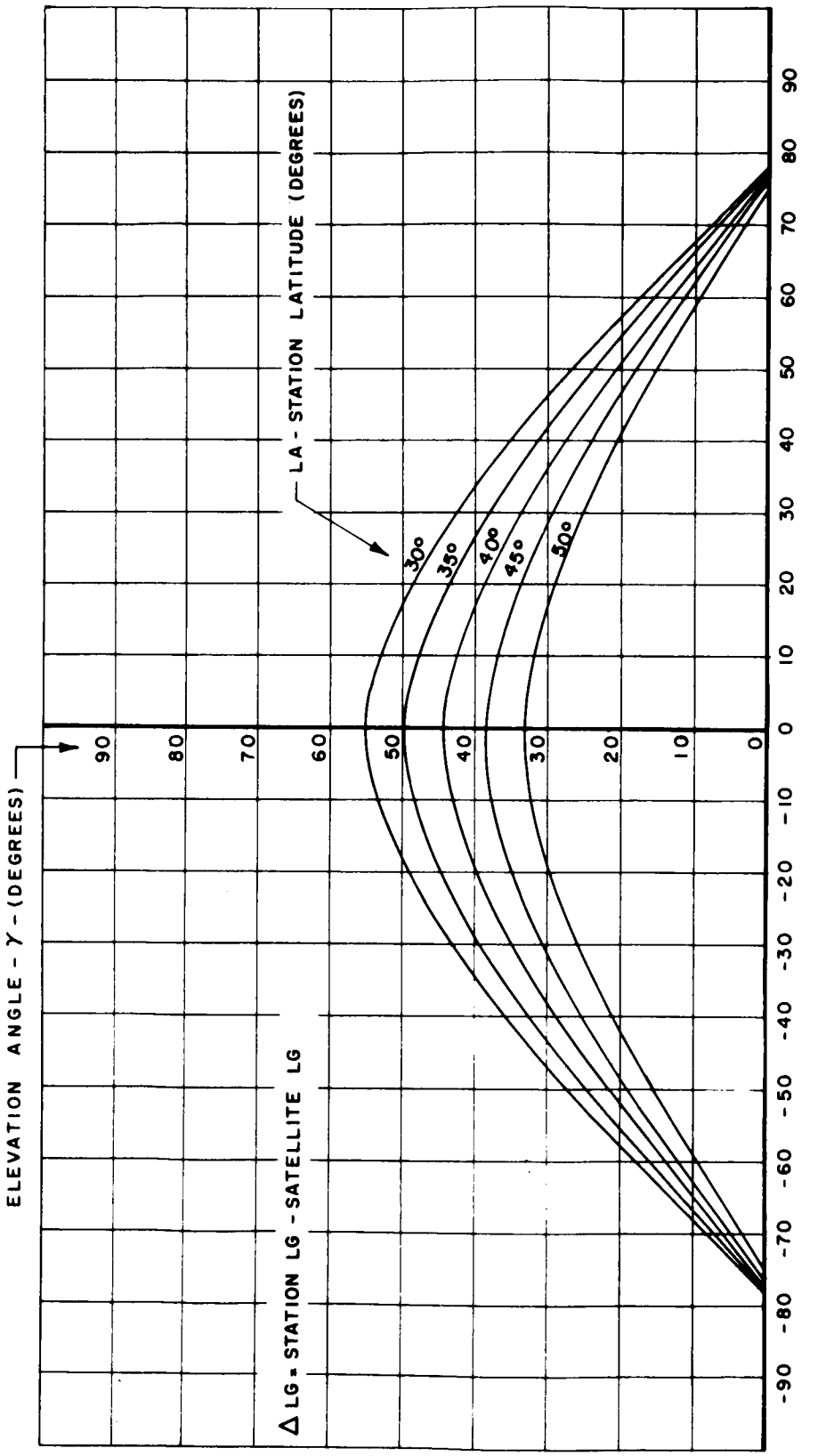

Figure 7-1. Elevation Angle as a Function of Ground Station Latitude and Longitude and of Synchronous Stationary Satellite Longitude

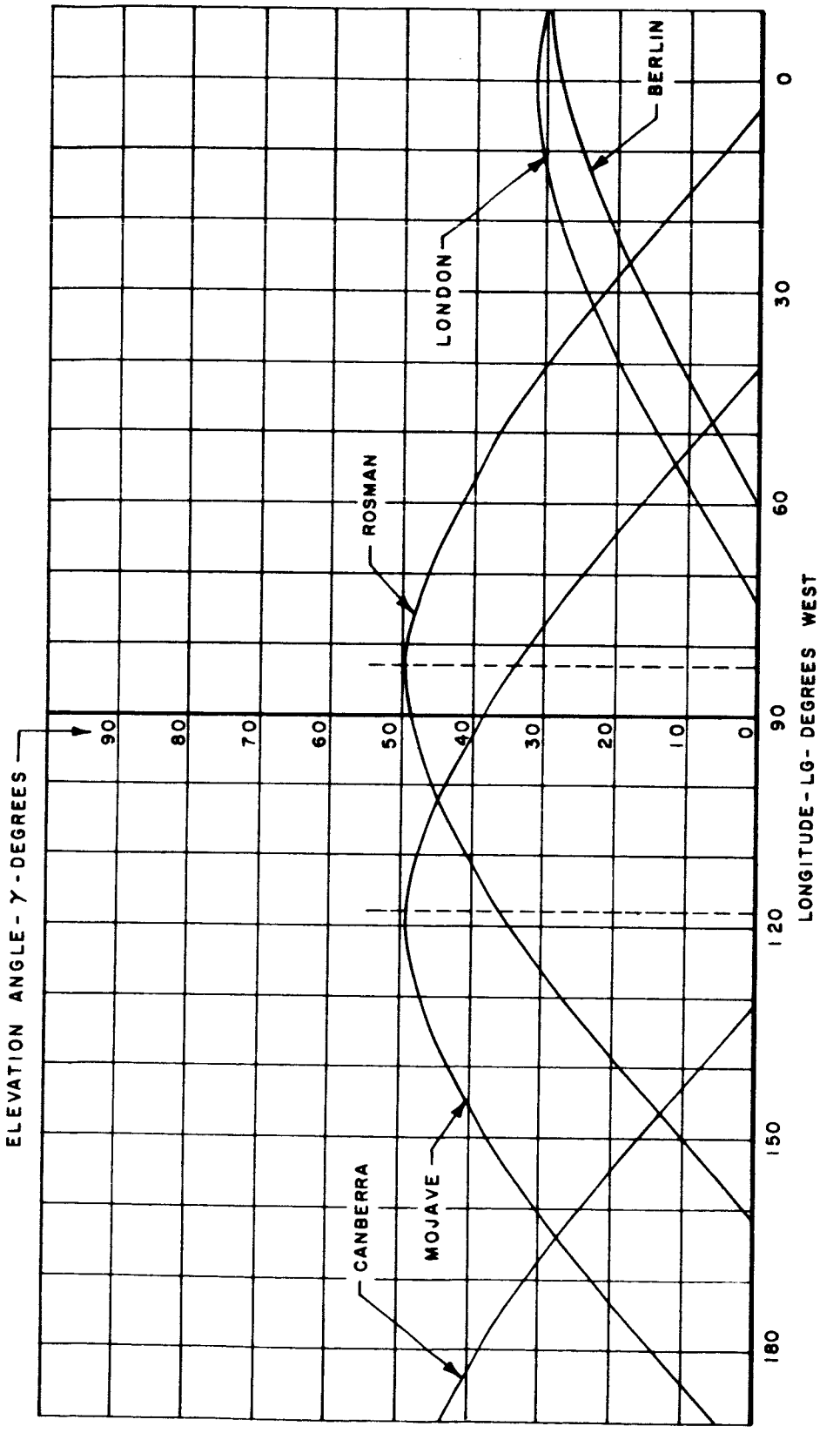

Figure 7-2. Elevation Angle vs Synchronous Satellite Longitude for the ATS Ground Stations

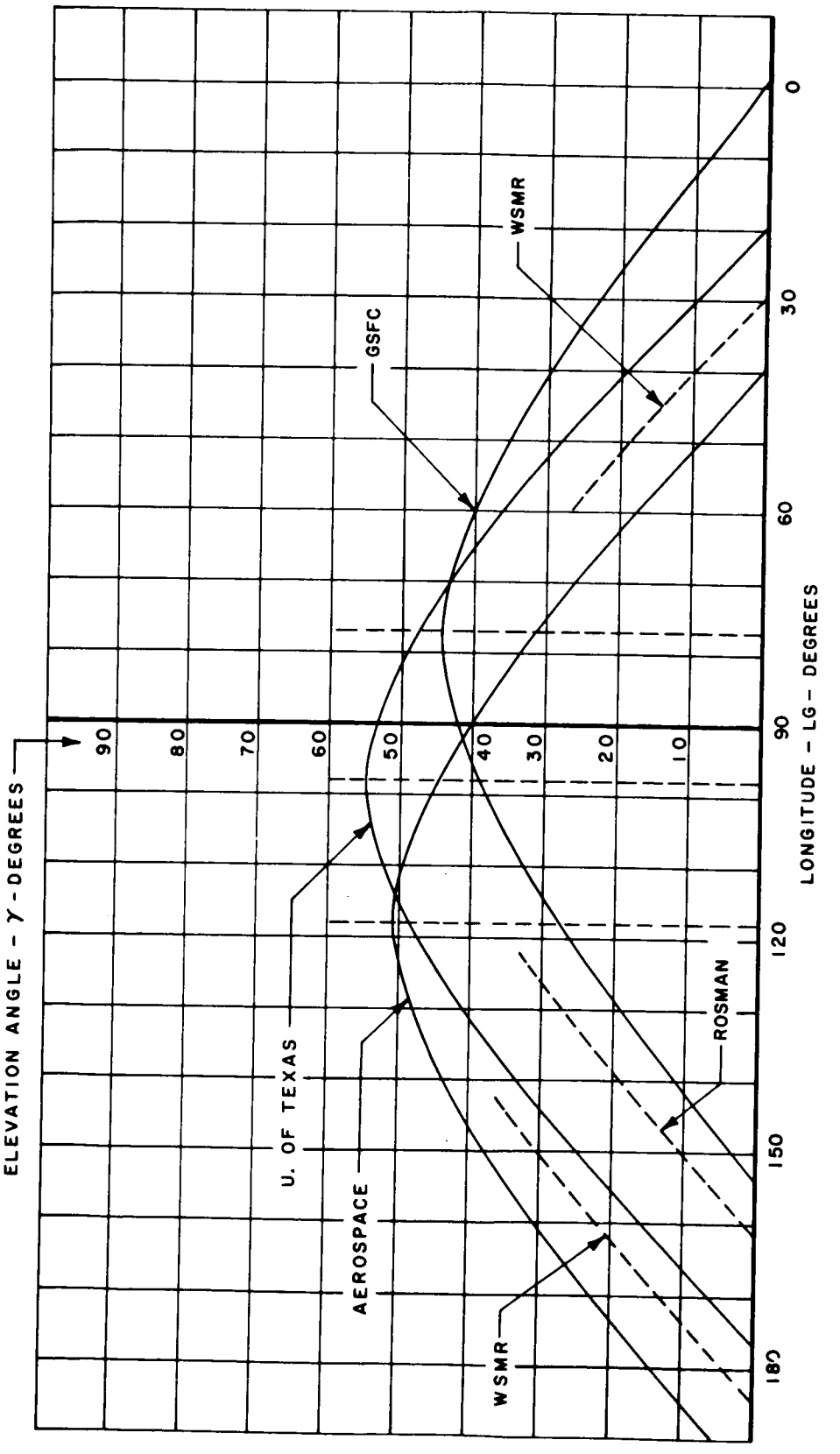

Figure 7-3 Elevation Angle vs. Synchronous Satellite Longitude for the Millimeter Experimental Ground Stations

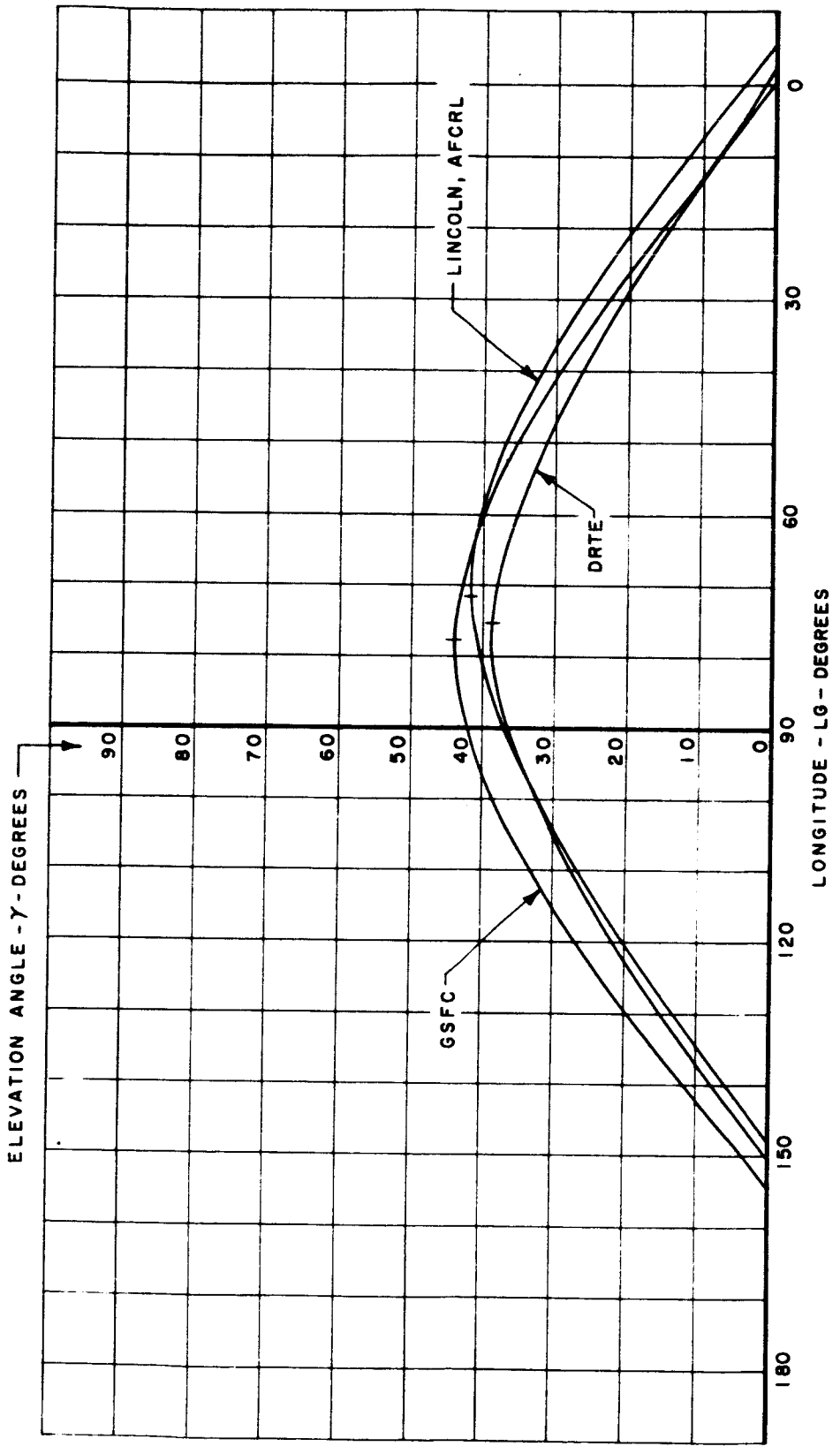

Figure 7-4. Elevation Angle vs Synchronous Satellite Longitude for the Millimeter Experimental Ground Stations

TABLE 7-3

ELEVATION ANGLE PROFILES FOR PROPAGATION EXPERIMENTS

Position	Station	Elevation Angle
PA-45	Aerospace	5°
	WSMR	15° *
	Univ. of Texas	24°
	DRTE	29°
	GSFC	33°
	Lincoln, AFCRL	35°
SA-30	Univ. of Texas	10°
	DRTE	21°
	GSFC	23°
	Lincoln, AFCRL	26°
PP-145	GSFC	7°
	Rosman	15° *
	Univ. of Texas	29°
	Aerospace	41°
SP-165	Univ. of Texas	10°
	WSMR	22° *
	Aerospace	31°

* Auxiliary Receiver

Some important conclusions can be drawn from Tables 7-2 and 7-3

a. A synchronous satellite in the secondary Atlantic position of 30° West longitude provides a satisfactory combination of down-links with the ground stations indicated.

b. A synchronous satellite in the primary Atlantic position of 45° West longitude or in the secondary Pacific position of 165° West longitude provides a satisfactory combination of down-links with the ground stations indicated, if a gap filler receiver is positioned near White Sands Missile Range.

c. A synchronous satellite in the primary Pacific position of 145° West longitude provides a satisfactory combination of down-links with the ground stations indicated, only if a gap filler receiver is positioned at Rosman.

d. The AFCRL and Lincoln stations are of marginal value for both Pacific positions.

7.1.2 Medium Altitude (6000 nmi) Satellites

The medium altitude satellite is a useful space platform with conduct propagation experiments. The angular elevation rate of the medium altitude satellite is slow enough (no faster than 0.025 degrees per second at 6000 nmi) to permit ample viewing time per pass with sufficient data samples per degree of elevation. On the other hand, the elevation angular rate is fast enough to complete a full elevation profile beofre significant weather changes can occur. Elevation coverage from the horizon to 30 degrees can take place well within an hour on many of the orbital passes.

Figure 7-5 shows the zero degree elevation coverage contours for a 6000 nmi satellite for ground terminals located near Los Angeles, California; Austin, Texas; Washington, D. C.; Boston, Massachusetts and Ottawa, Canada. The Ottawa location has been included to accommodate Canada's Defense Research Telecommunication Establishment (DRTE) in any planning they might have for participation in this program. As the coverage diagrams indicate, the altitude of this satellite is sufficiently high to permit simultaneous observation by many ground stations for two hours or more. Coverage contours for 0°, 10°, and 20° elevation angles were given for each station in Section 6.2 of the First Quarterly Report. Orbital characteristics for the 6000 n mile satellites are given in Appendix III of Volume II, Final Report.

A one-year viewing time profile was developed to: (1) estimate the number of satellite passes available to a ground station during any interval of time, (2) estimate the amount of viewing time per pass, and (3) estimate the total operational time on the satellite payload which is required to service all the ground stations during a given pass. The results of this profile show that the available viewing time is abundant, ranging from 35 passes (165-200

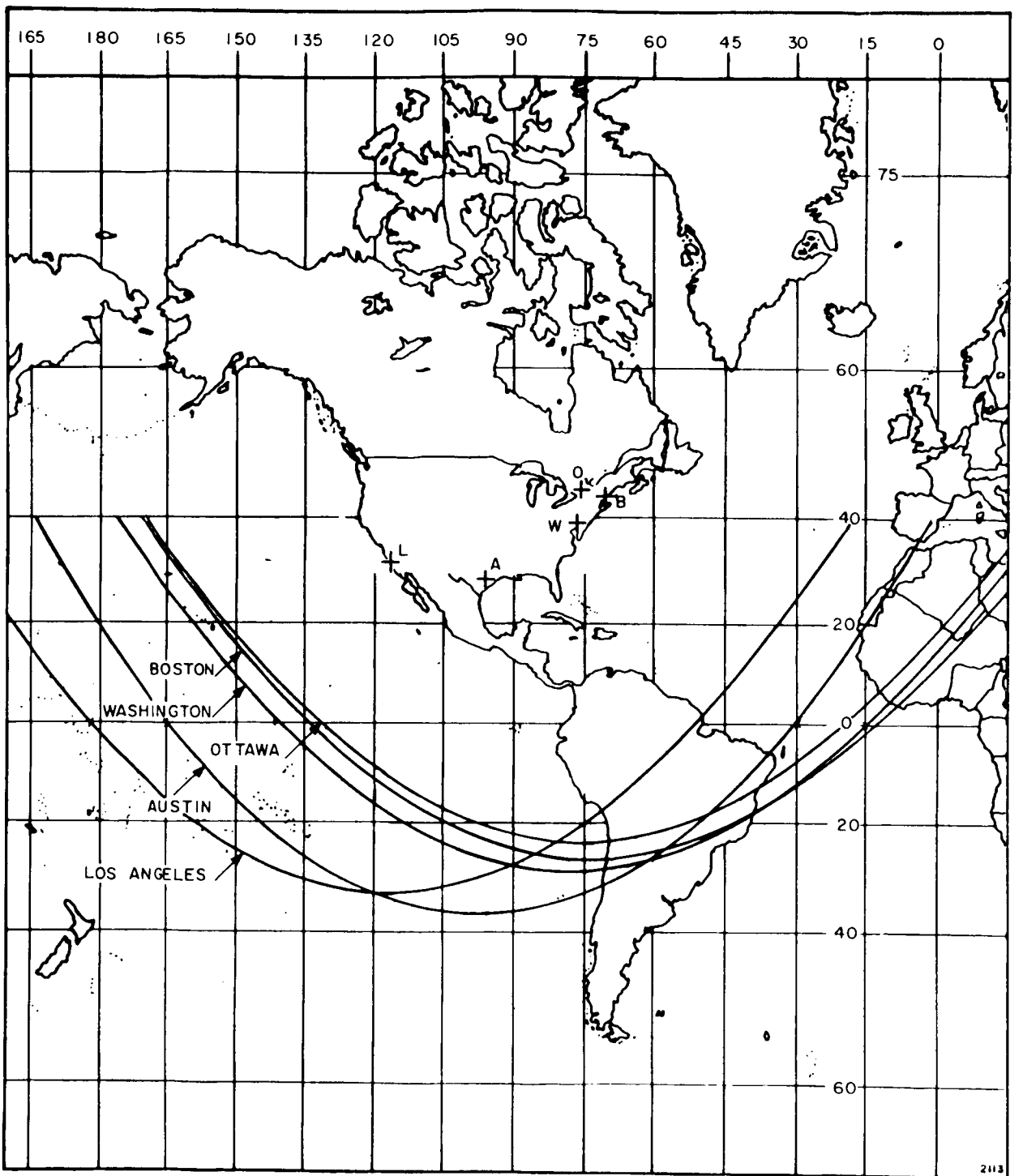

ZERO DEGREE ELEVATION COVERAGE
CONTOURS FOR A 6180 N. SATELLTE

Figure 7-5. Zero Degree Elevation Coverage Contours for a 6000 nmi Satellite

minutes per pass) every 13 days for Austin, Texas, to 31 passes (130-180 minutes per pass) every 13 days for Ottawa, Canada. For the same period of time, the maximum payload operational time ranges from 180-340 minutes for each of the 35 passes. Additional information about the one-year time profile can be found in Appendix IX of the First Quarterly Report.

7.1.3 Low Altitude (100-300 n miles) Satellites

The design of experiments using low altitude spacecraft would be based on the assumption that propagation experiments using aircraft, and medium to synchronous altitude unmanned or manned satellites have already been performed during preceding phases of the program. The preceding experiments would provide basic propagation data under highly controlled measurement conditions. This accurate knowledge of significant atmospheric influences on power density, modulation method, and receiver performance would permit valid conclusions to be reached as to the utility of this region of the spectrum. Finally, the preceding experiments would generate statistics relating to channel reliability as a function of time and zenith angle, under a representative series of meteorological conditions.

Low orbiting spacecraft are not ideal vechicles for basic propagation experiments. They are just too close to earth to permit reasonable time for gathering quantitative data by any one ground station. Multiple ground stations are expensive, especially since the spacecraft is traveling at high angular rates relative to the ground terminal. Low orbiting spacecraft do, however, offer payload capacities which often surpass tho e available at higher altitudes. Furthermore, the availability of man in a low orbiting spacecraft would be of inestimable value in determining the operational potential of millimeter-wave communications to support future manned spacecraft missions. The experiments with low orbiting spacecraft would be communication experiments demonstrating actual modulation methods expected to be employed in future systems. They would, in effect, verify the system performance inferred from the basic propagation data gathered during previous phases of the millimeter-wave communication propagation program. Typically, low altitude space-earth communications are restricted to short intervals (2-10 minutes) at each site during each orbital pass; nevertheless, these millimeter-wave channels are attractive for certain system applications. The advantages of aircraft as terminats in aerospace

communications have been recognized. They fly above a large portion of the sensible atmosphere and therefore provide a space-air communications channel which is essentially free of both water vapor and oxygen absorption. Because of their freedom from propagation effects and the altitude of the airborne terminal, these communication links offer a considerable increase in reliable communication time per orbital pass over that for space-earth channels. In addition, the transportability of the aircraft allows one to take advantage of certain orbits, not available to ground stations, where real-time transmission from spacecraft sensors is necessary.

Orbital periods and velocities for satellites at altitudes below 600 nautical miles are given in Figure 7-6. Additional orbital data for low altitude spacecraft is given in Section 4.3.4 in Volume II, Final Report. Communications time during an orbital pass between a satellit nd a given point on the Earth is the most important parameter when evaluating candidate satellites as platforms for space-earth propagation and communication experiments. The most useful curves for estimating communication time for a given orbital pass are shown in Figures 7-7 through 7-9 for spacecraft altitudes of 100, 200, and 300 nautical miles. These curves are approximations for communications time as a function of: minimum horizon in terms of elevation angle (γ), and minimum Earth's surface range between the ground terminal and the orbital plane. These curves show the profound effects that the minimum operating horizon has on the usefulness of low orbiting spacecraft. Calculations for all of these curves are based on the assumption that the ground terminal latitude is somewhat less than the orbit inclination.

Finally, a three dimensional sketch is given in Figure 7-10 which shows the shape of the ground station latitude-orbital inclination function for average total communication time for a 24-hour day in a 30-to 45-day mission. Communication time is maximum at points 1 and 2 in Figure 7-10 when the ground station is on the Equator and the satellite orbit is equatorial or when the ground station is on a Pole and the satellite orbit is polar. Table 7-4 gives the average communications time in hours per day for the above two cases at satellite altitudes of 100, 200, and 300 n miles. The communications time for an equatorial station and a polar orbit is also given. Communication time is zero for values of ground station latitude where:

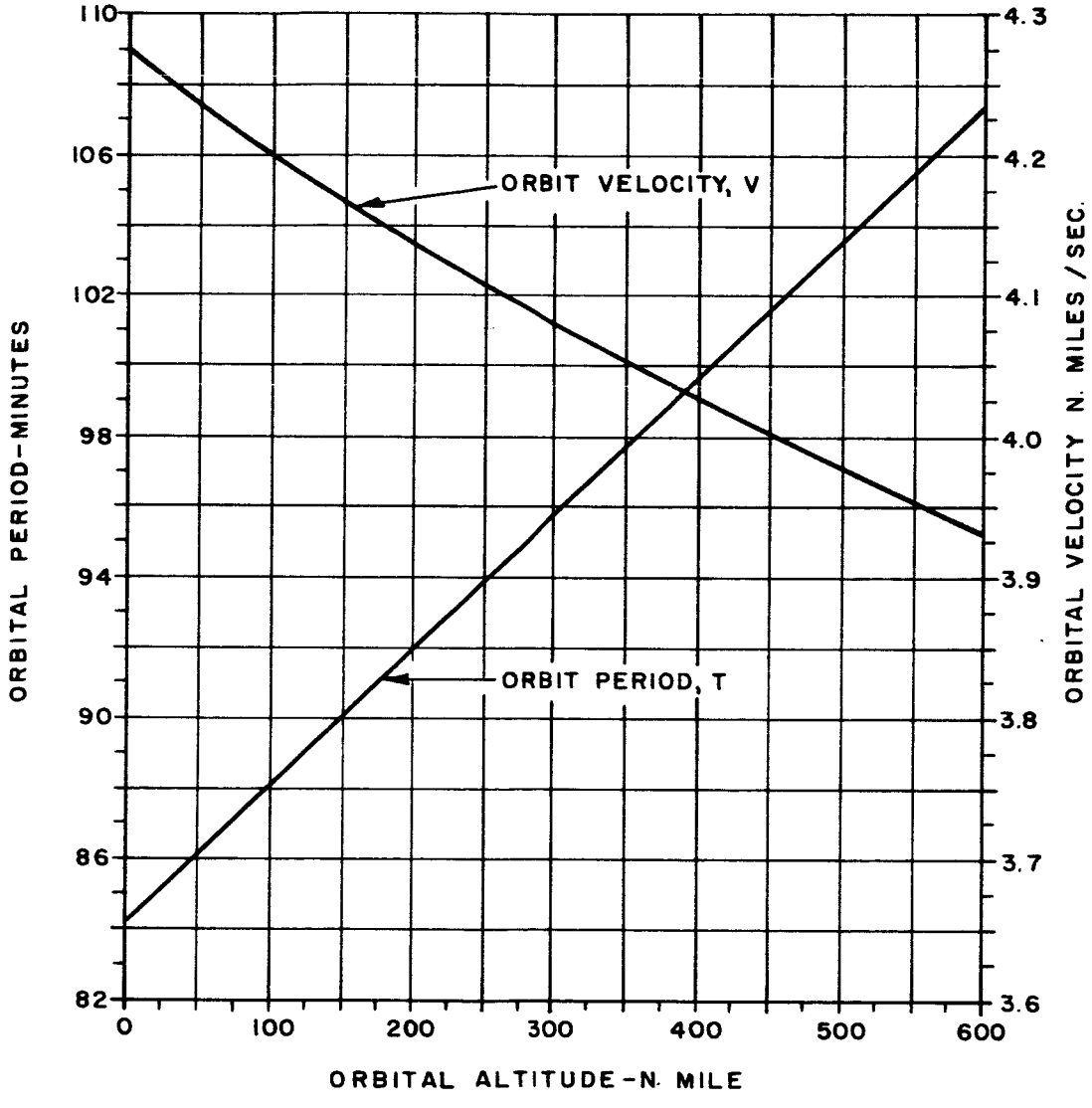

Figure 7-6 Orbital Period and Velocity Versus Altitude For Low Orbiting Spacecraft

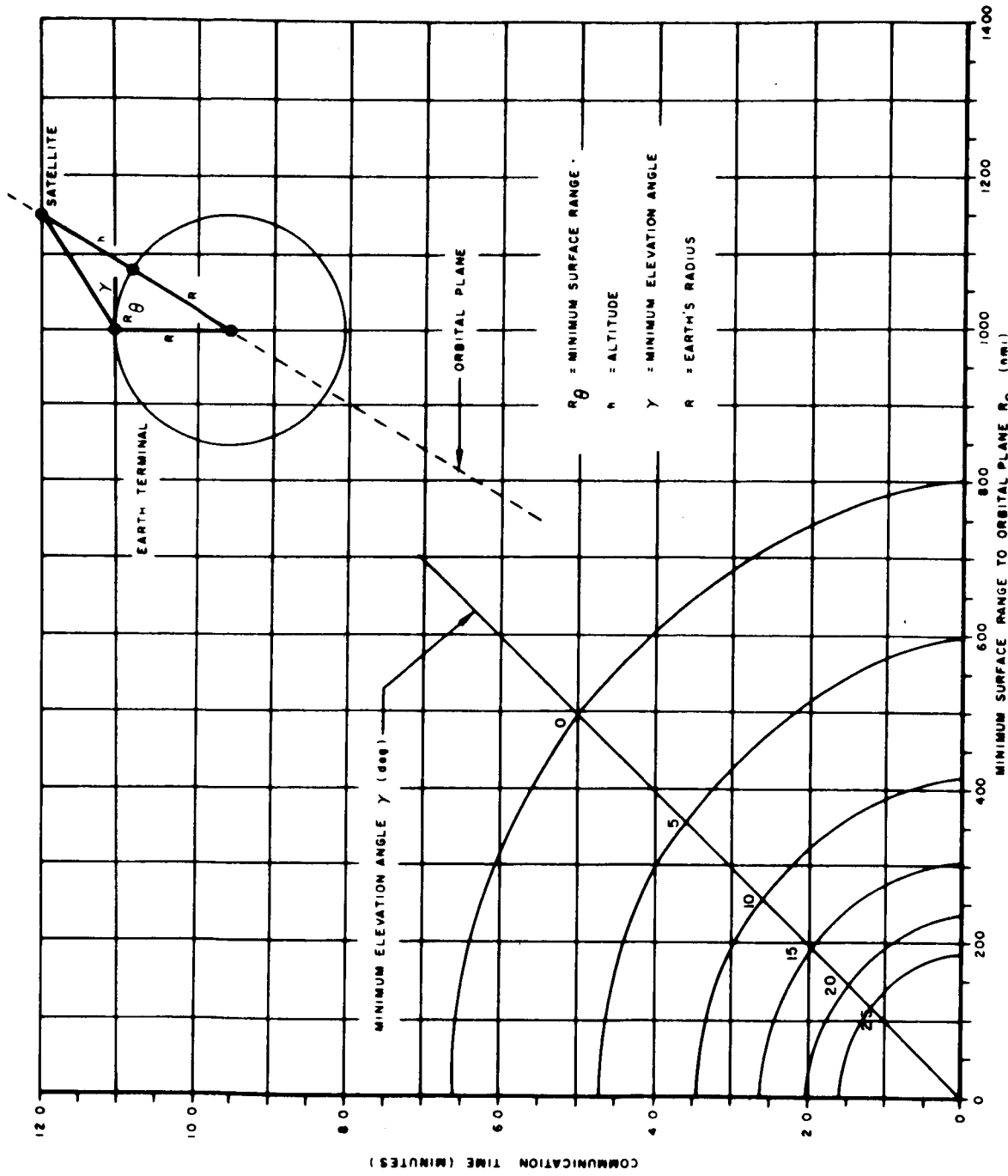

Figure 7-7. Communication Time for a 100 n. mi. Altitude Satellite Pass

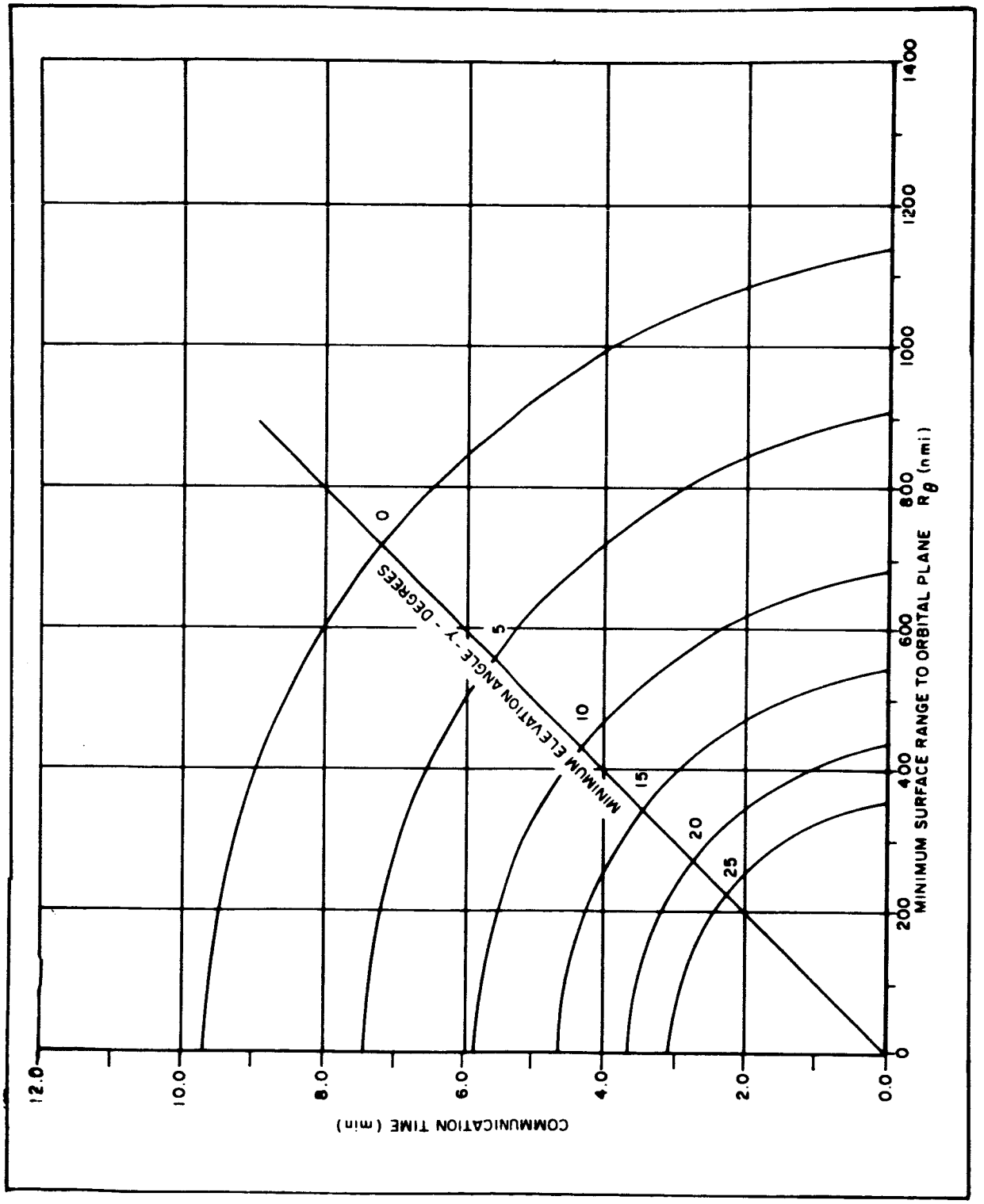

Figure 7-8. Communication Time For a 200 n mi. Altitude Satellite Pass

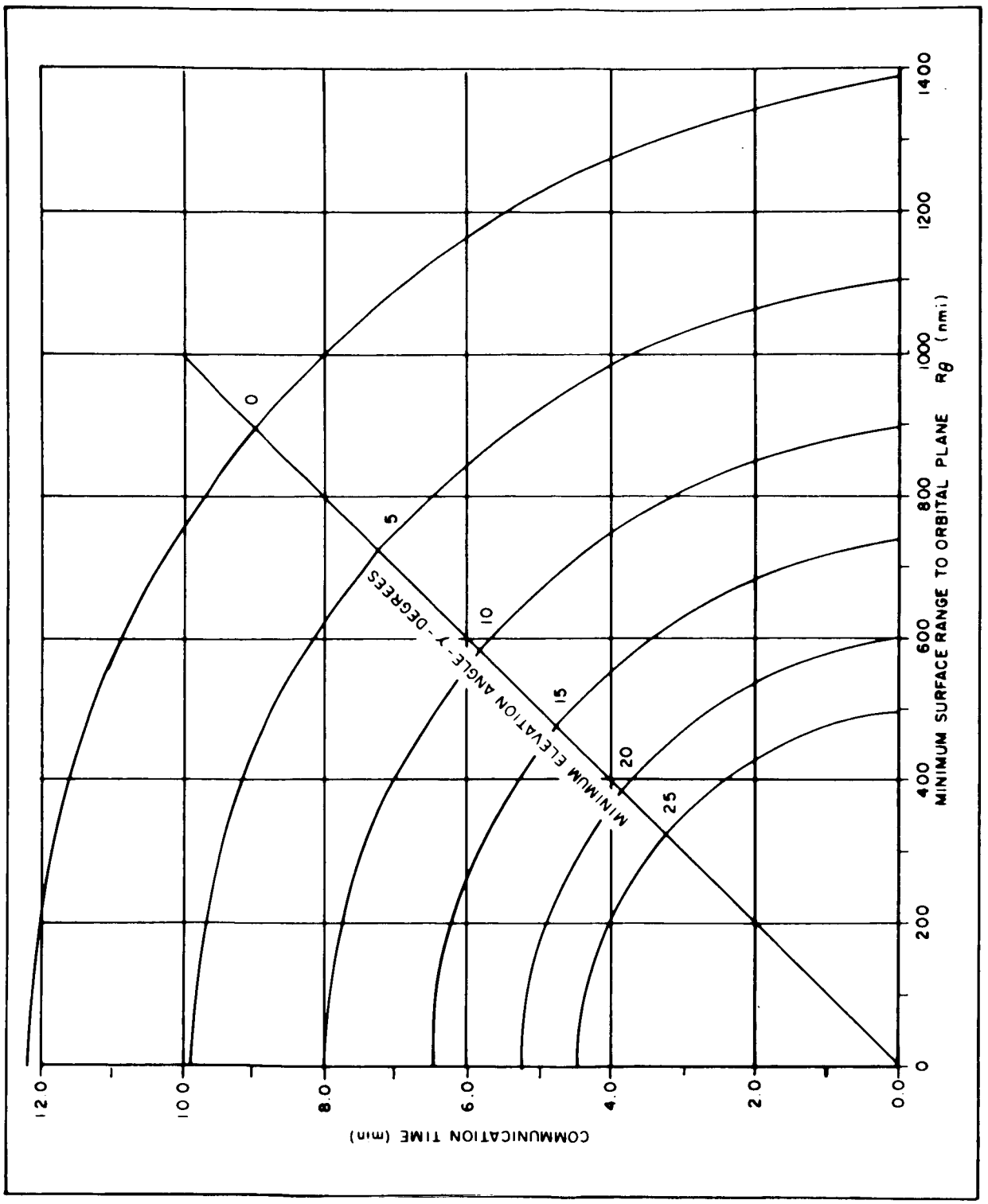

Figure 7-9. Communication Time For a 300 n mi. Altitude Satellite Pass

TABLE 7-4

AVERAGE COMMUNICATION TIME FOR LOW ALTITUDE SPACECRAFT

Orbital Inclination, Station Location	Communication Time - Hours		
	h = 100 n. mi. /2 = 13.5°	h = 200 n. mi. /2 = 19.0°	h = 300 n. mi. /2 = 23.1°
(1) 0° ; equatorial	1.8	2.5	3.1
(2) 90° ; equatorial	0.2	0.4	0.6
(3) 90° ; polar	1.9	2.5	3.1

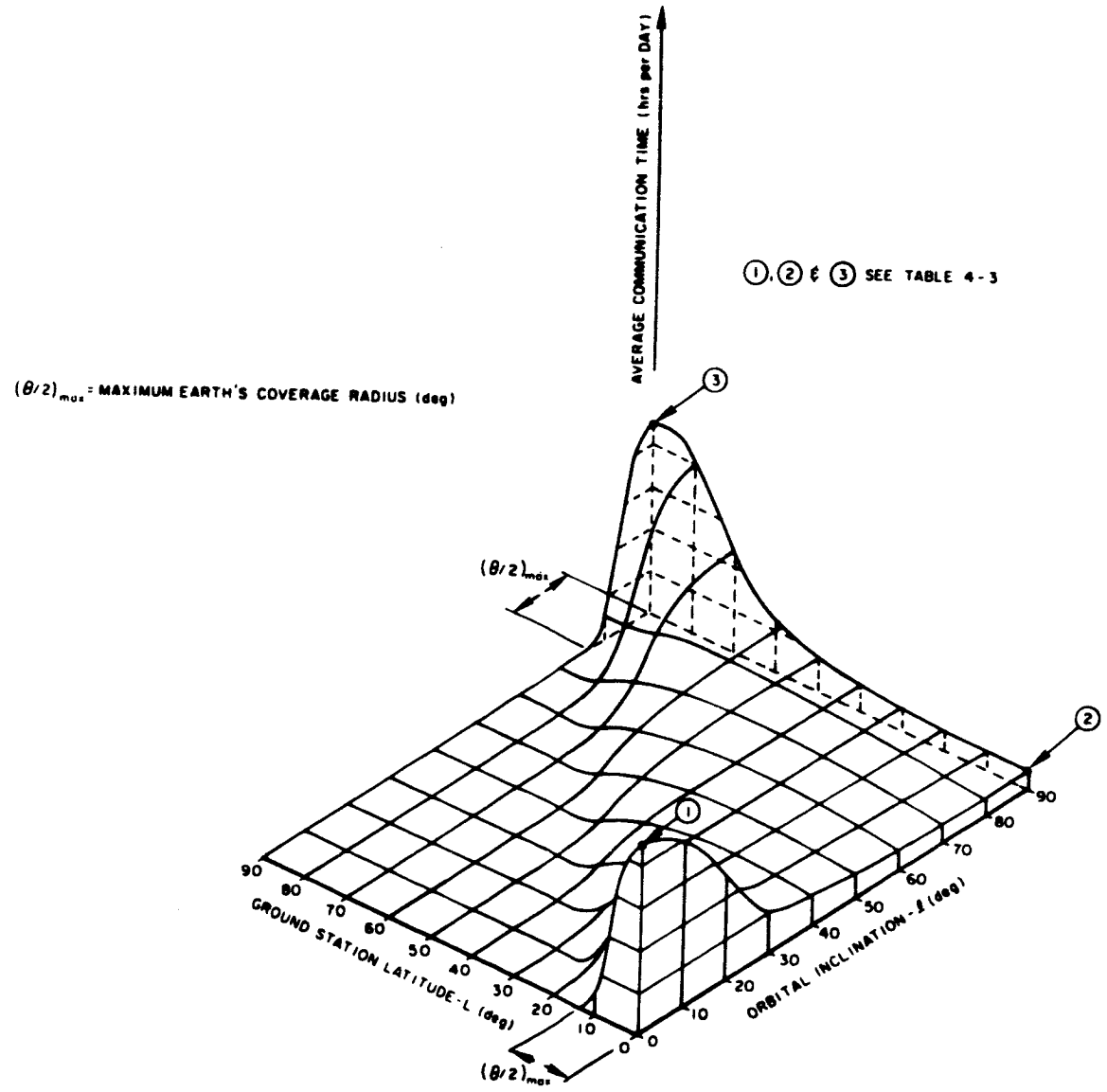

Figure 7-10 The Shape of the Ground Station Latitude/ Orbital Inclination Function.

$$L \geq \ell + \left(\theta/2\right)_{max}$$

$\theta/2$ is maximum when γ = zero degrees.

7.2 Experiment Design Using Manned Spacecraft

For the most part, this experiment design study was conducted with the Applications Technology Satellites (ATS) in mind. The specific ATS satellites are described as follows:

(a) ATS - A, MAGGE - Medium altitude, gravity gradient stabilized satellite at 28.5 degrees inclination.

(b) ATS - B and C, SASSE's - Synchronous altitude, spin stabilized stationary satillites.

(c) ATS-D and E, SAGGE's - Synchronous altitude, gravity gradient stabilized stationary satellites.

With the establishment of the NASA APOLLO Applications Program (AAP) (Formerly known as AES, APOLLO Extension System) and the Air Force Manned Orbiting Laboratory (MOL) Program, it was considered appropriate to include as much experiment design information as possible in these reports. This is the reason why an orbital analysis on low altitude spacecraft was given in the preceding section.

Table 7-4 gives a typical mission outline for the manned earth-orbital phase of the APOLLO Applications Program. This mission outline gives the orbits and mission times which are predominant, and is representative of the total experimental activity in which the spacecraft crew will be involved. The manned spacecraft experiment design must include careful consideration of the orbital, payload and mission time constraints placed by the specific spacecraft and its crew.

The use of man must be clearly defined by comparing the manned experiment with the comparable unmanned experiment in terms of specific experimental results, operational and equipment reliability, savings in weight and prime power, etc. Proper placement of instrumentation should be considered

TABLE 7-5

TYPICAL MISSION OUTLINE

FOR

12 THREE-MAN EARTH-ORBITAL FLIGHTS IN THE APOLLO APPLICATIONS PROGRAM

Flight No.	Mission Class	Altitude n miles	Inclination degrees	Duration days	Description
1	Remote Sensing of Earth's Surface	200	50	14	Earth mapping in visible and near-visible spectrum. Artificial gravity qualification. Medical.
2	Biomedical/Behavioral Technology	200	28 1/2	30	Biomedical/Behavorial Investigations. Lunar Orbit Survey System qualification.
3	Bioscience/Physical	200	28 1/2	45	Prolonged Weightlessness Effects. Zero-G behavior of solids, liquids and gases.
4	Space Operations/ Bioscience Laboratory	200	28 1/2	45	Rendezvous with Mission No. 3. Extravehicular cargo and personnel transfer. Rescue Operations. Spacesuit evaluation. Space Flight Effects on biological systems.
5	Remote Sensing of Earth's Atmosphere	200	83	45	Sun synchronous. Multi-spectral Sensors. Solar cell array erection and orientation.
6	Astronomy/Bioscience Laboratory No. 1	19,350	0	45	X-band, visual and IR spectral and photometric data. Deployable satellites. Extendable radio astronomy antenna
7	Artificial Gravity Laboratory	200	28 1/2	45	Evaluate Human Performance in Rotating Environment. Cable mounted CSM and LEM-Lab are rotated.
8	Remote Sensing of Earth's Surface and Atmosphere. Echo Observation	200	83	45	Sun synchronous. Multi-spectral Sensors. Solar Cell Array erection of orientation. CSM Inspection of Echo Satellite.
9	Space Physics and Subsurface Development	19,350	0	45	Space Environment near Earth. Aurora magnetic fields. Micrometeoroid fluxes. Life Support Communications. Satellite Launch
10	Astronomy/Bioscience laboratory No. 2	200	28 1/2	45	Optical Radio Astronomy. Micrometeorites. Gamma Rays. Biomedical.
11	Astronomy/ Logistics No. 1 and Bioscience Laboratory	200	28 1/2	45	Rendezvous with Mission 10. Cargo and Personnel Transfer Effects of flight duration beyond 45 days. Continue Optical and Radio Astronomy
12	Astronomy/ Logistics No. 2	200	28 1/2	45	Rendezvous with Mission 11. Extended Mission to total of 135 days. Cabin Atmosphere. Propellant Handling.

for the required astronaut interface within the Command Module (CM) and the necessary interconnections between the CM and the Service Module (SM) or the CM and a modified Lunar Excursion Module (LEM). The value of an EVA (extra vehicular activity) capability for the problem of antenna deployment and/or alignment after launch should be evaluated against alternative equipment locations.

Spacecraft integration and operational problems must be defined including experiment prelaunch installation and checkout, inflight maintenance or testing, effects on spacecraft subsystems, effects on spacecraft resources, and CM/SM separation for re-entry. Total weight and its distribution should be determined. Problems associated with the conduct of multiple experiments with the same equipment, concurrent experiments which compete for operator attention and special spacecraft orientation, and experiments by a non-specialist member of the crew should be defined. Environmental requirements peculiar to the experiment hardware should be specified, and packaging to achieve compability with the APOLLO operational environment should be determined.

Selection of experiment operational parameter sensors and programming controls would be made on the basis of the Unified S-band equipment data rates, signal levels, and anticipated experiments data system format. The data flow interface between the CM and the SM or LEM should be defined and hardware implications evaluated.

The final result of the experiment design study using manned orbiting spacecraft would be to define one or more typical 45 to 60-day mission profiles which can be considered. The profiles would describe the specifics of each millimeter experiment, the data to be obtained, the anticipated results, the application of the data, and the manner in which each experiment relates to other experiments. Each mission profile should be a schedule of events in the manned spacecraft mission which are pertinent to the millimeter communication experiments. Careful and thorough planning and scheduling of mission profiles would insure most efficient use of valuable experiment time. Results of these profiles would allow reasonably accurate costing of the complete communication experiment.

The mission profiles may vary with the spacecraft launching date because of the influence of the prevailing weather at the ground sites during that time of the year. For each mission, predetermined alternatives should include orbital coverage from ground sites and aircraft flight paths for each pass of the 45-day mission. Daily countdown procedures for calibration and check-out of each ground site and each aircraft should be defined and scheduled. Each aircraft flight plan, which may encompass experiment data collection on three or more consecutive orbital passes, should be defined in terms of type of aircraft, landing points, direction, altitude and speed, all related in time to the spacecraft orbit. All flights required for ground site and aircraft calibration and checkout, plus any flights required for aircraft-ground propagation data collection should be included.

A very important section of the mission profile would be the specification of the spacecraft crew's participation during the 45-day mission. Their duties may include calibration and maintenance checks, aid to acquisition, millimeter antenna steering and observation of signal displays. The duties of the personnel required to operate and maintain the ground and airborne experimental equipment should also be specified.

7.3 Use of Aircraft to Simulate Space-Earth Communication Links

A series of propagation experiments using aircraft, whose objectives are to determine the effects of the atmosphere on the characteristics of space-earth communications channels, would constitute a useful phase in the overall millimeter-wave propagation program.

This phase of propagation data collection should precede the final spacecraft equipment design phase for the space-earth experiments. Air-ground experiments, however, should not be considered as a satisfactory substitute for the complete space-earth experiments. As compared to satellites, slow moving aircraft which can fly above most of the sensible atmosphere are attractive as vehicles for conducting propagation experiments because they provide qualitative data, without the threat of additive noise, at less expense, within a shorter equipment design and fabrication period. This qualitative data would be helpful in designing more intelligent space-earth experiments which are more complete and which yield quantitative results.

An air-ground link could quickly provide fading data as a function of elevation angle for a variety of weather models. If the experiment is properly designed, a good assessment of the effects of multipath facing near the horizon could be obtained. In addition, coherence bandwidth as a function of elevation angle for a variety of weather conditions can be determined. One problem in instrumenting air ground experiments is to equip the ground terminal with an aircraft acquisition and tracking capability. It is desirable to determine the variance of the channel characteristics as a function of beamwidth including those very narrow beams, which are expected to be used in space-earth channels. These resulting large ground apertures, far bigger than necessary to complete an air-ground link, create an aircraft acquisition and tracking problem.

The features of aircraft instrumentation which make the air-ground phase of experiments practical are the lesser payload restrictions relative to those found aboard a spacecraft. Reliability requirements are much less because of the ability to correct malfunctions between flights. Ample prime power is available so that sufficient rf power levels can be achieved without regard to conversion efficiency and heat dissipation.

7.3.1 Effects of Aircraft Altitude and Velocity on Simulation

From a cost effectiveness standpoint, aircraft are not satisfactory substitutes for satellites when determining the complete characteristics of space-earth channels. Before giving specific reasons for this statement, it is important to briefly review the effects of the atmosphere on millimeter-wave propagation which are subject to distortion by aircraft speed and altitude.

Propagation of millimeter-waves through the atmosphere has an effect upon the maximum useful receiving aperature and the maximum useful receiver pre-detection integration time. The magnitude of these effects decrease with increasing ground terminal elevation angle and decrease with increasing distance between the receiving system and the perturbing medium. Spatial variations in index of refraction degrade lateral coherence, that is, they spoil the wavefront which is incident upon the receiving aperture. The amount of degradation in aperture gain due to these irregularities increases with aperture size. Variations in the degradation effect the signal facing spectrum along with variations in atmospheric absorption.

Temporal variations in index of refraction along the propagation path are caused by changes in the inhomogeneous atmosphere by circulation of air and the change of path position due to satellite movement with respect to the ground terminal. The degradation in aperture gain due to any temporal variations is reduced by the tracking system's ability to respond to slow variation in wave front tilt. In other words, the tracking system cancels out the low frequency spatial and temporal components of the two dimensional spectral density function for lateral coherence which is sketched in Figure 7-11.

Temporal variations also reduce the maximum useful pre-detection integration time because each spectral line in the waveform is doppler spread by changes in average speed of propagation over the total path. This pre-detection integration time, however, increases with increasing aperture size because of the averaging effects with a larger segment of wavefront.

The ideal experiment would provide a complete statistical model of this two-dimensional lateral coherence function and the accompanying cross-correlation function. However, for the early experiments, the effects of the propagation medium on spectral purity is partially masked by the short term instabilities of the millimeter-wave transmitter until such time that the much needed improvements in state-of-the-art have been accomplished. An indirect account of the effects on spectral purity can be obtained by observing the amplitude fading spectrum.

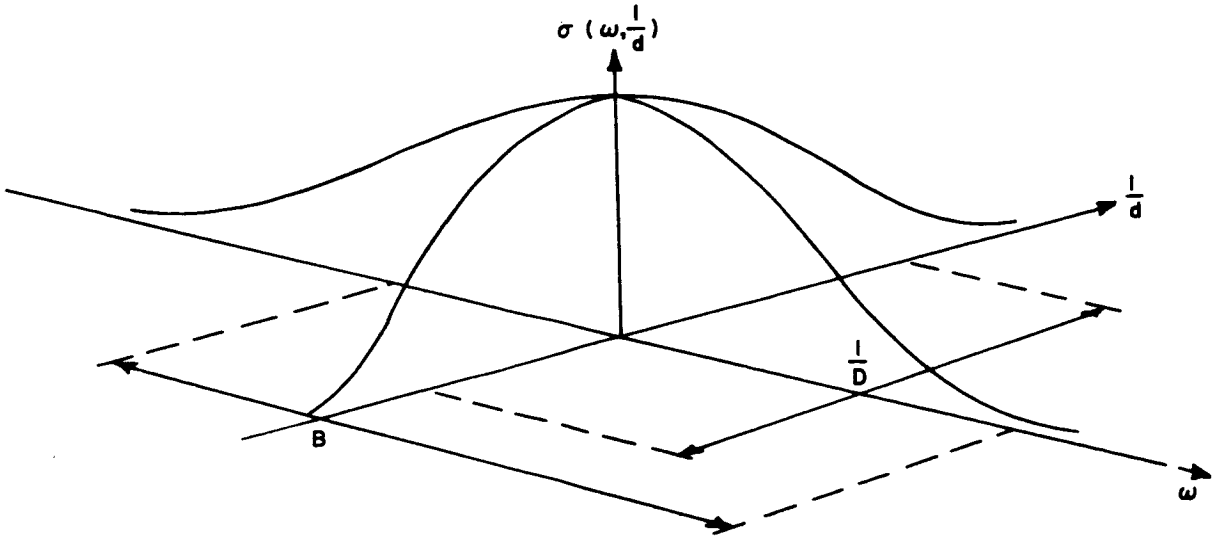

Figure 7-11 Two Dimensional Spectral Density Function For Lateral Coherence

The differences between space-earth channels and air-ground channels as discussed above might turn out to be insignificant but one cannot be completely sure until some measurements are made. To improve the simulation one should strive to use slow moving high altitude aircraft. The effects of atmospheric turbulence on the short term motion of the aircraft decreases with altitude. If the bulk of the perturbing medium happens to be near 8 to 15 thousand feet, then an air-ground channel with a high altitude aircraft (about 40 thousand feet) more nearly represents the space-earth channel. Also the higher the aircraft altitude and the slower the aircraft speed the smaller the apparent wind speeds. Everything that is done to improve simulation increases the costs of the aircraft flight tests. This leads the discussion to one final area -- cost effectiveness of aircraft tests versus cost effectiveness of spacecraft tests. A complete cost effectiveness story is not within the scope of this report, but certain preliminary ideas can be introduced.

The inability of the geometry of air-ground links to simulate the geometry of space-earth links creates certain atmospheric effects which preclude complete substitution of aircraft for spacecraft. There are three major reasons:

a. To determine the spatial dimension for lateral coherence, it is desirable to vary the width of the spatial filter - that is, change the effective receiving aperture size; and change the baseline distance between two spatial filters. Air-ground links for this purpose are difficult to implement because the aircraft is moving. Incidentally, low-orbiting spacecraft are even more undesirable because the spacecraft is seldom within view of the ground terminal. The satellite should be stationary when lateral coherence measurements are being performed because it greatly simplifies the ground instrumentation required.

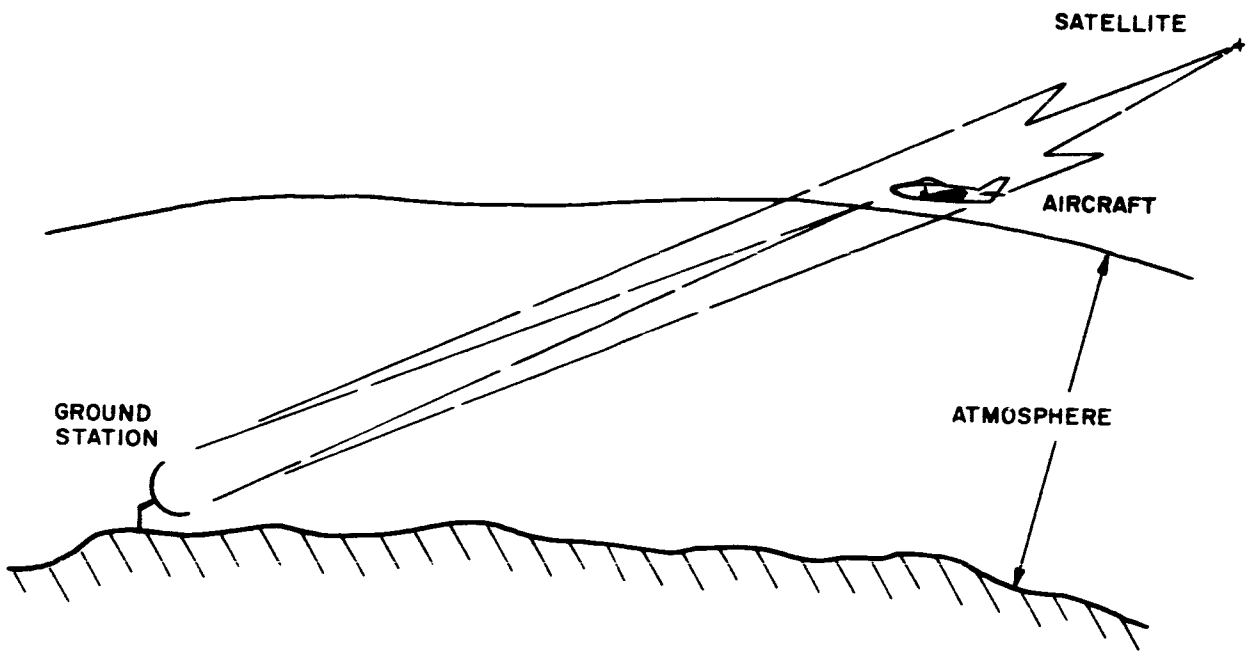

Figure 7-12 Dissimilarities of the Atmospheric Volume Involved in Space-Earth and Air-Ground Communication Channels

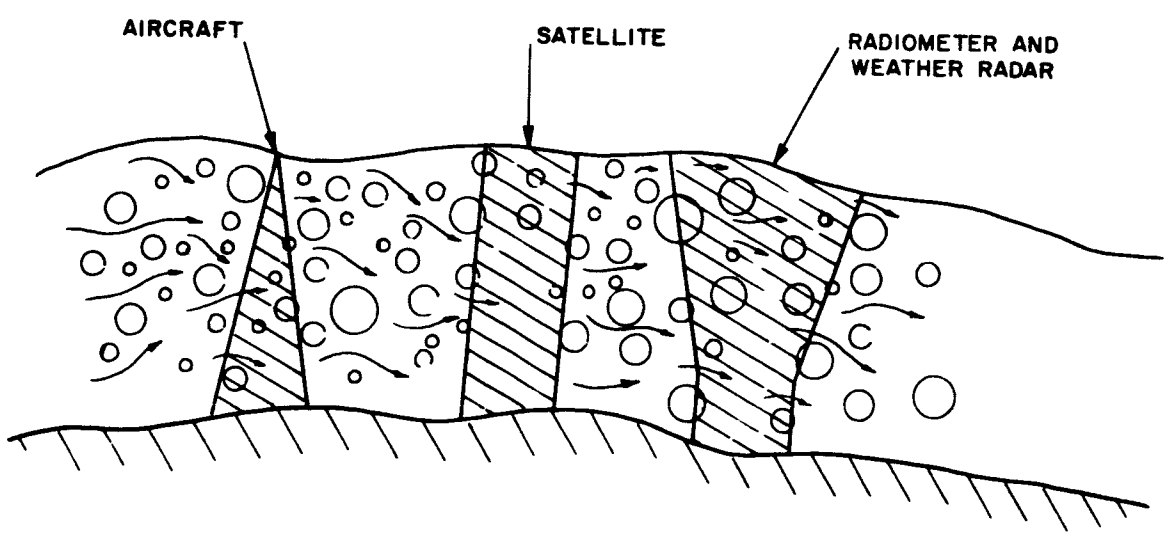

Figure 7-13 Comparison of Atmospheric Volume Involved in Radiometric and Radar Measurements with Atmospheric Volumes Which Affect Communications

b. The drawing in Figure 7-12 illustrates another reason why aircraft data could present results which do not truly simulate space-earth channels. An aircraft flies just above the sensible atmosphere and as a result the volume of the atmosphere which effects the channel is conical in shape with the apex at the aircraft and the base being the ground antenna. When a satellite is used, even a 100mile altitude satellite, the volume of the atmosphere approaches that of a cylinder whose diameter is equal to the diameter of the ground antenna. The effects on the channel are the same when the atmosphere is homogeneous. When the atmosphere is turbulent, especially at the higher altitudes, the difference in channel effects might become appreciable.

Another interesting point to make concerns the use of radiometers and weather radar. An essential input to the experiment results is sky temperature which gives a measure of total atmospheric absorption. Rainfall rates along the path of propagation as measured by a weather radar are also important. The volume of the atmosphere which affects the radiometer and radar measurements are also cones.

The apex of each of these cones is at the ground receiver dish (excluding the near field which is cylindrical) and its cone angle is equal to the beamwidth of the antenna. (See Figure 7-13). When the condition of the atmosphere is homogeneous, the effects are negligible, but when the atmosphere is turbulent, the effects might be significant. The final point to make, is that the inverted cone will more nearly represent a cylinder in the space-earth channel than it will represent a cone in the air-ground channel.

c. The third reason why aircraft data could present results which truly simulate space-earth channels is shown in Figure 7-14. Aircraft flying just above the sensible atmosphere cause the path of propagation to change in position. The movement of the aircraft introduces an apparent wind speed which is proportional to the velocity of the aircraft and proportional to the altitude at which the turbulence

exists. This apparent wind speed can be an order of magnitude greater than true wind speeds which are normally encountered. This "wind" effect is not too serious when simulating space-earth channels for low orbit spacecraft, but when simulating space-earth channels for high altitude spacecraft and deep space probes, there would be some question. Aircraft movement expands the two-dimensional spectral density function in the time domain and direct compression of the time scale may not necessarily simulate the long range channels.

7.3.2 Cost Effectiveness of Aircraft Tests

One of the objectives of the overall millimeter-wave propagation program is to provide the communication system designer with the necessary statistical knowledge to accurately assess the effects of the propagation medium on: the required effective radiated power and effective receiver sensitivity to achieve given nominal data transmission capacities; the signal fidelity or error rate probability or transmitted signals after propagation through the channel; and on the reliability or percentage of time these quantities and qualities are expected to prevail.

A typical work cycle with a stationary satellite which would be satisfactory for the propagation experiments would be to operate during a five day work week, ten to twelve times, spaced seasonally during the year. A full work week every four or five weeks may be the most attractive arrangement from a manpower scheduling point of view. This several week period between tests also provides an opportunity for examining data and making changes in test procedure and ground equipment before the next test.

Each work week could consist of four data collection sessions, four to six hours duration for each; and appropriately spaced so that each station collects data during dawn and dusk and near noon and midnight. These sessions include pre-test and post-test data collection check-out and calibration with the spacecraft simulator which is located at a remote boresight facility. No planning would be made with regard to weather since it is unpredictable and since work schedules must be established well in advance. Enough samples would be taken during the year which should result in a reasonable cross-section of the normal meteorological variables.

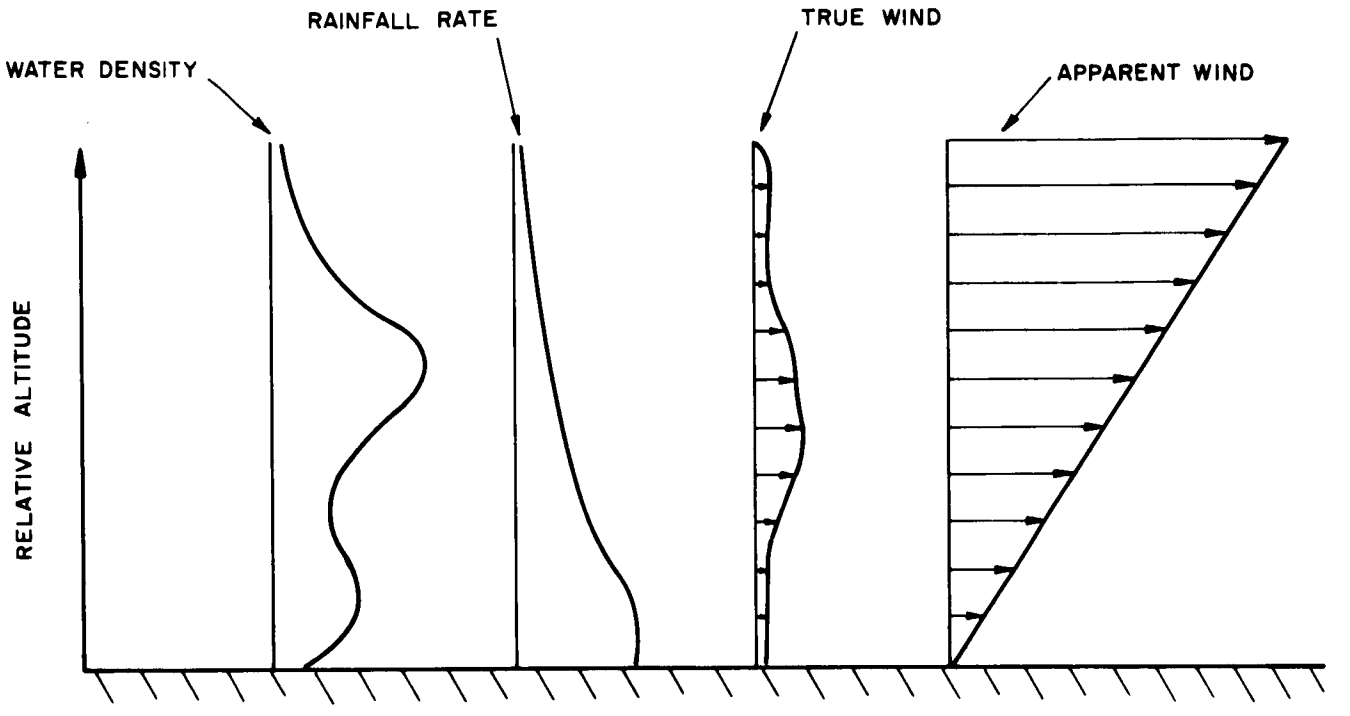

Figure 7-14 Apparent Wind Profile Caused by Aircraft Motion And Its Relation To True Wind, Rainfall Rate and Water Density Profiles

With three ground stations working in different parts of the country, this typical work cycle represents 864 hours of data. It is, of course, not necessary to statistically process all of the data collected in a four to six hour period, but it would be necessary to look for the occurrence of unusual propagation effects, to insure that what is processed, adequately represents the statistical model. If the expense of a high altitude aircraft is compared with the cost of a payload aboard a synchronous satellite to provide that many hours of good data, it can be shown that spacecraft can be very competitive with aircraft as platforms for conducting the propagation experiments. This is based on the assumption that the millimeter-wave experiment is one of several experiments being performed with the satellite such as in the case of the Applications Technology Satellites.

7.4 Up-Links Versus Down-Links

One question, which is continually being asked by those who are interested in millimeter-wave propagation experiments using satellites, is: Why not use millimeter-wave receivers in the satellite instead of millimeter-wave transmitters and thus enhance payload reliability, reduce prime power consumption and weight, and above all, make possible the implementation of these experiments within a shorter time scale? For the initial propagation experiments, it is recommended that down-links be used instead of up-links whenever possible. The reasons for this recommendation are given in this section with the synchronous ATS (Applications Technology Satellites) in mind as the primary candidate for the space platform.

The key to a successful experimental program which involves the assistance of several existing ground installations, each controlled by a different agency, depends on the ease with which these facilities can participate. This ease is measured in terms of expense for any modifications required (unless absorbed by NASA), compatibility with schedules of other activities which involve these facilities, the amount of co-ordination required with other agencies during the operational periods, and the immediate accessibility of the resulting data to the participating agencies.

All of the existing sites under consideration (See Section 9) are equipped with millimeter-wave receivers which are used in radio astronomy. Since these facilities use interchangeable rf heads to change frequency of operation, it is very reasonable to assume that new rf heads, specifically designed for propagation data collection, can be supplied to these facilities. If these existing facilities are to be equipped with transmitters, some serious equipment difficulties can arise. The University of Texas facility, for example, does not use a Cassegrain antenna and, to eliminate long waveguide runs, the transmitter would have to be mounted near the focal point of the parabolic dish. A new transmitter and antenna feed support structure would have to be installed.

Another very important reason for wanting to use satellite transmitters is that less co-ordination is required during the data collection operation. These facilities can receive test waveforms transmitted from the satellite with little or no co-ordination with GSFC except to obtain satellite ephemeris data and to plan the data collection schedules. Several stations can make measurements simultaneously without interfering with one another. When ground transmitters are used, co-ordination is much more difficult, the main reason being that a closed loop is required to confirm that the transmitted signal is being properly received. A closed loop would require that each ground facility be equipped to receive a beacon signal or a telemetry signal from the satellite which indicates that the transmit beam is properly pointed.

One objection to the down-link has been the high prime power requirements of the space transmitter. However, a good receiver local oscillator, especially one that is locked to a stable source, consumes almost as much power and, since it must be on longer than a space transmitter in order to accommodate each ground station individually, it is questionable whether the satellite receiver really provides much advantage in prime power.

One of the prime areas of interest in the propagation experiments is to define the lateral coherence function which was discussed in Section 7.3. This function is two-dimensional in that it describes the maximum useful antenna aperture and the maximum useful integration time of a space-earth channel. It is desirable in the initial experiments to determine at least some

of the points along the spatial axis (points along the frequency axis can be inferred from the amplitude fading spectral density function). These points are determined from measurements using multiple receiving apertures on the ground and, therefore, these measurements can only be made with a down-link.

An essential input to the experiment is sky temperature measurements which give a measure of total atmospheric absorption. The most meaningful measurements are made with ground radiometers which use antennas equivalent in size to those being used for the space-earth link. It is very difficult to share an antenna with a CW signal transmitter and a radiometric receiver. Use of two antennas is out of the question because of expense involved. The frequency of operation of the radiometer would have to be displaced from that of the transmitter by a substantial amount in order to preserve the sensitivity of the radiometer.

When up-links are used, the participating agencies do not have immediate access to the raw data which is being collected. There is a certain delay in obtaining this information which prevents the station operators from evaluating their performance in real time and taking corrective action. It appears certain that in addition to satisfying NASA's requirements, these agencies would want to make specific measurements or data recordings which fulfill some special requirements of their own (antenna pattern measurements is a prime example). When up-links are used, they do not have any of these liberties.

All of these negative features about up-links tend to discourage or prevent other agencies from participating in the propagation program. The absence of their participation means the loss of valuable data points. In addition to losing important weather models, their absence also means degradation in the evaluation profile if a synchronous satellite is used.

On the positive side there are some significant features of the up-link which are worth discussing. First of all, as will be apparent in Section 5.1, satellite receivers are simpler and easier to design. Inherent in the design is improved reliability and significantly lower power consumption expecially in the case of the 16 Gc and 35 Gc receivers. One area of increased reliability

is in signal acquisition because the ground transmitter and receiver local oscillator can now be stabilized with a crystal frequency source. A satellite transmitter could not be stabilized because of the prohibitive amounts of power required, especially at 35 Gc, when considering the ATS satellites.

Even though the positive points for use of up-links are discussed briefly it does not mean that they aren't important. An early space-earth experiment has to depend completely on present technology and a satellite receiver design is considerably closer to meeting longevity and environmental requirements than the present satellite transmitter design. The main question to be answered is: Does the cost of an up-link experiment merit the propagation data it produces? This question can only be answered at such time when a specific satellite has been declared available and actual commitments have been received from the participating agencies who have usable ground terminals.

7.5 Implementation of Measurement Waveforms

As discussed in Section 5.1, three types of test waveforms are considered: an AM waveform with two sidebands, a PAM waveform, which is a time quantized pulse amplitude modulated waveform, and a PAM/FM test waveform which involves a pulse amplitude modulated waveform on a frequency modulated carrier. This section of the report deals with the implementation of these proposed waveforms. It was concluded that the basic measurement waveform to be transmitted is a simple one (that is, a carrier and one pair of variably spaced AM sidebands), yet it will provide ample information on the propagation channel. Although other more sophisticated waveforms are discussed, these are left for use in future experiments which are based on the results of the initial experiments. A choice between an unmodulated carrier and a modulated carrier will be provided, with the modulating frequency being variable in several discrete steps up to at least 50 megacycles.

7.5.1 AM Test Waveform

The AM test waveform lends itself readily to implementation in that it does allow the use of a stabilized millimeter source as the carrier through the use of an inguide shunt-mounted semi-conductor modulator.

The sideband energy is introduced onto the stable carrier. It is felt, at this time, that this particular approach is realistic and within the state-of the-art, requiring a minimum amount of development work for implementations, when a reasonable transmitter power level is considered. This holds for frequencies from 10 through 35 Gc. This shunt type of modulation does allow the introduction of modulating signals ranging from dc on through approximately 25 to 50 mc. The upper limiting capability of these shunt modulators is somewhat determined by the indicent RF power which is being modulated. This is to say that the upper frequency limit of modulation is inversely proportional to the power being modulated. Above this frequency range, namely, from 8 mm to 3 mm, a major development program in the semiconductor material and the type of modulation techniques would be required. This modulation approach can be implemented with approximately a 20 db on-off ratio which is equivalent to an approximate index of modulation of 80 percent. This modulation index would prove to be most adequate for the evaluation of the communication channel. The limiting factors in the generation of this modulation index are the engineering trade-offs between insertion loss I_L and isolation Iso, namely, the switching ratio Iso:I_L of the modulator. Hence, if more than 80 percent modulation was required, this would be accompanied by a greater loss in carrier power due to I_L.

7.5.2 PAM Test Waveform

The second modulation to be considered is that of a PAM waveform. The implementation of the PAM Test Waveform is very similar to that discussed for the AM Test Waveform, in that an RF line modulation would be used. The major difference is that the modulation signals will now become a pulse train, and the output would be RF pulses which have a coherent stable characteristic. It is suggested that a 10 nanosecond pulse will be used with a one to two nanosecond rise time. This type of modulation can best be accomplished at a power level below 100 mw and at a wavelength below 8 mm. Since this technique does require the utilization of a duty factor, this approach of RF line modulation yields a reduction in average power which is proportional to the duty of the waveform generator. Therefore, it is felt that this modulated signal be followed by a coherent pulse amplifier such as a TWT, Pulse Klystron

Amplifier, and/or other devices. This would allow for boosting the peak power output to obtain an average power level which would provide adequate signal-to-noise ratio in the channelized receiver. This problem of generating peak power in coherent millimeter devices cannot be solved without a development in the RF source capability. This fact became quite evident during a survey of millimeter components.

The same results showed dramatically the limitations that are evident in today's millimeter source technology. Namely, the only devices capable of peak power equal to average power are found in the magnetron family and those are duty limited and provide only non-coherent signals, which would pose major problems in obtaining narrow-band predetection bandwidths.

7.5.3 PAM/FM Test Waveform

The pulse amplitude modulated FM test waveform can be implemented most readily through the utilization of a low power pulse amplitude FM signal generator followed by a final driver RF amplifier, such as TWT's and/or RF distributed amplifier techniques. Once again, the argument as presented in the preceding paragraph, as it relates to peak and average power devices, is applicable to this type of operation. Hence, the implementation of this system would be through the utilization of a low power FM oscillator followed by an RF line modulator whose output is fed directly to a high power transmitter amplifier device. Through the implementation of this technique, it is felt that this will more closely simulate an actual PAM/FM communication system, in that direct control of the PAM and direct control of the FM signals may be independent and may provide a coherent source for the purposes of implementing a channelized receiver.

7.6 Experiment Equipment Configurations

This section of the report deals with the proposed implementation of space flight hardware and existing or planned ground facilities which would be

needed in the initial propagation measurements program outlined in the summary. The proposed program satisfies the basic measurements requirements and uses a basic measurement waveform which can be readily implemented. In view of the existing and planned experimental millimeter wave facilities, the proposed experiments would make the best use of all the available equipment capabilities and, therefore, provide the best propagation data for the funds and payload space expended.

GSFC is developing a millimeter-wave experimental facility for performing space-earth communication/propagation experiments. This facility will serve as the major participant in this data collection program. Other facilities which are considered are those which presently exist at Aerospace Corporation, The University of Texas, Air Force Cambridge Research Laboratories (AFCRL), and Lincoln Laboratory.

7.6.1 Spacecraft Configuration

It is proposed that the 35 Gc and 16 Gc satellite transmitters be utilized. Each transmits a single AM double-sideband waveform with a variable modulation frequency which is received by several ground stations simultaneously. In addition, it is proposed that a 94 Gc receiver be carried aboard the satellite in order to receive an AM double-sideband waveform from a transmitter such as the one being developed for the Aerospace facility. The design details for the spacecraft equipment are given in Section 8.1.

At this point, it is desirable to restate a few of the many considerations which have led to the selection of this experiment. First and foremost, the availability of flight qualified hardware grossly limits the introduction of more sophisticated and/or higher frequency devices to be carried in the vehicle as transmitter sources, although it is well acknowledged that a transmitter source in the vehicle does present the most useful of all experimental approaches.

Secondly, the 35 Gc and 16 Gc transmitter power capabilities will range from a minimum useful radiated RF power of 200 milliwatts up to approximately 10 watts of RF power. These factors may again be considered as tradeoffs depending upon the time of the experiment, namely, the schedule of development and, the specific satellite which is available.

As will be noted, tubes are available which possess the capability of providing a suitable RF source which has been missile and/or aircraft flight tested, hence will provide the greatest factor of confidence in the system.

A third major consideration in the selection of this spacecraft configuration has been the availability of ground facilities and their ability to adequately interface with a communications experiment. It is most apparent that all sites presently available have been established and are presently utilizing radiometric systems as their main operational mode. In examining their capabilities, it is evident that, in order to achieve meaningful experimental data, a thorough site evaluation is necessary. This requires data on the facilities' operational capabilities at the frequencies at which the experiment is performed. The selection of a 35 Gc satellite transmitter was made primarily on the basis that all of the existing sites except Aerospace are presently performing at 35 Gc. Radiometric measurements have been made with these antenna facilities, either on extended targets or point sources, which have allowed them to perform sufficient antenna calibration and beam pattern measurements. Also, for the most part, all of these facilities have boresight facility measurements on their antenna and have established gain figures of antennas and pointing accuracy capabilities.

The selection of a 16 Gc satellite transmitter was made on the basis that it represents a logical point in the 10-100 Gc spectrum at which to perform propagation-communication experiments before entering the major area of atmospheric absorption.

Hence, for the above listed reasons, it was deemed most advisable that a 35 Gc and 16 Gc experiment be performed which allows the utilization of the University of Texas, Lincoln Laboratory and AFCRL facilities and could also include the recently developed Haystack facility as a possible receiver site for the evaluation of a large antenna aperture. Also, in conjunction with the vehicles transmitter capabilities, and with the presently planned 94 Gc transmitter capability at the Aerospace Corporation, it will be shown that the ability to piggy-back a 94 Gc receiver on the 35 Gc transmitter in the satellite does not grossly penalize the weight and power consumption of the payload. It is proposed that this be accomplished by utilizing the third harmonic of 35 Gc and an X-band IF technique which will allow the reception of 94 Gc signals. It is felt that this technique of utilizing a receiver in the spacecraft most readily interfaces with the Aerospace facility since they are presently instrumenting a one-hundred watt 94 Gc transmitter capability.

The 16 Gc satellite transmitter presently would interface with the Goddard Facility and the Canadian station for the Defense Telecommunication Research Establishment. The remaining facilities would have to be modified with receivers in order to participate at this frequency during the propagation experiments.

7.6.2 Ground Facilities Configurations

An evaluation of the existing and planned U.S. facilities is discussed in Section 9. The remainder of this section discusses the general ground equipment configuration and, the associated design details of the actual hardware are given in Section 8.2. A ground equipment list was given in Section 2.1.3 of the Second Quarterly. In order to provide a well coordinated propagation data collection program it is considered worthwhile that certain components on that list be purchased by NASA funds if necessary to insure that they be built to identical specifications. Commonality of equipment increases the value of experimental results and reduces data processing expenses.

GSFC Facility

The general equipment configuration for the GSFC facility is shown in Figure 7-15. An antenna system, consisting of a 15-foot parabolic reflector mounted on an elevation over azimuth pedestal with its 32-foot tower, is one of the major items in the GSFC facility. A receiver system, shown in Figure 7-16, is required for this antenna system in order to provide a ground terminal for experimental space-earth propagation links. It is intended that the antenna system will be equipped to track satellites via programmed ephemeris data utilizing a single lobe receiver pattern and by later modifications, it will be equipped to automatically track satellites by means of multiple channel millimeter-wave receivers. The final receiver system should consist of: interchangeable RF heads for specific frequencies within the 8 Gc to 94 Gc frequency range (mounted in a compartment behind the reflector); communication, radiometric and tracking IF receivers; signal processors; and analog data recorders. The radiometric IF receivers which share the same RF head as the Signal IF receivers are essential to the program as the chief source of correlative data.

The GSFC complex should also have a system of millimeter-wave signal sources to be installed at a remote location which operates with the receiver system in the main facility. The sources are required for antenna boresighting and beam pattern measurement. These signal sources with appropriate modulators will also establish ground-to-ground links, which will be useful in developing millimeter system technology to be applied to the instrumentation of space-earth experimental communication links. The signal sources should be designed and packaged such that the 94 Gc klystron and associated components can be used to drive a 94 Gc power amplifier employed in the antenna compartment at the main facility. The signal sources are illustrated in Figure 7-17.

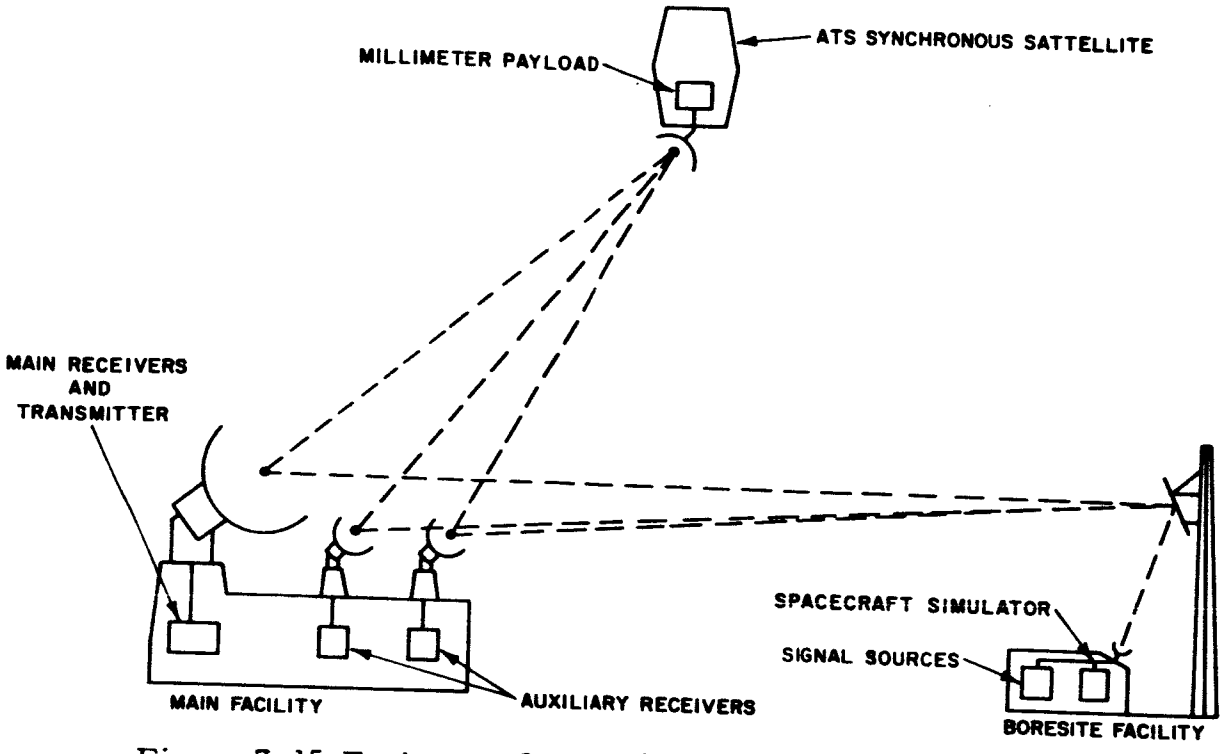

Figure 7-15 Equipment Layout for ATS Synchronous Satellite and GSFC Millimeter Experimental Ground Facility

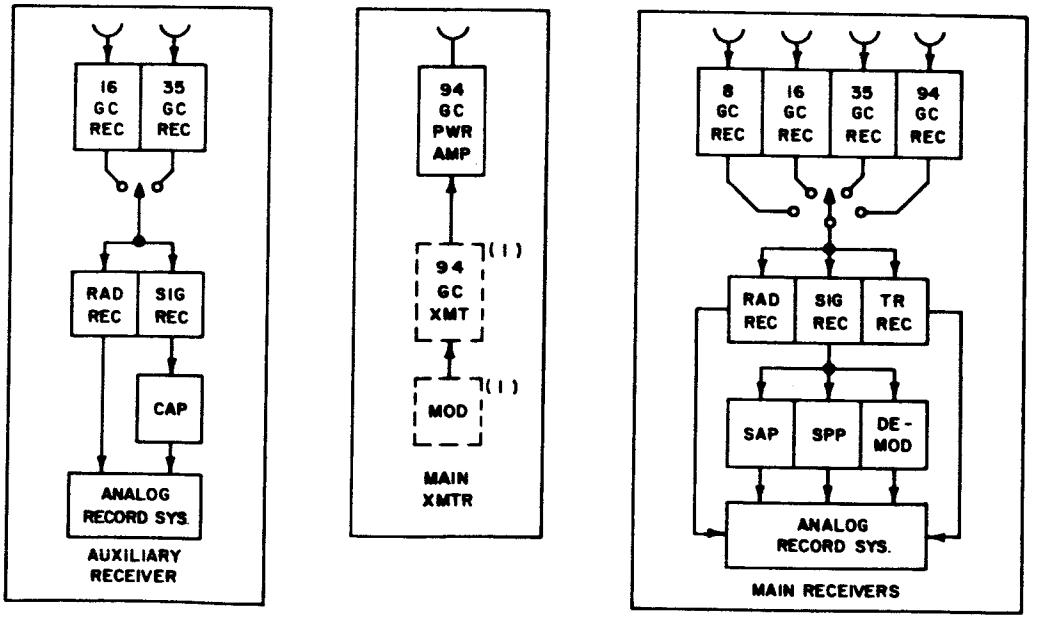

(I) BORROWED FROM SIGNAL SOURCES IN BORESITE FACILITY
CAP -- CARRIER AMPLITUDE PROCESSOR
SAP -- SIGNAL AMPLITUDE PROCESSOR
SPP -- SIGNAL PHASE PROCESSOR

Figure 7-16 Component Layout for GSFC Main Facility

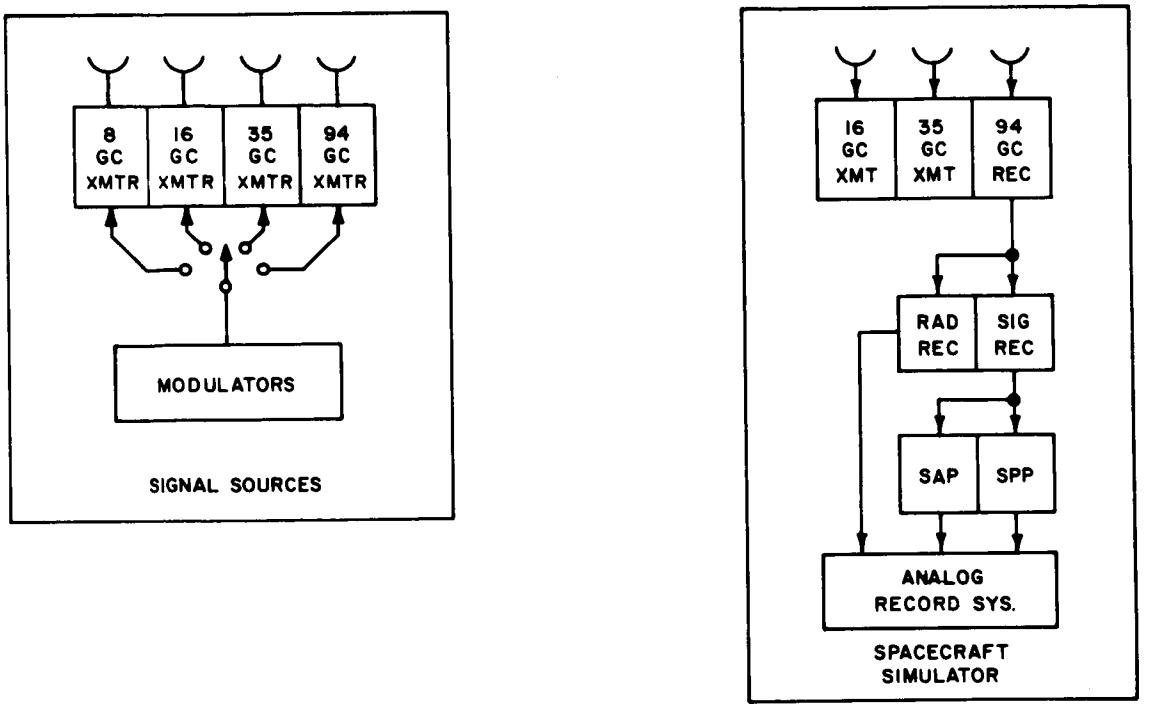

Figure 7-17 Equipment Layout for GSFC Boresight Facility

Also at this remote boresight facility, a spacecraft simulator is required which operates with the main facility and performs the same functions intended for the spacecraft equipment. For the GSFC facility this simulator can be the engineering model of the flight hardware which is recommended for the initial experiments. A spacecraft simulator is essential at the boresight installation for each participating facility in order to properly calibrate and checkout the data collection system before each data collection test.

Finally, auxiliary receivers are suggested which consist of subsystems that are identical to some of the main receiver subsystems and are incorporated into smaller antenna systems. These receivers are shown in Figure 7-19, where three possible modes of operation at the GSFC facility is presented. These three modes of operation can exist simultaneously and the data results to be obtained from these modes of operation are tabulated in Table 7-5.

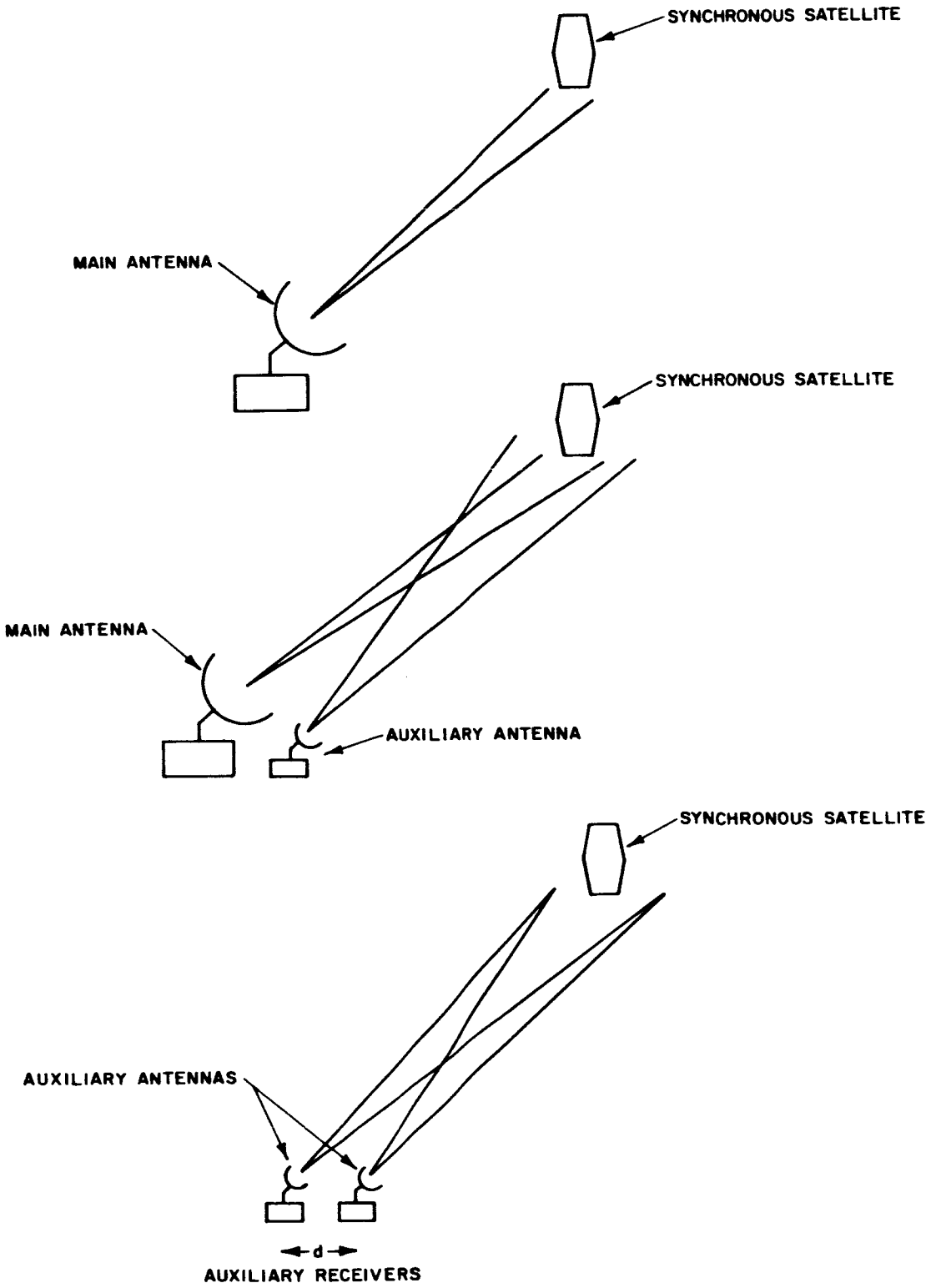

Figure 7-18 Modes of Operation at GSFC with a Synchronous Satellite

TABLE 7-6

PROPAGATION DATA RESULTS FOR DIFFERENT MODES OF OPERATION

Mode	Equipment	Data Results
1	Main Antenna	Atmospheric absorption, carrier amplitude fading, correlation of carrier and sideband fading and relative phase of sidebands as a function of AM modulation frequency by receiving signals at 16 Gc and 35 Gc and transmitting signals at 94 Gc. Wavefront tilt by observing tracking receiver error signals.
2	Main Antenna & Auxillary Antenna	Correlation of carrier fading for two different beamwidths by receiving signals at 16 Gc and 35 Gc.
3	Two Auxillary Antennas	Correlation of carrier fading as a function of distance, d, by receiving signals at 16 Gc and 35 Gc in two auxiliary receivers.
Future	Two Auxiliary Antennas and Two Mirrors	Correlation of carrier fading and reflective phase of received carriers as a function of distance, d.

The auxiliary receivers are considered good insurance for a successful propagation experiment associated with a synchronous satellite. The additional knowledge gained for the fractional increase in the total program cost is considered to be an excellent bargain.

The auxiliary receivers can also be moved to some other location such as Rosman, North Carolina, or WSMR, New Mexico, to assist in establishing an elevation profile of carrier fading statistics.

With the use of mirrors, Mode 3 could be expanded as shown in Figure 7-20. The reason for the mirrors is to allow the receivers to share a common millimeter-wave local oscillator so that relative phase measurements can be made. The data results obtained from this configuration are also given in Table 7-5. However, this configuration is not recommended as an initial experiment since its useful design depends upon results from Mode 3.

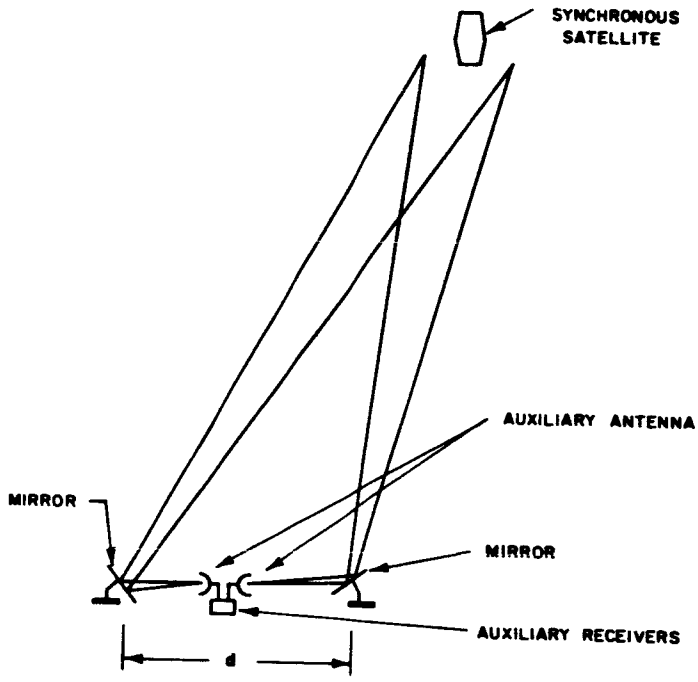

Figure 7-19 Possible Future Mode of Operation with Two Auxiliary Receivers

Other Facilities

The other facilities being considered should be equipped with new interchangeable RF heads which are custom-packaged to interface with the existing antenna system and specifically designed to operate with receiver IF units identical to those used in the GSFC facility. The packaging of the IF units, the signal processor and the analog recording system can be identical for all of the installations. A spacecraft simulator, whose subsystem electrical design is identical to the engineering model of the flight hardware, should be installed at each facility's boresight location. The system make-up of the simulators will vary depending upon the frequencies of operation at each facility.

sources, and presents the transfer equations which allow for the proper selection of the optimum loop closure for a given device. The selected loop is dependent on the control parameters and the types of RF sources under consideration in the utilization of different loop techniques that allow for either frequency locking or phase locking of RF sources. The loops discussed in the survey are generally applicable as either transmitter stabilizers or local oscillator AFC lock subsystems.

Appendix I of the Second Quarterly Report deals with a proposed development program designed to bridge the gap between the present state-of-the-art millimeter equipment and that equipment required for future satellite communication systems. These proposed systems are considered to be a logical extension of the spacecraft experiments described in this report and are designed to make maximum use of the presently available millimeter technology and the lower frequency microwave developments.

8.1 Spacecraft Equipment

The satellite transmitter and receiver block diagrams are shown in Figure 8-1. The two transmitters are considered to be the greatest power consuming devices aboard the satellite, and thus will receive prime emphasis.

8.1.1 35 Gc Satellite Transmitter

The efficiency of the 35 Gc transmitter tubes being considered ranges from 0.1 to 1.0 percent, and it should be noted that as the efficiency of the device is increased the prime power supplies decrease proportionately in size and weight. Two types of klystron oscillators capable of supplying 2 w and 200 mw respectively, are presently available. The efficiency of these two devices varies by almost one order of magnitude. This is due to the fact that as higher power outputs are attained, the standby power, such as filament power, becomes less significant in the accumulative prime power required. This continues to be the case as greater RF power is generated.

Section 8
EQUIPMENT DESIGN

This section of the report deals with the proposed implementation of ground station and space flight hardware, discussed in Section 7.6, which would be needed in the initial propagation measurements program. The proposed program satisfies the basic measurements requirements and uses a basic measurement waveform which can be readily implemented. In view of the existing and planned experimental millimeter wave facilities, the proposed experiments would make the best use of all the available equipment capabilities and, therefore, provide the best propagation data for the funds and payload space expended.

The hardware considered for the design of the payload modules consists mainly of state-of-the-art items which can be qualified for one year's operation in a spacecraft environment. The objective of the experiment is to gather propagation data and not to show feasibility of sophisticated millimeter-wave hardware. In those cases where suitable components are not available, component tests and breadboard activities required to complete a qualified design are identified.

By way of demonstrating feasibility of the proposed experiments, the RF component survey was concentrated on the definition of RF sources, since millimeter wave generation is deemed the most critical factor in the payload design. This survey, which was presented in Section 5.4 of the First Quarterly Report, represents the present state-of-the-art availability and also includes projections of presently active development programs and proposed programs.

Section 5.5 of the First Quarterly Report is a survey of frequency control methods implemented through the use of stabilization loop techniques in RF

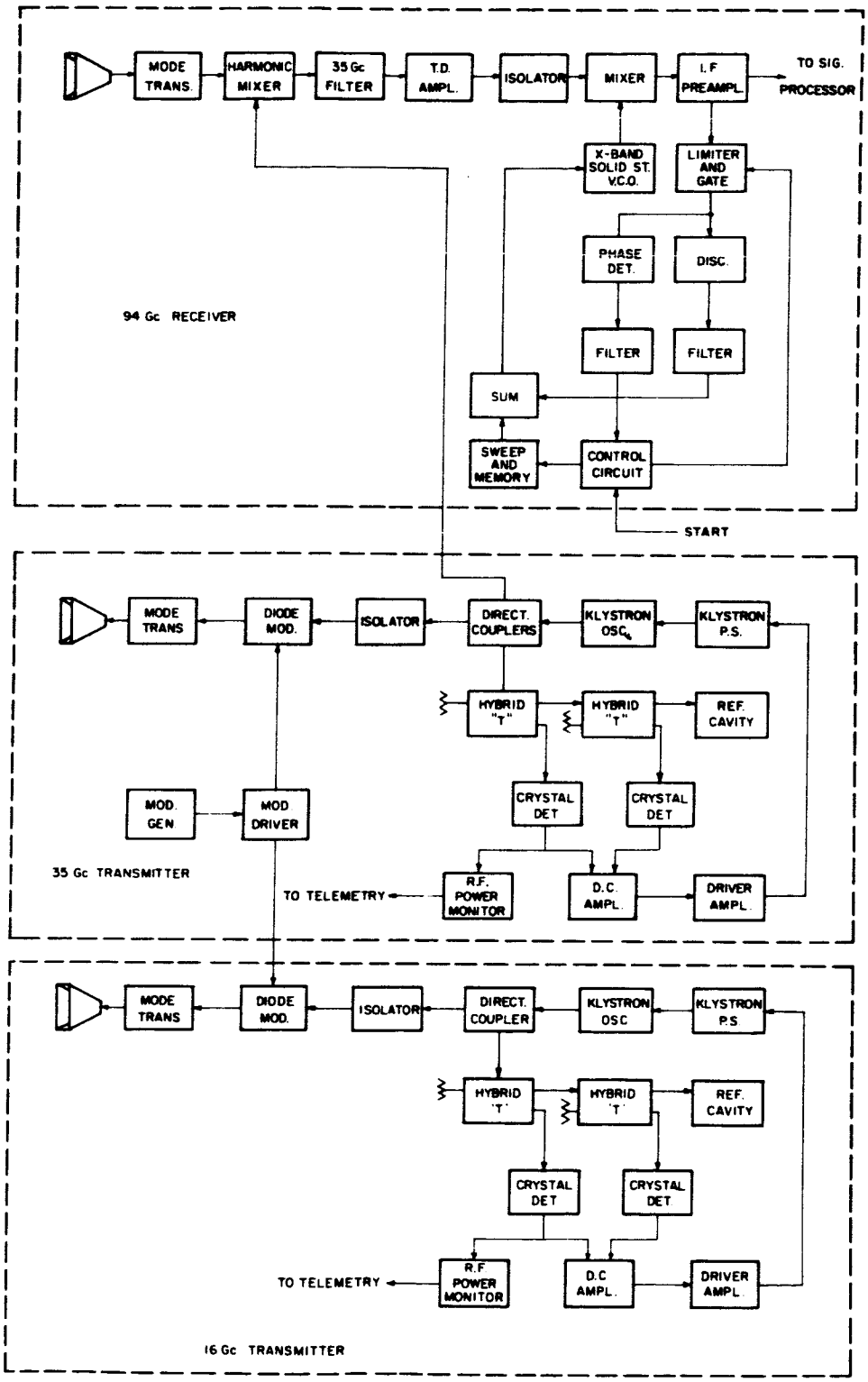

Figure 8-1 Satellite Transmitters and Receiver

The possibility of introducing a two-watt transmitter is within the state-of-the-art if one is willing to supply prime power in excess of 250 w. To supply the minimum useful output of 200 mw with present-day tubes, about 80 w of prime power must be supplied.

For this report the design of a 200 mw transmitter is presented because of the specified prime power restrictions and because it possibly represents the minimum useful experiment. Higher power designs will be discussed in subsequent reports. Referring to the 35 Gc transmitter in the block diagram of Figure 8-1, the total losses in the various coupling elements have been estimated conservatively to be a maximum of 3 db. Thus, the source must be capable of delivering a minimum of 400 mw of microwave power. It is further desirable to employ as the transmitter a device which has been derated as far as its power output is concerned, and ruggedized for missile applications.

One possibility is the I. T. T. F-2900 series Klystron. This klystron has been derated from an output of about 1 w to 400 mw. It is felt that no serious problem exists in operating this device at 400 mw output power. Another possible device is the Varian VA-283 reflex klystron with an output power of 400 mw. This tube has been designed for extreme environments in airborne applications.

The prime power required for a selected VA-283 or F-2900 is 77 w. The transmitting tube will be stabilized in frequency utilizing an AFC loop. The sampled power is derived from a directional coupler with a coupling coefficient of about 20 db. and an insertion loss not exceeding 0.5 db. The transmitted power, meanwhile, is applied to the input of a second directional coupler. Here, approximately 10 mw is coupled out and applied as the local oscillator drive to the 94 Gc receiver harmonic mixer. The output of this directional coupler is fed to a semiconductor AM shunt modulator. The insertion loss of the modulator is estimated at a maximum of 1.5 db.

The RF carrier is modulated at three independent modulation frequencies, i.e., 10 kc, 10 mc, and 50 mc. The change in modulation frequency is performed in a step manner and need not be done excessively fast as the propagation path of a 6000 nmi satellite will not change at a fast rate. The modulating signals are derived from the spacecraft reference and divided down to the proper frequencies. These frequencies are selectable either through a ground command or a simple, slow commutating switch aboard the satellite.

The modulator itself consists very simply of a varactor diode located in a shunt configuration in a $\pi/4$ length of waveguide. One side of the diode is at DC ground, while the other side is attached to a TNC connector center conductor via an RF bypass network. The drive power required is quite small, certainly below 100 mw. Thus, the modulator driver need not be very elaborate. A transistor buffer amplifier followed by an emitter follower ought to suffice. The modulated RF is now applied to the antenna through a short length of waveguide. The antenna is discussed in Section 3.1.4.

Table 8-1 is a tabulation of the weight, volume, and power consumed by the 35 Gc transmitter module. The weight of the module is well below the 25 pound limitation and according to the total volume, the transmitter can easily be packaged into the nominal 18 x 11 x 8 in. experiment package.

8.1.2 16 Gc Satellite Transmitter

As in the 35 Gc transmitter discussion, the 200 mw transmitted power case is presented because of the prime power restrictions. Here also the transmission losses in the transmitter system have been estimated at 3 db maximum and the source must, therefore, be capable of 400 mw of RF power in order to deliver 200 mw to the antenna system. The same qualities of a derated, rugged, reliable device are also desirable as in the 35 Gc case.

TABLE 8-1

35 Gc TRANSMITTER VOLUME, WEIGHT AND POWER

Item	Weight (oz)	Size (in.)	Prime Power Required (w)	Remarks
Diode Md.	2.	2x1x1		
Modulator Driver	4.	2x2x3	1.0	
Modulation Gen.	2.	1x1x2	0.2	
Directional Coupler	5.	2x2x1		
Isolator	3.	2x1x1		
Klystron (400 mw)	7.	3x2x2	56.0	ITT or Varian Selected Tube
Klystron Power Supply	64.	3x3x10	21.0	
Hybrid 'T'	4.	3x2x2		2 required
Cavity	8.	3x3x3		
Crystal Det.	2.	1x1x3		2 required
D. C. Amplifier	4.	2x2x3	1.0	
Driver Amplifier	4.	2x2x3	1.0	
Program Control	4.	2x2x3	0.5	
Waveguide	12.	2x2x12		
Connectors	16.	1x1x8		
Miscellaneous	16.	3x6x6		Coax cable and wire
TOTALS	9 lbs. 13 oz.	336 cu. in.	80.7 w	

A typical device under consideration is a selected Sperry type SOU-403 two-cavity klystron. This device is capable of 1w power output, but would be operated in a derated manner to improve reliability and to reduce power consumption. The prime power required for operation of a selected klystron would be about 72 w, which includes power supply conversion losses.

The transmitting tube will be stabilized in frequency by means of an AFC loop as shown in Figure 8-1. The operation of the loop is essentially the same as the one used in the 35 Gc transmitters and is described in the preceding section.

The RF carrier will be modulated in the same manner as the 35 Gc transmitter using the same type of diode modulator. The 16 Gc antenna is discussed in Section 8.1.4.

Table 8-2 is a tabulation of the weight, volume and power consumption expected in implementing the 16 Gc transmitter module.

8.1.3 94 Gc Satellite Receiver

As previously described in this section, the proposed satellite receiver will make use of a portion of the on-board generated RF energy from the unmodulated 35 Gc transmitter carrier. Through the implementation of this technique, the receiver's overall prime power consumption is drastically reduced. As an example, it would require approximately 60 to 80 w prime power to generate the necessary local oscillator signal for the first converter.

TABLE 8-2

16 Gc TRANSMITTER VOLUME, WEIGHT AND POWER

Item	Weight (oz)	Size (in.)	Prime Power Required (w)	Remarks
Diode Mod.	2.	2x1x1		
Modulator Driver	4.	2x2x3	1.0	
Modulation Gen.	2.	1x1x2	0.2	
Direct. Coupler	5.	2x2x1		
Isolator	3.	2x1x1		
Klystron (400 mw)	7.	3x2x2	35.0	Selected Sperry Type SOU-408 2 Cavity
Cavity	8.	3x3x3		
Hybrid 'T's	4.	1x1x1/2		2 required
Crystal Det.	2.	1x1x3		2 required
D. C. Amplifier	4.	2x2x3	1.0	
Driver Amplifier	4.	2x2x3	1.0	
Klystron Power Supply	64.	3x3x10	15.0	
Waveguide	16.	2x2x12		
Connectors	16.	1x1x8		
Miscellaneous	16.	3x6x6		Coax cable
TOTALS	9 lbs. 13 oz	343 cu. in.	53.2	

However, in the proposed implementation, the satellite 94 Gc receiver utilizes the previously generated 35 Gc signal as its first converter signal, and, through the use of a third harmonic converter receiver operation is feasible at the expense of 6 w or less. The proposed receiver and its interface with the transmitter is shown in Figure 8-1.

Once the 94 Gc signal has been received by the antenna, it is fed to the harmonic mixer where it is converted into the first IF. This first converter derives its local oscillator drive from the 35 Gc transmitter by means of a directional coupler. The third harmonic is generated in the nonlinear mixer diode and is used as the down converting signal in order to derive the X-band IF signal. It should be noted that this technique is not beyond the present state-of-the-art, considering the millimeter and submillimeter work being done by many in the field and, in particular, the capabilities of Raytheon's Santa Barbara Operation to utilize their wafer diodes as harmonic mixer elements for receiving systems in the millimeter and submillimeter regions. The X-band IF system consists of a tunnel diode amplifier which requires minimum power, yet provides adequate amplification to minimize the effects of the second stage noise figure. Considering that both of these devices represent state-of-the-art technology, this approach becomes quite practical.

The first IF is now followed by the second mixer which converts the X-band signal to a second intermediate frequency at approximately 200 mc with an instantaneous bandwidth of approximately 100 mc. The output of this IF is then fed directly to a triplexing device which, through high pass, low pass, and bandpass filtering, allows the selection of the carrier and its two associated sidebands. At this point the carrier filter output is utilized for closing the loop of the phase locked AFC system. This is accomplished by means of tuned narrow band amplifiers and limiters in order to provide the error signal for the phase comparator which drives the VCO. This VCO is a solid state, X-band oscillator which is tuned to the proper frequency in order to correct for doppler and other frequency shifts inherent in the

communications channel. This loop will be provided with an automatic sweep acquisition circuit which sweeps the VCO until a lock signal is derived from the phase comparator, and will also contain an override signal to prevent the VCO from locking onto one of the sidebands associated with the carrier. The following sections will describe in more detail how these two signals, the sweep and lock-on override signals, are derived from the signal processor.

Table 8-3 provides a reasonable weight, size, and power estimate of this particular receiver system. As can be seen from the tabulation, the totals for the incorporation of this receiver within the 35 Gc transmitter

TABLE 8-3

94 Gc RECEIVER VOLUME, WEIGHT AND POWER

Item	Weight (oz)	Size (in.)	Prime Power Required (w)	Remarks
Harmonic Mixer	6.	4x2x2		
Tunnel Diode Ampl.	6.	3x3x2	0.1	
Mixer Preamplifier	13.	6x3x2	0.5	
X-band Solid State Source	9.	3x3x3	3.4	
Band Pass Ampl.	2.	2x1x1	0.2	Parts only will build - 2 required
Video Amp. Σ	8.	3x3x2	0.2	Parts only will build-2 required
Second Mixer B. P. Ampl., Det.	5.	4x1x1	0.1	Parts only will build-2 required
3 Mixers & 3 Filters	4.	3x3x1	0.1	Parts only will build
Synth., Gates, F. D. C.	6.	3x3x2	0.5	Parts only will build
ϕ Det., Disc., Σ	5.	3x2x1	0.5	Parts only will build - 2 required
Limiter, Integ. ϕ shift, ϕ Det.	3.	3x1x1	0.5	Parts only will build - 2 required
Limiter & Gate	4.	2x2x1	0.4	Parts only will build
Waveguide	8.	2x2x12		
Connectors	16.	1x1x8		
Miscellaneous	16.	3x6x6		Coax and wire
TOTALS	7 lbs. 8 oz.	325 cu. in.	7.5 w	

burdens the prime power source by a very small amount. The combined weight and volume of the 35 Gc transmitter/94 Gc receiver package is still within the 25 lb. limitation and should fit into the nominal 18x11x8 in. experiment package.

8.1.4 Spacecraft Interfaces

There are three areas in which serious interface problems exist between millimeter-wave experiment modules and the ATS spacecraft. Several basic questions are yet unanswered in the areas of prime power, data transmission and the space-frame.

Prime Power

The electrical power subsystem[63] of the Applications Technology Satellite provides electrical power to the other spacecraft subsystems. The primary power source for both the medium and synchronous altitude satellites is a solar cell array. Battery cells are used to provide power during transient loads and solar eclipses.

The electrical power is delivered to the payloads through two busses. Each payload is connected to a bus through a payload regulator. The payload regulator controls voltage and ripple to the payload, and operates up to 136% of nominal full load current of the payload. Experiment payloads are also connected to the unregulated bus through a power switch in parallel with the regulator. This switch handles high current, short duration loads which exceed the regulator limit and are less than a defined maximum limit. The specific voltage, current and ripple parameters are given in Table 8-4.

The interface problem with the electrical power subsystem is a big one. The 35 Gc transmitter/94 Gc receiver module requires approximately 85 watts of prime power and the 16 Gc transmitter module requires approximately 55 watts of prime power. It is understood that the ATS spacecraft was designed with 25 watt experiments[64, 65] in mind. It is hoped that, since the millimeter-wave propagation data would be collected during only a small

fraction of the total operational life of the satellite, the power subsystem could accommodate the larger amounts of power on a time shared basis with other experiments.

TABLE 8-4

ELECTRICAL POWER SUBSYSTEM CHARACTERISTICS

APPLICATIONS TECHNOLOGY SATELLITE

Parameter	Limits
Voltage - Normal	
Unregulated Bus	-24.5 to -32.0 Vdc
Payload Regulator Output	-24 Vdc ± 2%
Battery	-24.5 Vdc at 25% discharge depth
Voltage - Transient	
Unregulated Bus (0.5 seconds max.)	-21 to -32 Vdc
Payload Regulator Output	-26 Vdc max.
Ripple	
Unregulated Bus	500 mV peak - peak
Payload Regulator Output	10 mV peak - peak
Current	
Solar Cell*	
SASSE	6.35 Amps
SAGGE	4.75 Amps
MAGGE	4.75 Amps
Battery	
SASSE	1.15 Amps for 1.15 hours
SAGGE	1.15 Amps for 1.15 hours
MAGGE	1.75 Amps for 0..75 hours
Life	75% of initial capacity after 3 years in orbit

*Not including battery charging current

Telemetry and Command

The telemetry and command subsystem[66] of the ATS satellite consists of three equipment groups:

a. Telemetry group, containing:
   1. Four transmitters
   2. Two PCM telemetry encoders
b. Command group, containing:
   1. Two receivers
   2. Two command decoders
c. Antenna group, containing:
   1. Two antenna hybrid baluns
   2. Two sets of antennas
   3. Two diplexers

This subsystem interfaces with the millimeter wave experiment to turn the experiment ON and OFF, to change modulation frequency, and possibly to encode and transmit data from the experiment. Interface with the command portion of this subsystem is not difficult and therefore will not be discussed in this section.

The telemetry portion of this subsystem, specifically the encoding and multiplexing functions, are marginal for handling the data from the millimeter wave experiment because of the experiment's high data rates on most of its outputs. Since it may be possible to reduce the data rates slightly, the subsystem's interface characteristics are discussed below. Maximum experiment data rates are given, based on specific configurations for using the telemetry subsystem.

All data outputs from the millimeter wave experiment are in analog form. Each output would be fed to an analog data encoder in the telemetry and command subsystem, which would convert the analog data into 9-bit digital words. These words would then be fed to the 64-channel main multiplexer,

the 64-channel submultiplexer, or the 32-channel submultiplexer. Pertinent characteristics of the telemetry equipment group are given in Table 8-5.

The millimeter wave experiment planned for the ATS satellite presently has 6 analog data outputs which must be telemetered to a ground station. Five of these outputs must be sampled at a high rate (that is, sampling rate of 0.1 second is desired), and the sixth output can be sampled at a slower rate. The minimum time in which all outputs could be sampled once by the telemetry and command subsystem would be:

$$6 \text{ words} \times 9 \text{ bits/word} \times \frac{1}{194.18} \text{ seconds/bit} = 0.248 \text{ seconds.}$$

This minimum sampling time could be approached in the actual experiment by using supercommutation on one of the submultiplexers, and by sampling the less critical outputs at a slower rate (e.g., sample every other cycle). For example, the 32-channel sub-multiplexer has 28 channels available for sampling analog data. The five millimeter wave experiment outputs requiring high sampling rates could be supercommutated (i.e., bridged) five times using 25 channels, and leaving three channels for super-commutating the sixth output. When the millimeter wave experiment is ON, the telemetry main multiplexer would be stopped at its channel 63, the 32-channel sub-multiplexer, and this submultiplexer operated at its maximum frame rate of 1.49 seconds. Five samples of the high-rate experiment data would be obtained in this time, or the average sampling time would be 0.30 seconds. If the 64-channel submultiplexer were used, the 5 high data channels could be supercommutated 11 times, leaving 5 submultiplexer channels for sampling the sixth experiment channel. The average sampling time would be 0.27 seconds.

The above average sampling rates are several times the desired rate of 0.10 seconds, but should not seriously restrict the experiment data. Thus, if either the 32-channel, or the 64-channel, submultiplexer could be allocated exclusively to the millimeter wave experiment, and if data from other

TABLE 8-5

PERTINENT CHARACTERISTICS OF THE TELEMETRY GROUP APPLICATIONS TECHNOLOGY SATELLITE, TELEMETRY AND COMMAND SUBSYSTEM

Parameter	Value
Bit rate	194.18 bits/second
Word Length	9 bits
Output	Split phase NRZ (Manchester Coding) (Binary 0 equals 0, 1 and binary 1 equals 1, 0)
Encoder Drive - Normal	Spacecraft clock, 1553 Hz ± 0.1%
- Backup	Internal oscillator, 1553 Hz ± 15%
Analog Encoder:	
Word sample time	9-bit sample (46.26 milliseconds)
Experiment loading -	
During sample	2.5 micro amps
During "not" sample	0.02 micro amps
Current transient applied to experiment at beginning of sample time for zero impedance experiment source	±25 milliamps max.
Voltage transient applied to experiment at beginning of sample time for infinite impedance experiment source	+15 Volts maximum -15 Volts minimum
Experiment data voltage range	0 V to -5.11 V
Experiment source impedance	≤ 10 K ohms
Experiment source allowed failures	Shorts to voltages ≤ +2 V Shorts to voltages less negative than -34 V
Accuracy	± 0.25% over-all for the 0 to -5.11 V input

TABLE 8-5 (cont)

Parameter	Value
Main Multiplexer:	
Number of channels	64
Channel allocation	
0, 1, 2	Frame synchronization, 27-bit word
3-bit 1	Encoder mode identification
3-bits 4-9	Submiltiplexer position identification
4 thru 17	Digital data inputs
18	Calibration reference
19 thru 61	Analog data direct
62	64-word analog submultiplexer
63	32-word analog submultiplexer
Frame period	2.97 seconds
Submultiplexer - 64-channel:	
Channel allocation	
0, 1, 2	Frame synchronization, 27-bit word
3	Calibration
4 thru 63	Analog data
Frame period - normal	190.09 seconds
Frame period - main multiplexer stopped at 64-channel submultiplexer	2.97 seconds
Submultiplexer - 32-channel:	
Channel allocation	
0, 1, 2	Frame synchronization, 27-bit word
3	Calibration
4 thru 31	Analog data
Frame period - normal	95.04 seconds
Frame period - main multiplexer stopped at 32-channel submultiplexer	1.49 seconds

experiments could be sampled periodically when the millimeter wave experiment was operating (e.g., operate the 32-channel submultiplexer for 40 frames, or 59.4 seconds, then the multiplexer for one frame, or 2.97 seconds, and then the 32-channel submultiplexer for 40 frames, etc.), the telemetry and command subsystem could be used to transmit the data from the millimeter wave experiment.

Communications Subsystem

The spacecraft communications subsystem [68] of the Applications Technology Satellite is a primary subsystem which has three modes of operation: a multiple access mode, a frequency translation mode, and a wideband data mode (for transmitting data from on-board experiments). In addition to its communications capability, each mode provides a low-power microwave carrier for ground station antenna tracking. The subsystem consists of:

a. Two complete, separate transponders
b. Two transmitters
c. Receiving and transmitting antenna subsystem

In addition, this subsystem may include secondary power supply equipment. The pertinent characteristics of the spacecraft communications subsystem are given in Table 8-6.

Instead of using the telemetry subsystem, the communications subsystem may be used in its wideband data mode to transmit the millimeter-wave experiment data. However, this experiment data would require additional processing before it is transmitted to ground stations by the communications subsystem. The six analog experiment outputs, each of which has a frequency band from dc to 10 cps, must be translated in frequency to selected locations within the 10 cps to 5 Mc video base band. These six signals, even with guard bands, would occupy only a small portion of the video base band,

TABLE 8-6

PERTINENT CHARACTERISTICS OF THE SPACECRAFT COMMUNICATIONS SUBSYSTEM -- APPLICATIONS TECHNOLOGY SATELLITE

Parameter	Value
Effective Radiated Power	
Synchronous Altitude	20.4 dbw
Medium Altitude	14.4 dbw
Tracking Beacon Power	20 ± 1 db below Effective Radiated Power
Frequency	
Transponder, 475025-106	
Input	6212.094 mHz
Output	4119.599 mHz
Beacon	4135.947 mHz
Transponder, 475025-107	
Input	6301.050 mHz
Output	4178.591 mHz
Beacon	4195.173 mHz
Maximum Bandwidth	25 mHz (in the Frequency Translation Mode)
Input Power (each transponder/ transmitter)	27 watts maximum (measured at regulator input with -28 Vdc)
Weight	
Antennas	15 lbs.
Transponders (2)	27 lbs.
Transmitters (2)	12 lbs.

TABLE 8-6 (cont)

Parameter	Value
Communications Transponder	
Wideband Data Mode	
Input Signal	Video
Base Band	10 Hz to 5 mHz
Input Voltage	1.0 V peak - peak
Input Impedance	75 ohms
Modulation Type	FM
Modulation Index	1.5
Maximum Deviation	7.5 mHz peak
Center Frequency	65.39 or 66.33 mHz
Output Linearity	10% deviation from a best fit line
Communications Transmitter	
Type	Traveling-wave Tube
Amplitude Response	< 0.05 db/mHz over a bandwidth of 25 mHz centered at the carrier frequency
Internally Generated Spurious Frequencies	At least 20 db below output carrier
Antennas	
Receiving Frequencies	6.150 to 6.350 GHz
Transmitting Frequencies	4.050 to 4.250 GHz
Isolation	70 db minimum
SASSE Mission (ATS-B)	
Receiver - Gain	7.8 db minimum
- Pattern	Symmetrical within ±0.5 db in the plane perpendicular to the spacecraft spin axis (Ø plane)
- Polarization	Linear, perpendicular to spin axis

TABLE 8-6 (cont)

Parameter	Value
Transmitter - Gain	18 db minimum
- Pattern	Conical
- Polarization	Linear, parallel to spin axis
SASSE Mission (ATS-C)	Mechanically despun antenna (GFE) for reception and transmission
SAGGE Missions	
Receiver - Gain	16.3 db minimum
- Pattern	Conical
- Polarization	Linear, perpendicular to spin axis
Transmitter - Gain	16.7 db
- Pattern	Conical
- Polarization	Linear, parallel to spin axis
Transmitter - Gain	10.5 db minimum
- Pattern	Conical
- Polarization	Linear, parallel to spin axis

leaving most of this band for simultaneous usage by other experiments.

Space Frame

The interface between the experiment equipment and the frame of the gravity gradient spacecraft poses a problem in two areas: the proximity of the experiment modules to the millimeter-wave antennas and, the placement of these antennas in their proper orientation toward earth. The volume and weight specifications of the equipment would not be difficult to meet.

The modules should be located in compartments which are on the earth side of the spacecraft. This minimizes waveguide runs and provides some flexibility in that the antenna could share compartment space with the

module. The effective radiated power required in a down-link is in the neighborhood of 20 dbw. With only 200 milliwatts of actual rf power available, the antenna gain must therefore be 27 db. This means that the antenna beam-width (7.5°) is smaller than the angle subtended by the earth and, therefore, the pointing of this antenna toward the United States depends upon the longitudinal position of the satellite and the accuracy of its gravity gradient stabilization sub-system. If the stabilization accuracy is within $\pm 3^{\circ}$ in pitch and roll and within $\pm 7^{\circ}$ in yaw, then a 7.5° beam can be effectively used. The size of a 16 Gc antenna (about 0.6 of a foot) presents a problem in that protrusions from the skin of the spacecraft is limited during launch.

8.1.5 Critical Component Tests and Breadboard Activities

This section describes the priority items which should be implemented in such a way that these design developments are available to the millimeter experiment designer prior to final commitment of final package design. These design development areas will require six months to one year for adequate evaluation of the proposed design approaches.

The best possible means of properly evaluating these key items is by constructing breadboard models and/or purchasing certain items whose performance specifications may be in doubt or improved upon by a better understanding of their performance.

Transmitter Breadboarding

Insofar as the 35 Gc and 16 Gc transmitters are concerned, three items fall under this category. First and foremost, the Pound discriminator should be built and thoroughly evaluated. This item is of the greatest importance for the following reasons:

a. The ultimate sensitivity is achieved when the receiver bandwidth is narrowed to 1 cps. Anything approaching this can only be obtained if the transmitter is stable to within this bandwidth. It is, therefore, well worthwhile to experimentally determine the best achievable stability without a major development program.

b. This form of microwave discriminator, although tried and true, has not been materially improved since its early use. With the advent of improved semiconductor diodes, klystrons and low-noise dc amplifiers, it should be possible by means of good design techniques, to improve the overall capability of the Pound discriminator.

The second key item in the transmitter is the shunt modulator. For this particular application, a modulation depth of 20 db or better is desirable. This feature by itself is not very difficult to achieve. The important point is that this modulation range must occur simultaneously with a very low insertion loss. The presently allocated insertion loss is 1.5 db for the modulator. Certainly this must not be exceeded, and, if possible, lowered to less than 1 db.

Two types of shunt modulators should be evaluated - the reflective type and the absorption type. The implementation of the reflective type is closest to present-day capabilities, but would require the introduction of low-loss millimeter wave isolation to prevent the reflected energy from reaching the stabilized transmitter source and any frequency converters supplied by this source.

The shunt modulator, therefore, should ideally be an absorption type of modulator. The desirability of this feature is the fact that when the modulator is in the non-transit bias position, all the non-transmitted energy will be absorbed. The only presently available true absorbing semiconductor modulator is the PIN diode. Therefore, the operation of a PIN diode modulator at 35 and 16 Gc must be thoroughly investigated and documented. The main evaluation of this device would be to determine the actual change in match due to a change in the percent modulation. This, then, would be compared with a reflective model coupled to an isolator.

To this end, two, or possibly three, suitable modulators should be purchased and tested. On the basis of these results, a decision would be

made as to the most suitable unit. As part of this work, any required modifications would be made.

A third critical item is the choice of the power supply. This unit must be capable of withstanding high accelerative forces during launch and remain highly stable with a minimal change in the output levels. Power supplies of the SCR type are generally in use in space applications, but are usually tailor-made for any specific experiment. A thorough search of manufacturers' literature should be made, circuit diagrams should be examined, and specifications should be scrutinized in order to arrive at the best choice.

Receiver Breadboarding

Three items in the receiver require early and special attention. The establishment of a firm foundation of knowledge and skill in these areas is somewhat lacking, as a general rule, and the best solution to problems of this nature is the construction of, and experimentation with, actual hardware.

The first of these key items is the harmonic mixer which receives signals at 94 Gc and uses the 35 Gc transmitter power for the local oscillator drive, thus delivering an IF signal at X-band. The loss and noise figure of this mixer has, of course, a direct relation to the sensitivity of the receiver and methods should be determined to optimize this sensitivity. For instance, it may be possible to obtain an improved performance by means of a small external diode bias. This bias would certainly improve the IF impedance with respect to that of the tunnel diode IF amplifier input, another crucial item.

The next key item is the IF amplifier itself. The stability, impedance match and lowest available noise figure must be firmly established. A shortcoming of the tunnel diode amplifier (its limited dynamic range), will be carefully studied and suitable technology will be applied to overcome this shortcoming. Low-pass filtering techniques will be employed to avoid diode burnout due to dc transients.

Thirdly, the carrier phase-lock loop must be scrutinized in minute detail. The S/N ratio values required for lock and unlock are still theoretical postulates. Thus, it is essential that a loop be constructed and various levels of signals plus noise be injected into the loop in order to gain a firm feel for the possible improvements in this unit.

In order to retrieve the upper and lower sidebands of the 94 Gc signal, it is, of course, necessary to maintain a stability in the satellite, comparable to that of the ground terminal transmitter. Considering that hardly any restrictions are imposed on the size, weight and volume of the ground equipment, it is expected that the transmitted signal will be stable indeed. Thus, an extremely tight loop is required and should be given early attention.

8.2 Ground Equipment

The ground equipment configurations which will be discussed here will be those which were introduced in Section 7.6.

8.2.1 Signal Sources

The signal sources which are used as transmitters to provide boresight signals for the purpose of generating antenna patterns and boresight accuracy measurements on the ground-based facility were described in Section 4.1 of the Second Quarterly Report. This equipment will also provide the GSFC facility with AM and FM capabilities in a ground-to-ground experimental communications link which would allow development of millimeter technology applicable to spacecraft systems and ground-based systems. In addition, these signal sources could eventually interface with higher power amplifier devices. Hence, these sources with their output of approximately one watt could then drive a 100 w transmitter or a 1000 w transmitter as would be required in a large, high data-rate space-earth communications system. The system would possess the capability of a wide deviation FM system and in addition would possess capability of pulse modulation and AM modulation.

8.2.2 Main Receivers

The main receiver system for the GSFC facility, as shown in the block diagram of Figure 8-2 represents the current thoughts on the present and the potential capabilities of the ground-based facility that would be required in order to operate with maximum capabilities in the total millimeter spectrum.

The block diagram has been divided into the four major sections, an RF head and three receiver IF sections, to facilitate the following of signal paths and function clarification. The approach has been to maintain as much equipment as possible in a common usage status relative to all changes in frequency associated with the millimeter experiments.

Interchangeable RF Receivers

The first part of the block diagram (left-hand side) shows the RF feed interface arrangement of each interchangeable RF head with the ground terminal antenna system which includes a 15 foot millimeter dish. A four horn cluster feed would be used, providing a quadrahorn, 2 or 3 db cross-over beam pattern.

Frequency changeover is accomplished by removing the entire front end section and replacing it with another module operating at a frequency. This modular arrange ment is similar to the technique employed in some types of microwave test equipment. Each frequency head will be packaged to mate into the remaining sections of the receiver by means of two of three waveguide joints plus power and signal connectors. This would allow changeover to a new frequency of operation to be accomplished in a relatively short time.

IF Receivers

The input RF section is followed by the receiver IF sections. The RF and IF sections interface by means of a diplexer operating at a high frequency. The receiver divides into three IF sections, the radiometric

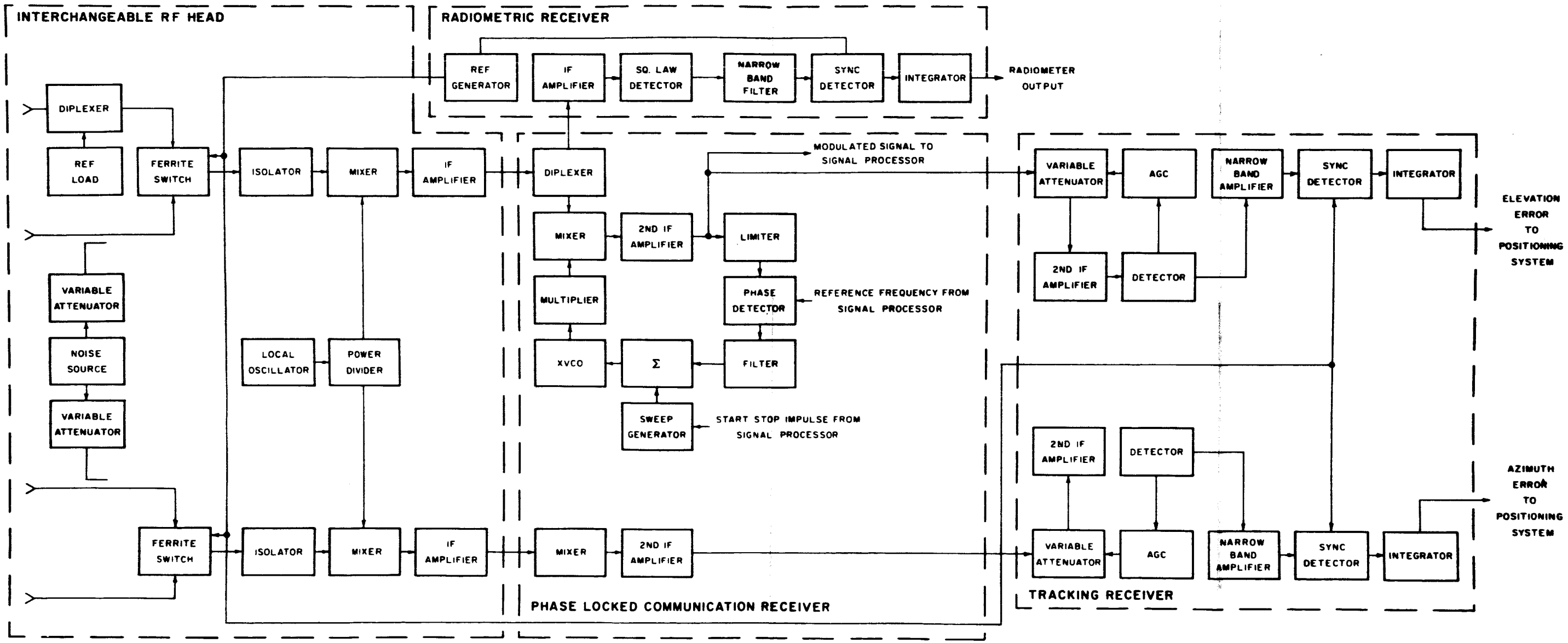

8-25

Figure 8-2 Ground Receiver System With Angle Tracking

IF receiver, the communication IF receiver, and the tracking IF receiver. Parts of the communications receiver serve a dual function in that they are also used in the tracking mode of operation. Tracking is accomplished by lobe switching, and error signals will be provided for use in closed loop servo operation of the antenna facility.

The outputs of the diplexer in the upper channel, as shown on the block diagram, are fed to two sections. One output is fed to the radiometric receiver section which is tuned to a different frequency relative to the second output of this diplexer. The remaining components of the radiometric receiver process the signal to complete the Dicke type radiometer measurements.

The second output from the upper diplexer is fed to a mixer pre-amplifier. The reference signal for this mixer and the lower channel mixer is obtained from a crystal VCO. The output of the second IF pre-amplifier goes to a carrier lock loop, the output of which controls the crystal VCO and causes the receiver to lock on the carrier. The output of this pre-amplifier is also fed to the tracking receiver where it is processed along with the lower channel signal, and generates the azimuth and the elevation error signals that would be required in order to angle track.

This implementation would allow this system to simultaneously provide radiometric signal processing in addition to a wide bandwidth for propagation test signal processing. This system also has very large predetection first IF bandwidth (500 - 700 mc) which inherently provides the system with longevity for future high data rate communications tests.

The radiometric system utilizes the following technique. A diplexer with a load at one port, is placed between one antenna feed horn and the ferrite switch. This port of the ferrite switch accepts the reference load power for the radiometer and the transmitted communication channel spectrum simultaneously. The second input port of this ferrite switch is attached to another antenna feed horn and this port accepts the radiated power of the

and the transmitted communication channel spectrum. Since the radiometer cannot measure the sky temperature, at the exact spectrum of the communication channel, its displaced spectrum is selected by the second diplexer located in the communication receiver. This configuration allows simultaneous operation of both the radiometer and communication receiver with no loss of input power or degradation of either system.

The tracking mode utilized beam switching to derive an error signal which is directly proportional to the difference in power of the energy in the communication channel at the inputs of both antennas. The measurement of the absolute temperature of the two beams would be accomplished by the pre-calibration of the receiver and the establishment of a primary baseline prior to the tracking of satellites and/or sources. It is felt that this technique is readily emplementable and would prove useful and valuable in the reduction of data during the real time evaluation of communications characteristics.

This basic lobe switch-track technique is proposed to be used at all frequencies since it does circumvent the problems associated with a phase sensitive amplitude monopulse system.

Alternate System

The system in Figure 8-2 exhibits a loss in gain due to the inefficient illumination of the dish and high spillover by the quadrahorn feed system. However, this should not be a problem if the adequate test signal strength is provided.

An improvement in received signal-to-noise density ratio may be realized throughthe use of a single horn primary feed system, at the expense of automatic tracking capability. This configuration shown in Figure 8-3 also allows simultaneous operation of both the Dicke radiometer and communications receiver. This type of system is more desirable when synchronous stationary satellites are used as the propagation platform.

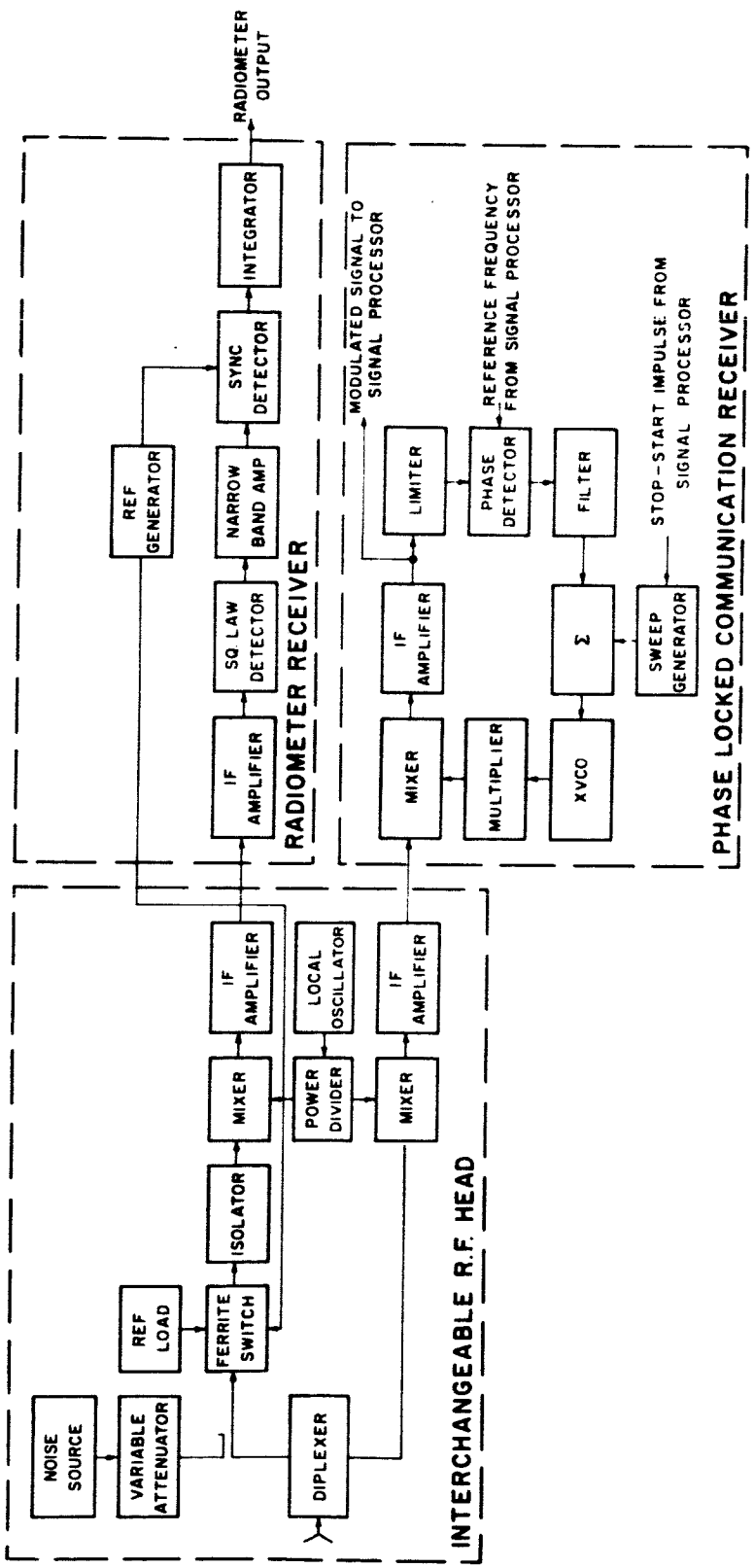

Figure 8-3 Ground Receiver System Without Automatic Tracking

8.2.3 Ground Transmitter (94 Gc)

This section deals with the requirements and capabilities of the ground transmitter operating at 94 Gc which would interface with the satellite receiver described in Section 8.1.3. As indicated in Section 5, the signal power analysis is based on a 10 w transmitter as the minimum capability. However, serious consideration should be given to a 100 w capability.

This transmitter can take the form of a low power driver such as klystron or distributed interaction klystron devices which can be amplitude modulated via a shunt modulation technique, as previously described in Section 8.1. This, then would be followed by a final driver amplifier which would transmit 10 to 100 w of RF power. This final driver amplifier could readily take the form of the presently developed Hughes TWT type of coherent millimeter amplifier.

This type of operation would prove to be most efficient in that the final driver stages may be operated in a saturated mode to optimize the power output of the last driver stage and minimize amplitude fluctuations due to the previously introduced AM technique. Hence, it is felt that this general philosophy would lend itself readily to solving the problems of generating high levels of millimeter power for ground based installations. Further detail on this particular approach would, by necessity, require a more detailed investigation into the actual operating characteristics of the final driver stages and its associated hardware.

This information, it is felt, will be available within the near future, due to the actual experience of the Hughes and Aerospace test and evaluation programs on these high power millimeter transmitter sources. Therefore, it is proposed that a continuing exchange of information with these two groups be such that the latest and most up to date information with regard to these

devices is introduced into the final design document of this study.

8.2.4 Auxiliary Ground Terminals

As indicated in the introduction to this report and as further outlined in Section 7.6, when one is forced with the implementation of a propagation experiment aboard a synchronous stationary satellite, the availability of an auxiliary transportable ground terminal which would perform as a gap filler in the elevation profile examination of the medium would prove to be a most useful and versatile piece of equipment from the experimenter's point of view.

Further use of this auxiliary station could be made by co-locating it with one of the larger fixed installations, for a period of time, to determine multipathing effects as a function of beam size. The availability of two of these auxiliary stations in a dual reflector variable baseline configuration would provide useful estimates on spatial decorrelation of amplitude fading.

As indicated in Section 7.6, this device need only determine flat frequency fading by providing amplitude data on the received carrier at the particular elevation angles prescribed. It is not deemed necessary that this particular auxiliary terminal possess the overall ground terminal capabilities as prescribed for the existing large antenna facilities. This terminal would be outfitted utilizing a transportable antenna and pedestal system which would allow for adequate positioning accuracy on a fixed satellite. The antenna system would consist of a parabolic reflector and, for purposes of transportability, a diameter of 10 ft. would be considered a reasonable trade-off.

When considering adequate signal levels, for measuring amplitude fading, a 10 ft. antenna appears to be sufficient. This antenna system would then be attached to a simple, accurate, hand positioned mount system which would allow for the handling and positioning of the antenna in a reasonable mechanical environment. The output of the antenna's feed system would interface directly with the conventional receiver front ends described in Section

8.2.2 and the signal processing required at the site would be simple amplitude detection and recording capabilities which will be described in Section 10. Once again it should be emphasized that phase coherent measurements need not be attempted at the auxiliary sites. It is felt that if phase coherence measurements of the signal are performed by a larger facility at an elevation angle less than the one in which the auxiliary site is located, then measurements at the auxiliary site would not be absolutely necessary. Hence, the primary function of the auxiliary terminal would be to supply a ground terminal which may be readily transportable to varying locations to establish statistical fading information on the signal under varying weather model conditions and also to provide a tool at the presently existing research ground terminals to perform variable aperture and spatial amplitude decorrelation measurements. One or more auxiliary receivers would allow greater versatility in the experiment program by maximizing the data output for a given payload within the spacecraft.

The design philosophy of the auxiliary ground terminal antenna system is based on the requirement that the antenna system must be easily transported from one location to another where the distance between the two sites could be several feet or several hundred miles. A moderate amount of set-up and tear down time would be required by a crew of two to three persons without the use of elaborate cranes or machinery. One consideration in this regard is to mount the antenna system on a flat bed trailer. Also, a compartment must be provided on the back of the dish assembly to be utilized for the mounting of the antenna feed and RF receiver components. This RF package would be readily interchangeable for operation at 16 Gc and 35 Gc.

Three antenna sizes have been investigated: 6, 8 and 10 ft. paraboloc type reflectors. The surface tolerance required of the reflector at 35 Gc is 0.02 in. The approach used by one manufacturer is to utilize spun aluminum fabrication techniques. Attaining this close tolerance increases the

cost considerably since the normal runout of surface tolerance for a 10 ft. dish utilizing this technique is ± 3/32 in. or about 0.09 in. The weight breakdown for the three basic dish sizes is as follows:

Size	Weight
6 ft.	105 lb.
8 ft.	125 lb.
10 ft.	240 lb.

The above weight includes a mounting plate on the back of the dish. The feed system would add about 50 lb to the weight for a total of 290-300 lb in the cases of the 10 ft. antenna. This is the weight to be supported by the pedestal.

A hand crank azimuth oven elevation pedestal with a three foot standoff, capable of handling the wind loads associated with the 10 ft. dish in 30 mph winds, would weight about 500 lb. This pedestal would have 0.1 deg pointing accuracy in azimuth and 0.15 deg for elevation. The pedestal and antenna would be capable of surviving 100 mph winds in the stow position with the antenna pointing at the zenith.

A light duty single axle flat bed trailer with the required rigidity and support jacks supplied would cost approximately 4,000 dollars. This would greatly aid the mobility feature required of the system. Due to clearance problems (and to prevent damage), the feed system and the antenna would be detached from the pedestal during the transporting phase. Containers could be built on to the trailer to house and protect the detached subassemblies while moving from site to site.

8.2.5 Equipment Performance Specifications

Preliminary specifications were given in Section 4.5 of the Second Quarterly Report to show equipment performance desired. The specific frequencies at which the equipment must operate have been selected from the

presently designated ground-spacecraft communications and space research bands in accordance with the ITU October 1963 Extraordinary Administrative Radio Conference (EARC) standards. The specific frequencies at which the RF equipment should operate are:

Nominal Frequency	Actual Band
8 Gc	8.40 - 8.50 Gc
16 Gc	15.25 - 15.35 Gc
35 Gc	34.2 - 35.2 Gc
94 Gc	93.0 - 95.0 Gc

Section 9
GROUND FACILITIES EVALUATION

This section is a summary of Section 6 in the First Quarterly Report, which evaluated the presently available millimeter facilities within the Continental United States, plus a new facility being established at Goddard Space Flight Center. These facilities and their geographic location are listed in Table 9-1.

TABLE 9-1

GROUND FACILITY GEOGRAPHICAL CHARACTERISTICS

Facility	Area	Latitude ^{o}N	Longitude ^{o}W
Aerospace	El Segundo, California	33.9	118.4
U. of Texas	Austin, Texas	30.5	97.7
GSFC	Greenbelt, Md.	39.7	76.8
AFCRL	Waltham, Mass.	42.4	71.2
Lincoln	Lexington, Mass.	42.5	71.3
Haystack	Tyngsboro, Mass.	42.7	71.4

The data presented in the First Quarterly Report, accumulated during the first study phase of this contract, was derived from reports published on the facilities and through direct communications with the personnel associated with each of these facilities. In particular, it evaluated the task of integrating these presently instrumented facilities into a millimeter communications experiment. Section 6 of the First Quarterly Report lists the characteristics of each of the facilities and notes the deficiencies of each of the facilities as related to their ability to perform in this millimeter communications experiment.

As a point of general interest, it can be noted that the facilities pre-

sented here do represent an excellent cross-section of engineering technology in the assembly of each of these facilities. This statement is exemplified in the fact that there are four basically different and unique approaches to the fabrication of high-precision parabolic reflectors. This cross-section of technology is shown most drastically in the invar honeycomb construction technique utilized by the University of Texas in direct contrast with the machined aluminum panel technique utilized by Aerospace Corporation. Further comparison can be drawn with the Lincoln Laboratory spun-cast technique, and finally, with a fourth fabrication technique utilizing a machined foamed plastic surface with two radii pendulous routing. All of these techniques have been utilized successfully for the fabrication of high precision parabolic reflectors.

In addition, several mount configurations and several servo drive configurations have been implemented and tested, these being, the differential torque drive technique utilized by the University of Texas, the hydraulic servo constant displacement type of drive implemented on the Aerospace facility, and the more conventional torque drive utilized by the AFCRL facilities.

Each of these facilities has been evaluated as a site, and performance measurements have been conducted on the gain, efficiency and antenna patterns, all in the millimeter regions. In addition, pointing accuracies and dynamic tracking accuracies have been checked primarily through the utilization of celestial body radio astronomy. Hence, it is felt that the designers of future millimeter facilities will have at their disposal many design curves and techniques which have been implemented and tested and, therefore, may be directly compared on a cost effectiveness basis. This, therefore, should allow a most excellent trade-off analysis to be performed which would allow the communications designer to choose the most efficient design and fabrication techniques for utilization in an operational satellite commun-

ications network.

By way of summary, Table 9-2 and Figure 9-1 have been included to compare various antenna system characteristics of the facilities.

TABLE 9-2

GROUND FACILITY ANTENNA SYSTEM CHARACTERISTICS

Facility	Type of Mount	Type of Antenna	Antenna Diameter
Aerospace	Equatorial	Cassegrain	15
U. of Texas ν	Equatorial	Feed at Focus	16
GSFC	Azimuth-Elevation	Cassegrain	15
AFCRL	Azimuth-Elevation	Cassegrain	29
Lincoln	Azimuth-Elevation	Degenerate Cassegrain	28
Haystack	Azimuth-Elevation	Cassegrain	120

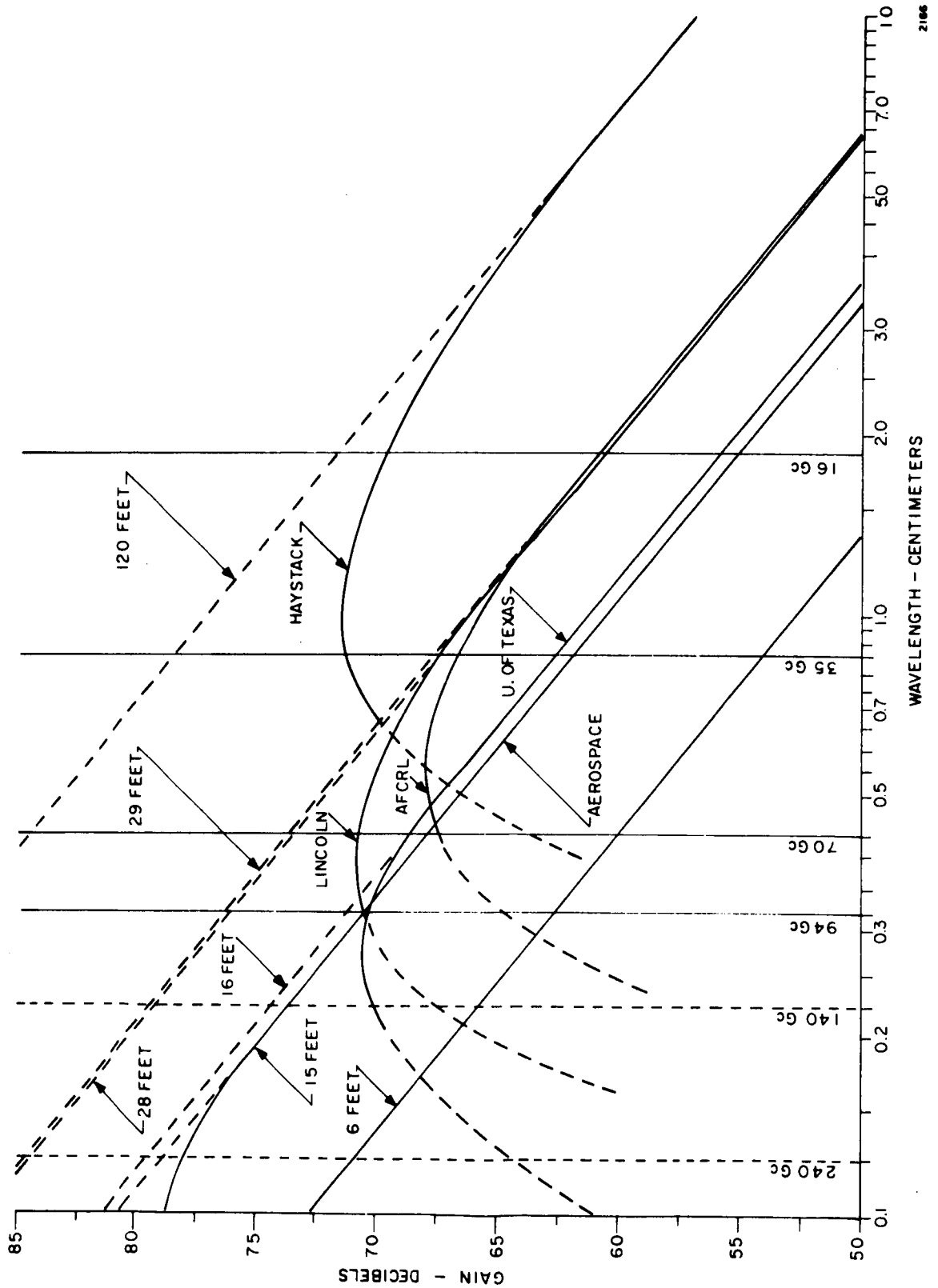

Figure 9-1. Antenna Gain at Ground Station Facilities

9.1 Millimeter Facilities and Capabilities

9.1.1 Aerospace Corporation

The Aerospace Space Radio Systems Facility was established to investigate the suitability of millimeter wavelength systems for space and missile applications involving, in particular, the practicality of constructing and operating a large aperture ground based antenna with tracking capabilities at a sea level site. The antenna has been operating with a 3.2 millimeter radiometer since December 1963, and performance has also been evaluated in its operation as a radio telescope. Primary emphasis was given to measurements made during the lunar eclipse of 30 December 1963, and radiometric data is being taken on the earth's atmosphere, the sun, the moon, and Venus.

Research programs on the use of the spectrum between 10 mm and 1 mm have been undertaken by this facility, and work has been done at 3.2 mm under the auspices of the Air Force Ballistic Systems and Space Systems Division to explore the technical and economic feasibility of using the millimeter spectrum for communications and radar.

The original program plan formulated at the facility was as follows:

a. Exploration of practical uses of the millimeter spectrum using millimeter components in such a manner that the requirements of the system would be similar to those placed on radar and communications equipment,

b. Investigate the ability to fabricate a relatively large antenna with exceptionally fine beamwidths and extremely fine tolerances on pointing accuracy and boresight stability, since this would determine the practicality of millimeter systems,

c. Gather basic propagation data

d. Provide a millimeter instrument to fill the important spectrum gap in radio astronomy observations with the associated unusual resolution capability of such an instrument.

It was felt that the proper approach was to build and operate a millimeter radio telescope, but with sufficient control and dynamic capability to permit subsequent tracking of near-earth satellites in communications and radar experiments. By this approach, the critical factors of large antenna design and cost was explored and, at the same time, immediate investigation into receiver type components was started and usefully employed. All of the pointing control, mechanical stability, alignment, calibration, and feed design problems were investigated.

A steerable 15 foot diameter parabolic antenna with surface tolerances adequate for efficient operation up to 1 mm was purchased along with an equatorial mount and servo system. This was installed on the roof of the Aerospace R &D Center in El Segundo, California. At the same time, digital data processing equipment was purchased and installed in the control penthouse at the same facility along with the remaining required support equipment.

The Space Radio Systems Facility consists of five basic elements:

a. A large aperture antenna supported by an equatorial mount and tower,

b. A hydraulic servo system capable of high pointing accuracy over a wide dynamic range of tracking rates,

c. A digital data processing unit which can adequately perform the functions of ephemeris computations, servo control, and data reduction,

d. Radiometric receivers and calibration equipment,

e. Boresighting capability to accomplish accurate alignment between the mechanical axis of the reflector and the multiple rf feed patterns.

9.1.2 University of Texas Facility

The University of Texas facility is a millimeter wave radio telescope which is installed at the University's field station. The precision 16 foot diameter parabolic antenna was designed for near optimum performance at wavelengths of approximately 4 millimeters and also possesses the capability of slightly degraded performance at 2 millimeters and 1 millimeter. The primary intent of the installation was to survey the surface of the moon which would allow the determination of surface characteristics and atmospheric contents. To date, the primary emphasis of the facility has been on assisting in the selection of the sites for the manned lunar landing. Through the utilization of its very narrow beamwidth, which is a few minutes of arc, it is possible to probe the lunar surface to determine the radiometric temperature variances as a function of frequency.

The utilization of this reflector is accomplished through its attachment to a high resolution equatorial mount. This mount facility is new in design and utilizes a differential torque drive technique to accomplish its high pointing accuracy capabilities. This mount, when coupled to the antenna which is fabricated with invar honeycomb, performs as a well integrated radio astronomy facility. Hence, the actual fabrication of this antenna facility was done through the implementation of an entirely new technique - the assembly of a temperature compensated precision reflector using invar as a major construction material. From the presently available measured data on this facility, it appears that the development and utilization of this technique has proved to be extremely successful.

The actual implementation of measurements hardware at the University of Texas has been primarily in the area of radiometric systems. These particular systems utilize a Dicke type of radiometric receiver with a 10 megacycle predetection bandwidth. These two receiving systems are built in such a manner that, via plug-in receiver heads at the reflector focus position, a choice of 35 Gc, 70 Gc, 100 Gc and 140 Gc operating frequencies available.

This is one of the few new facilities which utilizes a feed-at-focus primary feed system. It should be noted that for all other facilities under consideration, a Cassegrain technique or a modified degenerate Cassegrain technique is utilized for their feed system. Hence, the problems and limitations of introducing equipment at the primary focus of this main reflector are best exemplified by the basic weight limitations imposed by the structure. A feed weight of less than 40 pounds must be maintained in order to preserve surface and prime focus accuracy over the entire elevation operation of the main reflector. This inherent system limitation indicates the lack of adaptability for which this type of system lends itself; the difficulties of instrumenting a high power millimeter transmitter at the prime focus of this particular facility cannot be overcome.

A second limitation is related directly to the site's inability to perform during foul weather conditions. This ground base facility is housed within an observatory type dome which allows true fair weather operations without the adverse effects of radomes. The proposed solution to this particular problem could well be accomplished through the implementation of a thin film membrane radome material installed over the observatory dome window; this would provide adequate protection for all weather operation of the facility.

The next area of prime concern in utilizing this facility is the

relatively slow slew and track rate capability. In view of the primary mission of the facility having been established as a readiometric observatory, the slew and track capabilities have been tailor-made for celestial body observations. This has produced a system which is limited in its ability to perform on higher angular velocity targets such as 6000 mile satellites. Its capability in the hour angle axis is better than that of the declination axis because, in celestial work, the hour angle is the working axis of the radio observatory. It is felt that through the utilization of the present differential torque drive a higher slew and track rate may be accomplished if a relaxation of the dynamic pointing accuracy can be tolerated.

In summary, it is felt that the University of Texas facility, as presently assembled, provides a receiver aperture capable of receiving millimeter waves, but the primary limitations of the facility are associated with its servo and acquisition capabilities which would require modification if experiments with satellites other than synchronous are to be performed.

9.1.3 Air Force Cambridge Research Laboratories (AFCRL)

Initial information of the AFCRL facility was derived primarily through direct interview with the personnel at the facility. After the site survey had been completed, a report [68] was published on the facility. This facility consists primarily of a precision millimeter parabolic antenna system coupled to a high precision elevation over azimuth mount. The antenna system and associated mount assembly as presently assembled, uses a Cassegrain feed system, and is primarily instrumented for 35 Gc operation. This mode of operation, when coupled with the 29 foot antenna, generates a 0.07 degree antenna beam and yields a 66.7 db antenna gain at 35 Gc. This is comparable to a 45 percent efficiency at this frequency. The system servo capabilities (its elevation and azimuth mount drive rates), are well within those required for the performance of medium

altitude satellite track. The facility has the capability of approximately two degrees per second in each axis and is programmable through an eighteen bit digital code computer interface.

In summary, it is felt that the AFCRL 29-foot facility presents a real possiblity of being implemented into a millimeter communications experiment, and would be capable of performing either an active track mode or a programmed track mode for a 35 Gc experiment. The site's ability to perform above this frequency, it is felt, should be evaluated at a later time, after the present measurements of the facility have been completed and its true capability determined. It shall also be noted at this point that the AFCRL facility is an exposed facility, in that no protective radome is utilized. This leads to some operational problems during severe winter conditions, in that no antenna surface heating is introduced to allow for the removal of snow accumulated in the reflector. This method of operation would prove to be interesting during the winter season because a true evaluation of the potential of a totally exposed facility without radome protection could be made, especially with water and snow on the dish surface.

9.1.4 MIT, Lincoln Laboratory

Actually, Lincoln Laboratory possesses two millimeter facilities. Namely, the 28-foot spun cast precision system located at the Laboratory itself and the Haystack 120 foot radar installation. The 28 foot facility has been in existence for several years and has performed as a radio astronomy observatory both for the pure radiometric mode and as a radar astronomy instrument. This facility is limited by the mount's capability to perform satellite track missions since it utilizes a gun mount which has limited elevation and azimuth drive capability. This type of mount system, when coupled to the existing servo-drive capabilities, is limited by stiffness and in track rate, such that it would be most difficult to perform a track and acquisition mode on non-stationary satellites.

The Haystack facility was assembled as a radar research instrument and was primarily developed to prove the feasibility of, and to obtain design technology for, the fabrication of large precision parabolic antenna structures to introduce high resolution high precision mount capabilities to the radar field. The facility has a 120 foot parabolic receiving aperture capable of operating from 1 to 10 Gc. Note that the lower limit of frequency of 1 Gc is dictated by the present space frame radome of the facility. The upper frequency of 10 Gc is the frequency initially specified in the procurement of the facility. As shown in Figure 9-1, it is expected that reasonable operation at 35 Gc may be accomplished and that antenna gains in the order of 71 db will be realized with corresponding reduction in overall antenna efficency.

The design of the facility has allowed for the introduction of varied experiments through the utilization of plug-in room techniques which are located to the rear of the prime feed in the Cassegrain feed system. This approach will prove to be most satisfactory and a conversion of the facility from one mode of operation to an entirely different mode can be done within one hour.

This facility would prove to be most interesting as a ground terminal receiver for the proposed millimeter communication experiments because it would allow the evaluation of extremely large aperture antennas for millimeter systems. The facility has no mechanical limitation which directly conflict with the tracking requirements for satellites above 6,000 nautical miles. It can either be programmed to track the satellites using ephemeris data or it can be slaved to the Millstone Hill Radar which can skin-track the satellites. It is anticipated that a minimum of difficulty will be encountered in the utilization of this facility in the communications work.

9.1.5 Goddard Space Flight Center

A millimeter wave experimental ground facility is in the process of being implemented at the Goddard Space Flight Center in Greenbelt, Md. To date, GSFC has procured a 15 ft. spun-cast millimeter reflector. This parabolic reflector has the ability to perform up to a wavelength of 3 mm. Action has been taken to procure a high precision servo and mount assembly for the antenna.

9.2 Meteorological and Geographical Profiles

This is a summary of the geographical and meteorological characteristics [15] of the areas in which facilities under consideration for participation in the proposed millimeter experiments are located. The details were given in Section 6.3 of the First Quarterly Report. Figure 9-2 is a comparison of the monthly mean precipitation for each of the areas to be discussed.

9.2.1 Aerospace Facility

The Aerospace Corporation Space Radio Systems Facility (SRSF) is located on the roof of the two-story Building F at the Aerospace Research and Development Center in El Segundo, California. This "sea level" site in the Metropolitan area of Los Angeles is very near the Pacific Ocean. The boresight station for this 15 foot antenna facility is located on San Pedro Peak (1100 feet altitude) in the Palos Verdes Hills, a distance of eleven nautical miles to the south.

The climate of Los Angeles is normally pleasant and mild through the year. The Pacific Ocean is the primary moderating influence but coastal mountain ranges, lying along the north and east sides of the Los Angeles coastal basin, act as a buffer against extremes of summer heat and winter cold occurring in desert and plateau regions in the interior. An important,

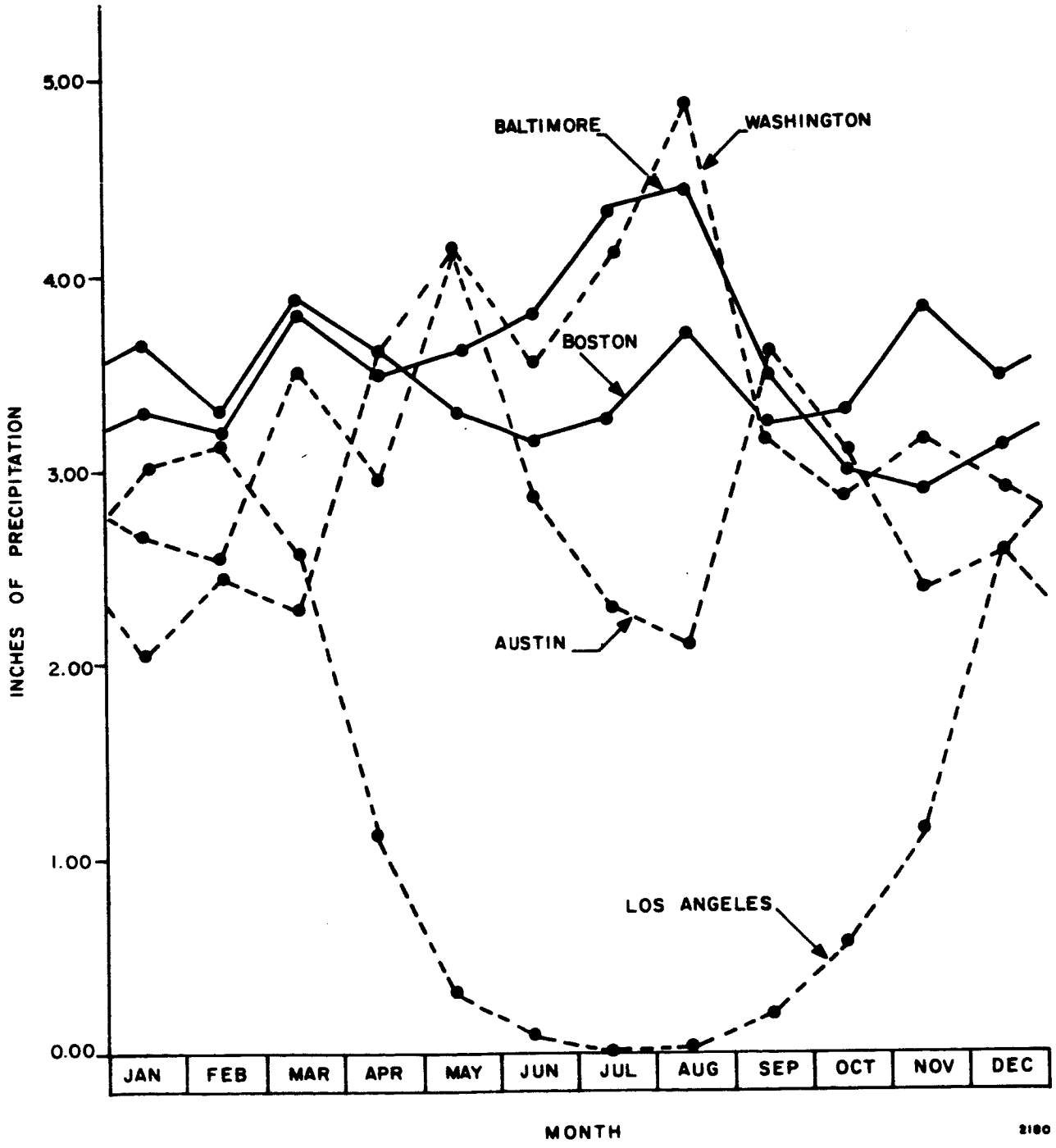

Figure 9-2 Mean Monthly Precipitation

and somewhat unusual aspect of the climate of the Los Angeles metropolitan area is the pronounced differences in temperature, humidity, cloudiness, fog, rain, and sunshine over fairly short distances. These differences are closely related to the distance from, and elevation above, the Pacific Ocean.

Like other Pacific Coast areas most rainfall comes during the winter with nearly 85 percent of the annual total occuring from November through March, while summers are practically rainless. As in many semiarid regions there is a marked variability in monthly and seasonal totals. Annual precipitation may range from less than a third of the normal value to nearly three times normal while some customarily rainy months may be either completely rainless or receive from three to four times the average for the month. Thunderstorms are infrequent.

Prevailing winds are from the west during the spring, summer, and early autumn, with northeasterly wind predominating the remainder of the year. Average wind speeds are rather low. At times the lack of air movement combined with a frequent and persistent temperature inversion is associated with concentrations of air pollution in the Los Angeles coastal basin and some adjacent areas. Low clouds are common at night and in the morning along the coast during spring and summer. Light fog may accompany the usual night and morning low clouds but dense fog is more likely to occur during the night and early morning hours of the winter months.

9.2.2 University of Texas

The radio telescope facility operated by the Electrical Engineering Research Laboratory of the University of Texas is located at the University of Texas field station just outside of Austin, Texas. The boresight station for this 16 foot antenna facility is installed in a University tower in the city nearly 7 miles away.

Austin, the capital city of Texas, is located on the Colorado

River. Elevations within the city vary from 400 feet to 700 feet above sea level. The climate is influenced by the nearness of the Gulf of Mexico which is the source of the maritime tropical air mass which moves over Austin with the prevailing south winds. However, surges of polar air in winter account for the frequent north winds experienced during December, January and February.

The normal annual temperature is 68.3 degrees. During winter the daily range in temperature is from about 60 degrees to about 40 degrees but wide variations from these figures and sudden changes occur as cold polar air replaces warm tropical air and vice versa. Daily range in temperature in summer averages from 74 in the early morning to 94 in the afternoons. The mean number of days with temperature below 32 degrees is 19 per year. These usually occur from late November to mid-March.

Annual rainfall has varied from 65 inches to as little as 11 inches, but the normal annual rainfall is 32.58 inches. Seventy percent of the years have totaled rainfall between 24 and 44 inches. Prolonged dry spells do occur and at times, all months of the year have seen little or no rain. There is no pronounced dry and wet season and rainfall is fairly well distributed throughout the year with a May normal of 3.71 inches and an August normal of 1.94 inches.

9.2.3 Cambridge Research Laboratories and Lincoln Laboratory

The AFCRL facility is situated 20 miles inland from Boston on Prospect Hill beside Route 128 in Waltham, Massachusetts. The 478 foot elevation of Prospect Hill permits excellent coverage near the horizon in all directions. The boresight station for this 29 foot antenna facility is located on Nobscot Hill in Sudbury, Massachusetts, which is about 10 miles west of Prospect Hill.

The Lincoln Laboratory 28-foot antenna radio telescope facility

is located on the roof of the main laboratory building at L. G. Hanscom Air Force Base in Bedford, Massachusetts. Hanscom AFB is about 25 miles west of Boston. The boresight station for this facility is located in Billerica, Massachusetts, 5 nautical miles away. Its elevation above sea level is 350 feet.

The Lincoln Laboratory 120-foot research facility for space communications, radar and radio astronomy is located at Tyngsboro, Massachusetts. The installation, which is named Haystack Experimental Facility is located approximately 30 miles northwest of Boston and about one-half mile from the Millstone Hill radar.

Three important influences are responsible for the main features of Boston's climate. First, the latitude (42° N) places the city in the zone of prevailing west to east atmospheric flow in which are encompassed the northward and southward movements of large bodies of air from tropical and polar regions. This results in variety and changeability of the weather elements. Secondly, Boston is situated on or near several tracks frequently followed by systems of low air pressure. The consequent fluctuations from fair to cloudy or stormy conditions reinforce the influence of the first factor, while also assuring a rather dependable precipitation supply. The third factor, Boston's east-coast location, is a moderating factor effecting temperature extremes of winter and summer.

Boston has no dry season. For most years the longest run of days with no measurable precipitation does not extend much more than two weeks. This may occur at any time of year. Much of the rainfall from June to September comes from showers and thunderstorms. During the rest of the year, low pressure systems pass more or less regularly and produce precipitation on an average of roughly one day in three. Coastal storms, or "northeasters," are prolific producers of rain and snow.

9.2.4 Goddard Space Flight Center

Goddard Space Flight Center is located near Greenbelt, Maryland, on the Baltimore-Washington Parkway about 10 miles from downtown Washington. Since GSFC is only 23 miles from the center of Baltimore, climatological summaries for both cities are given.

Washington lies at the western edge of the Middle Atlantic coastal plain, about 50 miles east of the Blue Ridge Mountains and 35 miles west of Chesapeake Bay at the junction of the Potomac and Anacostia Rivers. Elevations range from a few feet above sea level to about 400 feet in parts of the northwest section of the city.

Summers are warm and humid and winters mild; generally pleasant weather prevails in the spring and autumn.

There are no well pronounced wet and dry seasons. Thunderstorms, during the summer months, often bring sudden and heavy showers and may be attended by damaging winds, hail, or lightning. Tropical disturbances occasionally, during their northward passage, influence Washington's weather, mainly with high winds and heavy rainfall.

The Baltimore area lies about midway between the rigorous climate of the North and the mild South and adjacent to the modifying influences of the Chesapeake Bay and Atlantic Ocean to the east and the Appalachian Mountains to the west. Since Baltimore is near the path of most systems of low barometric pressure which move across the country, changes in wind direction are frequent and are the cause of the changeable character of the weather.

Rainfall distribution throughout the year is rather uniform. Severe drought during the growing season is infrequent. Rainfall during the growing season occurs principally in the form of thundershowers, and rain-

fall totals during these months vary appreciably, depending on the number of thundershowers which occur largely by chance in a given locality.

Section 10
SIGNAL PROCESSING

This section describes the signal processors which are used to transfer the phase and amplitude information contained in the received signals to analog storage on tape. A signal flow analysis was given in Section 5.2 of the Second Quarterly Report which described the energy spectrum at all points in the communication channel from the transmitter modulator to the phase and amplitude detectors in the signal processor. A summary of the signal level analysis is presented here which discusses the signal-to-noise ratios at major points in the receivers and signal processors. From the analysis summary a quick evaluation can be made of any experimental space-earth link.

10.1 Signal Processor Configuration

The block diagrams for the satellite and ground signal processors presented in Figures 10-1 and 10-2 are discussed. The two signal processor configurations to be implemented for this experiment, one for the 94 Gc receiver in the satellite, and a second more sophisticated configuration to be used for all frequencies at the ground stations, are compatible with the amplitude modulated test waveform with modulation frequencies of approximately 5 kc, 10 mc and 50 mc.

The signal processor interfaces directly with the phase-locked receiver in the IF communications receivers which were illustrated in Figures 8-1 and 8-2 of Sections 8.1 and 8.2. The phase-locked receiver translates the received energy spectrum down to the second IF frequency of 66 mc and removes the effects of doppler and any transmitter and receiver frequency source instability that are associated with the carrier frequency.

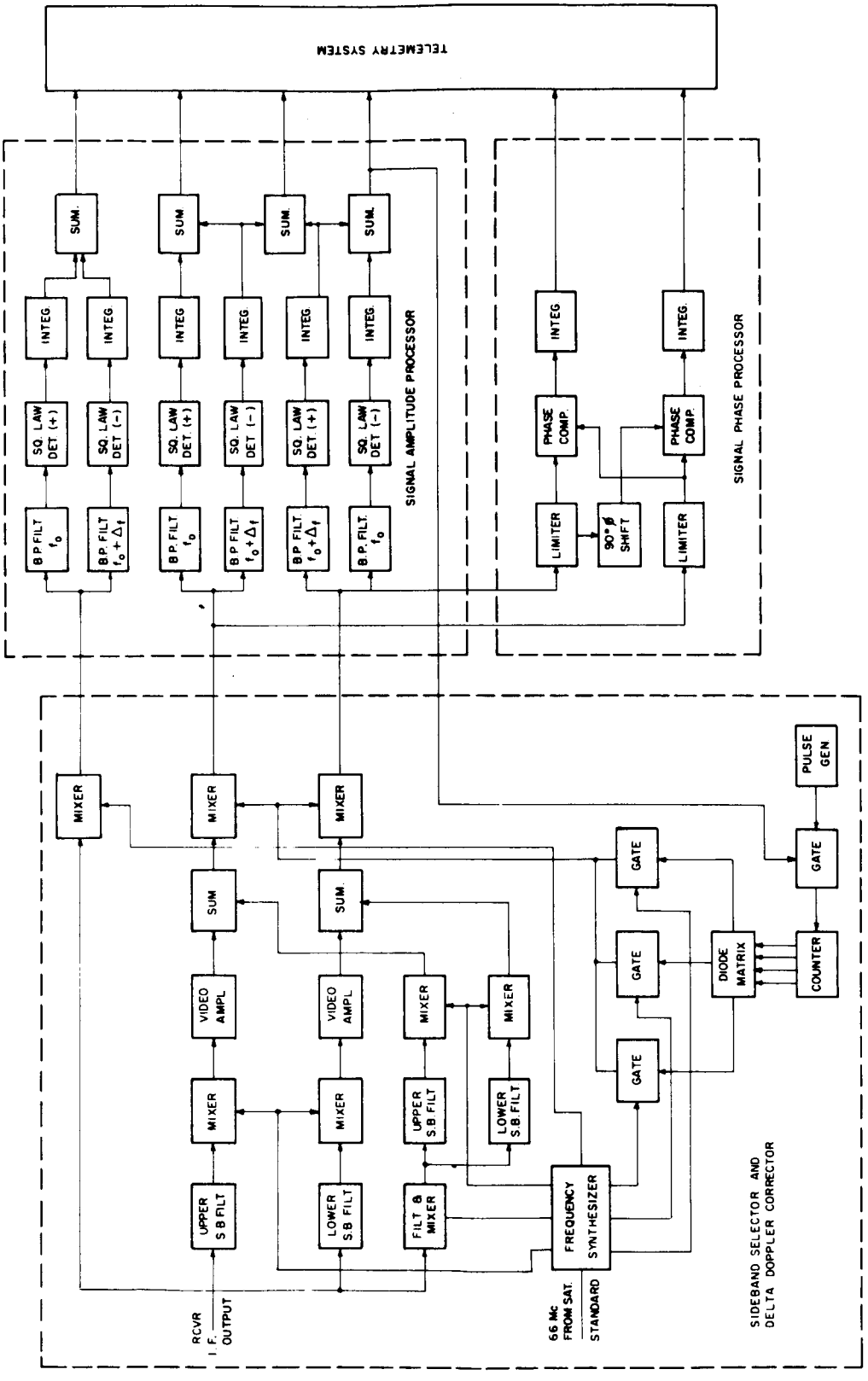

Figure 10-1 Satellite Signal Processor

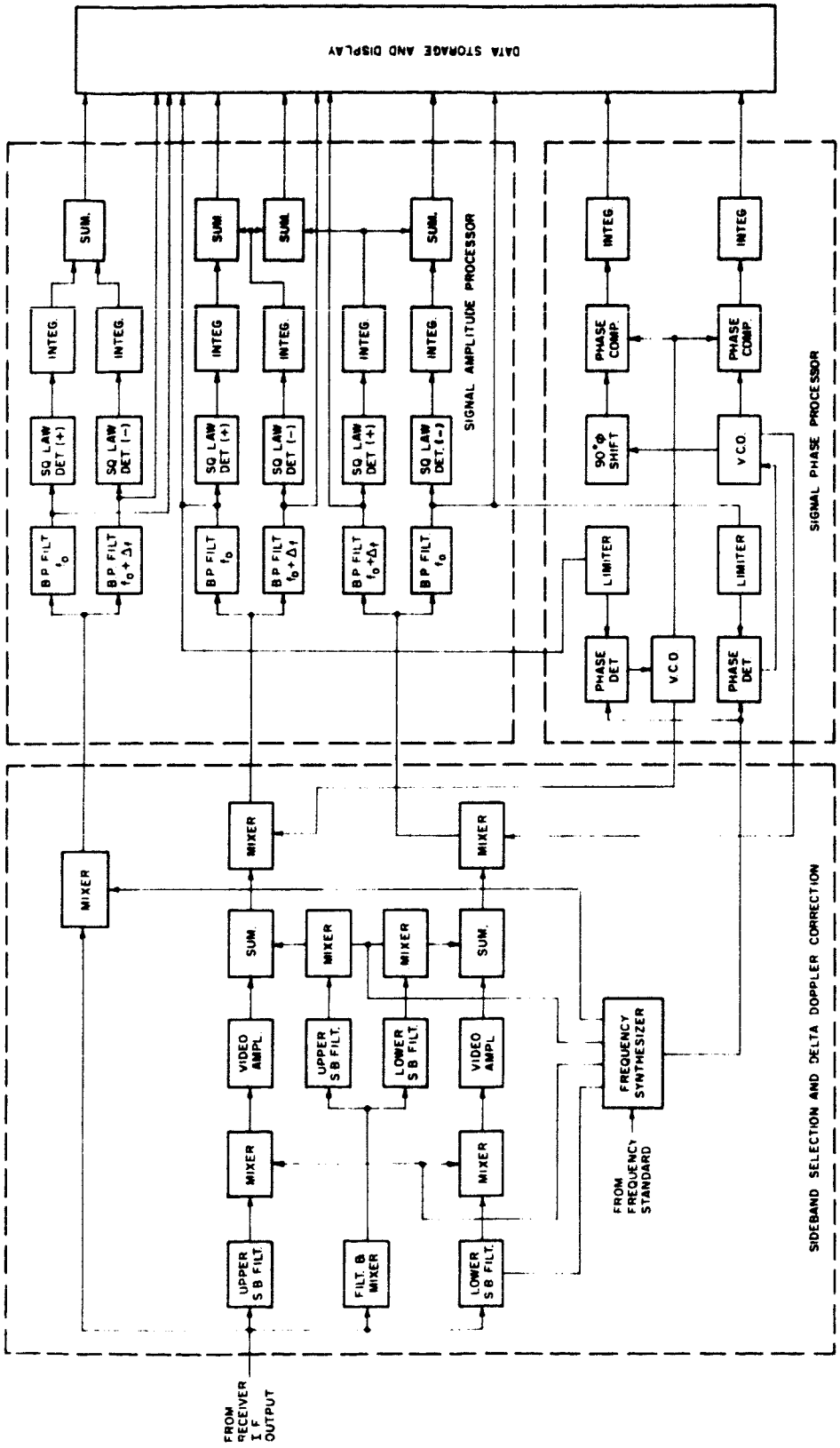

Figure 10-2 Ground Signal Processor

In addition to the signal processor description which follows, supplementary design information was given in Section 5.5 of the Second Quarterly Report.

10.1.1 Sideband Selection and Delta Doppler Correction

The energy in the received signal spectrum which is centered at 66 mc is separated into three distinct channels. The first of these channels, the upper sideband channel, begins with the upper sideband energy being amplified while all other energy is attenuated by the upper sideband filters. This energy is then transferred to a mixer in which the local oscillator is at 66 mc and the output, which is the lower conversion product, is selected by the video amplifier. This lower conversion product is the modulation frequency plus the delta doppler and any phase shift due to the communication channel. This energy due to the upper sideband is transferred through a summation network to a second mixer, the function of which is to translate this energy to a convenient frequency (10.7 mc) for predetection filtering and signal phase and amplitude processing.

The second channel, the lower sideband channel, performs the same processing as the first channel and translates the energy in the lower sideband to 10.7 mc. The third and last channel consists of a single mixer which translates the 66 mc carrier directly to 10.7 mc for additional processing.

This sideband selection and delta doppler correction process is readily implemented when the modulation frequency is 10 mc or 50 mc, however, for the case of the 5 kc modulation frequency, the received signal at 66 mc must be translated to a much lower frequency, namely, 6.6 mc, to perform the desired sideband separation. The sidebands are each translated to a center frequency equal to the modulation frequency and then inserted back into the higher modulation frequency channels through the summation networks.

In the ground receiver signal processors, the second mixer which translates each sideband to 10.7 mc is part of a phase locked loop which contains

a voltage controlled oscillator narrowed to 500 cps since the phase-locked loops cancel the delta doppler and any modulation frequency errors. All frequencies required for the translating functions are derived from the 66 mc frequency standard in the ground receiver. The fixed modulation frequencies (5 kc., 10 mc and 50 mc) dictates the values of the three frequencies required for the final translation to 10.7 mc. These three frequencies are applied manually to the second mixers in sequence and, in the event a signal appears at the output of the signal amplitude processor, the sequence is halted since the correct local oscillator frequency is selected. In the satellite receiver, these three frequencies are applied automatically.

10.1.2 Signal Amplitude Processing

The signal amplitude processor generates four data outputs which are directly proportional to the carrier power, the upper sideband power, the lower sideband power, and the differential gain of the upper and lower sideband channels.

The energy in the carrier channel is band limited and detected with a square law device, thus generating an output proportional to the input power. At low values of signal-to-noise ratio, the detected output, due to the noise power, would be in the same order of magnitude as the portion of the output due to the signal power. This DC voltage at the output of the detector, due to the input noise power, is eliminated by summing the same noise power at a frequency displaced from the signal which is provided by another square law detector with opposite polarity output. This configuration is the same for both the upper and lower sideband outputs. An additional summation network is utilized to monitor the differential gain in the two channels. All five outputs are fed directly to the analog recording system.

10.1.3 Signal Phase Processing

In the ground receivers, phase must be determined by comparing the outputs of the voltage controlled oscillators since all frequency and phase

variations are removed from the signal channel in this phase-locked loop. The two VCO signals are compared in in-phase and quadrature phase detectors which provide voltage outputs which represent 0 to 360 deg of phase rotation. The output of the phase comparator is integrated and buffer amplified such that direct interfacing with the analog recording system is provided.

In the satellite receiver, the signals are received and processed through tuned hard limiter circuits which provide in-phase and quadrature signals for processing through dual phase comparators. This provides and output from 0 to 360 deg of phase information. The output of the phase comparator is integrated and buffer amplified such that direct interfacing with the telemetry link is provided for the spacecraft.

10.1.4 Analog Data Storage and Presentation

The analog recording system in the gound terminal includes a tape recorder which stores the data for non-real time analog to digital conversion and digital computation. An analog strip line recorder is also provided to present the data in real time for purposes of monitoring, calibration and early interpretation of the raw data.

In addition to recording post detection signals which represent signal power and relative phase, the outputs of predetection filters would be translated to a frequency much lower than the 10.7 mc and stored on the same tape recorder.

10.2 Signal Flow Analysis

The signal flow analysis which was given in Section 5.2 of the Second Quarterly Report, describes the energy spectrum at all points in the communication channel at which a change in the energy spectrum takes place. The communication channel is considered to include the propagating medium and all circuitry located in the transmission line, from the generation of the test waveform in the satellite transmitter to the output of the signal

processor in the ground receivers. The satellite-to-ground channel was analyzed in detail and then the ground-to-satellite channel was discussed in terms of its significant differences.

10.3 Signal Level Analysis

The signal level analysis which was given in Section 5.3 of the Second Quarterly Report specified the signal levels and signal-to-noise ratios at major points in the communication channel.

The power at the input to the receiver is:

$$P_R = P_T G_T G_R \sigma L \qquad (10\text{-}1)$$

where:

P_T = input power to transmitter antenna

G_T = gain of transmitter antenna

G_R = gain of receiver antenna

σ = free space attenuation

L = polarization, and atmospheric losses

Free space attenuation is calculated as

$$\sigma = \left[\frac{\lambda}{4\pi R}\right]^2 \qquad (10\text{-}2)$$

where:

R = distance between the transmitting and receiving antennas

λ = wavelength of received energy

For a satellite directly over the ground station the free space attenuation is as shown in Table 10-1.

TABLE 10-1

FREE SPACE ATTENUATION FOR A SATELLITE

DIRECTLY OVER THE GROUND STATION

Frequency	16 Gc	35 Gc	94 Gc
Synchronous Satellite -db	207.8	214.6	223.2
6000 nmi Satellite -db	197.6	204.4	213.0

Slant range as a function of elevation angle for synchronous and 6000 nmi satellites is given in Appendix III of Volume II. From these two curves relative free space attenuation versus elevation angle was computed and is shown in Figure 10-3.

The atmospheric absorption used in this signal level analysis is based on the weather model established in Section 4-1.

The atmospheric absorption at 16 Gc, 35 Gc and 94 Gc which was computed from this weather model is given in Figures 4-5, 4-6 and 4-8. Propagation fading losses due to multipathing is one of the key parameters which will be measured during the experiment.

The total noise energy at the receiver input is the sum of the noise generated from within the receiver and the noise energy impinging on the antenna due to the radiation from the earth in the case of the 94 Gc satellite receiver and radiation from the atmosphere in the case of the 16 Gc and 35 Gc ground receivers. The noise power density at the receiver input is expressed as:

$$N_c = KT_o (FL-1) + KT_A \qquad (10-3)$$

where:

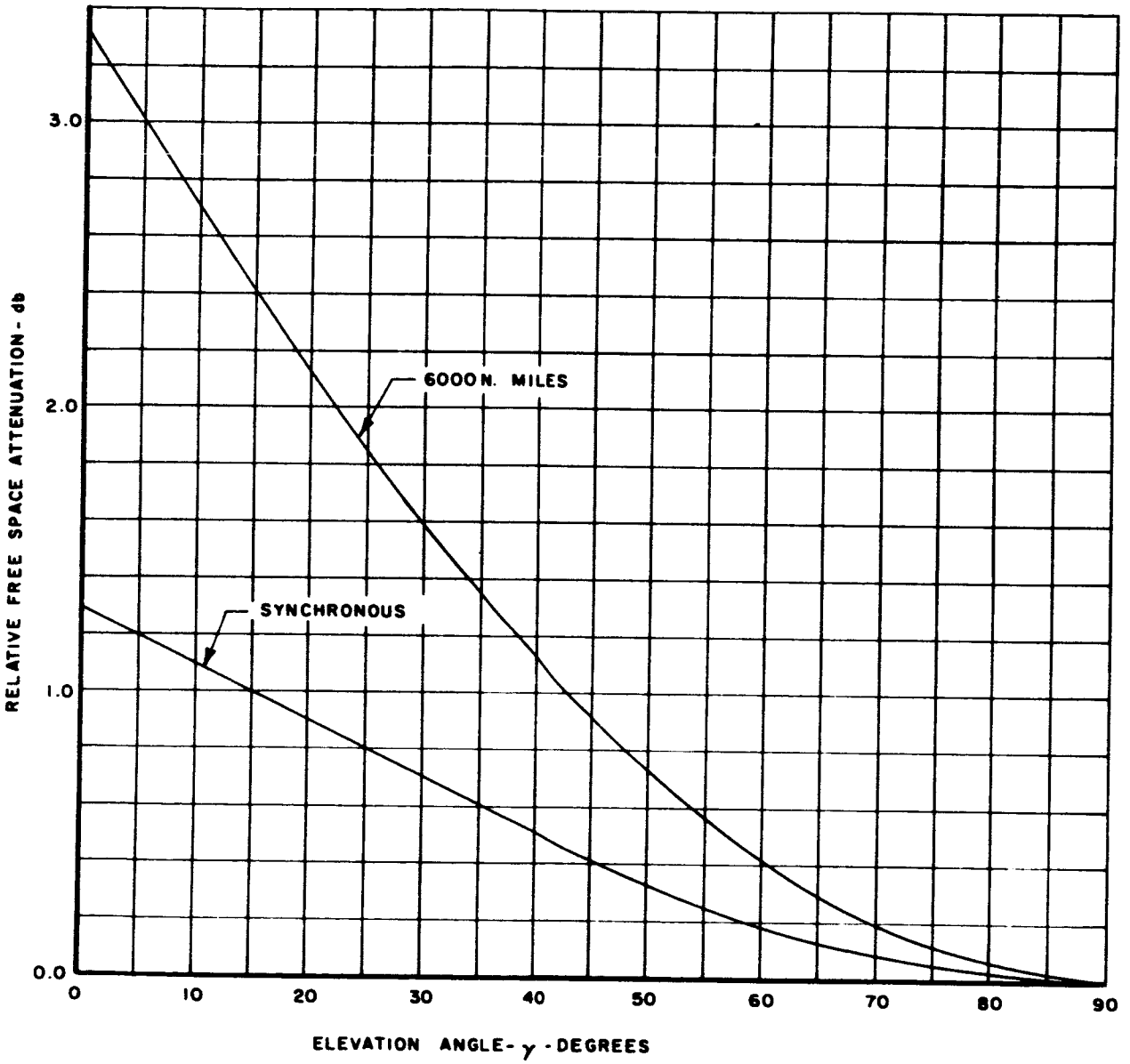

Figure 10-3. Relative Free Space Attenuation for Synchronous and 6000 nmi Satellites

N_c = noise power per cycle bandwidth

K = Boltzmann's constant = 1.38×10^{-23} watt-seconds/^{o}Kelvin

T_o = ambient temperature of system

F = receiver noise figure

L = receiver signal losses prior to mixer

T_A = effective antenna temperature

The effective temperature of the satellite antenna was given in Figure 4-19. Effective temperature of the ground antennas, which was derived in Section 4.2, is of interest mainly because it is a useful source of correlative data when making propagation measurements. As for receiver noise density, the receiver noise figures are so high: that is, 25 db for the 94 Gc satellite receiver, 15 db for the 35 Gc ground receiver and 12 db for the 16 Gc ground receiver; that the antenna temperature contribution is of little significance.

As the predetection bandwidth is increased beyond that occupied by the signal spectrum, the signal-to-noise ratio naturally decreases.

The signal flow analysis indicates that minimum predetection bandwidth in the receiver of a satellite-to-ground link is limited by the third IF frequency error. This error is a result of our inability to adjuct the reference oscillator in the frequency synthesizer so that the third IF frequency is perfectly aligned with the specified center frequency of the predetection filters. The third IF frequency error is:

$$\frac{\Delta\omega_3}{2\pi} = (k_o + r\,t)\left[\frac{\omega_3 + (\omega_m)_{max}}{2\pi}\right] = 83 \text{ cps} \qquad (10\text{-}4)$$

where k_o = initial adjustment error = 1×10^{-6}

r = oscillator drift rate = 1×10^{-9}/day

t = period of drift = 365 days

$\omega_3/2\pi$ = third IF frequency = 10.7 Mc

$1/2\pi\,(\omega_m)_{max}$ = maximum modulation frequency = 50 Mc

In addition to the above error, a second error $\frac{\Delta\omega_{mfg}}{2\pi}$ must be included which is a result of the filter manufacturer's inability to provide a center frequency equal to that which is specified. This error could be as much as 100 cycles.

Therefore, for synchronous and medium altitude satellite-to-ground links in which phase-locked loops are used in the sideband channels of the signal processor, the minimum predetection bandwidth is:

$$B_{min} = 2\left[\frac{\Delta\omega_3}{2\pi} + \frac{\Delta\omega_{mfg}}{2\pi}\right] = 366 \text{ cps} \qquad (10\text{-}5)$$

As a margin of safety, these errors are assumed to be of the same polarity and are not root mean squared.

For the ground-to-synchronous satellite links in which there are no phase-locked loops in the sideband channels to cancel transmitter modulation frequency error, $\frac{\Delta\omega_m}{2\pi}$, the minimum predetection bandwidth is increased.

$$\text{maximum } \frac{\Delta\omega_m}{2\pi} = (k_o + r\,t)\left[\frac{(\omega_m)_{max}}{2\pi}\right] = 68 \text{ cps} \qquad (10\text{-}6)$$

In this case the minimum predetection bandwidth is

$$B_{min} = 2\left[\frac{\Delta\omega_3}{2\pi} + \frac{\Delta\omega_{mfg}}{2\pi} + \frac{(\Delta\omega_m)_{max}}{2\pi}\right] = 502 \text{ cps} \qquad (10\text{-}7)$$

For the ground to medium altitude satellite links the absence of the phase-locked loops permits a delta doppler error. From Figure 3, Appendix III in

Volume II, the maximum doppler velocity, $\dot{r}_{max}$, is 4080 ft/sec. The maximum delta doppler error is:

$$\text{maximum } \frac{\Delta\omega_d}{2\pi} = \frac{(\omega_m)_{max}}{2\pi} \cdot \frac{\dot{r}_{max}}{C} = 207 \text{ cps} \qquad (10\text{-}8)$$

where C = velocity of light = 0.986×10^9 ft/second. The minimum predetection bandwidth is:

$$B_{min} = 2\left[\frac{\Delta\omega_3}{2\pi} + \frac{\Delta\omega_{mfg}}{2\pi} + \frac{(\Delta\omega_m)_{max}}{2\pi} + \frac{(\Delta\omega_d)_{max}}{2\pi}\right] = 916 \text{ cps} \qquad (10\text{-}9)$$

Signal-to-noise density for an unmodulated carrier from a satellite directly over the ground terminal is used as a reference point from which performance of the 16 Gc, 35 Gc and 94 Gc experiment links are developed. This reference calculation is also based on the complete absence of the atmosphere. For convenience, reference calculations for the 6000 nmi satellite are included in Tables 10-2 through 10-4 along with those for the synchronous satellite (19,300 nmi altitude).

For the synchronous satellite antenna, a 7^o beam is used which illuminates the Continental United States. A 23^o beam which illuminates the complete earth would have been preferable, but the additional 10 db gain is required for the propagation measurements. For the medium altitude satellite antenna, a 50 degree beam is used which illuminates the complete earth. Higher gain antennas will be difficult to implement on the medium altitude satellite since the satellite aspect with respect to a given point on earth is continually changing.

Since the synchronous satellite is stationary, the satellite antennas can be linear polarized and the linearly polarized ground antennas can be aligned to minimize polarization loss. When using a medium altitude satellite, the polarization alignment would be more difficult and therefore 3 db polarization

loss is assumed.

Tables 10-2 through 10-4 used a 15 ft diameter dish as a reference. Table 10-5 gives the variance from this reference for each ground facility being considered so that simple adjustments can be made in the signal-to-noise density values.

TABLE 10-2

SIGNAL ANALYSIS FOR 35 Gc DOWN-LINKS

WITH SYNCHRONOUS AND MEDIUM ALTITUDE SATELLITES

	Synchronous	Medium
Free Space Attenuation (λ= 8.6 mm) -db	214.6	204.4
Propagation Loss (zero loss as reference) -db	0.0	0.0
Satellite Antenna Gain -db	27.0	10.5
Ground Antenna Gain (15 ft, 55%)-db	- 61.9	61.9
Noise Density (T_o = 9200°K, N F = 15 db, T_A = o) -dbw/cps	- 189.0	-189.0
Transmitter Power (200 mw) -dbw	- 7.0	- 7.0
Polarization Loss -db	0.3	3.0
Received Signal Power (unmodulated carrier) -dbw	- 132.4	-141.4
Signal-to-Noise Density (unmodulated carrier) -db/cps	56.0	47.0
(modulated carrier)-db/cps	50.0	41.0
(each sideband) -db/cps	44.0	35.0

TABLE 10-3

SIGNAL ANALYSIS FOR 16 Gc DOWN-LINKS WITH SYNCHRONOUS AND MEDIUM ALTITUDE SATELLITES

	Synchronous	Medium
Free Space Attenuation (λ = 18.7 mm) -db	207.8	197.6
Propagation Loss (zero loss as reference)-db	0.0	0.0
Satellite Antenna Gain - db	27.0	10.5
Ground Antenna Gain (15 ft, 55%)-db	55.1	55.1
Noise Density		
(T_o =4500°K, N F= 12 db, T_A = o) -dbw/cps	- 192.1	-192.1
Transmitter Power (200 mw) -db	- 7.0	- 7.0
Polarization Loss -db	0.3	- 3.0
Received Signal Power (unmodulated carrier) -dbw	- 133.0	-142.0
Signal-to-Noise Density (unmodulated carrier)-db/cps	59.1	50.1
(modulated carrier) -db/cps	53.1	44.1
(each sideband) -db/cps	47.1	38.1

TABLE 10-4

SIGNAL ANALYSIS FOR 94 Gc UP-LINKS WITH

SYNCHRONOUS AND MEDIUM ALTITUDE SATELLITES

	Synchronous	Medium
Free Space Attenuation (λ = 3.2 mm) -db	223.2	213.0
Propagation Loss (zero loss as reference) -db	0.0	0.0
Satellite Antenna Gain -db	27.0	10.5
Ground Antenna Gain (15 ft, 55%) -db	70.5	70.5
Noise Density		
(T_o = 95,000^{o}K, NF=25 db, T_A =290^{o}) -dbw/cps	-179.0	-179.0
Transmitter Power (10 w) -dbw	10.0	10.0
Polarization Loss -db	0.3	3.0
Received Signal Power (unmodulated carrier)-dbw	-116.0	-125.0
Signal-to-Noise Density (unmodulated carrier)-db/cps	63.0	54.0
(modulated carrier)-db/cps	61.2	52.2
(each sideband)-db/cps	55.2	46.2

TABLE 10-5

REFERENCE CHART FOR VARIATION IN SIGNAL-TO-NOISE DENSITY FOR VARIOUS GROUND ANTENNAS

	35 Gc		16 Gc		94 Go	
Ground Facility	Antenna Gain	Variance	Antenna Gain	Variance	Antenna Gain	Variance
GSFC	61.9	0.0	55.1	0.0	68.5	-2.0
AEROSPACE	61.9	0.0	55.1	0.0	70.5	0.0
Univ. of TEXAS	62.4	0.5	55.6	0.5	70.5	0.0
AFCRL	66.7	4.8	60.8	5.7	-	-
LINCOLN	67.5	5.6	60.5	5.4	-	-
HAYSTACK	71.0	9.1	69.5	14.4	-	-
Auxiliary	58.4	-3.5	51.6	-3.5	-	-

A spacecraft or ground based receiving system must have a frequency acquisition and tracking capability since very small predetection bandwidths are required. The capability of any phase-lock receiver to acquire a signal and to stay in lock is a function of the input signal-to-noise density ratio, received signal frequency deviations and loop parameters.

Section 6 of Volume II illustrates the superiority of the band pass limiter over automatic gain control when optimizing the dynamic range of a phase tracking loop. Section 6 also explains that for the frequency offsets anticipated signal acquisition cannot be accomplished without sweeping the output frequency of the voltage controlled oscillator. A phase-lock receiver which employs bandpass limiting and frequency sweeping is shown in Figure 10-3. From the analysis given in Section 6, maximum frequency sweep rate versus loop-noise bandwidth for various values of signal-to-noise density were derived as shown in Figure 10-4. Since a 36 db signal-to-noise density ratio meets most of the requirements for experimental links, the maximum sweep rate for a 90% probability of acquisition will be 100 Kc per

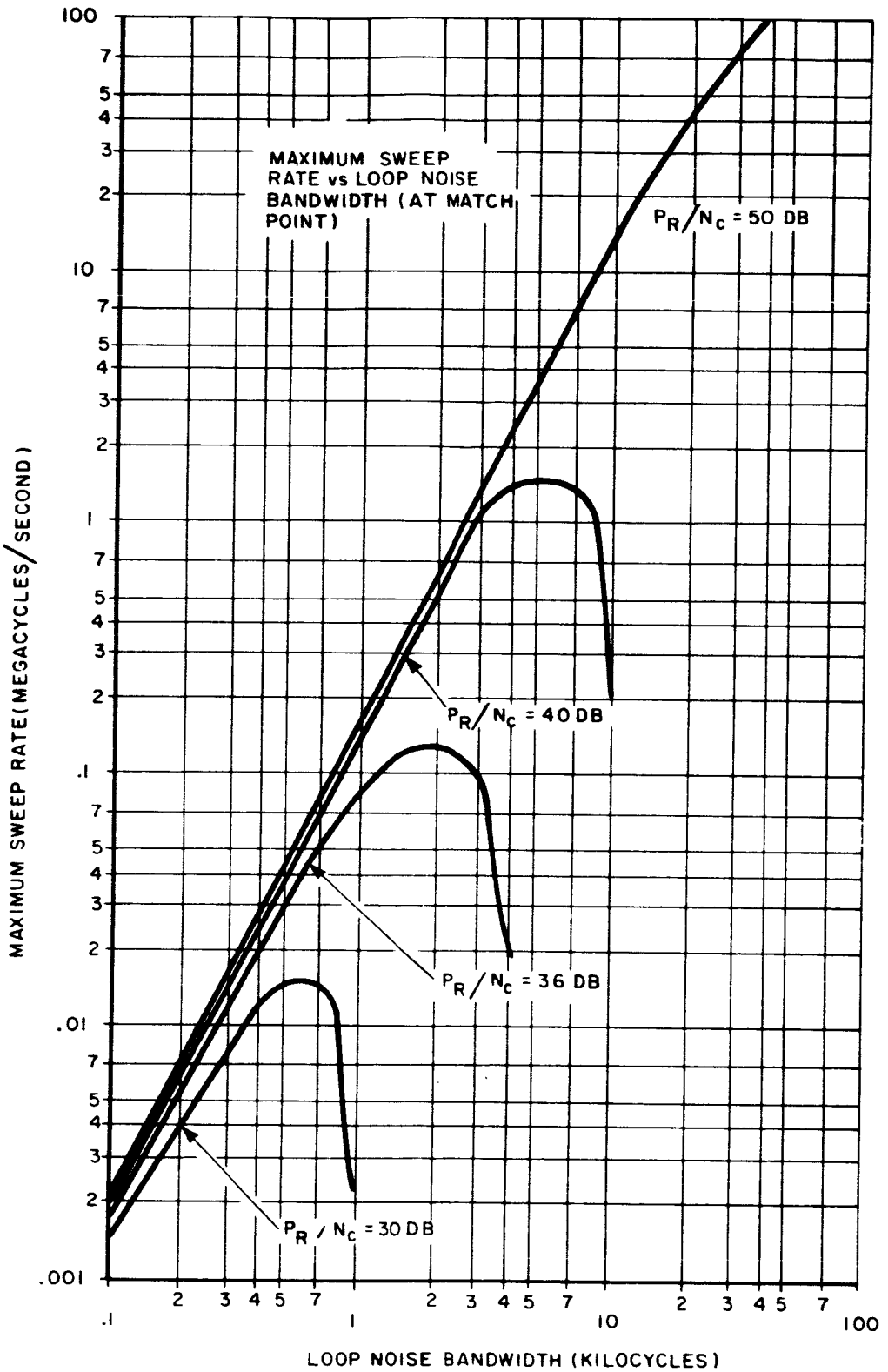

Figure 10-4 Maximum Sweep Rate vs Loop Noise Bandwidth (at Match Point)

second. In this case the loop noise bandwidth will be 2 Kc and, since the frequency offset under the worst conditions is 2 Mc, the sweep time will be 20 seconds.

The amplitude processor, in part, consists of a square law detection device, the voltage output of which is directly proportional to the power at its input. The output of an ideal square law detector is expressed as:

$$E_{DC} = \rho(P_S + P_N) \qquad (10\text{-}9)$$

where:

E_{DC} = direct current at detector output

ρ = detector transfer function

P_S = signal power at input to detector

P_N = noise power at input to detector

In addition, there exists amplitude fluctuations in the direct current component at the output of the detector due to the noise power at the detector input. The rms value of these fluctuations is defined as:

$$\overline{\sigma}_N = \frac{\rho P_N}{\sqrt{B\tau}} = \rho N_c \sqrt{\frac{B}{\tau}} \qquad (10\text{-}10)$$

where:

B = predetection bandwidth

τ = post-detection integration time

N_c = noise power density

Equation (10-9) defines the output voltage of the square law detector as a function of both signal and noise powers at the detector input. An output voltage that is a function of signal power only, has been generated by subtracting the same gain noise bandwidth product of a spectrum displaced from the desired signal spectrum. A block diagram of this approach was included in Section 10.1. The total noise fluctuation increases by the square root of two at the detector output; however, the output is now directly proportional to the input signal power. The voltage signal-to-noise ratio at this output may now be expressed as:

$$\frac{E_{dc}}{\sqrt{2}\sigma_n} = \frac{P_s}{N_c}\sqrt{\frac{\tau}{2B}} \qquad (10\text{-}11)$$

The minimum detectable change in amplitude is therefore:

$$\overline{A}_N = \frac{\frac{E_{dc}}{\sqrt{2}\sigma_n} + 1}{\frac{E_{dc}}{\sqrt{2}\sigma_n}} = \frac{\frac{P_s}{N_c}\sqrt{\frac{\tau}{2B}} + 1}{\frac{P_s}{N_c}\sqrt{\frac{\tau}{2B}}} \qquad (10\text{-}12)$$

and is plotted in Figure 10-5 for τ = 0.1 sec and for B = 500 cps. If the carrier phase-lock loop unlocks when the carrier signal-to-noise density becomes 27 db, then A_n max = 0.8 db on the carrier and 2.5 db on each sideband when the modulation index is unity.

The signal processor in the ground stations utilizes a phase lock loop in each sideband channel to cancel delta-doppler and modulation frequency error so that the predetection bandwidth can be minimized for better amplitude measurement. Relative phase of the sidebands is measured by comparing, in a phase detector, the outputs of the VCOs which establishes the minimum detectable change in relative phase.

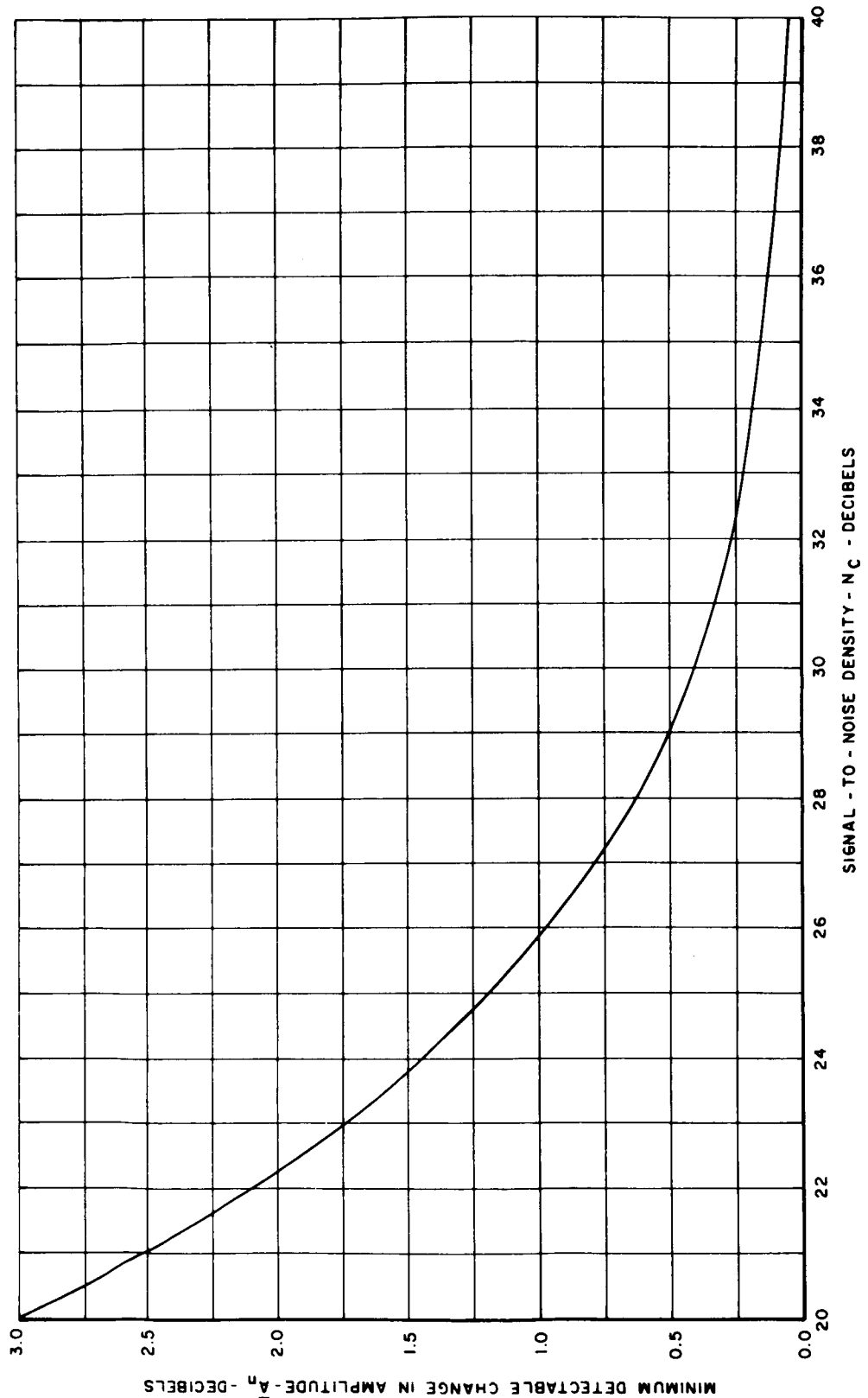

Figure 10-5. Minimum Detectable Change in Signal Amplitude

In the satellite the signal processor does not have phase lock-loops in the sideband channels and therefore the delta doppler and modulation frequency error establishes the predetection bandwidth. Relative phase of the sidebands is measured by comparing, in a phase detector, the actual sidebands themselves.

In either case the rms phase jitter or minimum detectable change in relative phase is expressed as:

$$\overline{\phi}_n = \frac{1}{\sqrt{\frac{P_s}{N_c}\,\tau}} \quad \text{radians} \tag{10-13}$$

The rms phase jitter versus signal-to-noise density is plotted in Figure 10-6 for $\tau = 0.1$ second. If the carrier phase-lock loop unlocks when the carrier signal-to-noise density becomes 27 db then $\left(\phi_n\right)_{max} = 0.14$ radians or degrees when the modulation index is unity.

Using the ground facilities discussed in Section 9, the assumed synchronous satellite positions identified in Section 7.1.1 and the signal level analysis just presented, the various experiment links were evaluated and the detailed results were given in Section 5.4 of the Second Quarterly Report. An evaluation of a typical link is given in Table 10-6.

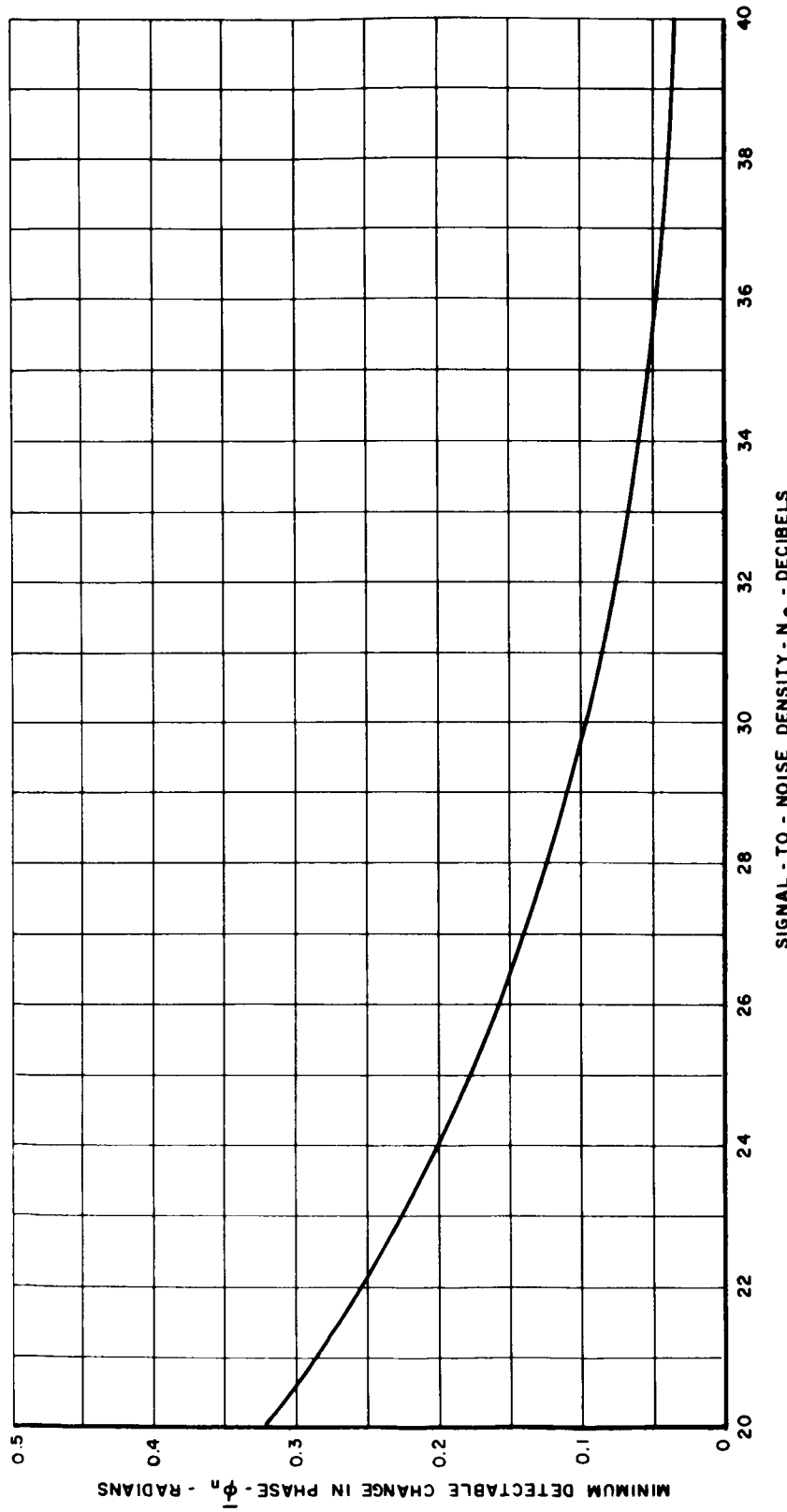

Figure 10-6. Minimum Detectable Change in Relative Phase

TABLE 10-6

EVALUATION OF A 35 GC EXPERIMENTAL LINK

Ground Station		GSFC
Satellite Position	(Table 7-2)	PA-45
Signal-to-Noise Density Reference (Unmodulated Carrier, 90° elevation, no atmosphere)	(Table 10-2)	56.0 db
Relative Free Space Attenuation (90° elevation vs. 33° elevation)	(Figure 10-3)	-0.6 db
Propagation Loss (cloudy, 33° elevation)	(Figure 4-6)	-0.9 db
Fading Loss (multipath)		-10.0 db
Antenna Gain Variance (15 foot reference)	(Table 10-5)	0.0 db
Beam Shape Loss (7° beam pointed at United States)		-2.0 db
Signal-to-Noise Density (unmodulated carrier)		42.5 db
(modulated carrier)		36.5 db
(each sideband)		30.5 db
Minimum Detectable Change in Sideband Amplitude	(Figure 10-5)	±0.4 db
Minimum Detectable Change in Relative Phase of Sidebands	(Figure 10-6)	±8 deg.

Section 11
DATA PROCESSING AND EVALUATION

The design of a millimeter propagation experiment is not complete without describing the data processing and evaluation required to define the parameters of the channel through the propagating medium.

Existing computer facilities are equipped to handle the data processing required for the propagation data collection program. Special-computer programs, which are based on the mathematics presented in this section, can be generated to provide estimates of the channel parameters. Little computation is required to infer, from these basic parameters, the effect of propagation on commonly used waveforms and modulation systems because this has already been done for similar effects at lower frequencies. Information on the estimation of system performance with these basic parameters was given in Section 6, and in the open literature such as References 58 through 62.

The first part of this section discusses the general concept of processing and evaluating millimeter propagation data taken from space-earth channels. The definitions of the channel parameters which apply to any communication channel were given in Section 3.2. The second part of this section summarizes Section 7 of Volume II, Final Report, which gives the mathematics for computing the millimeter channel parameters using the basic signal and correlative measurements that are specified in Section 5 of this report.

11.1 General Concept

The actual processing of the collected data can be performed by off-the-shelf equipment. The important consideration is that, when the experiment hardware is purchased, the data processing equipment must be specified in detail so that its procurement or lease becomes an integral part of the experiment design package. Labor required for data processing and analysis must be specified in the program plan.

Data to be used in the final description of the propagating medium will come from three principal sources. They are:

a. Spacecraft position data from a satellite tracking facility.

b. Amplitude and phase data either telemetered from spacecraft receivers or extracted from ground and airborne receivers.
c. Meteorological and radiometric data from correlative sensors.

Proper emphasis must be placed upon correlative sensors and correlative data processing. It does little good to determine atmospheric absorption, atmospheric noise, selective frequency fading and channel capacity unless we accurately classify the meteorological conditions existing during each measurement period and determine the probability of recurrence of each class of conditions during the annual cycle. Good correlative data will allow prediction of propagation effects for many future ground terminal locations from data taken with a few ground terminals.

Three phases of data processing will be considered for the experiments. They are:

a. Real-time on-site space, ground, and airborne data recording and processing which will be useful for operational monitoring and last minute changes in test schedule during the spacecraft pass or measurement interval.
b. Non-real-time on-site data processing which is necessary for short range test schedule planning for the subsequent spacecraft passes or measurement intervals.
c. Non-real-time off-site data processing performed by existing contractor and/or government computer facilities required to develop the final data in tabular and graphical form.

The taped analog data from the satellite and from all the ground facilities would be converted to digital form and processed at a central data processing facility. The relationship of this facility with the other facilities involved in the propagation data collection program is illustrated in Figure 11. 1.

Each ground facility receiver should be equipped with identical signal processors and analog tape recorders to minimize data processing expense. Each ground receiver would share its rf head with a radiometer in order to make sensitive sky temperature measurements using the same antenna beam. Short term and long term variations of antenna azimuth and elevation angle

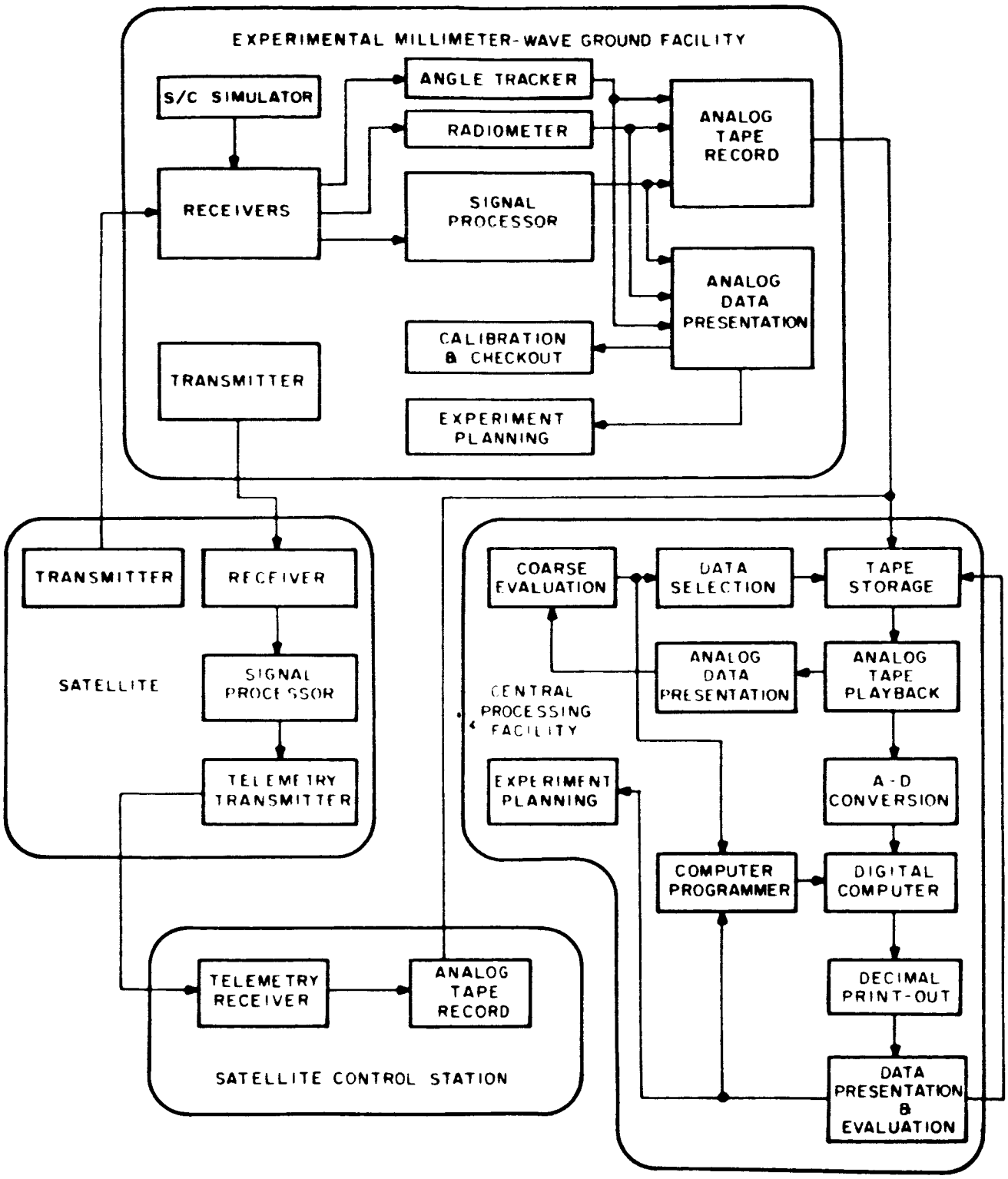

Figure 11-1 General Concept of Data Processing and Evaluation

are recorded on tape along with the signal amplitude, relative sideband phase and radiometric temperature. It should also be noted that the boresight installation for each of the participating ground facilities should be equipped for calibration and checkout purposes, with a spacecraft simulator which consists of the appropriate transmitters and/or receivers which function like those aboard the satellite.

Real-time analog strip line recorder presentations of the same data which is being recorded on magnetic tape will be made at each site for calibration, check-out and operational monitoring and to provide the co-operating agencies with immediate access to the raw data. A coarse evaluation on the analog presentations can be made at the site for the purposes of planning follow-on experiments.

An extensive quantity of data will result from the experimental program, and, of course, it is not necessary to statistically process all of the data collected. However, it is necessary to look for the occurrence of unusual propagation effects to insure that the data which is processed adequately represents the statistical model. When the magnetic tape arrives at the central processing facility, an analog presentation, similar to that made at the side, is made from the tape playback in order to select those samples of data which are to be processed. As more and more samples are processed it is expected that evaluation of these results will indicate improvements to be made in the computer program, and will choose new samples for computer processing and old samples for rerun.

The spacecraft position data taken by the tracking facility in the satellite control station is programmed into the computer in order to cancel out free space attenuation from the total path losses of the space-earth link. Calibration runs, just prior to the actual propagation tests, are performed with the spacecraft simulator so that the proper receiver and transmitter constants can be used at the central processing facility. During the test itself, operational performance is monitored by recording certain data on one or more channels of the magnetic tape. Pre-test calibration and operational monitoring is also performed on the spacecraft equipment and telemetered to the satellite control station with the raw propagation data.

11.2 Measurement of Channel Parameters

A variety of correlation functions and spectral densities are useful in the characterization of the millimeter communication channel. The quantities listed in Tables 11.2 and 11.3, can be used to determine the fundamental limitations imposed by the channel upon commonly used modulation schemes. Because of difficulties in implementing the hardware required to perform the propagation experiments, it is wiser to restrict the initial tests, in many instances, to the determination of the modified functions. The results of the initial tests can be used for the intelligent design of more complex tests which define the complete function.

The channel functions in Tables 11-2 and 11-3 that are the initial phase of the space-earth propagation experiments are:

a. Modified echo correlation function.
b. Spaced-frequency correlation function.
c. Modified echo power spectrum.
d. Modified spatial correlation function.
e. Modified spatial spectral density function.

In addition to these channel functions, other functions derived from radiometric data should be useful in investigating some of the causes of these channel functions. They are:

a. Sky temperature autocorrelation function.
b. Sky temperature - signal amplitude cross-correlation function,
c. Sky temperature spatial correlation function.

The correlation functions and spectral densities associated with the millimeter communication channel are defined by ensemble averages. However, an ensemble of received waveforms will never be available in practice and, therefore, these functions cannot be measured experimentally by ensemble averaging. Instead, time averages on individually received waveforms must be used. The interchange of ensemble and time averages is justified provided the ensemble is ergodic, in which case infinite time averages are entirely equivalent to ensemble averages.

A further compromise must be made in practice. Because of long-term equipment instabilities, the satellite passing over the horizon, etc.,

TABLE 11-2

CORRELATION FUNCTIONS

Name	Definition	Associated Quantities
Two-Dimensional Correlation Function	$R(\Delta f, \Delta\tau) = 2E\left[\tilde{s}_r^*(f - \frac{\Delta f}{2}, \tau - \frac{\Delta\tau}{2}) s_r(f + \frac{\Delta f}{2}, \tau + \frac{\Delta\tau}{2})\right]$	
Modified Two-Dimensional Correlation Function	$R(\Delta f, \Delta\tau) = 2E\left[\left\lvert\tilde{s}_r(f - \frac{\Delta f}{2}, \tau - \frac{\Delta\tau}{2})\ s_r(f + \frac{\Delta f}{2}, \tau + \frac{\Delta\tau}{2})\right\rvert\right]$	
Spaced Frequency Correlation Function	$R(\Delta f) = R(\Delta f, o) = 2E\left[\tilde{s}_r^*(f - \frac{\Delta f}{2}, \tau)\tilde{s}_r(f + \frac{\Delta f}{2}, \tau)\right]$	Coherence Bandwidth F_c
Modified Spaced-Frequency Correlation Function	$R(\Delta f) = R(\Delta f, o) = 2E\left[\left\lvert\tilde{s}_r(f - \frac{\Delta f}{2}, \tau)\ \tilde{s}_r(f + \frac{\Delta f}{2}, \tau)\right\rvert\right]$	Modified Coherence Bandwidth $\hat{F}_c$
Echo Correlation Function	$R(\Delta\tau) = R(o, \Delta\tau) = 2E\left[\tilde{s}_r^*(f, \tau - \frac{\Delta\tau}{2})\tilde{s}_r(f, \tau + \frac{\Delta\tau}{2})\right]$	Coherence Time τ_c
Modified Echo Correlation Function	$\hat{R}(\Delta\tau) = R(o, \Delta\tau) = 2E\left[\left\lvert\tilde{s}_r(f, \tau - \frac{\Delta\tau}{2})\ s_r(f, \tau + \frac{\Delta\tau}{2})\right\rvert\right]$	Modified Coherence Time $\hat{\tau}_c$
Spatial Correlation Function	$R(\Delta d, \Delta\tau) = 2E\left[\tilde{s}_r^*(d - \frac{\Delta d}{2}, \tau - \frac{\Delta\tau}{2})\tilde{s}_r(d + \frac{\Delta d}{2}, \tau + \frac{\Delta\tau}{2})\right]$	
Modified Spatial Correlation Function	$R(\Delta d, \Delta\tau) = 2E\left[\left\lvert\tilde{s}_r(d - \frac{\Delta d}{2}, \tau - \frac{\Delta\tau}{2})\ \tilde{s}_r(d + \frac{\Delta d}{2}, \tau + \frac{\Delta\tau}{2})\right\rvert\right]$	
Spaced-Antenna Correlation Function (Variable Separation)	$R(\Delta d) = 2E\left[\tilde{s}_r^*(d - \frac{\Delta d}{2}, \tau)\tilde{s}_r(d + \frac{\Delta d}{2}, \tau)\right]$	Coherence Aperture D_c
Modified Spaced-Antenna Correlation Function (Variable Separation)	$R(\Delta d) = 2E\left[\left\lvert\tilde{s}_r^*(d - \frac{\Delta d}{2}, \tau)\ \tilde{s}_r + \frac{\Delta d}{2}, \tau)\right\rvert\right]$	Modified Coherence Aperture $\hat{D}_c$
Spaced-Antenna Correlation Function (Constant Separation)	$R(\Delta\tau) = 2E\left[\tilde{s}_r^*(d, \tau - \frac{\Delta\tau}{2})\tilde{s}_r(d, \tau + \frac{\Delta\tau}{2})\right]$	Cross-Coherence Time T_p
Modified Spaced-Antenna Correlation Function (Constant Separation)	$\hat{R}(\Delta\tau) = 2E\left[\left\lvert\tilde{s}_r(d, \tau - \frac{\Delta\tau}{2})\ \tilde{s}_r(d, \tau + \frac{\Delta\tau}{2})\right\rvert\right]$	Modified Cross-Coherence Time $\hat{T}_p$

TABLE 11-3

SPECTRAL DENSITIES

Name	Definition	Associated Quantity
Scattering Function	$\sigma(\tau, f) = \iint R(\Delta f, \Delta\tau) e^{j2\pi\tau\,\Delta f + j2\pi f\,\Delta\tau} d\Delta f\, d\Delta\tau$	
Modified Scattering Function	$\sigma(\tau, f) = \iint R(\Delta f, \Delta\tau) e^{j2\pi\tau\,\Delta f + j2\pi f\Delta\tau} d\Delta f\, d\Delta\tau$	
Power Impulse Response	$\sigma(\tau) = \int \sigma(\tau, f)\, df = \int R(\Delta f)\, e^{j2\pi\tau\Delta f} d\Delta f$	Frequency Spread B
Modified Power Impulse Response	$\sigma(\tau) = \int \sigma(\tau, f)\, df = \int \hat{R}(\Delta f) e^{j2\pi\tau\Delta f} d\Delta f$	Modified Frequency Spread $\hat{B}$
Echo Power Spectrum	$\sigma(f) = \int \sigma(\tau, f)\, d\tau = \int R(\Delta\tau)\, e^{j2\pi f\Delta\tau} d\Delta\tau$	Time Spread L
Modified Echo Power Spectrum	$\sigma(f) = \int \sigma(\tau, f)\, d\tau = \int \hat{R}(\Delta\tau)\, e^{j2\pi f\Delta\tau} d\Delta\tau$	Modified Time Spread $\hat{L}$
Spatial Spectral Density Function	$\sigma(v, w) = \iint R(\Delta d, \Delta\tau) e^{j2\pi\tau\Delta d + j2\pi d\,\Delta\tau} d\Delta d\Delta\tau$	
Modified Spectral Density Function	$\sigma(v, w) = \iint R(\Delta d, \Delta\tau) e^{j2\pi\tau\Delta d + j2\pi d\Delta\tau} d\Delta d\Delta\tau$	
Power Spectrum (Variable Antenna Separation)	$\sigma(w) = \int \sigma(\tau, d)\, dd = \int R(\Delta d) e^{j2\pi\tau\,\Delta d} d\Delta d$	Wavefront Frequency Spread F_D
Modified Power Spectrum (Variable Antenna Separation)	$\sigma(w) = \int \sigma(\tau, d)\, dd = \int \hat{R}(\Delta d)\, e^{j2\pi\,\tau\Delta d} d\Delta d$	Modified Wavefront Frequency Spread $\hat{F}_D$
Power Spectrum (Constant Antenna Separation)	$\sigma(v) = \int \sigma(\tau, d)\, d\tau = \int R(\Delta\tau) e^{j2\pi d\,\Delta\tau} d\Delta\tau$	Lateral Velocity Spread V
Modified Power Spectrum (Constant Antenna Separation)	$\sigma(v) = \int \sigma(\tau, d)\, d\tau = \int \hat{R}(\Delta\tau)\, e^{j2\pi d\Delta\tau} d\Delta\tau$	Modified Lateral Velocity Spread $\hat{V}$

coherent waveform observations for indefinitely long periods cannot be made, so that only finite, rather than infinite, time averages are feasible. The result of using finite duration observations is that an estimate of the correlation function or spectral density is obtained rather than the actual function. The estimate is subject to statistical variations and it is upon these variations that we focus our attention.

The estimation of correlation functions and spectral densities on the basis of finite duration observations has been treated in detail by Blackman and Tukey[69], Bello[70], Hannan[71], Watts[72], and Bendat[73]. Use of these studies has been made in the writing of Section 7 of Volume II.

Section 12
BIBLIOGRAPHY

1. Kailath, T., "Channel Characteristics of Time-Invariant Dispersive Channels," Lectures on Communications System Theory, Edited by E. Baghdady, McGraw Hill, 1961.

2. Sunde, E. D., "Digital Troposcatter Transmission and Modulation Theory," The Bell System Technical Journal, January, 1964, pp. 143-153.

3. Price, R., "Statistical Theory Applied to Communication Through Multipath Disturbances," Lincoln Laboratory, Tech. Report No. 34, September, 1953.

4. Kailath, T., "Sampling Models for Linear Time Variance Filters," Technical Report 352, MIT, May, 1959.

5. Green, P. E., Jr., "Radar Astronomy Measurement Techniques," Technical Report 282, Lincoln Laboratory, M. I. T., Lexington, Mass.; December 1962.

6. Gallager, R. G., "Characterization and Measurement of Time and Frequency Spread Channels," Technical Report 352, Lincoln Laboratories, M. I. T., Lexington, Mass.; April, 1964.

7. Price, R. and Green P. E., Jr., "Signal Processing in Radar Astronomy-Communication via Fluctuating Multipath Media," Technical Report 234, Lincoln Laboratory, M. I. T., Lexington, Mass.; October, 1960.

8. Kennedy, R., "Design Considerations from Ionospheric Channels" Raytheon Internal Memo. BL-1039; July 1964.

9. Lebow, I. L., et al., "The West Ford Belt as a Communications Medium" Proc. IEEE, 52, 5, pp. 543-563; May 1964.

10. Bello, P. A. and Nelin, B. D., "The effect of Frequency Selective Fading on the Binary Error Probabilities of Incoherent and Differentially Coherent Matched Filter Receivers," IEEE Trans. on Communication Systems, pp. 170-186; June 1963.

11. Van Trees, H. L., Class Notes for Course 6.576, Massachusetts Institute of Technology; Spring 1965.

12. Straiton, A. W. and Tolbert, C. W., "Factors Affecting Earth-Satellite Millimeter Wavelength Communications," IEEE Transactions on Microwave Theory and Techniques, September, 1963.

13. Rogers, T. F., "An Estimate of Influence of the Atmosphere on Airborne Reconnaissance Radar Performance," AFCRL, January, 1953.

14. Gunn, K.L. S., "The Microwave Properties of Precipitation Particles", and T. W. R. East, Quarterly of the Journal of the Royal Meteorological Society, 80, October, 1954.

15. "Local Climatological Data with Comparative Data", Weather Bureau, U.S. Dept. of Commerce, 1963.

16. "Rainfall Frequency Atlas of U. S. for Durations from 30 minutes to 24 hours and Return Periods from One to 100 Years", Technical Paper 40, Weather Bureau, U. S. Department of Commerce.

17. MIT Radiation Laboratory Series, Volume 13, 1948.

18. Kessler,E. III and Atlas,David "Model Precipitation Distributions" Aero/Space Engineering, Dec. 1959, pp 36-40.

19. Air Force Cambridge Research Labs, "Handbook of Geophysics for U. S. Air Force Designers", Chapter 6.

20. Lilley, A.E., & Meeks, M. L., "The Microwave Spectrum of Oxygen in the Earth's Atmosphere", Journal of Geophysical Research, Vol. 68, No. 6, March 15, 1963.

21. Blevis, B.C.,"Losses Due to Rain on Radomes and Antenna Reflecting Surfaces: IEEE Transactions on Antennas and Propagation", January, 1965.

22. Grant, E. H, Buchanan, T. J., and Cook, H. F., "Dielectric Behavior of Water at Microwave Frequencies", Journal of Chemical Physics, Volume 26, January, 1957.

23. Leaderman, H.and Turner, L.A., "Theory of the Reflection and Transmission of Electromagnetic Waves By Dielectric Materials", in "Radar Scanners and Radomes", MIT Radiation Laboratory Series, Volume 26, 1948.

24. Gibble, D., "Effects of Rain or Transmission Performance of a Satellite Communications System", IEEE International Convention, March, 1964.

25. Barton, D.A. etal, "Report of the Ad Hoc Panel on Electromagnetic Radiation" Final Report, Air Force Systems Command Contract AF18 (600) - 1895, February 1963.

26. Millman, G. H., "Atmospheric Effects on VHF and UHF Propagations" Proceedings IRE August 1958.

27. Smith, E. K., and Weintraub, S. "The Constants in the Equation for Atmospheric Refractive Index at Radio Frequencies" Proceedings IRE August 1953.

28. Westinghouse Electric Corporation, "Navigation Satellite System" Volume 1, January 1964.

29. Thompson, M. C., Janes, H. B., and Kirkpatrick, R. W., "An Analysis of Time Variations in Tropospheric Refractive Index and Apparent Radio Path Length", J. Geophys Res., Volume 65, January, 1960, pp. 193-201.

30. Barton, D. K., "Reasons for the Failure of Radio Interferometers to Achieve their Expected Accuracy", Proc. IEEE, Volume 51, No. 4, April 1963, pp. 626-27. (See also pp. 485-90 in "Radar System Analysis", Prentice-Hall, Inc., 1964).

31. Janes, H. B., and Thompson, M. C., "Errors Induced by the Atmosphere in Microwave Range Measurements", Radio Science (Sec. D of NBS Journal of Research), Volume 68D, No. 11, pp. 1229-1235, November, 1964.

32. Norton, K. A., "Effects of Tropospheric Refraction in Earth-Space Links", XIVth General Assembly of URSI, Japan, September, 1963.

33. Crain, C. M., Straiton, A. W., and Von Rosenberg, L. E., "Statistical Survey of Atmospheric Refraction Variation", IRE Trans. on Antennas and Propagation, October, 1953.

34. Hatch, R. W., Bennett, S. B., and Kinzer, T. P., "Telstar Communications Tests", Bell System Tech. Jour., June, 1963.

35. Jordan, T., "Electromagnetic Theory", McGraw Hill.

36. Bergmann, R. G., "Physics Review", Volume 70, 1946.

37. Tatarsky, V. I., "Wave Propagation in a Turbulent Medium", McGraw-Hill Book Co., Inc., New York, 1961. Also see, Krasilnikov, V.A., and Tatarsky, V. I., "Atmosphere Turbulence and Radio Wave Propagation", in Monograph on Radio Wave Propagation in the Troposphere, Elsevier Publishing Co., New York, 1962.

38. Maio, A. D., Castelli, J. P., and Harney, P. J., "Wavefront Distortion Due to Atmospheric Inhomogeneities" in Proceedings 1964 World Conference on Radio Meteorology, Boulder, Colorado.

39. Muchmore, R. B., and Wheelon, A. D., "Frequency Correlation of Line-of-Sight Signal Scintillations", IEEE Trans. Antennas and Propagation, Jan., 1963.

40. Brookner, E., "Synthesis of an Arbitrary Bank of Filters by Means of a Time-Variable Network", IRE Conv. Record, Part 2, 1961, pp. 221-235.

41. Gallager, R. G., "Characterization and Measurement of Time-and-Frequency Spread Channels", Technical Report, Lincoln Laboratory, April 1964.

42. Corrington, M. S., "Variation of Bandwidth with Modulation Index in Frequency Modulation", IRE, October 1947.

43. Goldwater, F. T., "Low Cost Digital System Records Weather Data", Electronics, January 1964.

44. Barrett, A. H., and Chung, V. K., "Method for the Determination of High Altitude Water-Vapor Abundance from Ground-Based Microwave Observations", Journal of Geophysical Research, Vol. 67, No. 11, October 1962.

45. Battan, L. J., "Radar Meteorology", The University of Chicago Press, Chicago, 1959.

46. Kessler, E., " Use of Radar Measurements for the Assessment of Areal Rainfall", U.S. Weather Bureau presentation at 17th Session of WMO Executive Committee, Geneva, Switzerland, May 1965.

47. Atlas, D., "Angels in Focus," 1964 World Conference on Radio Meteorology, Boulder, Colorado.

48. Geotis, S. G., "On Sea Breeze Angels", 1964 World Conference on Radio Meterorology, Boulder, Colorado.

49. Doviak, R. J., Goldhirsch, J., and Lombardini, P. P., "Electromagnetic Scattering from Electron Irregularities in an Inhomogeneous Electron Density Distribution", Raytheon Company Report FR-65-275, 18 August 1965.

50. Ottersen, H., "Occurrence and Characteristics of Radar Angels Observed with a Vertically-Pointing Pulse Radar", 1964 World Conference on Radio Meteorology, Boulder, Colorado.

51. Plank, V. G., Atlas, D., and Paulsen, W. H., "The Nature and Detectability of Clouds and Precipitation as Determined by 1.25 cm Radar", Journal of Meteor. Vol. 12, No. 4, August 1955.

52. Hitschfield, W. and Bordan, J., "Errors Inherent in the Radar Measurement of Rainfall at Attenuating Wavelengths", Journal of Meteor, Vol. 11, No. 1, February 1954.

53. Hathaway, S. D. and Evans, H. W., "Radio Attenuation at 11 kmc and Some Implications Affecting Relay System Engineering", Bell Systems Tech. Journal, Vol. 38, January 1959.

54. Brown, E. N., and Braham, R. R., Jr., "Precipitation Particle Measurements in Cumulus Congestion", Journal of Atmos. Sciences, Vol. 20, No. 1, January 1963.

55. Braham, R. R., Jr., "Cumulus Cloud Precipitation as Revealed by Radar - Arizona 1955", Journal of Meteor., Vol. 15, No. 1, pp. 75-83, February 1958.

56. Kerr, R. B., Propagation of Short Radio Waves, McGraw-Hill Book Co., New York, 1947.

57. Deir Mendjian, D., "Complete Scattering Parameters of Polydispersed Hydrometeors in the $\lambda 0.1$ to $\lambda 10$ cm Range", 1964 World Conference on Radio Meteorology, Boulder, Colorado.

58. Turin, G. L., "Error Probabilities for Binary Symmetric Ideal Reception through Nonselective Slow Fading and Noise", IRE, September 1958.

59. Lindsey, W. C., "Error Probabilitiss for Rician Fading Multichannel Reception of Binary and N-ary Signals", IEEE Trans, on Information Theory, October 1964.

60. Lindsey, W. C., "Error Probabilities for Random Multichannel Reception of N-ary Signals", (Original Version of Reference 2).

61. Sunde, E. D., "Digital Troposcatter Transmission and Modulation Theory", The Bell System Technical Journal, January 1964.

62. "Intermodulation Distortion in Analog FM Troposcatter Systems", The Bell System Technical Journal, January 1964, Part 2, pp. 399-435.

63. "Performance Requirements, Electrical Power Subsystem", GSFC Specification No. ATS S2-0120, April 1965.

64. "Spacecraft Interface Specification for Advanced Technology Experiments", GSFC RFP 233-621671-16, 4 September 1964.

65. "Opportunities for Participation in Space Flight Investigation", Office of Space Science and Applications, NASA, Washington, D. C., January 1965.

66. "Spacecraft Telemetry and Command Subsystem", GSFC Specification No. ATS S2-0140, 10 December 1964.

67. "Spacecraft Communications Subsystem", GSFC Specification No. ATS S2-0130, 15 December 1964.

68. Keane, L. M., "The AFCRL 29 ft. Millimeter-Wave Antenna," Air Force Cambridge Research Laboratories, AFCL-65-726, October, 1965.

69. Blackman, and Tukey, J. W., "The Measurement of Power Spectra from the Point of View of Communication Engineering", Dover Publications, Inc., New York 1958.

70. Bello, P. A., "Measurement of the Complex Time-Frequency Channel Correlation Function", Radio Science Journal of Research NBS/USNCURSI, Vol. 68D, No. 10, October 1964.

71. Hannan, E. J., "Time Series Analysis", Methuen and Co., Ltd., London, and John Wiley and Sons, Inc. New York, 1960.

72. Watts, D. G., "Optimal Windows for Power Spectra Estimation", Mathematics Research Center, United States Army, University of Wisconsin, MRG Report No. 506, September 1964. Also, available as ASTIA AD-607-822.

73. Bendat, J. S., "Principles and Applications of Random Noise Theory", John Wilen and Sons, Inc. 1958.